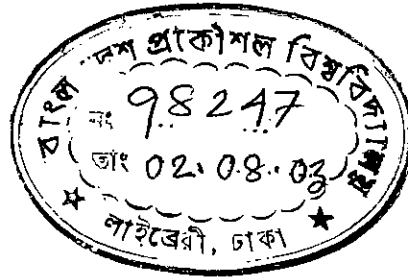


**Computation of Deflections of Edge Supported Reinforced Concrete  
Slabs Under Service Loads**

by

**Md. Ruhul Alam**



**MASTER OF SCIENCE IN CIVIL ENGINEERING (STRUCTURAL)**

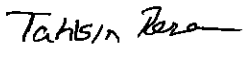


#98247#


**Department of Civil Engineering  
BANGLADESH UNIVERSITY OF ENGINEERING AND TECHNOLOGY,  
DHAKA  
2003**

The thesis titled “Computation of Deflections of Edge Supported Reinforced Concrete Slabs Under Service Loads”, Submitted by Md. Ruhul Alam, Roll No: 040004302F, Session: April 2000, has been accepted as satisfactory in partial fulfillment of the requirement for the degree of Master of Science in Civil Engineering (Structural) on 29<sup>th</sup> June, 2003.

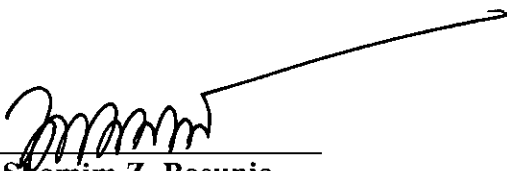
### BOARD OF EXAMINERS

1.   

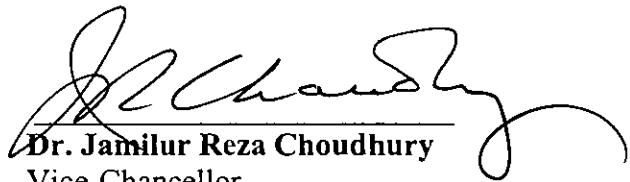
---

**Dr. Tahsin Reza Hossain**  
Associate Professor  
Department of Civil Engineering  
BUET, Dhaka. **Chairman**  
(Supervisor)
  
2.   

---

**Dr. Sk. Sekender Ali**  
Professor and Head  
Department of Civil Engineering  
BUET, Dhaka. **Member**  
(Ex-officio)
  
3.   

---

**Dr. M. Shamim Z. Bosunia**  
Professor  
Department of Civil Engineering  
BUET, Dhaka. **Member**
  
4.   

---

**Dr. Jamilur Reza Choudhury**  
Vice-Chancellor  
BRAC University  
Dhaka. **Member**  
(External)

## CANDIDATE'S DECLARATION

It is hereby declared that this thesis or any part of it has not been submitted elsewhere for the award of any degree or diploma (except for publication).



Md. Ruhul Alam

## ACKNOWLEDGEMENT

The author would like to express his sincere appreciation and gratitude to his supervisor, Dr. Tahsin Reza Hossain, Associate Professor, Department of Civil Engineering, Bangladesh University of Engineering and Technology (BUET), for his constant guidance, generous help, invaluable suggestions, continued encouragement and remarkable patience throughout the process of completion of this thesis.

The author is indebted to the Department of Civil Engineering, BUET, Civil Engineering Library, BUET Central Library, and Computer Center authorities for their facilities that were enjoyed by the author.

The author pays his deepest homage to his parents, whom he believes to be the cardinal source of inspiration for all his achievements.

## ABSTRACT

Excessive deflection of reinforced concrete slabs can cause severe serviceability problems. In recent years, realistic estimation of slab deflection under service loads has become more important due to the increasing use of high-strength materials and due to the use of ultimate limit state design which generally result in thinner members. This thesis is mainly concerned with computation of deflections of two-way edge supported slabs. Deflection calculation of slabs is complicated and time consuming due to the fact that it is affected by cracking, creep and shrinkage etc. The main objective of the current work is to develop a simplified method for prediction of immediate and long-term deflections of two-way edge supported slabs.

The work started with the elastic analysis of two-way edge supported slabs. Two finite element softwares, FE-77 and ANSYS have been used to analyze slabs with different end conditions. Moment and deflection coefficients charts have been prepared for easy calculation of elastic and immediate deflections.

Hossain (1999) developed a nonlinear FE module, which was incorporated in the finite element software FE-77, to model effect of cracking. This has been used in the current work after proper validation against experimental results. A detailed parametric study has been carried out and it has been observed that most of the edge supported slabs are cracked even under service loads if restraint shrinkage is considered. Results of the parametric study show that deflection increase due to cracking is only influenced by level of cracking, aspect ratio and boundary conditions.

Finally design charts have been proposed for easy calculation of immediate deflections of edge supported slabs. Charts are also validated by comparing with experiments results. As for long-term deflection, ACI Code (2002) multiplier approach has been used. ACI Code thicknesses are found to be adequate for most of the slabs with usual panel size and loading as the incremental and total deflections are within tolerable limits. Comparison between results of FE analysis and design chart method have been shown good agreement. With the help of these charts, a designer can easily calculate immediate as well as long-term deflections of edge supported slabs.

# CONTENTS

<b>CANDIDATE'S DECLARATION</b>	iii
<b>ACKNOWLEDGEMENT</b>	iv
<b>ABSTRACT</b>	v
<b>CONTENTS</b>	vi
<b>LIST OF FIGURES</b>	xi
<b>LIST OF TABLES</b>	xviii
<b>LIST OF SYMBOLS</b>	xx
<b>CHAPTER 1 INTRODUCTION</b>	1
1.1 Background	1
1.2 Scope and Objective of the Research Work	2
1.3 Outline of the Thesis	2
<b>CHAPTER 2 LITERATURE REVIEW</b>	4
2.1 Introduction	4
2.2 Behavior of Edge Supported Slab	5
2.3 Serviceability	8
2.4 Deflection Calculation by Uncracked Model	9
2.4.1 Simpson's method	9
2.4.2 Navier's Solution for Simply Supported Rectangular Plates	9
2.4.3 Levy's Solution for Rectangular Plate	10
2.4.4 The Strip Method	10
2.4.5 Deflection of Two-way Slab by Lagrange Equation	10
2.4.6 Finite Element Method	11
2.5 Deflection Calculation by Cracked Model	12
2.5.1 ACI Method Using Branson's Crack Model	12
2.5.2 Nilson's Approach	14

2.5.3 Gilbert Crack Model	17
2.5.4 Polak Approach	18
2.5.5 Scanlon and Murraray Approach	19
2.5.6 Jofriet and McNeice Approach	21
2.5.7 Hossain's Model	22
2.6 Long-term Deflection	22
2.6.1 ACI Method	23
2.6.2 Model Code 90, (MC-90) Method	24
2.7 Creep and Shrinkage	25
2.7.1 Creep and Shrinkage Coefficient	26
2.7.2 Deflection Due to Creep	26
2.7.3 Deflection Due to Shrinkage	27
2.8 Restraint Cracking	28
2.9 Construction Load	30
2.10 Deflection Control	31
2.10.1 ACI Code Provisions for Deflection Control	32
2.10.2 Gilbert Method	33
2.10.3 Hwang and Chang Method	33
2.11 Permissible Deflection	34
2.12 Conclusion	35
<b>CHAPTER 3 ELASTIC FINITE ELEMENT ANALYSIS</b>	<b>36</b>
3.1 Introduction	36
3.2 Mesh Sensitivity Analysis	36
3.2.1 Moment Coefficient	37
3.2.2 Deflection Coefficient	37
3.2.3 Mesh Sensitivity for FE-77 and ANSYS	38
3.3 Comparison of Deflections Calculated by FE-77 and ANSYS	42
3.4 Comparison of Moment Coefficients	44
3.5 Comparison of Deflection Coefficients	53
3.6 Comparison of Midpoint Deflection of One-way Slab	59
3.7 Comparison of Deflection for Full 3-D Building Model and Single Slab Model	61

3.8 Deflection and Moment Coefficients of Edge Supported Slabs	64
3.9 Conclusion	66
<b>CHAPTER 4 NONLINEAR FINITE ELEMENT ANALYSIS</b>	<b>67</b>
4.1 Introduction	67
4.2 Description of Hossain's Nonlinear Finite Element Program Module	68
4.3 Sequence of Analysis	69
4.4 Incorporation of ACI Method	71
4.5 Formation of [E] Matrices	72
4.6 Comparison of Experimental Results	73
4.6.1 McNeice Corner Supported Slab	73
4.6.2 McNeice One-way Slab	77
4.6.3 Shukla and Mittal Slabs	78
4.7 Sensitivity Analysis	81
4.8 Effect of Different Parameters on Deflection	83
4.8.1 Effect of Load on Elastic and Immediate Deflection of Slab	83
4.8.2 Effect of Concrete Strength on Deflection	86
4.8.3 Effect of Reinforcement on Deflection	87
4.8.4 Effect of Slab Thickness on Deflection	88
4.9 Deflection Limitations	90
4.10 Deflection against Live Load	92
4.11 Deflection Ratio vs. Stress Ratio Curve	94
4.11.1 Effect of Span Length	94
4.11.2 Effect of Applied Load and Slab Thickness	100
4.11.3 Effect of Live Load and Concrete Strength	105
4.11.4 Effect of Live Load, Concrete Strength and Span Length	107
4.11.5 Effect of Modulus of Rupture of Concrete	112
4.11.6 Effect of Aspect Ratio	113
4.12 Conclusion	114



<b>CHAPTER 5 DEFLECTION ESTIMATION USING DESIGN CHARTS</b>	116
5.1 Introduction	116
5.2 Selection of Parameters	116
5.2.1 Slab Thickness	117
5.2.2 Loading	117
5.2.3 Supported Conditions	117
5.2.4 Span Ratio and Span Length	118
5.2.5 Reinforcement Ratio	118
5.2.6 Material Properties	118
5.3 Mesh Sensitivity of the Modeling	119
5.4 Moment and Deflection Coefficients for Calculation of Deflection	120
5.5 Deflection Ratio vs. Stress Ratio Curve	120
5.6 Calculation of Elastic and Immediate Deflection of Slab	126
5.6.1 Calculation of Elastic Deflection of Slab	126
5.6.2 Calculation of Immediate Deflection of Slab Using Design Charts	127
5.7 Comparison of Immediate Deflection with FE Analysis	128
5.8 Validation of the Design Charts with Experimental Results and FE Analysis	131
5.9 Conclusion	133
 <b>CHAPTER 6 ESTIMATION OF LONG-TERM DEFLECTION</b>	 134
6.1 Introduction	134
6.2 Example Showing Short- and Long-term Deflections Estimation	134
6.2.1 Long-term Deflection Calculation from FE Analysis	135
6.2.2 Long-term Deflection Calculation from Design Charts	136
6.3 Parametric Study Showing Adequacy of Thickness	137
6.3.1 Live Load	137
6.3.2 Concrete Strength	139
6.3.3 Slab Thickness	140
6.3.4 Panel Size	142
6.4 Conclusion	144

<b>CHAPTER 7 CONCLUSIONS AND RECOMMENDATIONS</b>	145
7.1 Introduction	145
7.2 Conclusions	146
7.3 Recommendations for Future Work	148
<b>REFERENCE</b>	149
<b>APPENDIX</b>	153

## LIST OF FIGURES

### CHAPTER 2

2.1	Slab action at a corner.	5
2.2	Comparison of panels on beam and columns	7
2.3	Variation of moments across the width of critical sections assumed for design	8
2.4	Typical plate bending element with 12 degrees of freedom	12
2.5	Live load deflection analysis	16
2.6	Gilbert model	18
2.7	Uniaxial time-dependent behavior of concrete: generalize representation	25

### CHAPTER 3

3.1	Variation of positive moment coefficient $C_a(+)$ with number of element, for case-1	39
3.2	Variation of deflection coefficient with number of element, for case-1	40
3.3	Variation of positive moment coefficient $C_a(+)$ with number of element for case-2	40
3.4	Variation of negative moment coefficient $C_a(-)$ with number of element for case-2	41
3.5	Variation of deflection coefficient with number of element for case-2	41
3.6	Variation of moment coefficient $C_a(+)$ with slab span ratio, for case-1	45
3.7	Variation of moment coefficient $C_b(+)$ with slab span ratio, for case-1	46
3.8	Variation of moment coefficient $C_a(+)$ with slab span ratio, for case-2	46
3.9	Variation of moment coefficient $C_a(-)$ with slab span ratio, for case-2	47
3.10	Variation of moment coefficient $C_b(+)$ with slab span ratio, for case-2	47
3.11	Variation of moment coefficient $C_b(-)$ with slab span ratio, for case-2	48
3.12	Variation of moment coefficient $C_a(+)$ with slab span ratio, for case-3	48
3.13	Variation of moment coefficient $C_b(+)$ with slab span ratio, for case-3	49
3.14	Variation of moment coefficient $C_b(-)$ with slab span ratio, for case-3	49
3.15	Variation of moment coefficient $C_a(-)$ with slab span ratio, for case-4	50

3.16	Variation of moment coefficient $C_a(-)$ with slab span ratio, for case-5	50
3.17	Variation of moment coefficient $C_a(-)$ with slab span ratio, for case-6	51
3.18	Variation of moment coefficient $C_b(-)$ with slab span ratio, for case-7	51
3.19	Variation of moment coefficient $C_a(-)$ with slab span ratio, for case-8	52
3.20	Variation of moment coefficient $C_a(-)$ with slab span ratio, for case-9	52
3.21	Variation of deflection coefficient with span ratio for short direction, for case-1	53
3.22	Variation of deflection coefficient with span ratio for long direction, for case-1	54
3.23	Variation of deflection coefficient with span ratio for short direction, for case-2	54
3.24	Variation of deflection coefficient with span ratio for long direction, for case-2	55
3.25	Variation of deflection coefficient with span ratio for short direction, for case-3	55
3.26	Variation of deflection coefficient with span ratio for long direction, for case-3	56
3.27	Variation of deflection coefficient with span ratio for short direction, for case-4	56
3.28	Variation of deflection coefficient with span ratio for long direction, for case-4	57
3.29	Variation of deflection coefficient with span ratio for short direction, for case-8	57
3.30	Variation of deflection coefficient with span ratio for long direction, for case-8	58
3.31	Variation of deflection coefficient with span ratio for short direction, for case-9	58
3.32	Variation of deflection coefficient with span ratio for long direction, for case-9	59
3.33	Full 3-D modeling of the building with slab and beam	62
3.34	Figures of different slab cases	63

## CHAPTER 4

4.1	Flow chart showing the sequence of calculation	70
4.2	Details of corner-supported two-way slab tested McNeice	74
4.3	Load-deflection curve for the corner supported slab at node-7	75
4.4	Load-deflection curve for the corner supported slab at node-69	75
4.5	Load-deflection curve for the corner supported slab at node-147	76
4.6	Load-deflection curve for the corner supported slab at node-157	76
4.7	Details of simply supported one-way slab tested by McNeice	77
4.8	Load versus deflection curve for the simply supported one-way slab tested by McNeice	78
4.9	Details of edge supported two-way slabs tested by Shukla and Mittal	79
4.10	Load verses deflection curves for the edge supported Shukla and Mittal slab S-8 using FE-77 analysis	80
4.11	Load verses deflection curves for the edge supported Shukla and Mittal slab S-11 using FE-77 analysis	80
4.12	Load verses deflection curves for the edge supported Shukla and Mittal slab S-12 using FE-77 analysis	81
4.13	Comparison of elastic and immediate deflection of slab with respect to number element, for case-1	82
4.14	Comparison of elastic and immediate deflection of slab with respect to number element, for case-2	83
4.15	Details of slab modeling with FE meshing, for case-8	85
4.16	Comparison of elastic and immediate deflection of slab, for case-8	85
4.17	Variation of mid point deflection of slab with respect to concrete strength and modulus rupture of concrete, for case-2	86
4.18	Variation of immediate deflection of slab with % reinforcement, for case-2	88
4.19	Variation of elastic and immediate deflection of slab for varying thickness with constant live load, for case-1	89
4.20	Variation of elastic and immediate deflection of slab for varying thickness with constant live load, for case-2	90
4.21	Variation of immediate deflection slab for application of full load with varying span length and slab thickness, for case-2	92

4.22	Variation of immediate deflection of slab with varying live load, for case-4	93
4.23	Variation of deflection ratio vs. stress ratio curve of edge supported slab, for case-1, $f_r = 0.62\sqrt{f'_c}$ N/mm <sup>2</sup>	96
4.24	Variation of deflection ratio vs. stress ratio curve of edge supported slab, for case-2, with varying slab thickness, $f_r = 0.62\sqrt{f'_c}$ N/mm <sup>2</sup>	97
4.25	Variation of deflection ratio vs. stress ratio curve of edge supported slab, for case-3, $f_r = 0.62\sqrt{f'_c}$ N/mm <sup>2</sup>	97
4.26	Variation of deflection ratio vs. stress ratio curve of edge supported slab, for case-4, $f_r = 0.62\sqrt{f'_c}$ N/mm <sup>2</sup>	98
4.27	Variation of deflection ratio vs. stress ratio curve of edge supported slab, for case-1, $f_r = 0.33\sqrt{f'_c}$ N/mm <sup>2</sup>	98
4.28	Variation of deflection ratio vs. stress ratio curve of edge supported slab, for case-2, with varying slab thickness, $f_r = 0.33\sqrt{f'_c}$ N/mm <sup>2</sup>	99
4.29	Variation of deflection ratio vs. stress ratio curve of edge supported slab, for case-3, $f_r = 0.33\sqrt{f'_c}$ N/mm <sup>2</sup>	99
4.30	Variation of deflection ratio vs. stress ratio curve of edge supported slab, for case-4, $f_r = 0.33\sqrt{f'_c}$ N/mm <sup>2</sup>	100
4.31	Variation of deflection ratio vs. stress ratio curve of slab for varying live load and slab thickness, for case-1, $f_r = 0.62\sqrt{f'_c}$ N/mm <sup>2</sup>	103
4.32	Variation of deflection ratio vs. stress ratio curve of slab for varying live load and slab thickness, for case-2, $f_r = 0.62\sqrt{f'_c}$ N/mm <sup>2</sup>	103
4.33	Variation of deflection ratio vs. stress ratio curve of slab for varying live load and slab thickness, for case-1, $f_r = 0.33\sqrt{f'_c}$ N/mm <sup>2</sup>	104
4.34	Variation of deflection ratio vs. stress ratio curve of slab for varying live load and slab thickness, for case-2, $f_r = 0.33\sqrt{f'_c}$ N/mm <sup>2</sup>	104
4.35	Variation of deflection ratio vs. stress ratio curve of slab for varying live	

	load and concrete strength, for case-2, $f_r = 0.62\sqrt{f'_c}$ N/mm <sup>2</sup>	106
4.36	Variation of deflection ratio vs. stress ratio curve of slab for varying live load and concrete strength, for case-2, $f_r = 0.33\sqrt{f'_c}$ N/mm <sup>2</sup>	107
4.37	Variation of deflection ratio vs. stress ratio curve of slab for varying live load, concrete strength and span length, for case-4, $f_r = 0.62\sqrt{f'_c}$ N/mm <sup>2</sup>	109
4.38	Variation of deflection ratio vs. stress ratio curve of slab for varying live load, concrete strength and span length, for case-5, $f_r = 0.62\sqrt{f'_c}$ N/mm <sup>2</sup>	109
4.39	Variation of deflection ratio vs. stress ratio curve of slab for varying live load, concrete strength and span length, for case-8, $f_r = 0.62\sqrt{f'_c}$ N/mm <sup>2</sup>	110
4.40	Variation of deflection ratio vs. stress ratio curve of slab for varying live load, concrete strength and span length, for case-4, $f_r = 0.33\sqrt{f'_c}$ N/mm <sup>2</sup>	110
4.41	Variation of deflection ratio vs. stress ratio curve of slab for varying live load, concrete strength and span length, for case-5, $f_r = 0.33\sqrt{f'_c}$ N/mm <sup>2</sup>	111
4.42	Variation of deflection ratio vs. stress ratio curve of slab for varying live load, concrete strength and span length, for case-8, $f_r = 0.33\sqrt{f'_c}$ N/mm <sup>2</sup>	111
4.43	Variation of deflection ratio vs. stress ratio curve of slab for varying rupture strength of concrete, for case-1	112
4.44	Deflection ratio vs. stress ratio curve of two-way edge supported slab, for case-1, $f_r = 0.62\sqrt{f'_c}$ N/mm <sup>2</sup>	113
4.45	Deflection ratio vs. stress ratio curve of two-way edge supported slab, for case-2, $f_r = 0.33\sqrt{f'_c}$ N/mm <sup>2</sup>	114

## CHAPTER 5

5.1	Deflection ratio vs. stress ratio chart of two-way edge supported slab, for case-1, $f_r = 0.33\sqrt{f'_c}$ N/mm <sup>2</sup>	122
5.2	Deflection ratio vs. stress ratio chart of two-way edge supported slab, for case-2, $f_r = 0.33\sqrt{f'_c}$ N/mm <sup>2</sup>	122

5.3	Deflection ratio vs. stress ratio chart of two-way edge supported slab, for case-3, $f_r = 0.33\sqrt{f'_c}$ N/mm <sup>2</sup>	123
5.4	Deflection ratio vs. stress ratio chart of two-way edge supported slab, for case-4, $f_r = 0.33\sqrt{f'_c}$ N/mm <sup>2</sup>	123
5.5	Deflection ratio vs. stress ratio chart of two-way edge supported slab, for case-5, $f_r = 0.33\sqrt{f'_c}$ N/mm <sup>2</sup>	124
5.6	Deflection ratio vs. stress ratio chart of two-way edge supported slab, for case-6, $f_r = 0.33\sqrt{f'_c}$ N/mm <sup>2</sup>	124
5.7	Deflection ratio vs. stress ratio chart of two-way edge supported slab, for case-7, $f_r = 0.33\sqrt{f'_c}$ N/mm <sup>2</sup>	125
5.8	Deflection ratio vs. stress ratio chart of two-way edge supported slab, for case-8, $f_r = 0.33\sqrt{f'_c}$ N/mm <sup>2</sup>	125
5.9	Deflection ratio vs. stress ratio chart of two-way edge supported slab, for case-9, $f_r = 0.33\sqrt{f'_c}$ N/mm <sup>2</sup>	126
5.10	Deflection ratio vs. stress ratio chart of two-way edge supported slab, for case-1, $f_r = 0.62\sqrt{f'_c}$ N/mm <sup>2</sup>	131
5.11	Load-deflection curve for Shukla and Mittal slab, S-8	132
5.12	Load-deflection curve for Shukla and Mittal slab, S-11	132
5.13	Load-deflection curve for Shukla and Mittal slab, S-12	133

## CHAPTER 6

6.1	Variation of incremental deflection with varying live load for a corner panel	138
6.2	Variation of total deflection with varying live load for a corner panel	138
6.3	Variation of incremental deflection with varying live load and concrete strength for a corner panel	139
6.4	Variation of total deflection with varying live load and concrete strength for a corner panel	140
6.5	Variation of incremental deflection with varying slab thickness for a corner panel	141



6.6	Variation of total deflection with varying slab thickness for a corner panel	142
6.7	Variation of incremental deflection with varying span length and live load for corner panel	143
6.8	Variation of total deflection with varying span length and live load for corner panel	143

## APPENDIX A

A1	Deflection ratio vs. stress ratio chart of two-way edge supported slab for case-1, $f_r = 0.62 \sqrt{f'_c}$ N/mm <sup>2</sup>	154
A2	Deflection ratio vs. stress ratio chart of two-way edge supported slab for case-2, $f_r = 0.62 \sqrt{f'_c}$ N/mm <sup>2</sup>	154
A3	Deflection ratio vs. stress ratio chart of two-way edge supported slab for case-3, $f_r = 0.62 \sqrt{f'_c}$ N/mm <sup>2</sup>	155
A4	Deflection ratio vs. stress ratio chart of two-way edge supported slab for case-4, $f_r = 0.62 \sqrt{f'_c}$ N/mm <sup>2</sup>	155
A5	Deflection ratio vs. stress ratio chart of two-way edge supported slab for case-5, $f_r = 0.62 \sqrt{f'_c}$ N/mm <sup>2</sup>	156
A6	Deflection ratio vs. stress ratio chart of two-way edge supported slab for case-6, $f_r = 0.62 \sqrt{f'_c}$ N/mm <sup>2</sup>	156
A7	Deflection ratio vs. stress ratio chart of two-way edge supported slab for case-7, $f_r = 0.62 \sqrt{f'_c}$ N/mm <sup>2</sup>	157
A8	Deflection ratio vs. stress ratio chart of two-way edge supported slab for case-8, $f_r = 0.62 \sqrt{f'_c}$ N/mm <sup>2</sup>	157
A9	Deflection ratio vs. stress ratio chart of two-way edge supported slab for case-9, $f_r = 0.62 \sqrt{f'_c}$ N/mm <sup>2</sup>	158

## LIST OF TABLES

### CHAPTER 2

2.1	Minimum thickness of slabs without interior beams	33
2.2	Maximum allowable computed deflections	35

### CHAPTER 3

3.1	Parameters used in FE analysis	42
3.2	Comparison of elastic deflection of slab performed by FE-77 and ANSYS	43
3.3	Midpoint deflections for different types of support	60
3.4	Comparison of one-way slab deflection for different support conditions	60
3.5	Comparison of deflection calculated from single slab model and full 3-D building model	63
3.6	Deflection coefficients for elastic deflection of two-way edge supported slab center, considering short direction	65
3.7	Moment coefficients for calculation of maximum stress in the slab	66

### CHAPTER 4

4.1	Parameters for elastic and immediate deflection of slab for varying load	84
4.2	Parameters for calculation of elastic and immediate deflection of slab for varying slab thickness	89
4.3	Immediate deflections versus span length of slab for different span length and slab thickness for full load, for case-2	91
4.4	Immediate deflection of slab with varying live load, for case-4	93
4.5	Panel dimension of slab different slab cases	94
4.6	Slab thickness for slab case-2	95
4.7	Stress ratio and deflection ratio with changing live load and slab thickness for case-1, $f_r = 0.62\sqrt{f'_c}$ N/mm <sup>2</sup>	101
4.8	Stress ratio and deflection ratio with changing live load and slab thickness for case-2, $f_r = 0.62\sqrt{f'_c}$ N/mm <sup>2</sup>	101

4.9	Stress ratio and deflection ratio with changing live load and slab thickness for case-1, $f_r = 0.33\sqrt{f'_c}$ N/mm <sup>2</sup>	102
4.10	Stress ratio and deflection ratio with changing live load and slab thickness for case-2, $f_r = 0.33\sqrt{f'_c}$ N/mm <sup>2</sup>	102
4.11	Data for varying concrete strength of slab	105
4.12	Data for varying live load of 6096 mm × 606 mm slab	106
4.13	Common parameters used FE analysis	107

## CHAPTER 5

5.1	Comparison of calculated and FE analyzed deflections for different slab cases	130
-----	---	-----

## CHAPTER 6

6.1	Slab thickness predicted from ACI Code 1963 and ACI Code 2002	141
-----	---	-----

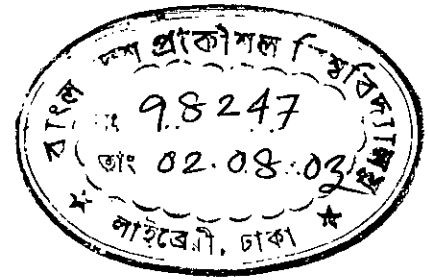
## LIST OF SYMBOLS

The following notation is used in the thesis:

$f'_c$	Concrete cylinder strength
$t, h$	Thickness of section
$d$	Effective depth of section
$E_c$	Modulus of elasticity of concrete
$E_s$	Modulus of elasticity of steel
$n$	Modular ratio = $E_s/E_c$
$f_r$	Modulus of rupture of concrete
$y_t$	Distance from neutral axis to the tension face
$I_{ut}$	Moment of inertia of uncracked section
$I_g$	Gross moment of inertia without reinforcement
$I_{eff}$	Effective moment of inertia of concrete cross section
$I_{cr}$	Moment of inertia of cracked section
$I_{e1}$	Effective moment of inertia in the major principal direction
$I_{e2}$	Effective moment of inertia in the minor principal direction
$M_{cr}$	Cracking moment as defined by ACI
$M_1$	Major principal moment
$M_2$	Minor principal moment
$\Delta_i$	Immediate deflection
$A_s$	Tensile reinforcement
$A'_s$	Compression reinforcement

$l$	Span length
$a, l_a$	Span length in short direction
$b, l_b$	Span length in long direction
$w$	Uniform transverse load
$\nu$	Poisson's ratio
$\rho$	Tensile steel percentage
$\rho'$	Compressive steel percentage
$\xi$	Time-dependent coefficient for additional long-term deflection
$[E]$	Elasticity matrix in x-y directions
$[E']$	Elasticity matrix in principal directions
$E_x, E_y$	Reduced Young's moduli of cracked concrete in x and y-directions
$t, h$	Slab thickness
$\nu_x, \nu_y$	Reduced Poisson's ratios of cracked concrete in x and y-direction
$c$	Moment coefficient
$C_a$	Moment coefficient in short direction
$C_b$	Moment coefficient in long direction
$f$	Developed stress from elastic FE analysis
$f_y$	Yield strength of reinforcing steel
$f'_c$	Concrete cylinder compressive strength
$n$	Modular ratio = $E_s/E_c$
$\delta$	Elastic deflection of slab
$D_a$	Deflection coefficient in short direction
$D$	Flexural rigidity of solid slab
$c_n$	Depth of neutral axis

$\alpha_n, \alpha_t$	Modification factors to include the effect of cracking, creep and shrinkage in the [E'] matrices
$\beta_1$	Takes into account the bond properties of bars
$\beta_2$	Takes into account the deterioration of tension
$\epsilon_{cs}$	Shrinkage strain
$\sigma_1, \sigma_2$	Stress in the outer fiber of the section in principal direction
$\psi_1(t_0), \psi_1(t)$	State 1 curvature at time $t_0$ and $t$
$\psi_2(t_0), \psi_2(t)$	State 2 curvature at time $t_0$ and $t$
$\psi_m(t_0), \psi_m(t)$	Mean curvature at time $t_0$ and $t$



## CHAPTER 1

### INTRODUCTION

#### 1.1 Background

A structure or a part of a structure, reaches a limit state when it becomes incapable of fulfilling its function or when it no longer satisfies the conditions for which it was designed. Two categories of limit state normally have to be considered, ultimate limit states corresponding to failure or collapse and serviceability limit states at which deflection and cracking become excessive. The basic aim of structural design is to ensure that a structure should fulfill its intended function throughout its life time without excessive deflection and cracking or collapse and this aim must of course be met with due regard to economy and durability. Modern structural engineering tends to produce more economic structures through gradually improved methods of design and the use of higher strength materials. There is tendency among designers to produce thinner sections. As for slabs a slight decrease in thickness may save huge volume of concrete and the dead load of structure also reduces significantly. However, the designer must not forget the possibilities of excessive deflection and cracking associated with thinner slabs. Generally different codes ensure serviceability through minimum thickness provisions. The ACI Code (1963, 2002) suggests guidelines for selecting thickness of two-way edge supported slabs. However, these guidelines are for normal range of loading and geometric parameters. The designer may want to use thinner slabs without jeopardizing serviceability in situations where load is small. Use of thinner slabs is also permitted by ACI Code as long as deflections are calculated and within tolerable limits. At the same time situation may arise where ACI Code thickness may not be adequate. In such conditions, it is important to predict short and long-term deflections accurately to ensure serviceability limit state design.

## **1.2 Scope and Objectives of the Research Work**

Two-way edge supported slabs are very common types of slab. Sometimes it is important for the designer to estimate the deflection accurately to ensure serviceability conditions. However, reinforced concrete is not elastic, homogenous, isotropic material as required by linear slab theories. Concrete possesses a comparatively low tensile strength and reinforced concrete slabs contain cracks even in service load range. Long-term deflections are also affected by creep and shrinkage of concrete. The finite element methods to numerically model slab deflections are complicated and time consuming. The main aim of this work is to develop an easy method of deflection estimation. To achieve this goal the objectives are set as follows:

- To model numerically the deflection behavior of two-way edge supported slabs considering cracking.
- To carry out a parametric study to identify effects of different material and geometric parameters on deflection.
- To produce a set of design charts which will be useful in prediction of deflection.
- To calculate long-term deflections using ACI multiplier approach.
- To study the adequacy of ACI minimum thickness provisions.

It is hoped that with the successful completion of the work, it would be possible for the designer to estimate the short- and long-term deflections of slabs using simplified design charts. A reasonable prediction of deflection will help the designer to choose the slab thickness needed from serviceability point of view.

## **1.3 Outline of the Thesis**

The thesis consists of 7 chapters and 1 appendix, which are outlined in this section.

**Chapter 1-** General background to the research program and summary of aims and objectives.



**Chapter 2-** Behavior of edge supported slabs; deflection calculation methods by uncracked and cracked models, and long-term deflection by ACI method and MC-90 methods are discussed. Deflection due to creep and shrinkage are pointed out. Restraint cracking, construction load, deflection control and permissible deflection limits are discussed.

**Chapter 3-** Elastic analysis of different edge supported slabs are performed using softwares FE-77 and ANSYS and results are compared. Moment coefficients and deflection coefficients of edge supported slabs are calculated and proposed for calculation of elastic deflection. Moment coefficients are also compared with ACI moment coefficients.

**Chapter 4-** Hossain's (1999) nonlinear FE module is discussed for calculation of immediate deflection of edge supported slab considering cracking. The performance of this model is verified against experimental results. A thorough parametric study is carried out to identify the effects of different material and geometric parameters on immediate deflections of edge supported slab.

**Chapter 5-** Nine sets of design charts are proposed for calculation of immediate deflection of slabs with nine different boundary conditions. The calculation procedures of elastic and immediate deflection of edge supported slab are discussed with example.

**Chapter 6-** Long-term deflection calculation of edge supported slabs with the help of FE-77 analysis and also with the design charts are discussed. The adequacy of ACI minimum thickness of slab is also studied.

**Chapter 7-** Conclusions and recommendations for future work are presented.

**Appendix A-** Deflection ratio vs. stress ratio curves of two-way edge supported slabs without consideration of restraint cracking.

## CHAPTER 2

### LITERATURE REVIEW

#### 2.1 Introduction

Reinforced concrete slabs are relatively thin, flat, structural elements, whose main function is to transmit load normal to their plane. In strength design, the members are so proportioned that they will have a proper safety margin against failure under a hypothetical overload state. It is also important that the member performance in normal service be satisfactory. This performance, termed as serviceability, is not guaranteed simply by providing adequate strength. Service load deflection under full load may be excessively large, or long-term deflections due to sustained load may cause damage to partition walls. There are other serviceability related problems like visually disturbing wide tension cracks, vibrations causing discomfort etc.

In the past, questions of serviceability were dealt with indirectly, by limiting the stresses in concrete and steel at service loads to the rather conservative values that had resulted in satisfactory performance. Now, with strength design methods in general use that permit more slender members through more accurate assessment of capacity, with higher strength materials further contributing to the trend toward smaller member sizes, such indirect method will no longer do. ACI Code (2002) proposes minimum slab thickness to ensure serviceability and at the same time allows thinner slabs if deflection calculation permits so. ACI Code also provides a simple deflection calculation procedure.

## 2.2 Behavior of Edge Supported Slab

Engineers sometimes attempt to visualize the response of slab to loading by imagining them to behave as a system of beams, and this can sometimes lead to features being overlooked. Slabs are surprisingly difficult structures to analyze, and solutions are often too complicated for important aspects of behavior to be immediately apparent.

If individual loads are considered first, it is apparent that a concentrated load on a slab supported on its edge is likely to create a zone of sagging moments about its point of application. When a portion of a slab is bent about any axis, Poisson's ratio effect causes a curvature, of opposite sign to the main bending curvature, about the orthogonal axis. Thus, application of equal and opposite couples about two edges causes a saddle shape to form. This effect and the inherent torsional stiffness, produces a tendency for slab to lift off support at corners. In Fig. 2.1, a corner of a slab resting on two walls is shown. The deflection profile on diagonal A-A' due to loading is compared with that of a series of beams. If uplift is prevented, hogging moments are created in the corner zone of the slab, and top steel is required to prevent excessive cracking.

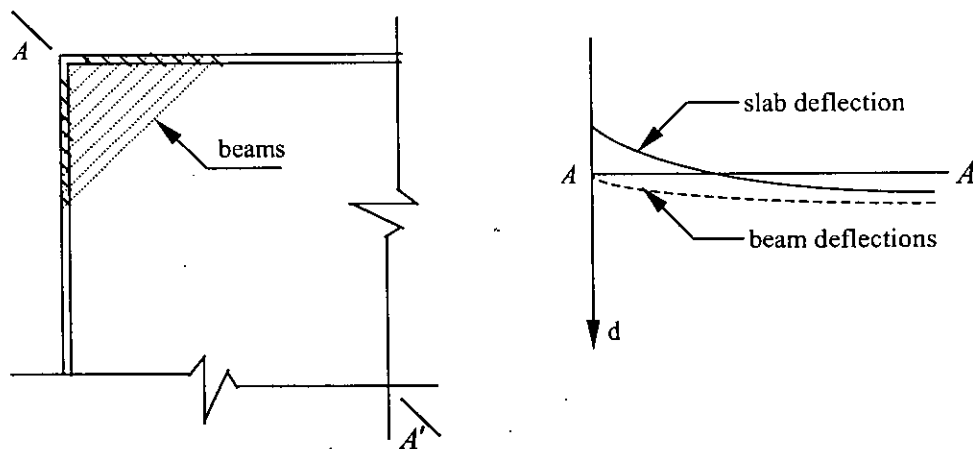
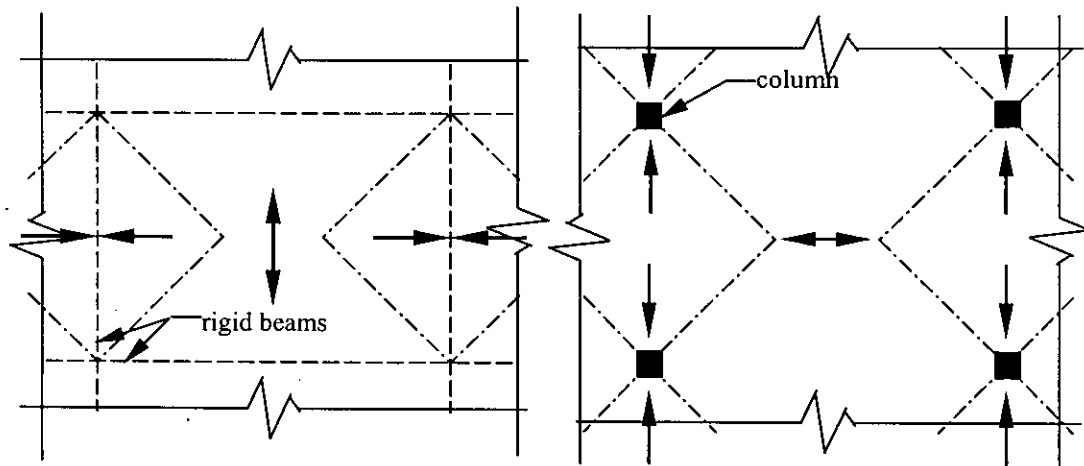
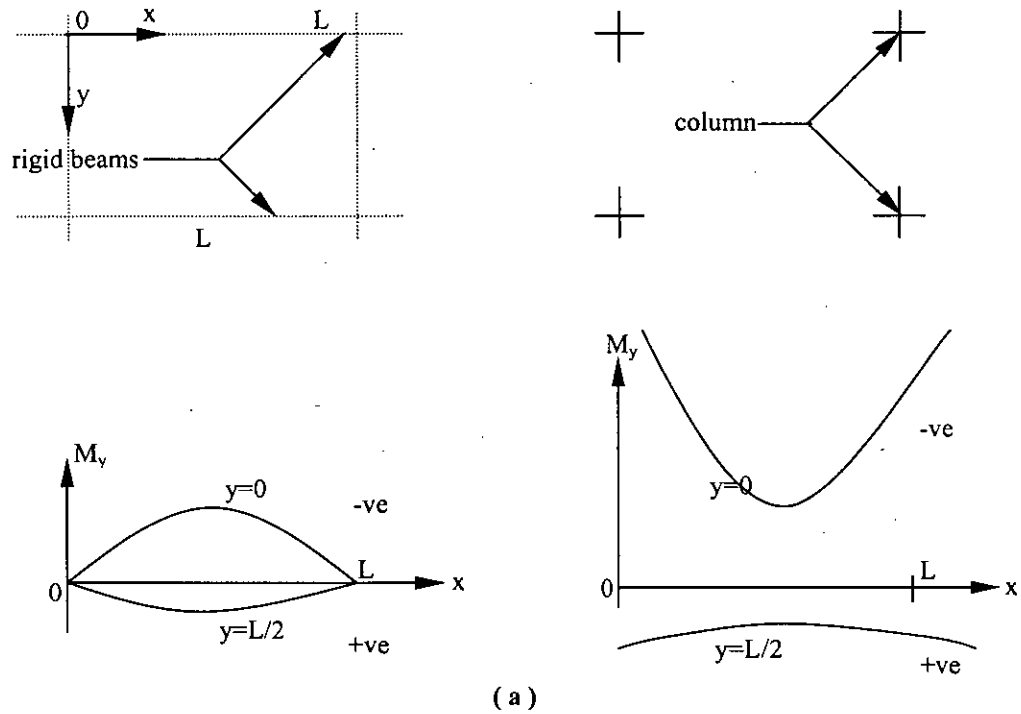


Figure 2.1 Slab action at a corner.

Because of the complicated nature of slab action, the distribution of load to the supporting structural system can differ substantially from that of a set of beams. In addition, although the reactions of the beams are statically determinate, those from the slab are not and their values can be very sensitive to the stiffness of the bearings provided.

The distribution of load in a panel of a large slab depends greatly on the nature of the supporting structural system. In Fig. 2.2, the bending moment distribution on the center and the support lines of square panels of two large slabs subjected to a uniform loading and supported on regular grids are compared. For the first slab the supports on the grid lines are stiff beam or walls, and the maximum moments occur in the center regions, between the support lines. For the second slab, which is supported on columns at the intersections of the grid lines, the maximum moments occur in the vicinity of the grid lines. For rectangular panels, slabs supported on stiff beams span primarily between the long beams, but the same panels supported on a grid columns span primarily in the long direction, and the transverse moments are confined to a limited width either side of the grid lines.

The largest moment in the edge supported slab occurs at midspan of the short strip and that moment reduces proportionately at the edge strip. The variation of moment in long strip is similar. These variations in maximum moment across the width and length of a rectangular slab are accounted for in an approximate way in most practical design methods by designing for a reduced moment in the outer quarter of the slab in each direction. In the edge strips the design moment is assumed to decrease from its full value at the edge of the middle strip to one-third of this value at the edge of the panel. This distribution is shown for the moments  $M_a$  in the short span direction and  $M_b$  in the long span direction in Fig. 2.3.



**Figure 2.2** Comparison of panels on beam and columns (a) Slab panels on rigid beams and columns; (b) load distribution in rectangular panels; adapted from Cope & Clark (1984)

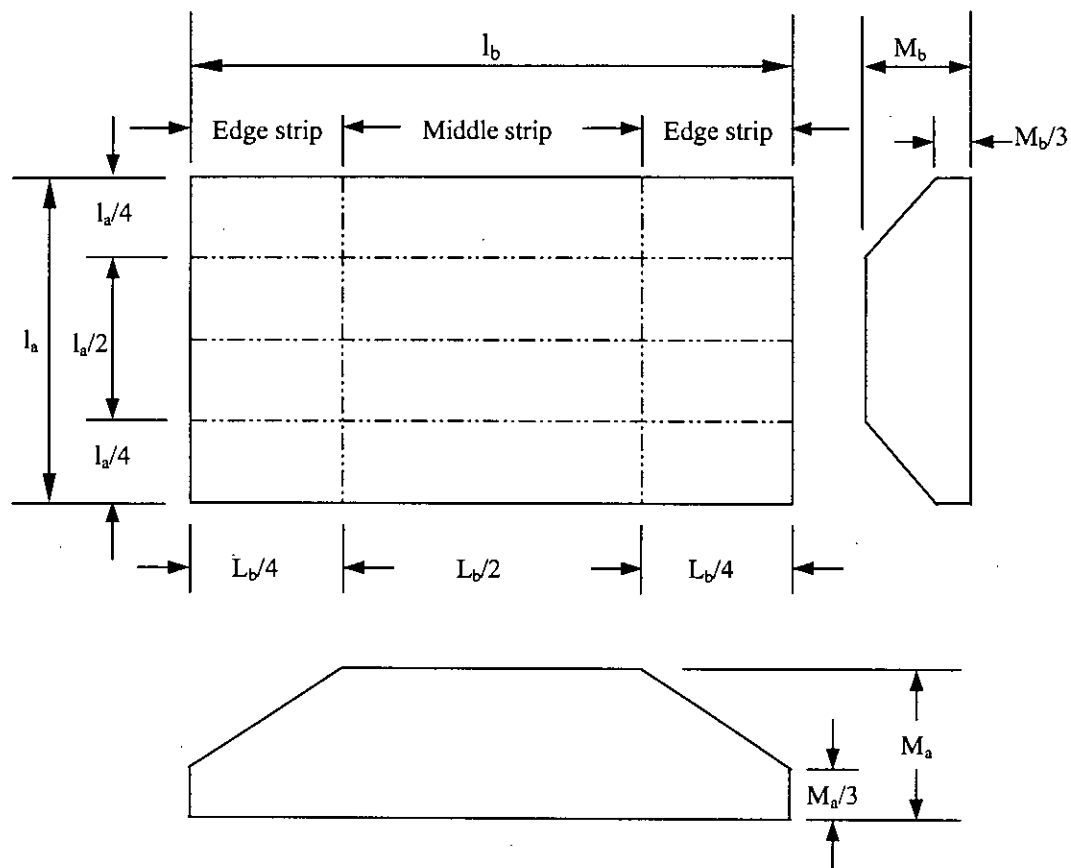


**Figure 2.3** Variation of moments across the width of critical sections assumed for design.

### 2.3 Serviceability

In strength design methods members are so proportioned that they will have a proper safety margin against failure in flexure or shear, or due to inadequate bond and anchorage of the reinforcement. The member is assumed to be in a hypothetical overload state for this purpose. It is also important that member performance in normal service be satisfactory, when loads are those actually expected to act, i.e. when load factors are 1. This is not guaranteed simply by providing adequate strength. Service load deflections under full load may be excessively large, or long-term deflections due to sustained loads may cause damage. Tension cracks in beams may be wide enough to be visually disturbing, or may even permit serious corrosion of reinforcing bars. This and other questions, such as vibration or fatigue, require

consideration. Serviceability studies are carried out based on elastic theory, with stresses in both concrete and steel assumed to be proportional to strain. The concrete on the tension side of the neutral axis may be assumed uncracked, partially cracked, or fully cracked, depending on the loads and material strengths.

Two approaches can be applied to the problem of control of serviceability by deflection:

- (a) Direct control method through the prediction of deflection by mathematical computations. The slab or plate relative stiffness can be so proportioned that the predicted deflection falls within acceptable limit.
- (b) Indirect control method through the limitation of the geometry to qualitatively accepted values of the span-to-depth ratios.

The second approach is expectedly more conservative in many instances, while the first approach requires more effort on the part of the designing engineer.

## **2.4 Deflection Calculation by Uncracked Model**

The calculation procedures of elastic deflection of edge supported slab are discussed in this section. The analytical methods for calculation of elastic deflection are briefly discussed. From finite element analysis the elastic deflection of slab can also be calculated.

### **2.4.1 Simpson's Method**

This method is applicable only for simply supported rectangular plates under various loadings. For uniformly distributed load, the maximum deflection occurs at the center of the plate and deflects symmetrically. Due to complicated mathematical equations this is difficult to use. Details can be obtained from Ugural (1999).

### **2.4.2 Navier's Solution for Simply Supported Rectangular Plates**

This method is applicable for simply supported rectangular plates under various kinds of loadings. This approach was introduced by Navier in 1820. Solution of the

bending problem employs the Fourier series for load and deflection. Details of this method is described in Ugural (1999).

### 2.4.3 Levy's Solution for Rectangular Plate

The Levy's method is applicable to the bending of rectangular plates with particular boundary conditions on the two opposite sides and arbitrary conditions of support on the remaining edges. To overcome the difficulty of Navier's solution an important approach was developed by M. Levy in 1900. Details can be obtained from Ugural (1999).

### 2.4.4 The Strip Method

The strip method is a simple approximate approach, for computing deflection and moment in a rectangular plate with arbitrary boundary conditions. In this method, the plate is assumed to be divided into two systems of strips at right angle to one another, each regarded as functioning as a beam. The method permits qualitative analysis of the plate behavior with ease but is less adequate, in general, in obtaining accurate quantitative results. However, that because this method always gives conservative values for both deflection and moment, it is often employed in practice. Details of the strip method can be obtained from Ugural (1999).

### 2.4.5 Deflection of Two-way Slab by Lagrange Equation

The classical theory of elasticity- assuming thin plates of constant thickness, small deflections and low stress levels- has expressed the deflection relationship as a Lagrangian equation:

$$\frac{\partial^4 a}{\partial x^4} + 2 \frac{\partial^4 a}{\partial x^2 \partial y^2} + \frac{\partial^4 a}{\partial y^4} = \frac{w}{D} \quad (2.1)$$

where,

a = deflection of the plate

w = transverse load per unit area

D = flexural rigidity per unit width =  $\frac{Eh^3}{12(1-\nu^2)}$



Finite difference method can be used to solve the above differential equation to get deflections of slabs.

#### 2.4.6 Finite Element Method

In this method, the slab is divided into a number of subregions or finite elements, which are generally triangular, rectangular or quadrilateral in shape. They are considered interconnected only at discrete points, called nodes, at the corners of the individual elements. The continuous displacement quantities are expressed in terms of a finite number of displacements  $w(x, y)$ , called degrees of freedom at the nodes. Therefore, for a rectangular plate bending element having 12 degrees of freedom, for instance,

$$[F] = [K][D] \quad (2.2)$$

where,

$[D]$  =  $12 \times 1$  column vector consisting of vertical displacements and rotations about each horizontal axis of each of the four corners.

$[K]$  =  $12 \times 12$  element stiffness matrix relating nodal forces and the corresponding displacements.

$[F]$  =  $12 \times 1$  column vector consisting of transverse forces and bending moments at the nodes.

The main problem in the application of the finite element method to linear elastic slab systems in general is to obtain a suitable force-displacement relationship between the nodal forces and the corresponding displacements at the nodal degrees of freedom. A further complication, in applying the method to reinforced concrete, is the derivation of a suitable set of constitutive relations to model the slab behavior under various loading conditions.

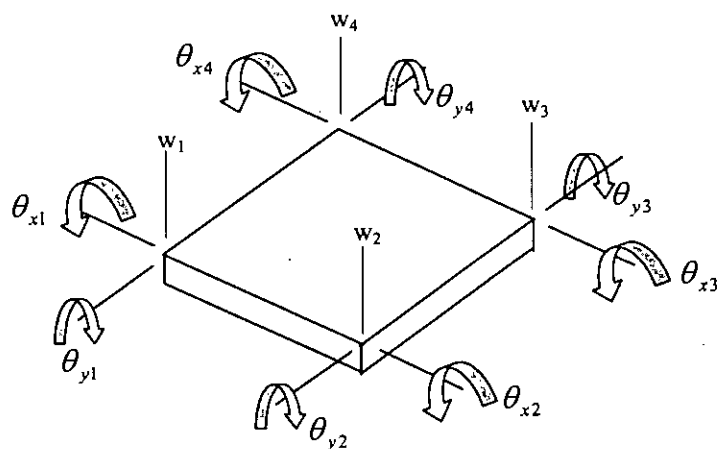


Figure 2.4 Typical plate bending element with 12 degrees of freedom.

## 2.5 Deflection Calculation by Cracked Model

In normal service load most of the edge supported slabs are cracked because of the stresses greater than modulus of rupture of concrete. In this situation the instantaneous slab deflection (termed as immediate deflection) will be excess than elastic deflection. The calculation methods of immediate deflection are discussed in this section.

### 2.5.1 ACI Method Using Branson's Crack Model

Elastic deflections can be expressed in the general form

$$\Delta = \frac{f(\text{loads, spans, support})}{EI} \quad (2.3)$$

where,  $EI$  is the flexural rigidity and  $f(\text{loads, spans, supports})$  is a function of the particular load, span, and support arrangement. The particular problem in reinforced concrete structures is therefore the determination of the appropriate flexural rigidity  $EI$  for a member consisting of two materials with properties and behavior as widely different as steel and concrete.

If the maximum moment in a flexural member is so small that the tension stress in the concrete does not exceed the modulus of rupture  $f_r$ , no flexural tension cracks will occur. The full, uncracked section is then available for resisting stress and providing rigidity. The effective moment of inertia for this low range of loads is that of the uncracked, transformed section  $I_{ut}$ , and  $E_c$  is the modulus of elasticity of concrete. For this load range, the elastic deflection is

$$\Delta_{iu} = \frac{f}{E_c I_{ut}} \quad (2.4)$$

At higher loads, flexural tension cracks are formed. In addition, if shear stresses exceed and web reinforcement is employed to resist them, diagonal cracks can exist at service loads. In the region of flexural cracks the position of the neutral axis varies: directly at each crack it is located at the level calculated for the cracked, transformed section; midway between cracks it dips to a location closer to that calculated for the uncracked transformed section. Correspondingly, flexural-tension cracking causes the effective moment of inertia to be that of the cracked transformed section in the immediate neighborhood of flexural-tension cracks, and closer to that of the uncracked transformed section midway between cracks, with a gradual transition between these extremes.

It is seen that the value of the local moment of inertia varies in those portions of the beam in which the bending moment exceeds the cracking moment of the section

$$M_{cr} = \frac{f_r I_{ut}}{y_t} \quad (2.5)$$

where  $y_t$  is the distance from the neutral axis to the tension face and  $f_r$  is the modulus of rupture. The exact variation of  $I$  depends on the shape of the moment diagram and on the crack pattern, and is difficult to determine. This makes an exact deflection calculation impossible.

Branson (1976), (1977) proposed an equation for calculation of effective moment of inertia between uncracked and fully cracked section of a simple beam considering tension stiffening. ACI 318-02 (2002) proposed that, for the calculation of deflection immediately after application of load, an effective value of moment of inertia using

Branson's equation should be used. ACI Code used a power  $n = 3$  in Branson's equation:

$$I_{eff} = \left(\frac{M_{cr}}{M_a}\right)^n I_{ut} + \left[1 - \left(\frac{M_{cr}}{M_a}\right)^n\right] I_{cr} \quad \text{and} \quad I_{ut} \quad (2.6)$$

where,

$I_{ut}$  = moment of inertia of the gross uncracked concrete section

$I_{cr}$  = moment of inertia of the cracked transformed concrete section

$M_{cr}$  = cracking moment of the reinforced concrete beam

$M_a$  = maximum values of bending moment in the span

Extensive documented studies (Branson, 1977) have shown that deflections of beam as well as slab are reasonably predicted by Branson's equation:

$$\Delta_{ic} = \frac{f}{E_c I_{eff}} \quad (2.7)$$

### 2.5.2 Nilson's Approach

Nilson (1997) has presented deflection calculation procedure of edge supported slab. Edge supported slabs are typically thin relative to their span, and may show large deflections even though strength requirements are met, unless certain limitations are imposed in the design to prevent this. The calculation of deflections for slab is complicated by many factors, such as the varying rotational restraint at the edges, the influence of alternative loading arrangements, varying ratio of side length, and the effects of cracking, as well as the time-dependent influences of shrinkage and creep. However, the deflection of an edge supported slab can be estimated with reasonable accuracy, based on the moment coefficients used in the flexural analysis. The deflection components of concern are usually the long-term deflections due to sustained loads and the immediate deflection due to live load.

Maximum live load deflection will be obtained when the live load acts on the given panel, in a checkerboard pattern. Therefore, live load deflection should be based on the maximum positive moments found corresponding to that loading arrangement, together with statically consistent negative moments at the supported edges.

This will be illustrated for the slab in Fig. 2.5a, considering the middle strip of unit width in the long direction of the panel. The variation of moment for a uniformly distributed load is parabolic, and the sum of the positive and average negative moments must be

$$M = \frac{1}{8} w_b l_b^2 \quad (2.8)$$

where,  $w_b$  is the fractional part of the load transmitted in the long direction of the panel (Fig. 2.5c). If full fixity were obtained at the supports, the negative moment is

$$M_{neg} = \frac{1}{12} w_b l_b^2 = \frac{2}{3} M \quad (2.9)$$

and the positive moment is

$$M_{pos} = \frac{1}{24} w_b l_b^2 = \frac{1}{3} M \quad (2.10)$$

The coefficients for maximum live load positive moments are derived assuming 50 percent fixity. The maximum positive moment  $M_b$  as obtained, shown in Fig. 2.5c, and the statically consistent negative moments are one-half the positive moment  $M_b$ .

Deflection calculations are thus based on the parabolic moment diagram, with maximum ordinate  $M_b$  at mid span and negative end moments one-half of that value.

The midspan live load deflection,  $\Delta_l$ , of the slab strip shown Fig. 2.5b, can be found based on the moment diagram of Fig. 2.5c. For the slab with both edges continuous,

$$\Delta_l = \frac{3}{32} \frac{M_b l_b^2}{E_c I_{eff}} \quad (2.11)$$

where  $M_b$  = Maximum positive live load moment

$E_c$  = Modulus elasticity of concrete

$I_{eff}$  = Effective moment of inertia of the concrete cross section of unit width

$\Delta_l$  = Mid span live load deflection

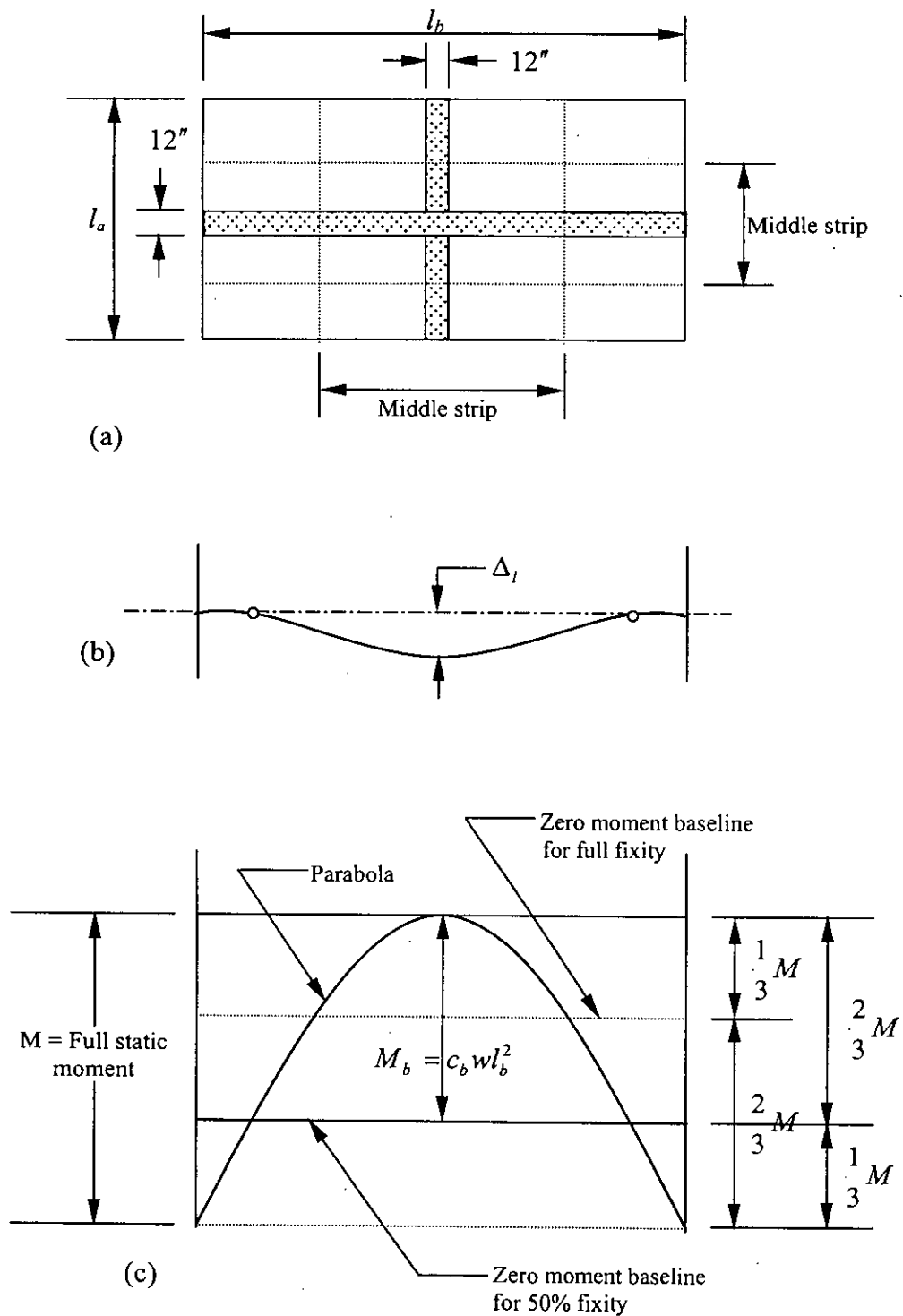


**Figure 2.5** Live load deflection analysis: (a) plan of slab; (b) deflection curve for unit strip; (c) diagram for maximum positive live load moment.

For the special case of slab where edges are completely free of restraint, the mid span deflection is

$$\Delta_l = \frac{5 M_b I_b^2}{48 E_c I_{eff}} \quad (2.12)$$

The dead load deflection is based on the moment diagram found using maximum dead load positive moment assuming all panels are loaded. The mid span dead load deflection  $\Delta_d$ , for both ends continuous, is

$$\Delta_d = \frac{1 M_b I_b^2}{16 E_c I_{eff}} \quad (2.13)$$

where,  $M_b$  is the dead load positive moment. For the special case where both ends are free of restraint, the midspan dead load deflection is

$$\Delta_d = \frac{5 M_b I_b^2}{48 E_c I_{eff}} \quad (2.14)$$

### 2.5.3 Gilbert Crack Model

Gilbert (1983), (1988) proposed an approach for modeling tension stiffening. An area of concrete located at the tensile-steel level is assumed to be effective in providing tension stiffening. Figure 2.6 shows an average cross-section of a singly reinforced member. Like the other tension stiffening models, the properties of this average cross-section are between those of the fully cracked section and the uncracked cross-section between the primary cracks. The tensile concrete area  $A_{ct}$ , which is assumed to contribute to the flexural stiffness after cracking, depends on the magnitude of the maximum applied moment  $M$ , the area of tensile reinforcement  $A_{st}$ , the amount of concrete below the neutral axis, the tensile strength of concrete (i.e. the cracking moment  $M_{cr}$ ), and the duration of the sustained load.

Based on short-term test results, the following empirical formula for  $A_{ct}$  was proposed:

$$A_{ct} = \beta_1 \beta_2 [0.21 b_w d - n A_{sn}] \left( \frac{M_{cr}}{M} \right)^2 \quad (2.15)$$

where,  $\beta_1 = 1$  and 0.5 for high bond bars and for plain bars, respectively. According to EC2-91 (1991),  $\beta_2 = 0.8$  and 0.5 for first loading and for loads applied in a

sustained manner (or for a large number of load cycles), respectively. When  $M < M_{cr}$ , the term  $(M_{cr}/M)$  in Eqn. (2.15) is taken as unity.

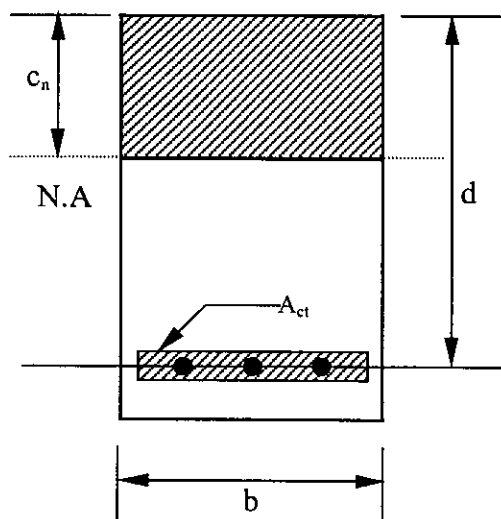


Figure 2.6 Gilbert model: adapted from Gilbert (1988)

#### 2.5.4 Polak Approach

Polak (1996) has adapted a detailed finite element formulations based on the layered approach. The layered approach, through the rigorous treatment of the states of strain and stress can model complex behavior of both thin and thick plates. The results of finite element effective stiffness analyses are compared to both experimental results and the results in the layered analyses. Polak commends that the layered approach is a detailed, versatile and comprehensive approach to modeling nonlinear behavior of members subjected to bending. And the effective stiffness approach is simpler and less time consuming. For typical slab systems, the effective stiffness formulations can provide results with accuracy comparable to the accuracy of the layered approach.

Polak modified the materials stiffness as follows:



$$[D]=\begin{bmatrix} \frac{E_x h^3}{12(1-\nu_x \nu_y)} & \frac{\nu_x E_y h^3}{12(1-\nu_x \nu_y)} & 0 & 0 & 0 \\ \frac{\nu_y E_x h^3}{12(1-\nu_x \nu_y)} & \frac{E_y h^3}{12(1-\nu_x \nu_y)} & 0 & 0 & 0 \\ 0 & 0 & \frac{G_1 h^3}{12} & 0 & 0 \\ 0 & 0 & 0 & G_2 h & 0 \\ 0 & 0 & 0 & 0 & G_3 h \end{bmatrix} \quad (2.16)$$

where, cracked shear moduli of concrete

$$G_1 = G \alpha_x \alpha_y$$

$$G_2 = G \alpha_x$$

$$G_3 = G \alpha_y$$

$$\text{where, } \alpha_x = \frac{I_{ex}}{I_{gx}} \quad (2.17)$$

$$\alpha_y = \frac{I_{ey}}{I_{gy}}$$

$E_x, E_y$  = reduced Young's moduli of cracked concrete in x and y-directions

$t$  = element thickness

$\nu_x, \nu_y$  = reduced Poisson's ratios of cracked concrete on x and y-directions.

Polak also checked the sensitivity of the proposed formulation when applied to the analysis of slabs with different reinforcement ratios, boundary conditions, and reinforcement orientations.

### 2.5.5 Scanlon and Murraray Approach

Scanlon & Murraray (1982) proposed an FE method to model cracking in reinforced concrete slabs. The method utilized a secant-stiffness formulation and used a modified anisotropic plane-stress relationship to include the effect of cracking. Specialized for orthotropy, the stress-strain relationships are expressed by:

$$\begin{Bmatrix} \sigma_x \\ \sigma_y \\ \tau_{xy} \end{Bmatrix} = \begin{bmatrix} \frac{E_x}{(1-\nu_x\nu_y)} & \frac{\nu_x E_y}{(1-\nu_x\nu_y)} & 0 \\ \frac{\nu_y E_x}{(1-\nu_x\nu_y)} & \frac{E_y}{(1-\nu_x\nu_y)} & 0 \\ 0 & 0 & G_{xy} \end{bmatrix} \begin{Bmatrix} \varepsilon_x \\ \varepsilon_y \\ \gamma_{xy} \end{Bmatrix} \quad (2.18)$$

Moment-curvature relationships are obtained by integrating over the slab depth to obtain:

$$\begin{Bmatrix} M_x \\ M_y \\ M_{xy} \end{Bmatrix} = \begin{bmatrix} \frac{E_x h^3}{12(1-\nu_x\nu_y)} & \frac{\nu_x E_y h^3}{12(1-\nu_x\nu_y)} & 0 \\ \frac{\nu_y E_x h^3}{12(1-\nu_x\nu_y)} & \frac{E_y h^3}{12(1-\nu_x\nu_y)} & 0 \\ 0 & 0 & \frac{G_{xy} h^3}{12} \end{bmatrix} \begin{Bmatrix} \psi_x \\ \psi_y \\ \psi_{xy} \end{Bmatrix} \quad (2.19)$$

Based on the analysis of the uncracked slab, moments in  $x$  and  $y$  directions,  $M_x$  and  $M_y$ , can be calculated for each element.

Scanlon & Murraray (1982) used the Branson's (1977) equations (Eqn. 2.6) with power  $n = 3$  to calculate the reduced flexural second moment of area in both  $x$  and  $y$  directions. Reduction in flexural stiffness in each direction can be accounted for using the ACI Building Code equation (Eqn. 2.6) in both  $x$  and  $y$  directions:

$$I_{ex} = \left( \frac{M_{cr}}{M_x} \right)^3 I_g + \left[ 1 - \left( \frac{M_{cr}}{M_x} \right)^3 \right] I_{crx} \quad (2.20)$$

$$I_{ey} = \left( \frac{M_{cr}}{M_y} \right)^3 I_g + \left[ 1 - \left( \frac{M_{cr}}{M_y} \right)^3 \right] I_{cry}$$

where,  $M_{cr}$  can be obtained from Eqn. (2.5). Material properties are modified as follows to reflect the reduction in stiffness due to cracking:

$$\begin{aligned} E_x &= \alpha_x E_c \\ E_y &= \alpha_y E_c \end{aligned} \quad (2.21)$$

$$v_x = \alpha_x v$$

$$v_y = \alpha_y v$$
(2.22)

where,

$$\alpha_x = \frac{I_{ex}}{I_{gx}}$$

$$\alpha_y = \frac{I_{ey}}{I_{gy}}$$
(2.23)

The analysis is then repeated using the reduced elastic constants until a stable condition is achieved. Scanlon & Murrery (1974) expected some reduction in effective shear modulus due to cracking. However, they used the uncracked value of shear modulus in the analysis before and after cracking since, according to them, a quantitative reduction is difficult due to the effects of dowel action and aggregate interlock. Tam & Scanlon (1986) also used an uncracked value of shear modulus in their analysis.

### 2.5.6 Jofriet and McNeice Approach

Jofriet & McNeice (1971) presented an FE method using a bilinear moment-curvature relationship based on Branson's (1977) equation. The approach used a tangent-stiffness formulation. The Branson formula does not yield directly the tangent-stiffness rigidity of a region after cracking but rather the secant rigidity. Using a least-square fit, an equivalent tangent-stiffness equation was proposed. Before cracking, the uncracked rigidity was defined by

$$R_u = E_c I_u$$
(2.24)

in which  $E_c$  = modulus of elasticity of concrete and  $I_u$  = the moment of inertia of the cross-section including the effect of reinforcement. After cracking, the rigidity was approximated as

$$R_c = \frac{(r-1)I_g I_{cr}}{rI_g - I_{cr}} E_c$$
(2.25)

in which  $r$  = a factor that is related to the reinforcing steel percentage,  $\rho$ .  $I_{cr}$  is the moment of inertia of the fully cracked transformed section given by

$$I_{cr} = \frac{1}{3}c_n^3 + \rho nd(d - c_n)^2 \quad (2.26)$$

where  $c_n$  is the depth of the neutral axis defined as

$$c_n = d \left[ \sqrt{2\rho n + (\rho n)^2} - \rho n \right] \quad (2.27)$$

### 2.5.7 Hossain's Model

Hossain (1999) has developed a nonlinear finite element (NLFE) module to calculate the deflection of reinforced concrete slabs which is based on a global plate stiffness approach. The program is novel since it incorporates an incremental approach to calculate deflections due to a time-varying load. The global plate stiffness approach was adopted, rather than the more complex and time-consuming layered element approach, since work by others including Polak (1996) suggests that the accuracy of both methods is comparable. The global plate stiffness approach has the added benefit of being consistent with the methods given in MC-90 (1990) and EC2 (1992) for calculating the curvature of cracked sections. This model is used in the current work and will be discussed in detail in Chapter 4.

### 2.6 Long-term Deflection

Initial deflections are increased significantly if loads are sustained over a long period of time, due to the effects of shrinkage and creep. These two effects are usually combined in deflection calculation. Creep generally dominates, but for some types of members, shrinkage deflections are large and should be considered separately. Creep deformations are directly proportional to the compressive stress up to and beyond the usual service load range. They increase asymptotically with time and, for the same stress, are larger for low-strength than for high-strength concretes.

Long-term deflection due to creep and shrinkage are influenced by many variables, including load intensity, mix components, mix proportions, age of slab at first loading, curing conditions, presence of compressive reinforcement, relative humidity

and temperature. While time-dependent deflection of slabs has not been studied extensively, it is generally known that time-dependent deflections may be about two to three times initial elastic deflections (Yu and Winter, 1960), and often result in unsatisfactory service load performance. Time-dependent deflection of a reinforced concrete beam in flexure at any time,  $t$ , is given by

$$\Delta(t, t_0) = \underbrace{\Delta_D(0) + \Delta_L(0)}_{\text{short-term deflection}} + \underbrace{\Delta_D^c(t, t_0) + \Delta_L^c(t, t_0) + \Delta^s(t, t_0)}_{\text{time-dependent deflection}} \quad (2.28)$$

*dead load*      *live load*      *creep deflection due to dead load, and sustained live load*      *warping due to shrinkage*

The ultimate deflection with respect to time is obtained by substituting ultimate values of creep and shrinkage into the time-dependent terms.

### 2.6.1 ACI Method

Deflection estimation procedure in ACI Code (2002) is simple where long-term deflections are calculated from instantaneous deflection by using multiplier. ACI Code 9.5.2 specifies that additional long-term deflections  $\Delta_l$ , due to the combined effects of creep and shrinkage shall be calculated by multiplying the immediate deflection  $\Delta_i$  by the factor

$$\lambda = \frac{\xi}{1 + 50\rho'} \quad (2.29)$$

where,  $\rho' = \frac{A'_s}{bd}$  and  $\xi$  is a time-dependent coefficient that varies from 0 to 2.

In Eqn. (2.29) the quantity  $\frac{1}{(1 + 50\rho')}$  is a reduction factor that is essentially a section property, reflecting the beneficial effect of compression reinforcement  $A'_s$  in reducing long-term deflections, whereas  $\xi$  is a material property depending on creep and shrinkage characteristics. For simple and continuous span, the value of  $\rho'$  used in Eqn. (2.29) should be that at the mid section, according to the ACI Code, or that at the support for cantilevers.

Values of  $\xi$  given in the ACI Code and Commentary are satisfactory for ordinary beams and one-way slabs, but may result in underestimation of time-dependent

deflections of two-way slabs, for which Branson (1977) has suggested a five-year value of  $\xi = 3.0$ .

### 2.6.2 Model Code 90, (MC-90) Method

MC-90 (1993) model gives method of deflection calculation considering the effects of cracking, shrinkage and creep. Curvatures are calculated in state 1 (reinforced concrete member is free from cracks) and state 2 (tensile stress of concrete member is assumed to be resisted entirely by reinforcement) considering reinforcement both in the tension and the compression zones. The curvature in state 1 at time of application of load,  $t_0$  is given by:

$$\psi_1(t_0) = \frac{M}{E_c(t_0)I_1} \quad (2.30)$$

where,

$M$  = principal moment

$E_c(t_0)$  = modulus of elasticity of concrete at time  $t_0$

$I_1$  = moment of inertia of uncracked transformed section around the centroid of the transformed section.

The curvature in state 2 at time  $t_0$  is given by:

$$\psi_2(t_0) = \frac{M}{E_c(t_0)I_2} \quad (2.31)$$

where,

$I_2$  = moment of inertia of cracked transformed section around the centroid of the transformed section and lies on the neutral axis.

When short-term deflection is of interest, the mean curvature is calculated using following equation:

$$\psi_m(t_0) = (1 - \zeta)\psi_1(t_0) + \zeta\psi_2(t_0) \quad (2.32)$$

where,

$$\zeta = 1 - \beta_1\beta_2 \left( \frac{M_r}{M} \right)^2 \quad (2.33)$$

The method proposed by MC-90 (1993) and EC2-91 (1991) to calculate the mean short-term curvature can also be extended to calculate long-term curvatures. The

additional curvature due to creep and shrinkage can be calculated using the approach by Ghali & Frave (1994) described below combined with the curvatures for states 1 and 2 according to MC-90 (1993) approach at time  $t$  which are given by

$$\psi_1(t) = \psi_1(t_0) + \Delta\psi_1 \quad (2.34)$$

$$\psi_2(t) = \psi_2(t_0) + \Delta\psi_2 \quad (2.35)$$

so that the mean curvature at time  $t$  is given by

$$\psi_m(t) = (1 - \zeta)\psi_1(t) + \zeta\psi_2(t) \quad (2.36)$$

where  $\zeta$  is given by Eqn. (2.33) with  $\beta_2 = 0.5$ .

## 2.7 Creep and Shrinkage

**Creep** is a property of continuing to deform over considerable lengths of time at a constant stress or load. The nature of creep process is shown in Fig. 2.7. Any workable concrete mix contains more water than is needed for hydration. If the concrete is exposed to air, the larger part of this free water evaporates in time, the rate and completeness of drying depending on ambient temperature and humidity conditions. As the concrete dries, it shrinks in volume, probably due to the capillary tension that develops in water remaining in the concrete. **Shrinkage**, which continues at a decreasing rate for several months, depending on the configuration of the member, is a detrimental property of concrete in several respects.

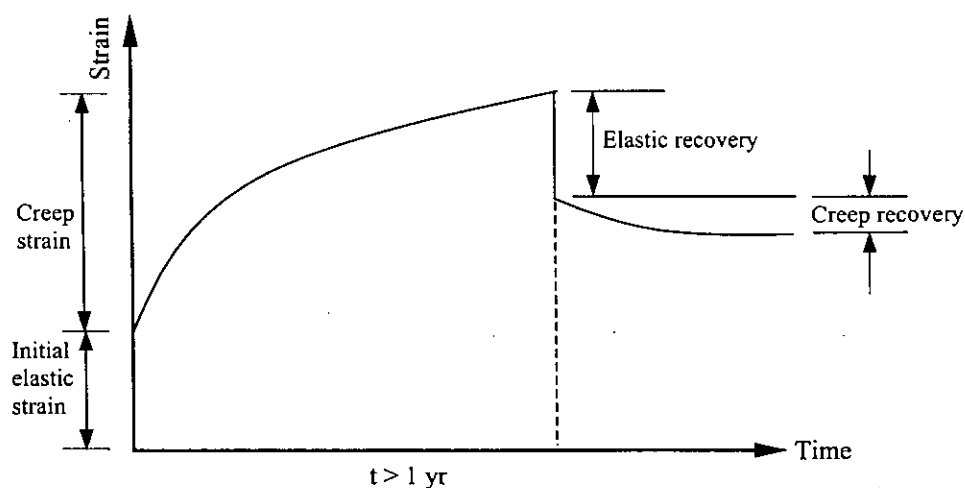


**Figure 2.7** Uniaxial time-dependent behavior of concrete: generalized representation

### 2.7.1 Creep and Shrinkage Coefficient

Deflections are a function of the age of concrete at the time of loading due to the long-term effects of shrinkage and creep, which significantly increase with time. ACI 435 (1978) suggested that the values for concrete ultimate creep coefficient and ultimate shrinkage strain can be estimated as 1.60 and  $400 \times 10^{-6}$ , respectively. These values correspond to the following condition:

- 70 percent average relative humidity
- Age of loading, 20 days for both moist and steam cured concrete
- Minimum thickness of component, 6 in. (152 mm)

ACI 209 (1971, 1982, 1992) recommended a time dependent model for creep and shrinkage under standard conditions as developed by Branson, Christianson, and Kripanarayanan (1971, 1977). The term "standard conditions" is defined for a number of variables related to material properties, the ambient temperature, humidity, and size of members.

### 2.7.2 Deflection Due to Creep

Two approaches are widely used (Kong *et al.*, 1983) for the determination of flexural deflection due to concrete creep. Both are based on a constant stress history, and both utilize short-time deflection as a measure of initial concrete strain. One approach utilizes the increased strain due to creep in combination with the initial strain,  $\epsilon_0$ , to define an effective modulus of elasticity,  $E'_c(t)$

$$E'_c(t) = \frac{\sigma_0}{\epsilon_0 [1 + \alpha(t, t_0)]} \quad (2.37)$$

where,  $\sigma(0)$  is the initial stress and  $\alpha(t, t_0)$  is the creep coefficient (ratio of creep strain to initial elastic strain) for concrete at time  $t$ , loaded at time  $t_0$ . Then, the effective modular ratio becomes

$$n'_c(t) = \frac{E_s}{E'_c(t)} = \frac{E_s}{E_c(t)} [1 + \alpha(t, t_0)] = n [1 + \alpha(t, t_0)] \quad (2.38)$$

The effective modulus and effective modular ratio may be used in lieu of  $E_c(t)$  and  $n(t)$  to predict the effects of creep.



An approach which has gained wide acceptance, both because of its ease of application and excellent correlation with experimental results, relates the creep effect to the short-time deflection as given in Eqn. (2.39):

$$y^c(t, t_0) = K_r^c \alpha(t, t_0) y(0) \quad (2.39)$$

where,  $K_r^c$  is a reduction factor empirically determined to relate creep strain to curvature.

According to Model Code 90 the creep strain expressed as follows:

Under sustained stress, the strain increases with time due to creep and the total strain-instantaneous plus creep at time  $t$  is:

$$\varepsilon_c(t) = \frac{\sigma_c(t_0)}{E_c(t_0)} [1 + \phi(t, t_0)] \quad (2.40)$$

where, the coefficient  $\phi$  represent the ratio of creep to the instantaneous strain; its value increases with the decrease of age at loading  $t_0$  and the increase of the length of the period  $(t - t_0)$  during which the stress is sustained. The value also depends on quality of concrete, ambient temperature and humidity as well as the dimension of the element considered.

The strain  $\varepsilon_c(t)$  is expressed in MC-90 by the equation:

$$\varepsilon_c(t) = \frac{\sigma_c(t_0)}{E_c(t_0)} \left[ 1 + \frac{E_c(t_0)}{E_c(28)} \phi_{CEB}(t, t_0) \right] \quad (2.41)$$

### 2.7.3 Deflection Due to Shrinkage

Deflection of beams due to shrinkage may be predicted from

$$y^s(t, t_0) = K_{sh} \phi_{sh}(t, t_0) L^2 \quad (2.42)$$

where,  $\phi_{sh}(t, t_0)$  is the curvature ( $M/EI$ ). The general practice is to assume that the reinforcing steel along the span is constant when determining  $K_{sh}$ . For continuous beams, the curvature is assumed to be the same value in the mid-span region (positive curvature for normal gravity type loading) and in the negative-curvature region near the end of the pans, with the inflection points arbitrarily taken at the span quarter points. Values of  $K_{sh}$  based on these conditions and using a constant

value of  $\phi_{sh}(t, t_0)$  (with approximate signs for negative curvature) are 0.125, 0.625, and 0.5 for a simply supported beam, fixed end beam, and cantilever beam, respectively.

According to Model Code 90 the shrinkage or swelling at any time  $t$  (days) may be estimated by:

$$\varepsilon_{cs}(t, t_s) = \varepsilon_{cs0} \beta_s(t - t_s) \quad (2.43)$$

where,  $\beta_s(t - t_s)$  is a function describing the development of shrinkage or swelling with time, given by:

$$\beta_s(t - t_s) = \left( \frac{t - t_s}{350(h_0/100)^2 + t - t_s} \right)^{0.5} \quad (2.44)$$

where,  $h_0$  (mm) is the notional size of the member,  $\varepsilon_{cs0}$  is the notional shrinkage.

## 2.8. Restraint Cracking

In two-way reinforced concrete slabs built monolithically with supporting column and wall elements, in-plane shortening due to shrinkage and thermal effects is restraint. The restraint is provided by a combination of factors, including embedded reinforcement, attachment to structural supports, and lower shrinkage rates of previously placed adjacent panels when slab panels are placed at different times. Nonlinear distribution of free shrinkage strains across the cross-section may also be a contributing factor.

Service load moments in two-way slabs are often of the same order of magnitude as the code-specified cracking moment,  $M_{cr}$ . Deflection calculations made using the code-specified modulus of rupture will often result in an uncracked section being used when cracking may actually be present due to a combination of flexural stress and restraint stress.

ACI 318 specifies the modulus of rupture for deflection calculations as  $0.62 \sqrt{f'_c}$  MPa ( $7.5 \sqrt{f'_c}$  psi). Laboratory test data, summarized in ACI 209R, indicate values ranging from  $0.5 \sqrt{f'_c}$  Mpa ( $6$  to  $12 \sqrt{f'_c}$  psi).

For slab sections with low reinforcement ratios, approaching minimum reinforcement, the difference between cracked and uncracked flexural stiffness is significant. It is important; therefore, to account for effects of any restraint cracking that may be present. Unfortunately, the extent of restraint cracking is difficult to predict. To account for restraint cracking in two-way slabs, Rangan (1976) suggested that column strip deflections be based on the moment of inertia of a fully cracked section,  $I_{cr}$ , and that middle strip deflections be based on  $(I_g + I_{cr})/2$ . Good agreement was reported between calculated and field measured deflections.

A more general approach was proposed by Scanlon and Murray (1982). They suggested that the effect of restraint cracking be included by introducing a restraint stress,  $f_{res}$ , that effectively reduces the modulus of rupture for calculating  $M_{cr}$ , i.e.

$$M_{cr} = \frac{f_e I_g}{y_t} \quad (2.45)$$

where,  $f_e = f_r - f_{res}$

A value of  $0.32 \sqrt{f'_c}$  MPa ( $4 \sqrt{f'_c}$  psi), or about half of the value specified in ACI 318, was proposed for the reduced effective modulus of rupture. This approach was investigated by Tam and Scanlon (1986) and has produced good correlation between calculated deflection and reported mean field-measured deflections [Jokinen and Scanlon 1985; Graham and Scanlon 1986(b)]. Ghali (1989) has also used the idea of reduced modulus of rupture and demonstrates the calculation of restraint stress due to reinforcement in the presence of uniform shrinkage.

An additional consideration is that the moments used in design for strength are based on some redistribution of moments. The distribution of design moments does not reflect the high peaks of moment adjacent to columns that occur in uncracked slabs.

Deflection calculations based on moment distributions used for design, therefore, tend to under-predict the effects of cracking.

For slab system in which significant restraint to in-plane deformations may be present, it is recommended by ACI Committee 435 (1991) that a reduced effective modulus of  $0.33\sqrt{f'_c}$  MPa ( $4\sqrt{f'_c}$  psi) be used to compute the effective moment of inertia,  $I_e$ . A procedure for implementing this approach in finite element analysis is given by Tam and Scanlon (1986).

## 2.9 Construction Load

Relatively high construction loads applied to young slabs with low tensile strengths and low elastic moduli will cause extensive flexural cracking and large initial deflection. The high applied stress/developed strength ratio may cause significant creep, generally non-recoverable, resulting in large long-term deflections. Construction loads on the lower slabs in the supporting assembly may often exceed the service loads regardless of the number of floors used to support the newly cast slabs unless appropriate construction methods are used. Sbarounis (1984a) suggested that, in fact, a certain combinations of design loads, slab thickness, and span the calculated overloads are close to the ultimate strength of the slabs. Construction loads are evidently related to the method of re-propping adopted and the number of floors which are back-propped. The following three systems of back-propping are used:

1. In low-rise buildings, floors can be continuously propped back to ground in which case construction loads are zero.
2. The most recently cast slab is struck and is allowed to deflect under its self-weight before any re-props are installed. The re-props are initially only lightly tightened and, consequently, initially carry only a nominal load.
3. The most recently struck slab is not allowed to deflect under its self-weight when struck and the supporting props are, consequently, initially stressed.

Grundy & Kabaila (1963) developed a procedure for calculating the load ratio  $W_{\text{construction}}/W_{\text{dead}}$  for each slab for propping system 3. They assumed linear elastic behavior and infinitely rigid props. They found that the maximum load ratio was greater than 2 even if four levels of back-props were used. The maximum construction load is considerably reduced if system 2 is adopted with two or more levels of back-propping. Liu *et al.* (1988) developed a computer-based computational procedure using the same assumptions as Grundy & Kabaila (1963) for rapid calculation of construction loads imposed on slabs which can be extended to examine whether the slab loads are greater than the available strength at each step of construction in high-rise buildings.

### **2.10 Deflection Control**

Excessive deflections can lead to cracking of supporting walls and partitions, ill-fitting of doors and windows, poor roof drainage, misalignment of sensitive machinery and equipment, or visually offensive sag. It is important, to maintain control of deflections, so that members designed mainly for strength at prescribed overloads will also perform well in normal service.

In the past, deflection was achieved indirectly, by limiting service load stress in concrete and steel to conservatively low values. The resulting members were generally larger, and consequently stiffer, than those designed by current methods based on strength. In addition, stronger materials are now in general use, and this, too, tends to produce members of smaller cross section that are less stiff than before. Because of these changes in conditions of practice, deflection control is increasingly important.

There are presently two approaches. The first is indirect and consists in setting suitable upper limits on the span-depth ratio. This is simple, and it is satisfactory in many cases where spans, load and load distributions, and member sizes and proportions fall in the usual ranges. Otherwise, it is essential to calculate deflections

and to compare those predicted values with specific limitations that may be imposed by codes or by special requirements.

### 2.10.1 ACI Code Provisions for Deflection Control

The indirect approach of deflection control is providing the minimum slab thickness of two-way edge supported slab and the limitations have given satisfactory results. ACI Code (1963) suggests the minimum thickness is equal to 3.5 inch or panel perimeter divided by 180 for special case of two-way slabs supported on four sides by relatively deep, stiff, edge beams. It has been used extensively since 1963 for slabs supported at the edges by walls, steel beams, or monolithic concrete beams having a total depth not less than about 3 times the slab thickness. The more general unified method of two-way system analysis found in more recent edition of ACI Code (2002) contains three equations governing minimum slab thickness. These equations account for the relative stiffness of slab and edge beams, the ratio of long to short panel side dimensions, and conditions of restraint along the edges.

#### ACI Code (2002) thickness: slab with beams on all sides

The parameter used to define the relative stiffness of the beam and slab spanning in either direction is  $\alpha$ . Then  $\alpha_m$  is defined as the average value of  $\alpha$  for all beams on the edges of a given panel. According to ACI Code (2002), for  $\alpha_m$  equal to or less than 0.2, the minimum thickness of Table 2.1 shall apply.

For  $\alpha_m$  greater than 0.2 but not greater than 2.0, the slab thickness must not be less than

$$h = \frac{l_n (0.8 + f_y / 200,000)}{36 + 5\beta(\alpha_m - 0.2)} \quad (2.46)$$

and not less than 5.0 in.

For  $\alpha_m$  greater than 2.0, the slab thickness must not be less than

$$h = \frac{l_n (0.8 + f_y / 200,000)}{36 + 9\beta} \quad (2.47)$$

and not less than 3.5 in.,

where,  $l_n$  = clear span in long direction, in.

$\alpha_m$  = average value of  $\alpha$  for all beams on edges of a panel

$\beta$  = ratio of clear span in long direction to clear span in short direction

**Table 2.1** Minimum thickness of slabs without interior beams.

Yield stress $f_y$ (psi)	Without drop panel			With drop panel		
	Exterior panels		Interior panels	Exterior panels		Interior panels
	Without edge beams	With edge beams		Without edge beams	With edge beams	
40,000	$l_n/33$	$l_n/36$	$l_n/36$	$l_n/36$	$l_n/40$	$l_n/40$
60,000	$l_n/30$	$l_n/33$	$l_n/33$	$l_n/33$	$l_n/36$	$l_n/36$
75,000	$l_n/28$	$l_n/31$	$l_n/31$	$l_n/31$	$l_n/34$	$l_n/34$

### 2.10.2 Gilbert Method

Gilbert (1985) proposed a simple design-oriented procedure for control of deflections in reinforced concrete slab system. A rational and reliable expression for the maximum allowable span to depth ratio of beams, proposed by Rangan (1982) was extended to the entire range of reinforced concrete flexural members including two-way edge supported slabs, flat slabs and flat plates. The data used for the calibration of the procedure were obtained from an extensive series of computer experiments with reinforced concrete slabs, using a nonlinear finite element model. Details of the method can be found in Gilbert (1985).

### 2.10.3 Hwang and Chang Method

Hwang and Chang (1996) proposed two alternative design procedures for deflection control. One with fewer parameters is written in a form of minimum thickness requirements. The other, allowing more flexibility in choices, involves the direct calculation of mid panel deflections. Both procedures suggested are simple; however

various factors influencing deflections of two-way slab systems (loading intensity, slab geometrical configuration, material properties, cracking phenomena, slab discontinuity, long-term effects and allowable limits) have been considered. These techniques were provided with instructive examples as well as comparison with the available experimental data and ACI 318-89 were made. Details of the method can be found in Hwang & Chang, 1996.

### **2.11 Permissible Deflection**

To ensure the satisfactory performance in service, the ACI Code (2002) imposes certain limits on calculated deflections. These limits are given in Table 2.2. Limits depends on whether or not the member supports or is attached to other nonstructural elements, and whether or not those nonstructural elements are likely to be damaged by large deflections. When long-term deflections are computed, that part of the deflection that occurs before attachment of the nonstructural elements may be deducted. The last two limits of Table 2.2 may be exceeded under certain conditions, according to the ACI Code.



**Table 2.2** Maximum allowable computed deflections

Type of member	Deflection to be considered	Deflection limitation
Flat roofs not supporting or attached to nonstructural elements likely to be damaged by large deflections.	Immediate deflection due to the live load L	$\frac{l}{180}$
Floors not supporting or attached to nonstructural elements likely to be damaged by large deflections.	Immediate deflection due to the live load L	$\frac{l}{360}$
Roof or floor construction supporting or attached to nonstructural elements likely to be damaged by large deflections.	That part of the total deflection which occurs after attachment of the nonstructural elements, the sum of the long-term deflection due to all sustained loads, and the immediate deflection due to any additional live load	$\frac{l}{480}$
Roof or floor construction supporting or attached to nonstructural elements not likely to be damaged by large deflections		$\frac{l}{240}$

## 2.12 Conclusion

In this chapter the behavior of edge supported slab has been discussed. Importances of serviceability are pointed out. The deflection calculation methods of slab by analytical and numerical approaches have been discussed for uncracked and cracked conditions. Long-term deflection calculation using ACI multiplier approach and Model Code 90 are presented. Deflection due to creep and shrinkage are explained. Restraint shrinkage cracking, construction load, deflection control and permissible deflection are discussed. The main concern of this work is deflection computation of edge supported slabs. Finite element method is a widely used numerical technique for analysis of such structures. However, computation of slab deflection is complicated due to the presence of cracking which makes the problem nonlinear even under service loads. Also, the effects of creep and shrinkage need to be included in long-term deflection calculation. With an aim to include all these effects in deflection calculation, the current work starts with an analysis which is presented in the next chapter.

## CHAPTER 3

### ELASTIC FINITE ELEMENT ANALYSIS

#### 3.1 Introduction

In Chapter 2, the importance of keeping slab deflections within tolerable limits are discussed in detail. Different codes and authors proposed minimum thickness guidelines which aim to ensure serviceability of slabs. At the same time, different deflection calculation procedures are discussed in detail in the previous chapter. Different crack models to simulate the loss of stiffness due to cracking, long-term models to represent creep, shrinkage etc. have been discussed. In the current chapter, elastic finite element analysis is introduced. Two general purpose finite element softwares, namely FE-77 (1999) and ANSYS (1997) are used for analysis of edge supported slabs.

The purposes of this chapter are to compare the results of finite element analysis with results from ACI Code and other authors and to prepare simplified charts for easy calculation of elastic deflections and moments. At first, a mesh sensitivity analysis has been carried out to decide a reasonable mesh size for obtaining correct results.

#### 3.2 Mesh Sensitivity Analysis

To obtain correct results from finite element analysis it is important to determine the optimum number of elements in each direction. For this purpose,  $1/4^{\text{th}}$  portions of square slabs have been modeled with varying number of elements for calculation of midpoint deflection and stress. From this analysis the mesh sensitivity of both software FE-77 and ANSYS has been compared in the form of moment coefficient

and deflection coefficient of two-way edge supported slabs. The calculation procedures of moment coefficient and deflection coefficient are discussed below.

### 3.2.1 Moment Coefficient

The stress developed at the support and midspan of two-way edge supported slab can be calculated from finite element analysis. From FE results the bending moment,  $M$  developed at any point of the slab can be calculated from flexural formula as follows:

$$M = \frac{f b t^2}{6} \quad (3.1)$$

where,

$M$  = bending moment

$f$  = flexural stress

$b$  = width of slab taken as unity

$t$  = total depth of slab

The bending moment coefficients at support and midspan for long and short directions of two-way edge supported slab can be computed from the formula:

$$c = \frac{M}{w l^2} \quad (3.2)$$

where,

$M$  = bending moment

$w$  = load on the slab per unit area

$l$  = span length of the slab in the respective direction

$c$  = moment coefficient

### 3.2.2 Deflection Coefficient

The deflection coefficient of two-way edge supported slab is calculated by the formula:

$$D = \frac{\delta E}{w l^4 / t^3} \quad (3.3)$$

where,

$\delta$  = total deflection of slab

$E$  = modulus elasticity of concrete

$w$  = total uniform applied on the slab

$l$  = span length of the slab in the respective direction

$t$  = thickness of the slab

### 3.2.3 Mesh Sensitivity for FE-77 and ANSYS

Mesh sensitivity of softwares FE-77 and ANSYS has been studied by comparing the results of moment coefficients and deflection coefficients with varying mesh sizes. The mesh sensitivity analysis helps to decide a reasonable mesh size for further runs so that correct results can be obtained from finite element analysis. Two types of slab, one is all end discontinuous (case-1) and other is all end continuous (case-2) have been analyzed. The mesh sensitivity analysis of two-way edge supported slab for the calculation of midpoint deflection and developed stress at support and midspan of slab, the elastic finite element modeling has been performed with varying the number of elements for same dimension and aspect ratio and loading. For this purpose, 1/4<sup>th</sup> portion of a square slab has been modeled with varying number of elements ( $4 \times 4 = 16$  to  $20 \times 20 = 400$ ) for slab case-1 and ( $4 \times 4 = 16$  to  $18 \times 18 = 324$ ) for slab case-2 and other parameters have been taken as unchanged. For FE-77 nine noded plate element and for ANSYS eight noded shell element have been used in the modeling. The other parameters used are as follows:

- Slab dimension is 4572 mm  $\times$  4572 mm (15 ft  $\times$  15 ft)
- Slab thickness equal to panel perimeter divided by 180 i.e.,  $t = 101.6$  mm
- The total load applied on the slab is 6.22 kN/m<sup>2</sup> (130 psf)
- $E_c = 20685$  N/mm<sup>2</sup> ( $3 \times 10^6$  psi)
- $f_y = 413.7$  N/mm<sup>2</sup> (60000 psi)
- $f'_c = 20.7$  N/mm<sup>2</sup> (3000 psi)
- Poisson's ratio,  $\nu = 0.18$
- Modular ratio,  $n = 10$

From the FE analysis the moment coefficients and deflection coefficients have been calculated from Eqns. (3.2) and (3.3) respectively. The variations of positive moment coefficient,  $C_a(+)$  and deflection coefficient against number of element have been presented in Figs 3.1 and 3.2 for slab case-1. Figures 3.3 and 3.4 show the variation of positive moment coefficient,  $C_a(+)$  and negative moment coefficient,  $C_a(-)$  and Fig. 3.5 shows the variation of deflection coefficient against number of element for slab case-2.

It has been observed that the variations of moment coefficients and deflection coefficients remain almost unchanged due to change in mesh size for slab case-1. For case-2 the coefficients are slightly different for mesh size less than  $10 \times 10$ . Change of moment coefficients and deflection coefficients are slight if mesh size is equal or finer than  $10 \times 10$  for  $1/4^{\text{th}}$  portion of a square panel.

Hence mesh density mentioned above, i.e.  $10 \times 10$ , may give more accurate results for both FE program. Further finite element analyses will be performed with the mesh size greater or equal to  $10 \times 10$  for  $1/4^{\text{th}}$  portion of each square slab.

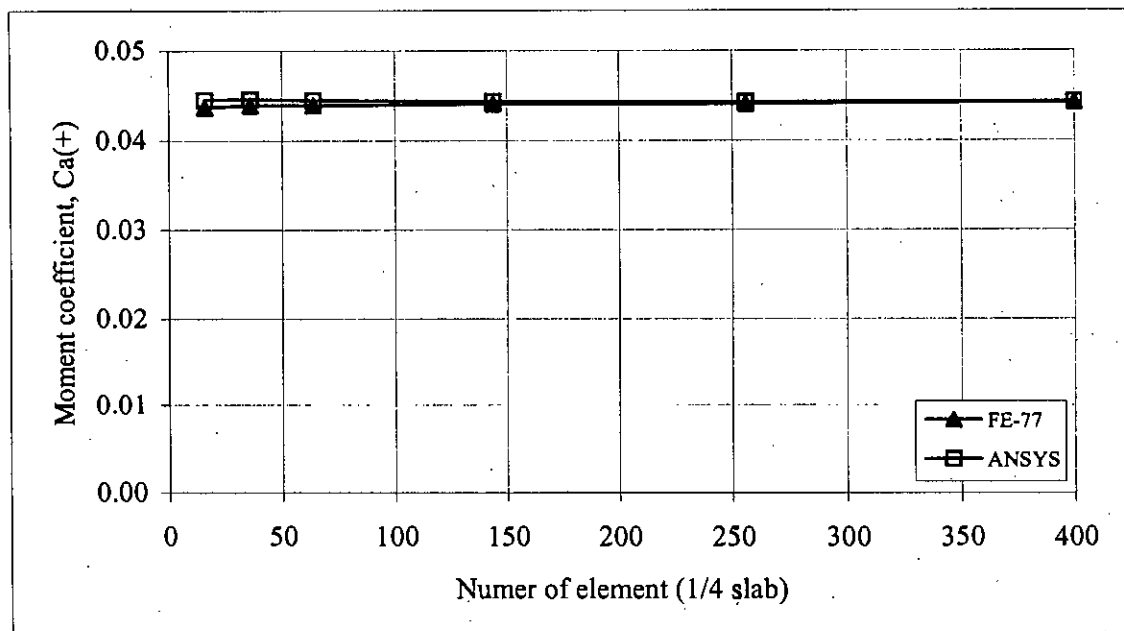


**Figure 3.1** Variation of positive moment coefficient  $C_a(+)$  with number of element, for case-1, aspect ratio,  $m = 1.00$

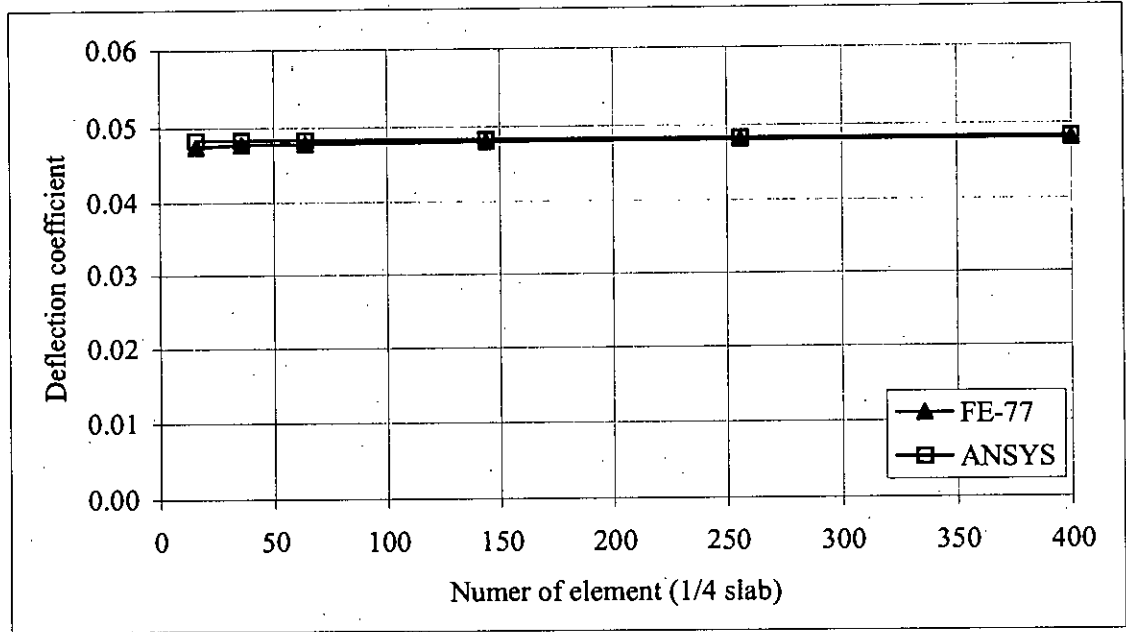


**Figure 3.2** Variation of deflection coefficient with number of element for case-1, aspect ratio,  $m = 1.00$

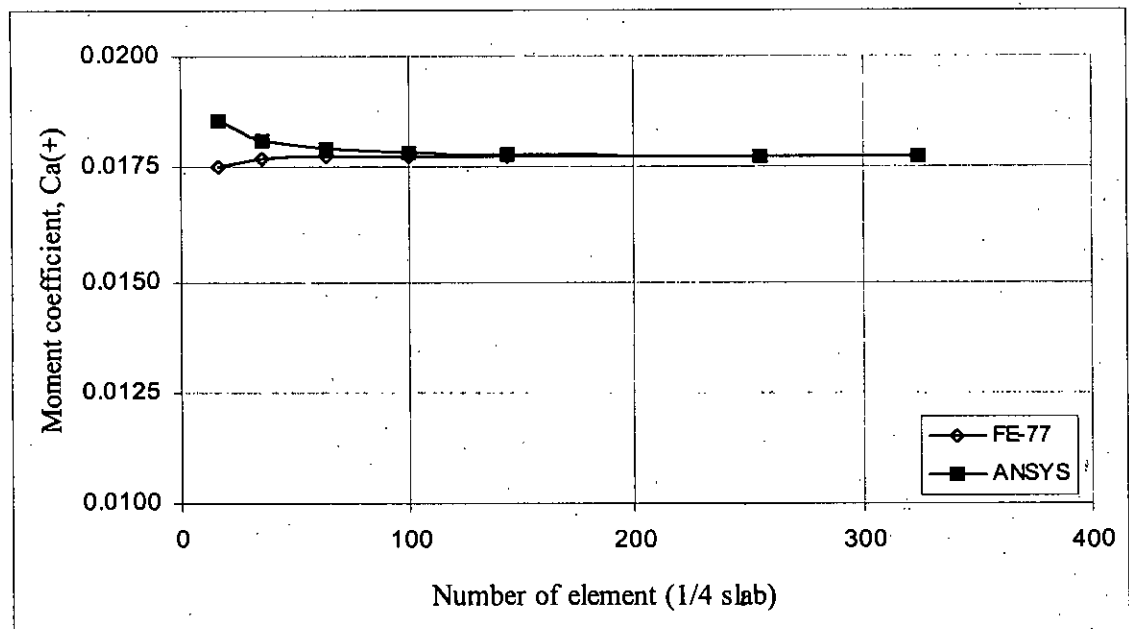


**Figure 3.3** Variation of positive moment coefficient  $C_a(+)$  with number of element, for case-2, aspect ratio,  $m = 1.00$

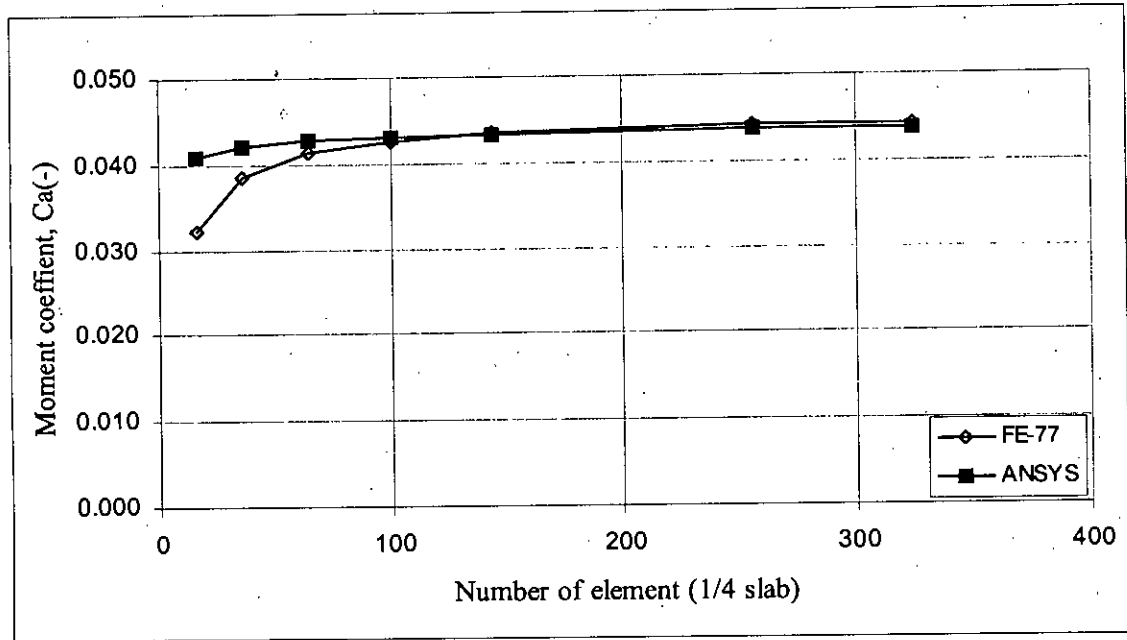


Figure 3.4 Variation of negative moment coefficient  $C_a(-)$  with number of element, for case-2, aspect ratio,  $m = 1.00$

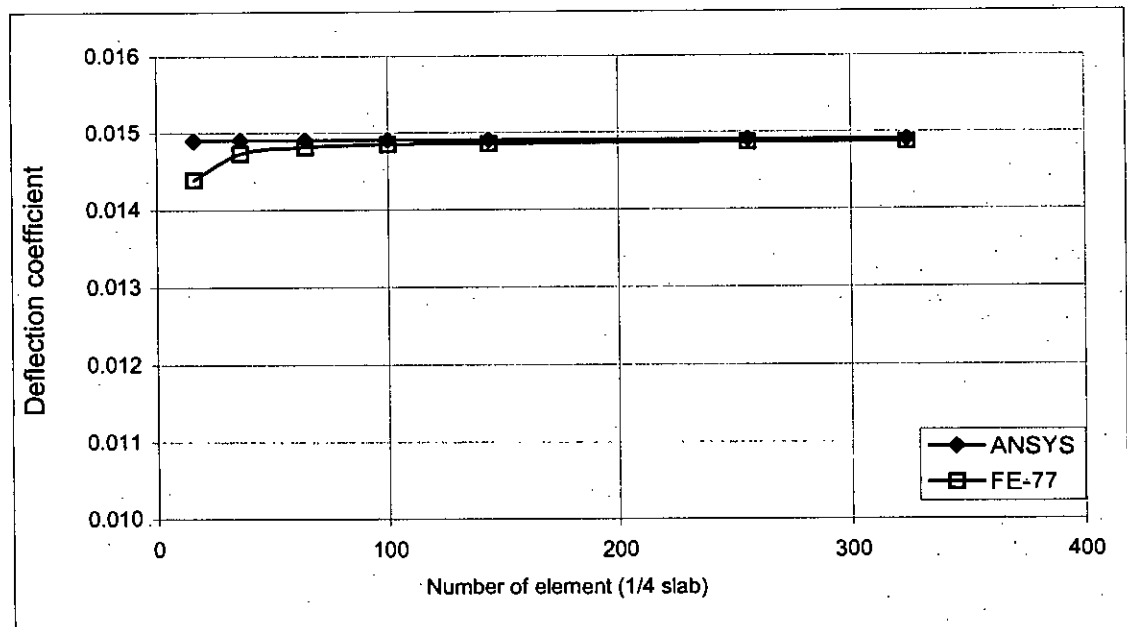


Figure 3.5 Variation of deflection coefficient with number of element for case-2, aspect ratio,  $m = 1.00$

### 3.3 Comparison of Deflections Calculated by FE-77 and ANSYS

Elastic deflection of different types of edge supported slabs are calculated using both FE-77 and ANSYS. The results are compared in this section. For this purpose a large number of finite element analysis has been performed by FE-77 and ANSYS with same dimension, aspect ratio and properties of slab with different boundary conditions. The common parameters used in all the FE analyses are presented in the Table 3.1.

**Table 3.1** Parameters used in FE analysis

Slab thickness	$E_c$ (N/mm <sup>2</sup> )	$f'_c$ (N/mm <sup>2</sup> )	Poisson's ratio	Modular ratio
Perimeter/180	20685	20.7	0.18	10

For different loadings, aspect ratio and slab thickness, the predicted results of elastic deflections from both FE analyses are presented in the Table 3.2 for different categories of slab. It is clearly observed that the both softwares FE-77 and ANSYS have given almost same results of elastic deflection.



**Table 3.2** Comparison of elastic deflection of slab performed by FE-77 and ANSYS

Aspect ratio	Slab dimension (mm × mm)	Slab thickness (mm)	udsl (kN/m <sup>2</sup> )	Elastic deflection (mm)											
				Case-1		Case-2		Case-3		Case-4		Case-8		Case-9	
				FE-77	ANSYS	FE-77	ANSYS	FE-77	ANSYS	FE-77	ANSYS	FE-77	ANSYS	FE-77	ANSYS
1.00	7620 × 7620	169.33	9.0174	14.57	14.63	4.477	4.485	6.807	6.824	7.813	7.845	5.685	5.694	5.685	5.694
0.90	7620 × 6858	160.87	8.8179	13.30	13.36	4.060	4.068	6.908	6.927	7.109	7.143	5.470	5.481	4.885	4.894
0.80	7620 × 6096	152.40	8.6184	11.59	11.65	3.462	3.470	6.758	6.779	6.130	6.159	4.999	5.008	3.954	3.961
0.70	7620 × 5334	143.93	8.4189	9.50	9.54	2.724	2.730	6.252	6.272	4.913	4.944	4.249	4.261	2.969	2.978
0.60	7620 × 4572	135.47	9.4164	8.18	8.22	2.206	2.214	6.080	6.101	4.094	4.119	3.736	3.745	2.314	2.323
0.50	7620 × 3810	127.00	9.2169	5.46	5.49	1.359	1.366	4.545	4.563	2.613	2.624	2.492	2.494	1.386	1.393

### 3.4 Comparison of Moment Coefficients

Moment coefficients of two-way edge supported slab have been calculated by the FE programs FE-77 and ANSYS. From both FE analyses, the middle strip moment coefficients have been calculated at midspan and the support of the slab. The calculated results are also compared with the ACI (1963) moment coefficients and those calculated by Chowdhury (2000).

The parameters taken in the modeling of FE-77 and ANSYS are discussed below. The number of element considered for  $1/4^{\text{th}}$  part of a square slab has been  $16 \times 16 = 256$ , and for aspect ratio less than 1.00, the number of element has been considered proportionally to the respective aspect ratio. The 9-noded and 8-noded shell element has been used for the program FE-77 and ANSYS respectively. Other parameters used are:

- Concrete compressive strength =  $20.7 \text{ N/mm}^2$
- The modulus of elasticity of concrete =  $20685 \text{ N/mm}^2$
- Poisson's ratio = 0.18
- Modular ratio = 10
- Slab thickness = Panel perimeter / 180.
- The aspect ratios ( $m = a/b$ ) are taken from 0.50 to 1.00.

where,

a = length of slab in short direction.

b = length of slab in long direction.

Various cases of slabs have been modeled with different aspect ratios. The positive moment coefficients  $C_a(+)$  for short direction,  $C_b(+)$  for long direction and negative coefficients  $C_a(-)$  for short direction,  $C_b(-)$  for long direction are calculated from FE analyses. The results obtained from both FE analyses are compared with the ACI moment coefficient and those computed by Chowdhury (2000). The variation of moment coefficients for different categories of slabs have been plotted in Figs 3.6 to 3.20. From the figures, it has been clearly observed that both programs FE-77 and ANSYS have produced identical curves of moment coefficients. The coefficients

calculated by Chowdhury (shown in figure as legend SRC) are incorporated with the FE-77 and ANSYS results.

For most of the slab cases, some variation of coefficients has been found for different FE analyses and ACI coefficients. The ACI moment coefficients are based on elastic analysis and also account for inelastic redistribution. On the other hand the coefficients calculated from FE softwares are based on only elastic analysis.

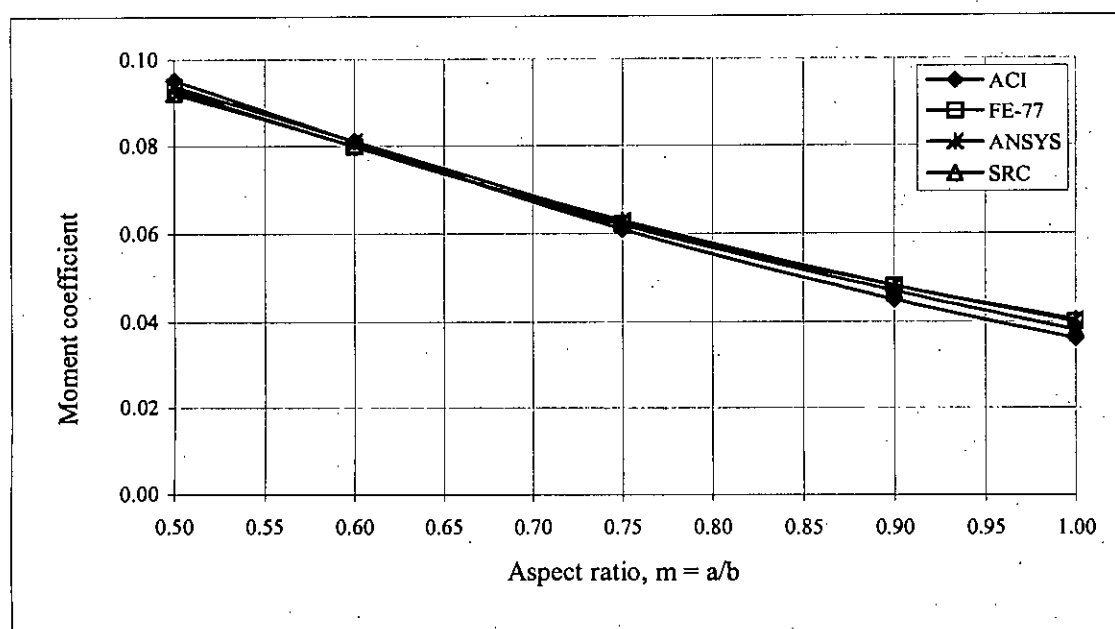


Figure 3.6 Variation of moment coefficient  $C_a(+)$  with slab span ratio for case-1.

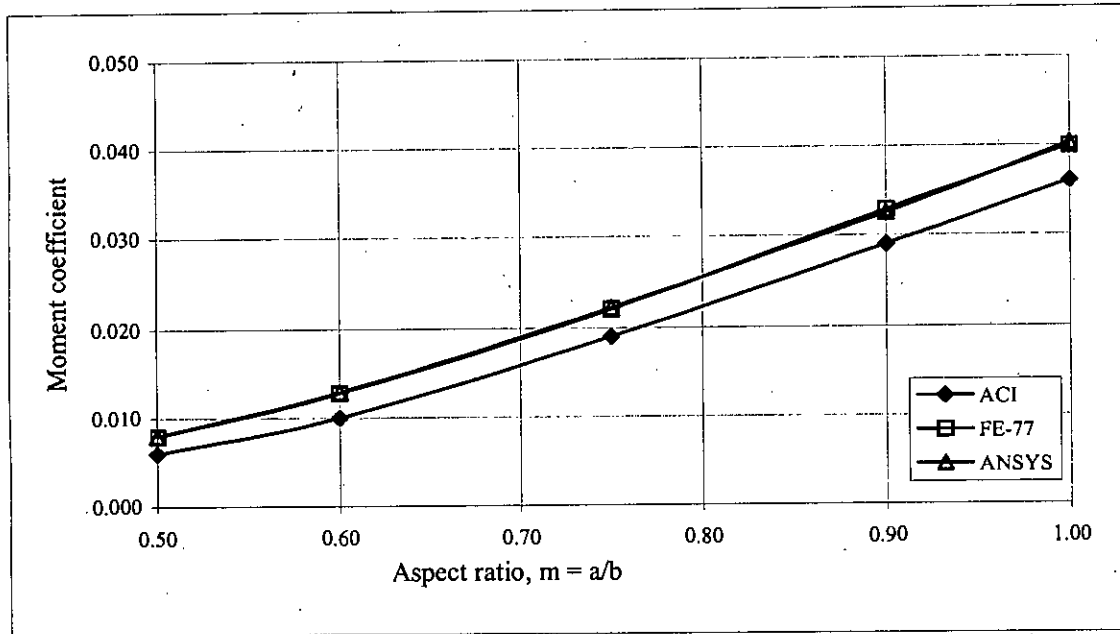


Figure 3.7 Variation of moment coefficient  $C_b(+)$  with slab span ratio for case-1.

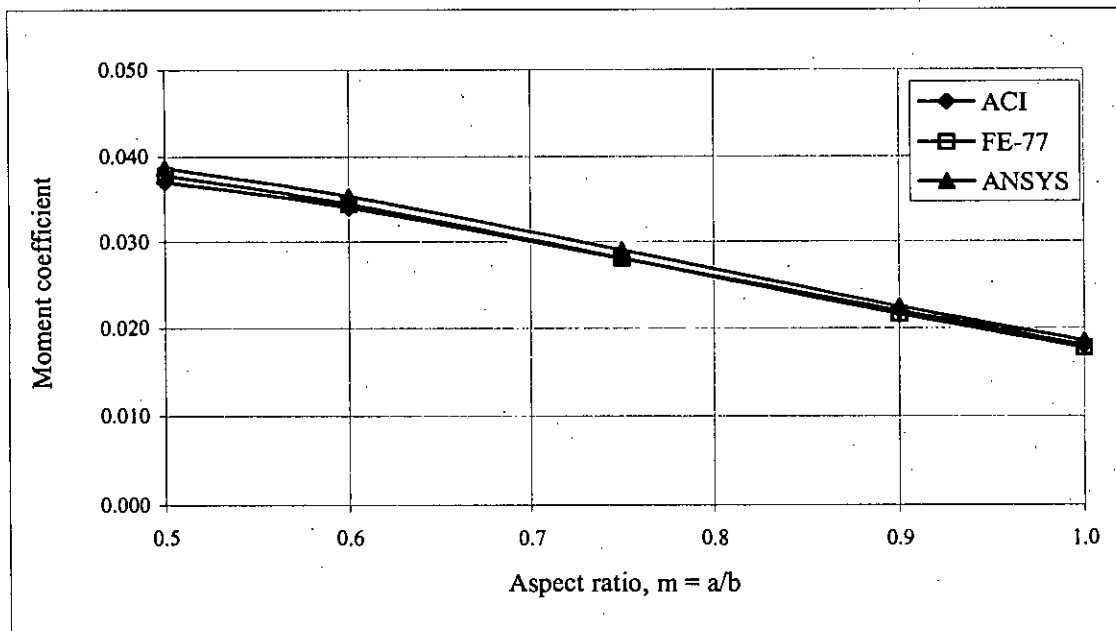


Figure 3.8 Variation of moment coefficient  $C_a(+)$  with slab span ratio for case-2.

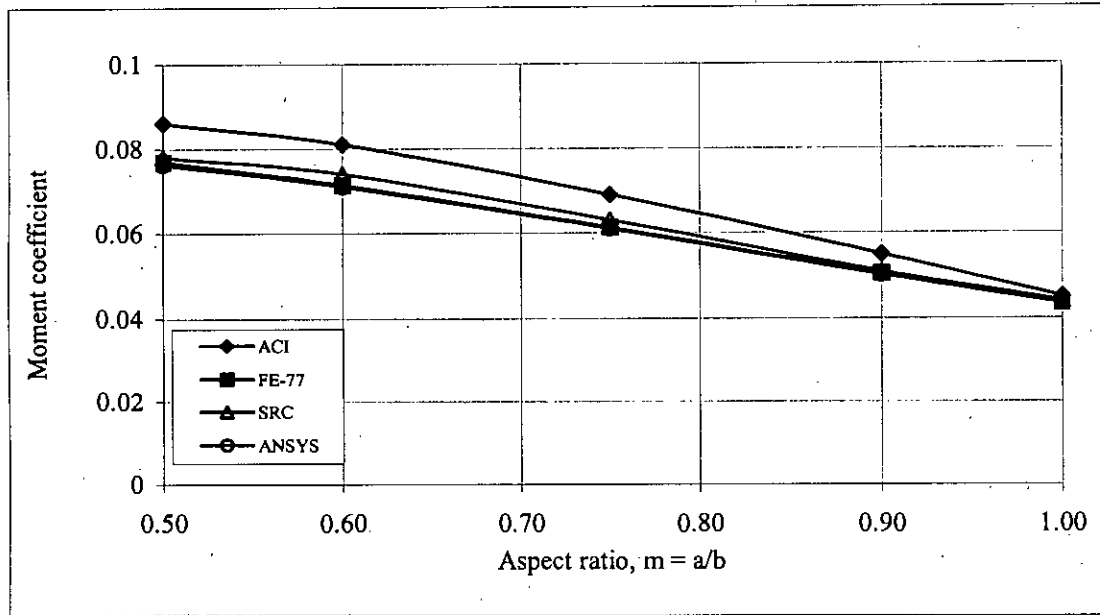


Figure 3.9 Variation of moment coefficient  $C_a(-)$  with slab span ratio for case-2.

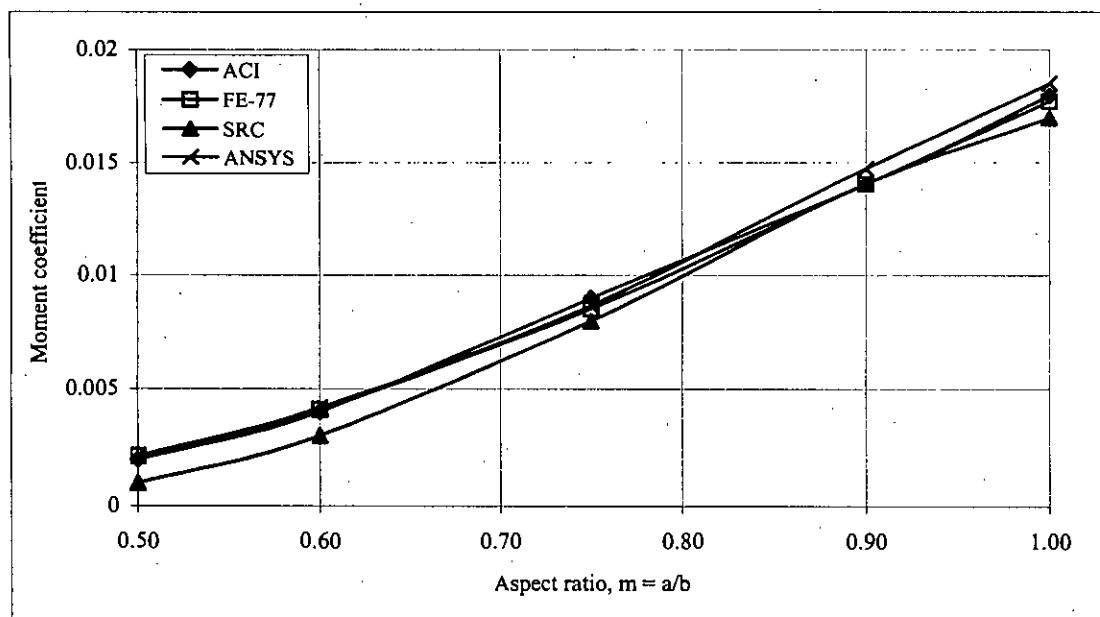


Figure 3.10 Variation of moment coefficient  $C_b(+)$  with slab span ratio for case-2.

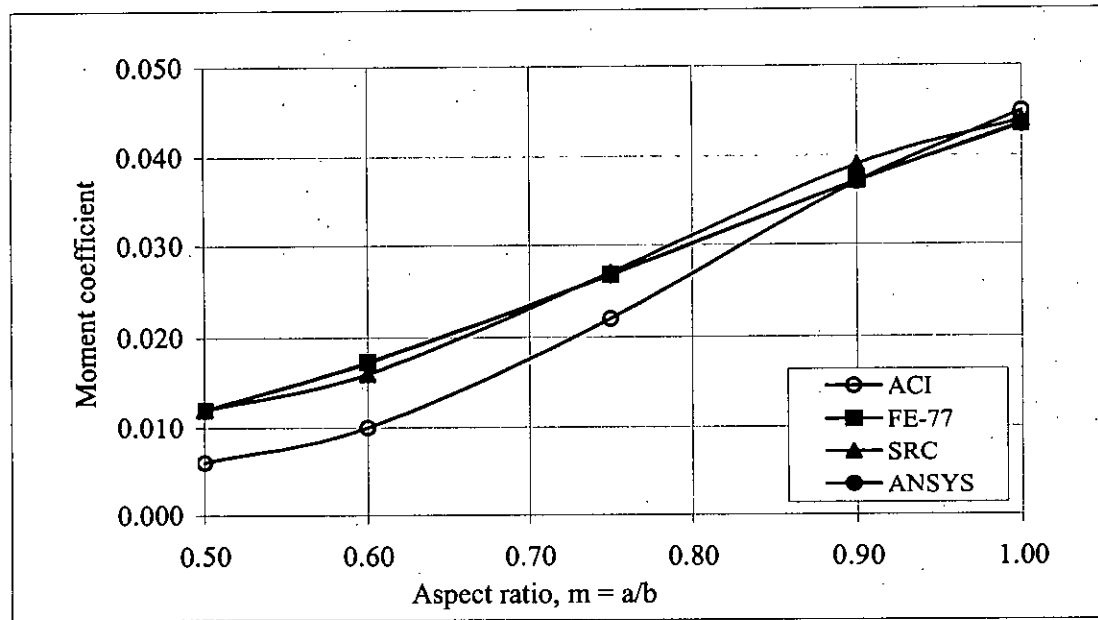


Figure 3.11 Variation of moment coefficient  $C_b(-)$  with slab span ratio for case-2.

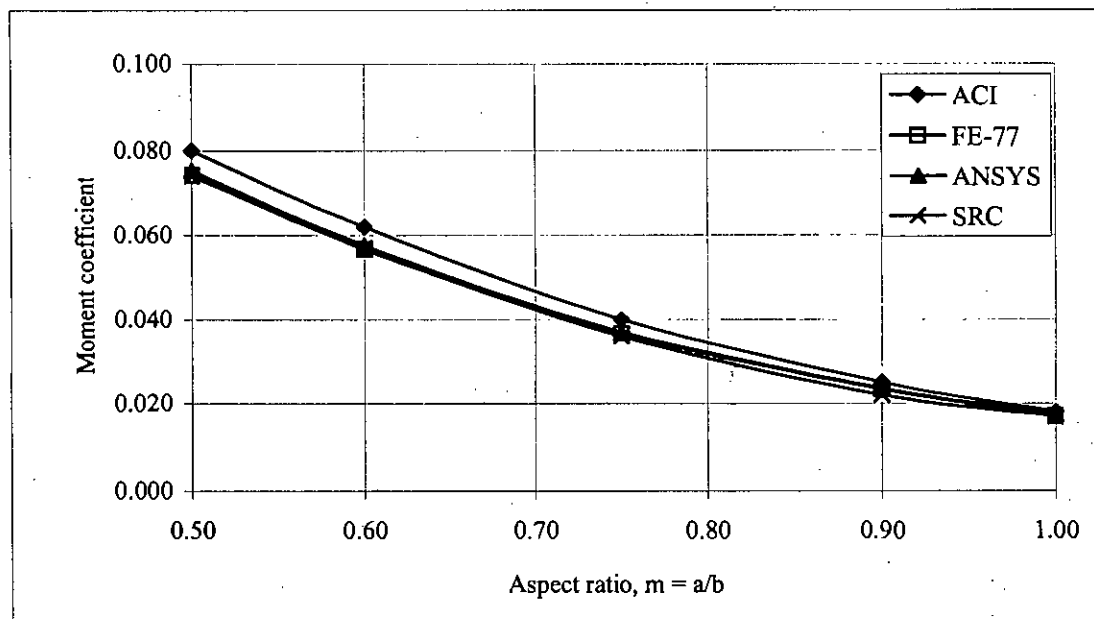


Figure 3.12 Variation of moment coefficient  $C_a(+)$  with slab span ratio for case-3.

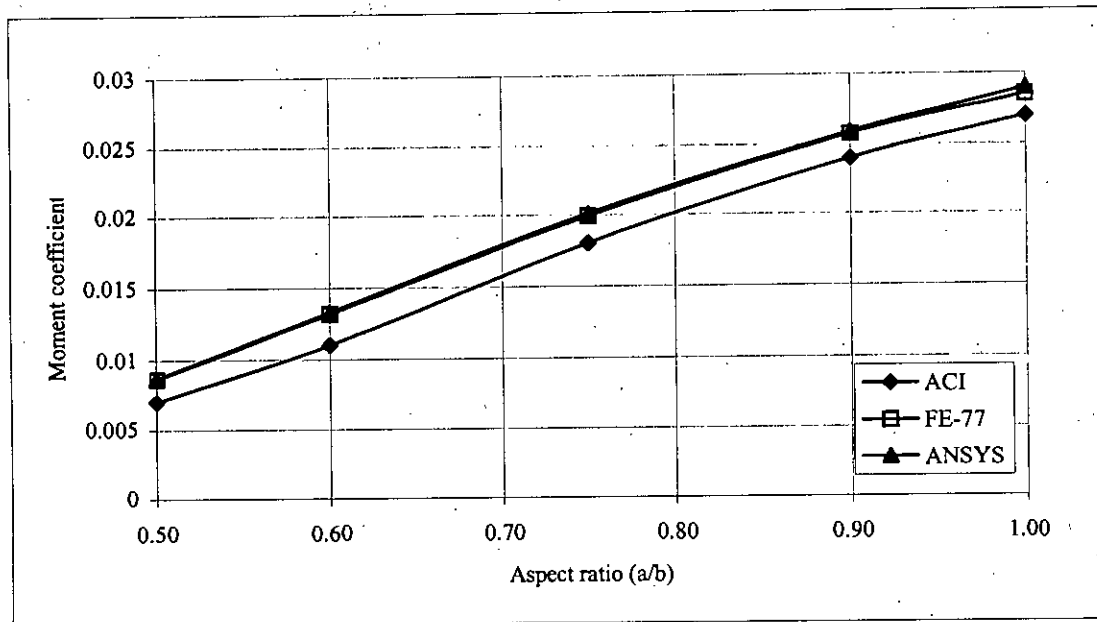


Figure 3.13 Variation of moment coefficient  $C_b(+)$  with slab span ratio for case-3.

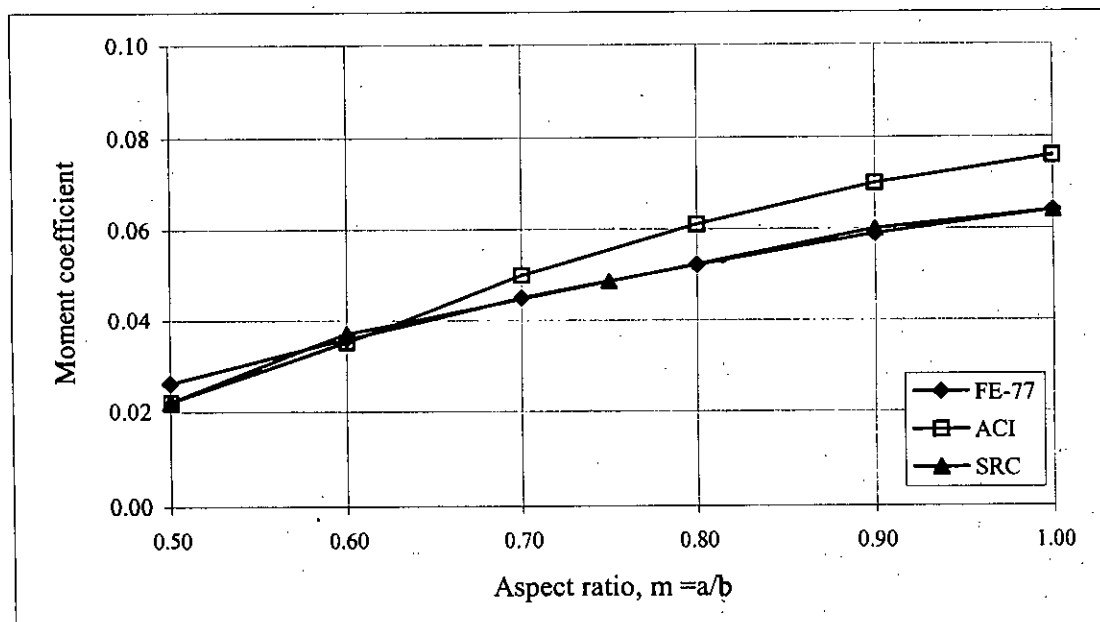


Figure 3.14 Variation of moment coefficient  $C_b(-)$  with slab span ratio for case-3.

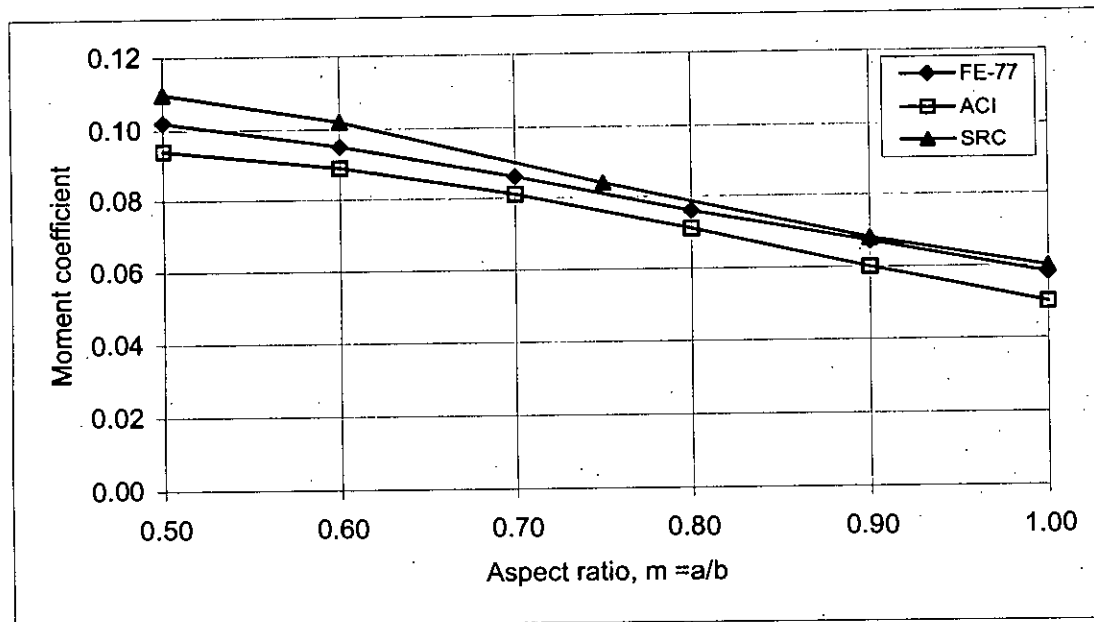


Figure 3.15 Variation of moment coefficient  $C_a(-)$  with slab span ratio for case-4.

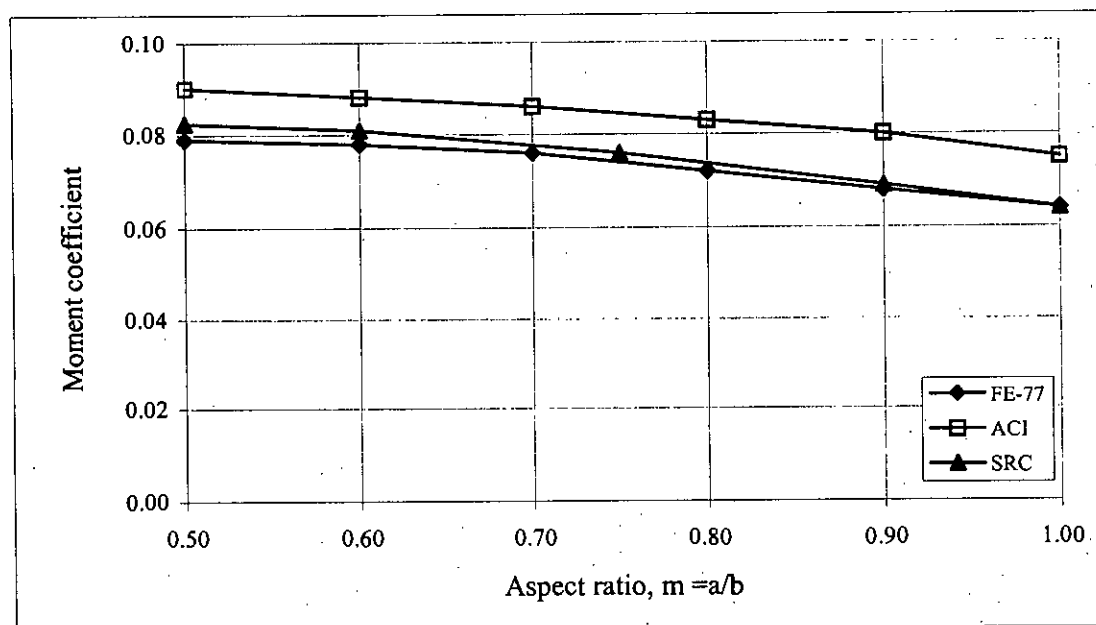


Figure 3.16 Variation of moment coefficient  $C_a(-)$  with slab span ratio for case-5.



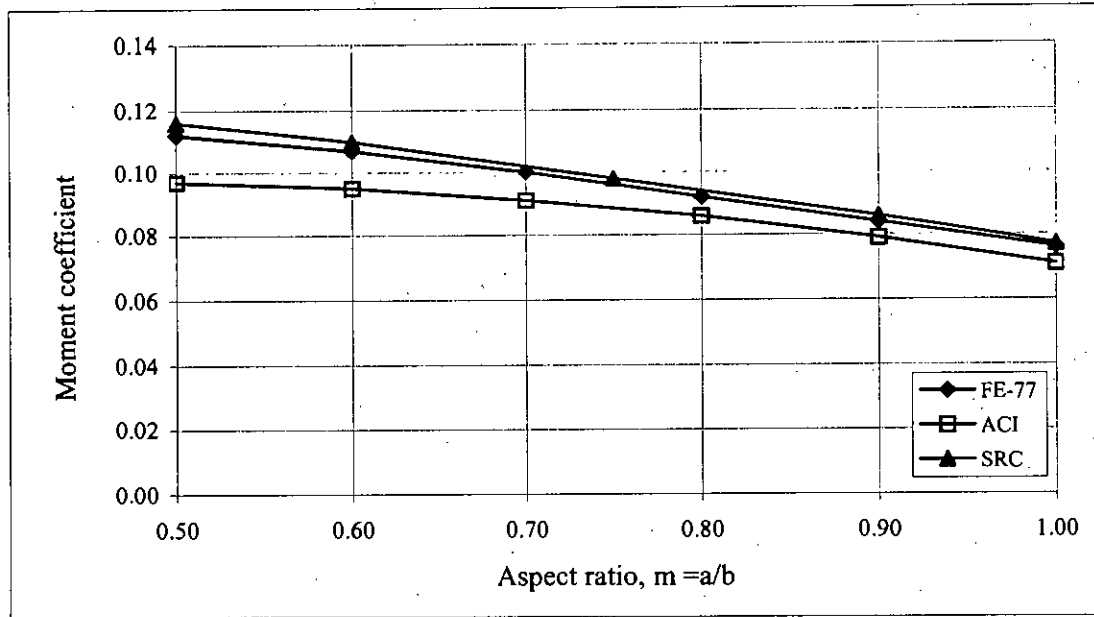


Figure 3.17 Variation of moment coefficient  $C_a(-)$  with slab span ratio for case-6.

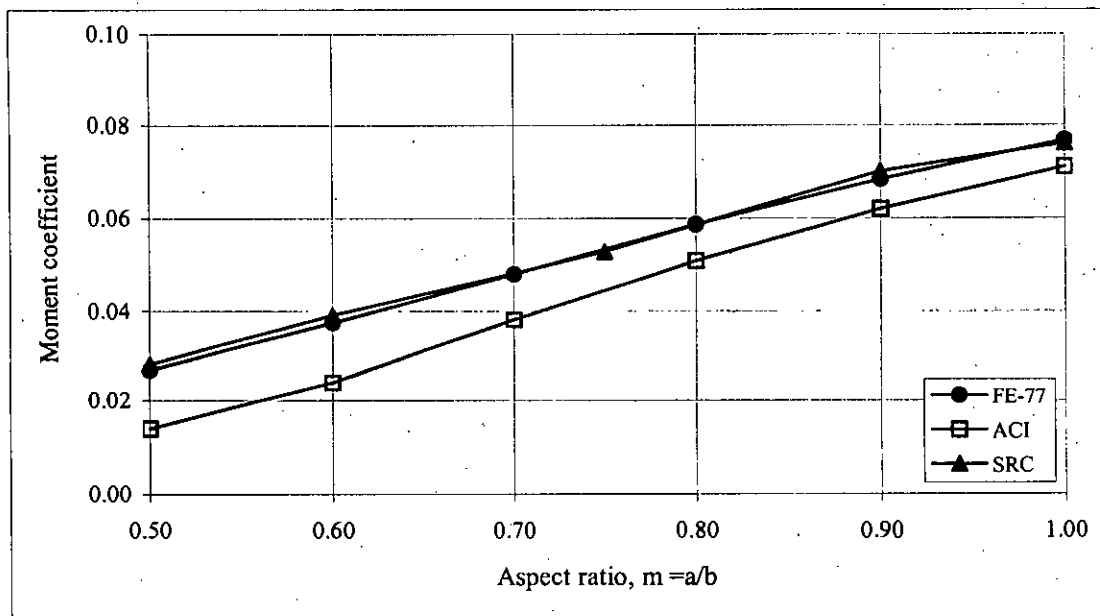


Figure 3.18 Variation of moment coefficient  $C_b(-)$  with slab span ratio for case-7.

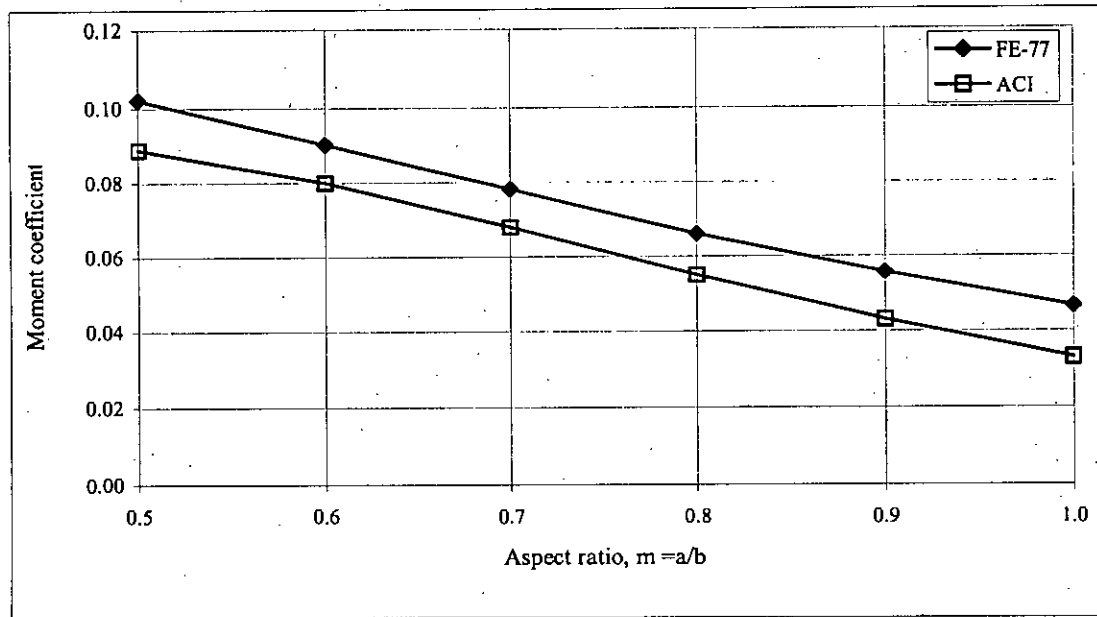


Figure 3.19 Variation of moment coefficient  $C_a(-)$  with slab span ratio for case-8.

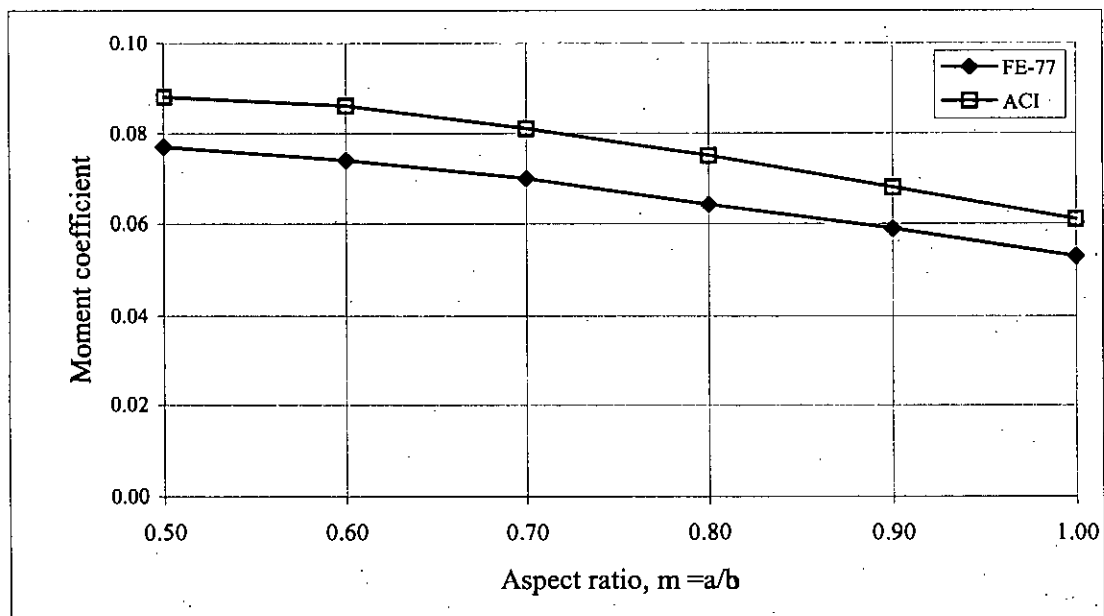


Figure 3.20 Variation of moment coefficient  $C_a(-)$  with slab span ratio for case-9.

### 3.5 Comparison of Deflection Coefficients

The deflection coefficients have been calculated by using the finite element program FE-77 and ANSYS for different aspect ratio and slab cases. The parameters for both FE analyses have been considered same as section 3.4. The variations of deflection coefficients are presented in Figs 3.21 to 3.32 for short direction and long direction. Both FE-77 and ANSYS produced identical results and some small variations have been observed with the coefficients computed by Chowdhury (2000) (shown in figure as legend SRC) for two-way edge supported slabs.

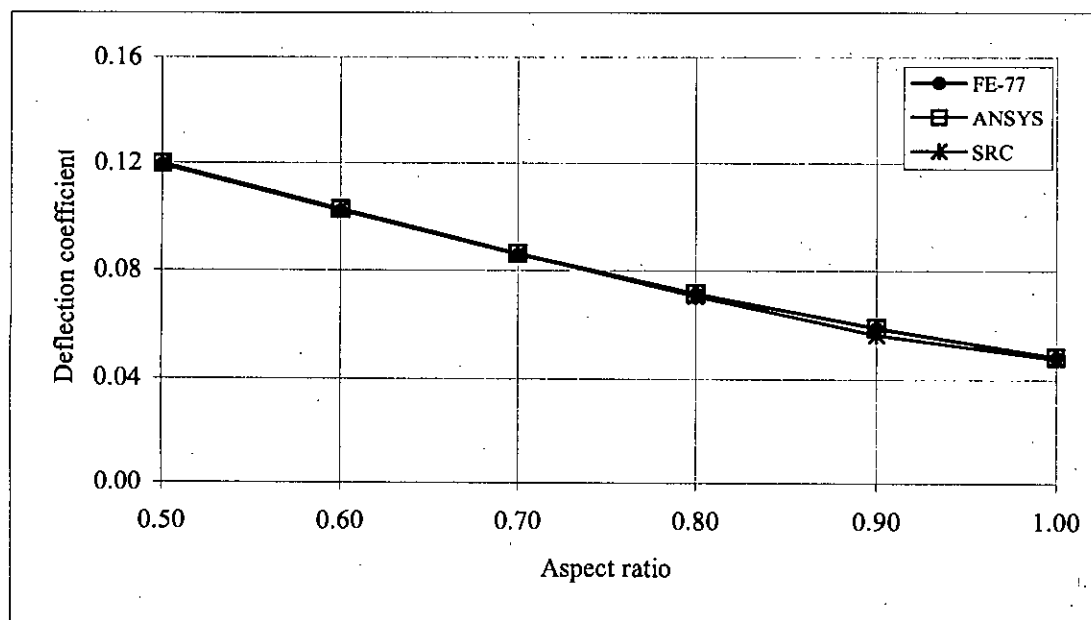


Figure 3.21 Variation of deflection coefficient with span ratio for short direction, case-1.

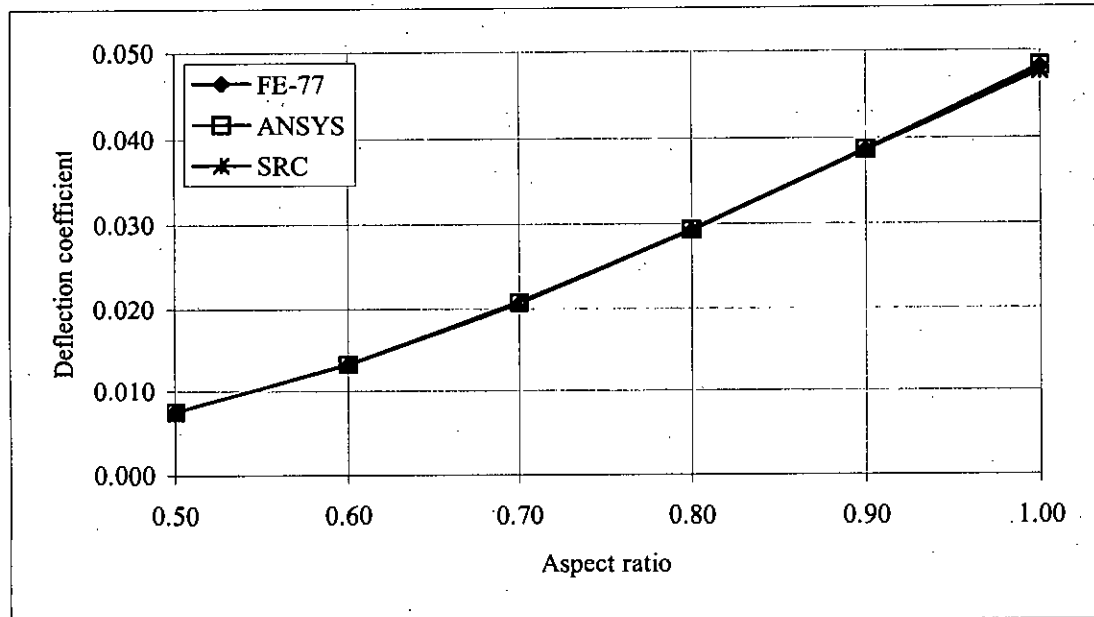


Figure 3.22 Variation of deflection coefficient with span ratio for long direction, case-1.

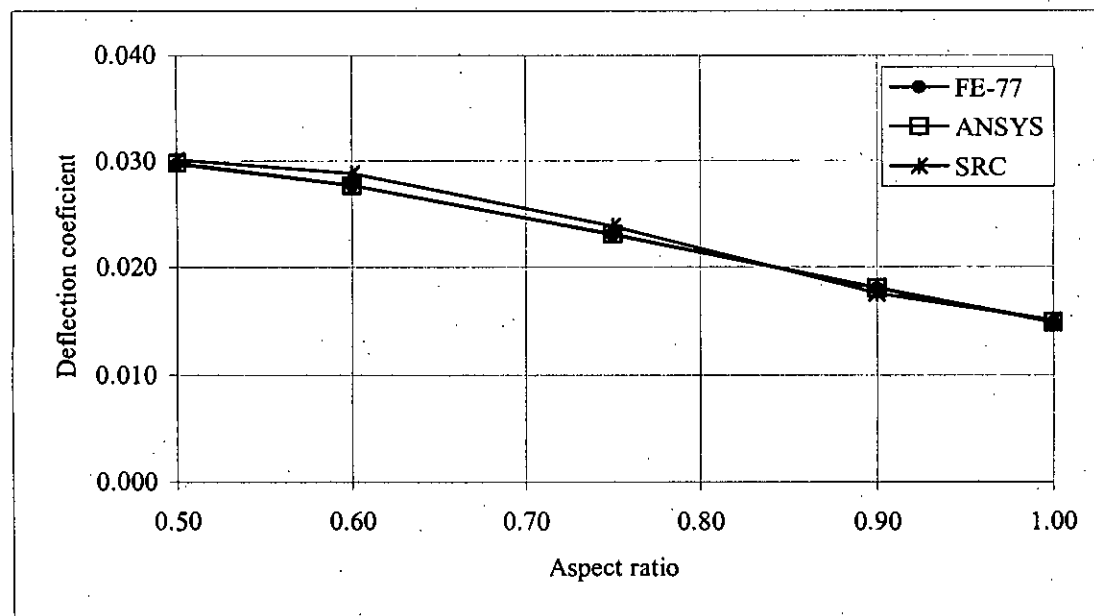


Figure 3.23 Variation of deflection coefficient with span ratio for short direction, case-2.

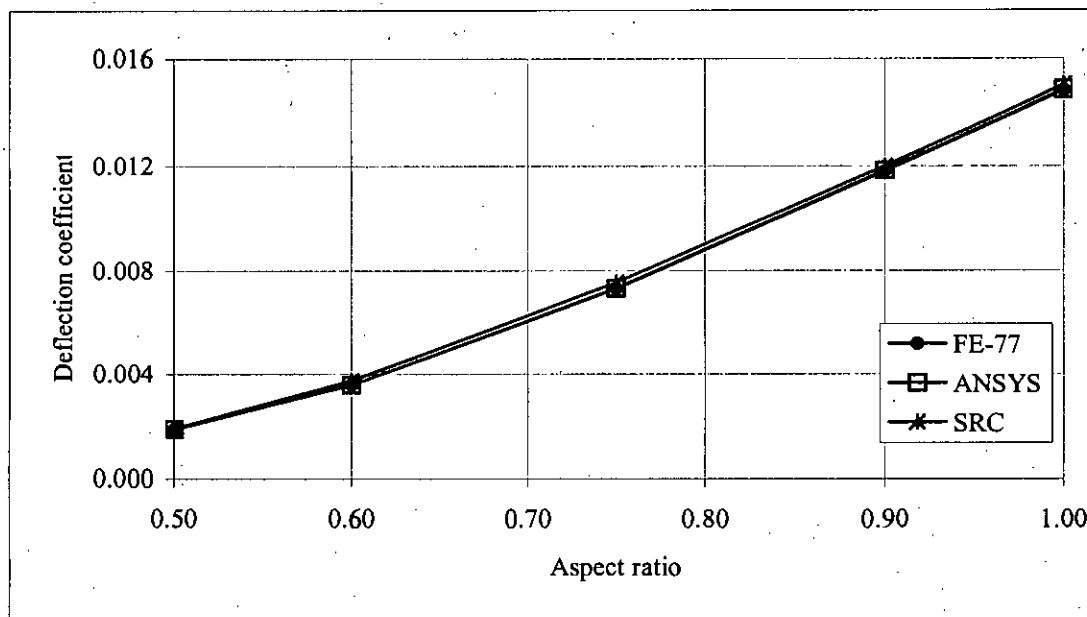


Figure 3.24 Variation of deflection coefficient with span ratio for long direction, case-2.

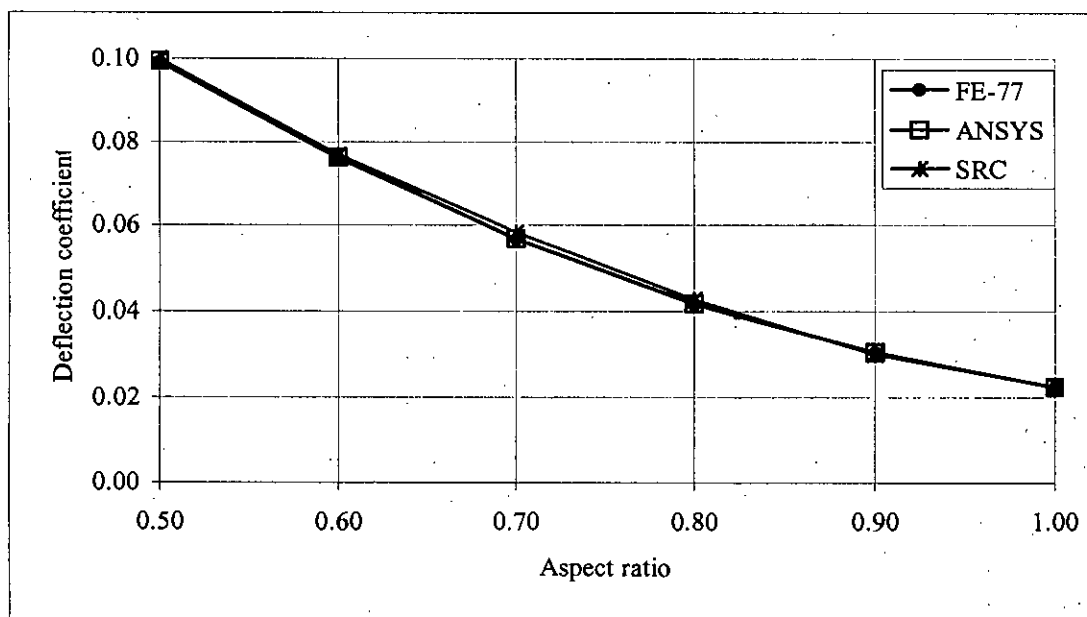


Figure 3.25 Variation of deflection coefficient with span ratio for short direction, case-3.

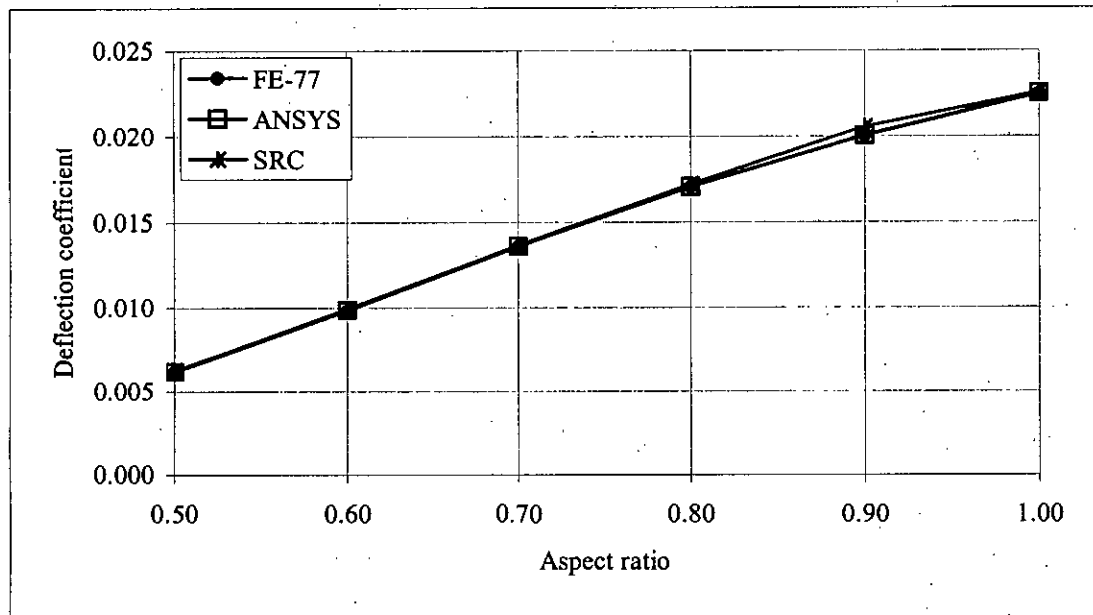


Figure 3.26 Variation of deflection coefficient with span ratio for long direction, case-3.

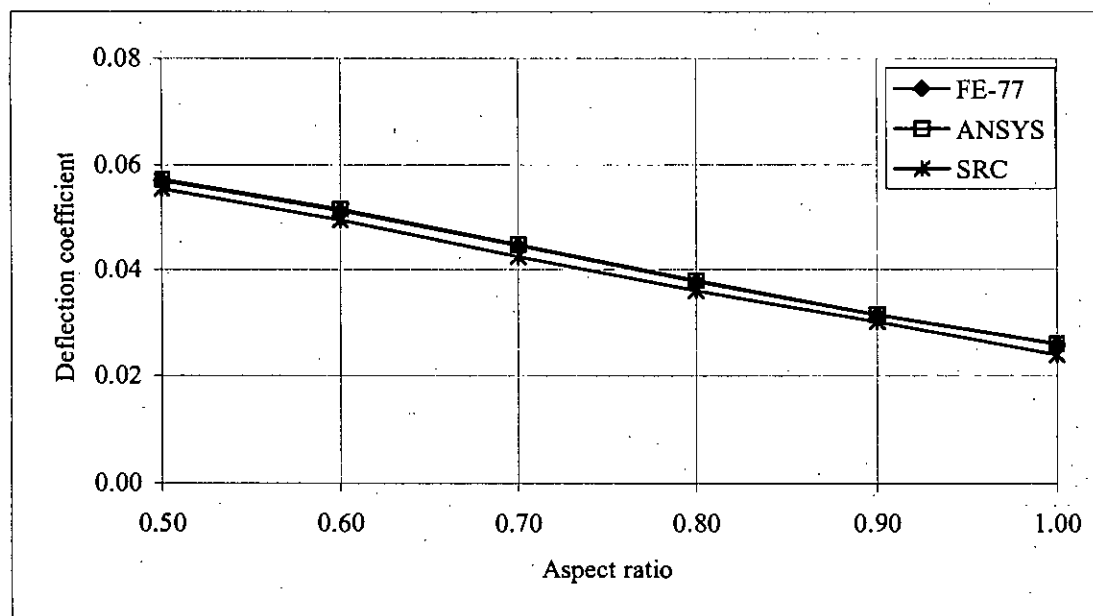


Figure 3.27 Variation of deflection coefficient with span ratio for short direction, case-4

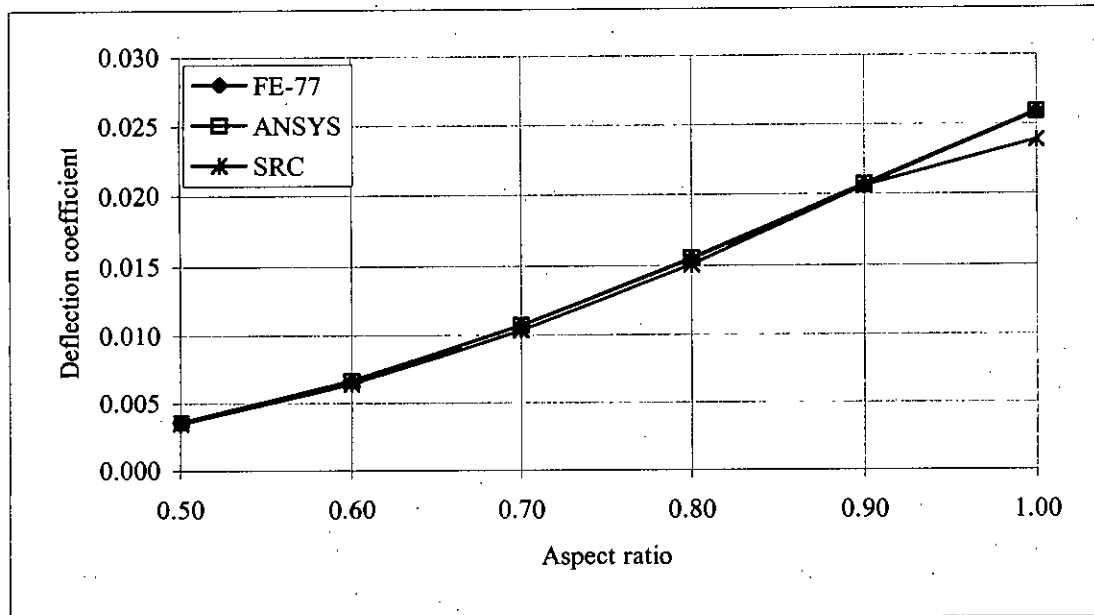


Figure 3.28 Variation of deflection coefficient with span ratio for long direction, case-4.

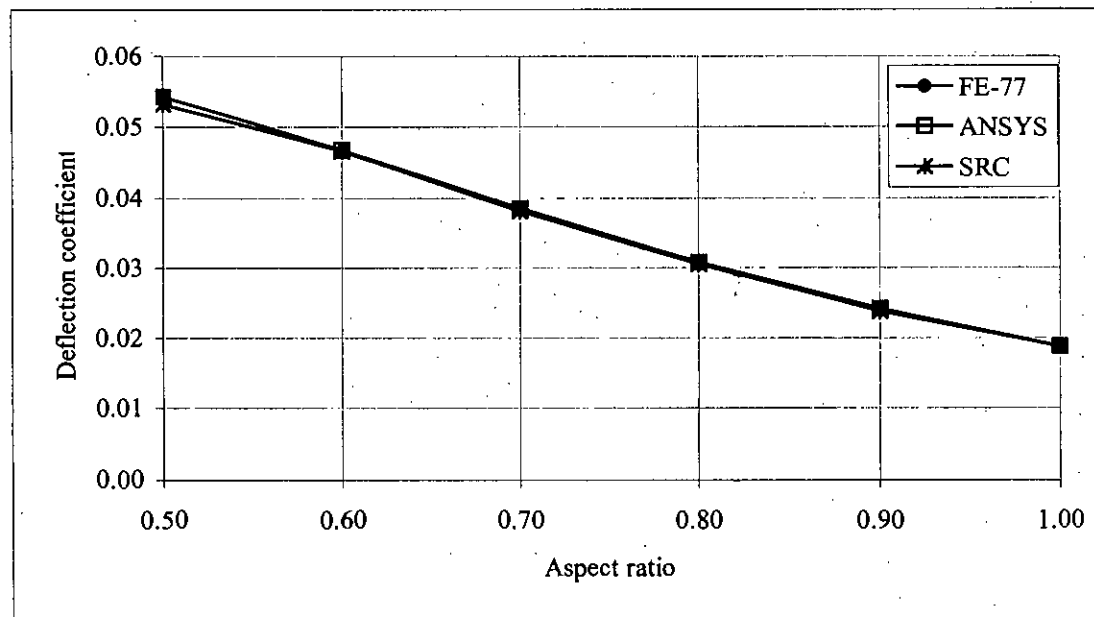


Figure 3.29 Variation of deflection coefficient with span ratio for short direction, case-8.

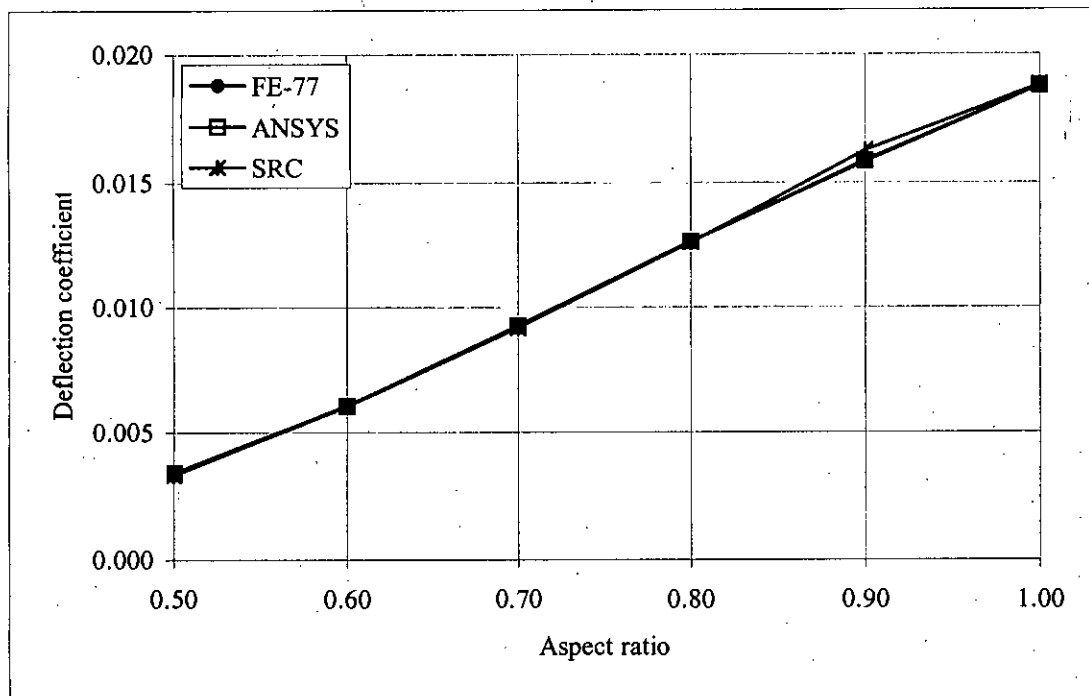


Figure 3.30 Variation of deflection coefficient with span ratio for long direction, case-8.

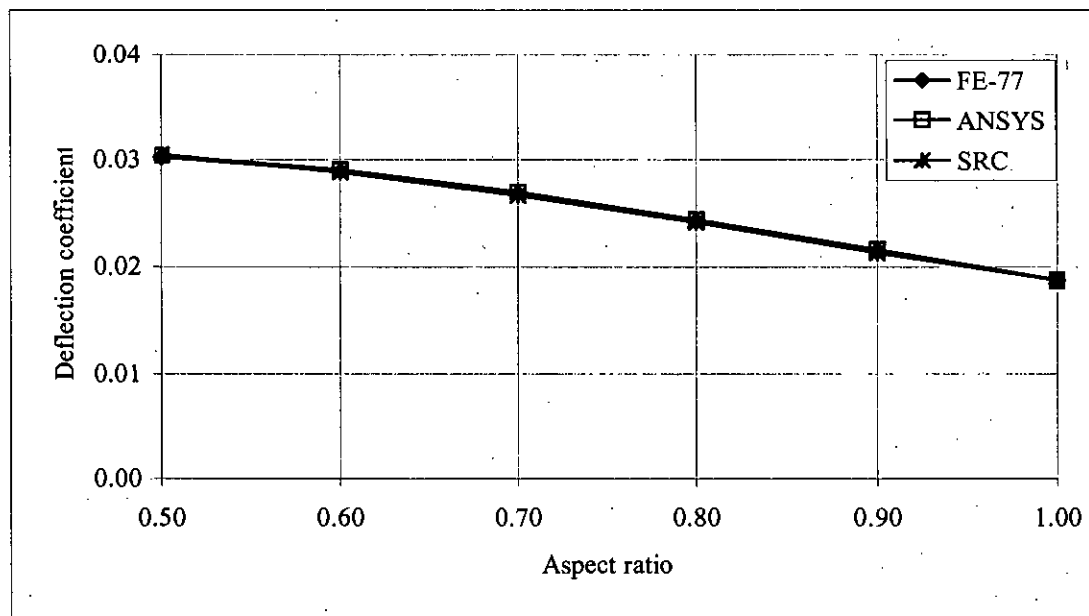
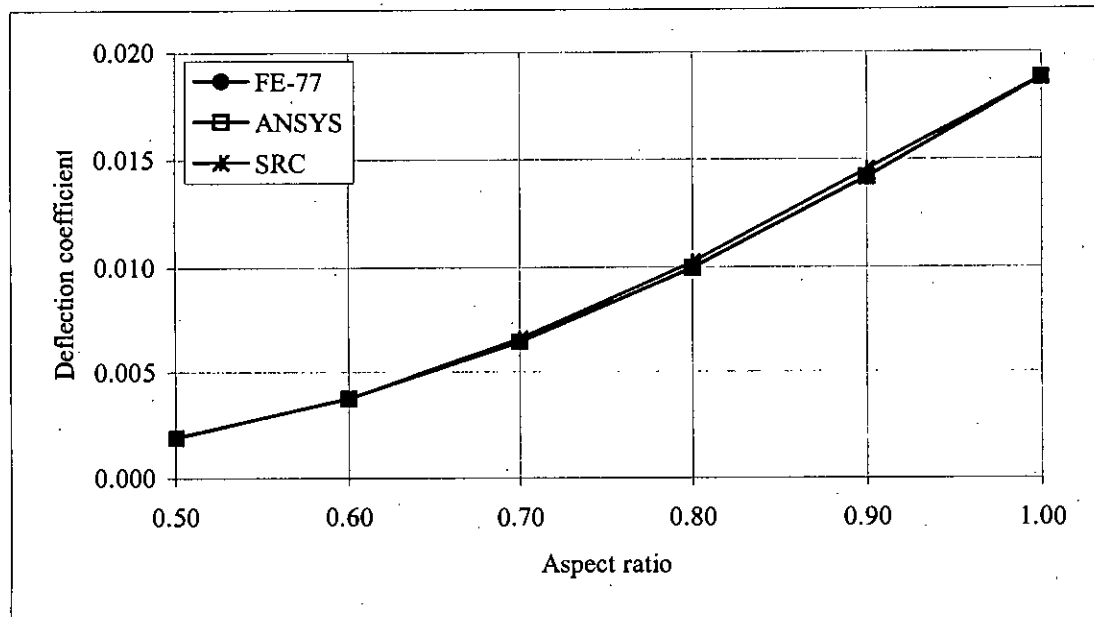


Figure 3.31 Variation of deflection coefficient with span ratio for short direction, case-9.





**Figure 3.32** Variation of deflection coefficient with span ratio for long direction, case-9.

### 3.6 Comparison of Midpoint Deflection of One-way Slab

The formulae for midpoint deflections of beam or one-way slab for different support conditions are tabulated in the Table 3.3. Using finite element analysis both FE-77 and ANSYS the midpoint deflections have been computed with the following parameters:

Span length of slab = 3048 mm

Slab thickness = 89 mm

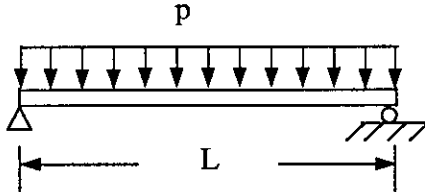
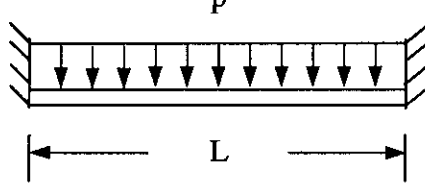
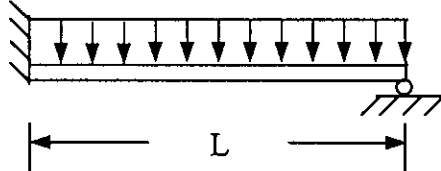
Total uniform load = 7.12 kN/m<sup>2</sup>

Modulus of elasticity of concrete,  $E_c = 20685 \text{ N/mm}^2$

Poisson's ratio  $\nu = 0.18$

The calculated results of deflections from both the FE analyses and calculated using formulae are shown in the Table 3.4. It has been observed that almost same results have been obtained from FE analyses and from formulae.

**Table 3.3** Midpoint deflections for different types of support

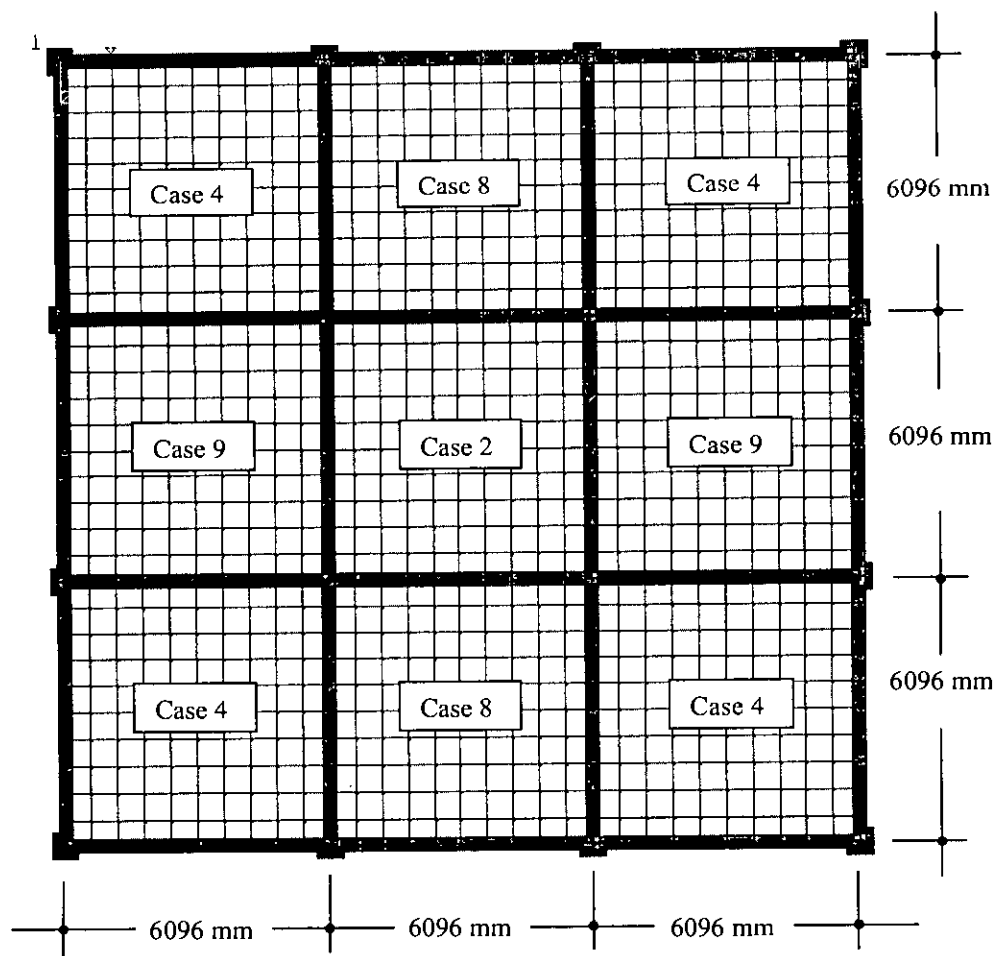
Beam with support condition	Deflection at midspan
	$w_c = 5pl^4 / 384EI$
	$w_c = pl^4 / 384EI$
	$w_c = pl^4 / 192EI$

**Table 3.4** Comparison of one-way slab deflection for different support conditions

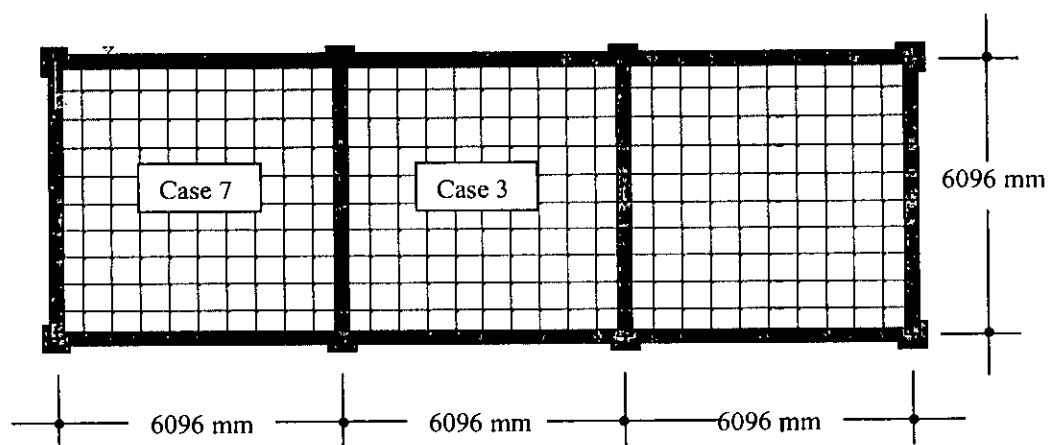
Support condition	Deflection (mm)				
	From formula	From FE analysis			
		FE-77		ANSYS	
			% variation wrt formula		% variation wrt formula
One end hinged and other end roller	6.590	6.6051	0.230	6.6136	0.36
Both end fixed	1.318	1.3170	0.080	1.3240	0.45
One end fixed and other end roller	2.636	2.6359	-0.004	2.6450	0.34

### 3.7 Comparison of Deflection for Full 3-D Building Model and Single Slab Model

In all the analyses performed so far, single slab panels were modeled with different boundary conditions. A more correct approach of modeling would be to consider multiple panels as in the real structure with beams and columns. This approach, though more rigorous and logical, will definitely involve more computational time. To check the correctness of using single panel analysis, parallel single panel and multiple panel analyses have been carried out for the same structure using ANSYS. For full 3-D modeling a  $3 \times 3$  span of column beam structure has been considered shown in Fig. 3.33(a). For full modeling the column dimension is  $381 \text{ mm} \times 381 \text{ mm}$  ( $15'' \times 15''$ ), beam dimension is  $305 \text{ mm} \times 610 \text{ mm}$  ( $12'' \times 24''$ ), slab thickness is  $135.4 \text{ mm}$  ( $5.33 \text{ inch}$ ) and center to center distance of columns has been considered as  $6096 \text{ mm}$  ( $20 \text{ ft}$ ). In full 3-D modeling the beam size has been considered as  $254 \text{ mm} \times 508 \text{ mm}$  ( $10'' \times 20''$ ) for slab cases 6 and 7. The mesh density of slab for both modeling has been taken same i.e.  $10 \times 10$  for each panel. For full modeling each beams are divided into 10 divisions. The relevant material properties for both modeling have been considered the same. The other common parameters are modulus of elasticity concrete,  $E_c = 20685 \text{ N/mm}^2$ , Poisson's ratio,  $\nu = 0.18$  and total load applied on the slab is  $14.37 \text{ kN/m}^2$  ( $300 \text{ psf}$ ). The calculated deflections for both analyses are presented in the Table 3.5 for different slab cases. From FE analysis single slabs deflections are found slightly higher than full 3-D modeling of the building and it is conservative for the calculation of elastic deflection of edge supported slab. Hence single slab modeling for calculation of elastic deflection is conservative and less time consuming than 3-D full building modeling.



(a)



(b)

Figure 3.33 Full 3-D modeling of the building with slab and beam.

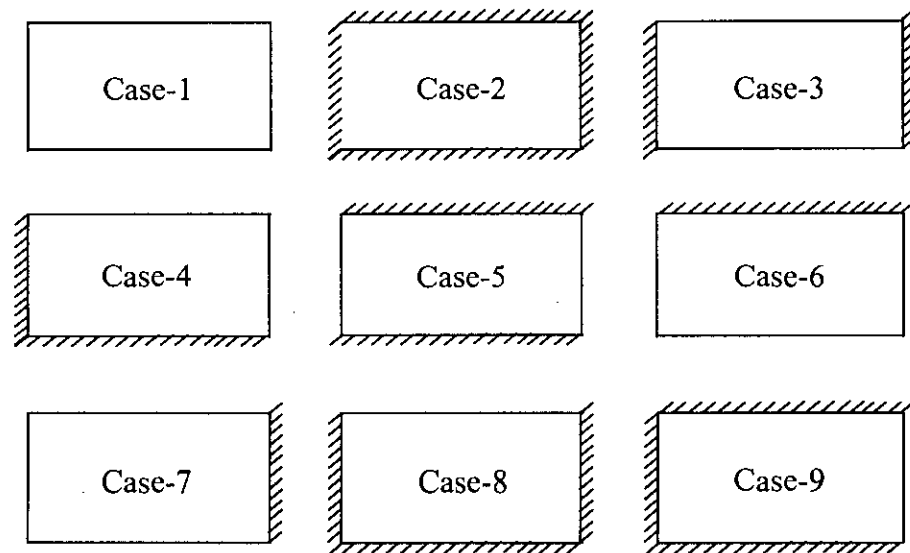


**Figure 3.34** Figures of different slab cases (A crosshatched edge indicates that the slab continues across, or is fixed at, the support; an unmarked edge indicates a support at which torsional resistance is negligible).

**Table 3.5** Comparison of deflection calculated from single slab model and full 3-D building model

Slab case	Deflection (mm)		% variation wrt full model
	Single panel model	Full 3-D model	
Case-2	5.77	5.05	14.2
Case-3	8.64	8.28	4.4
Case-4	9.73	8.89	9.4
Case-5	8.64	8.28	4.4
Case-6	12.67	12.11	4.7
Case-7	12.67	12.11	4.7
Case-8	7.19	6.75	6.5
Case-9	7.19	6.75	6.5

98247

### 3.8 Deflection and Moment Coefficients of Edge Supported Slabs

From finite element analysis, it has been found that the results of FE-77 and ANSYS are identical which are discussed in the sections 3.3 to 3.6. The moment coefficients are found different against ACI moment coefficients because of consideration of inelastic redistribution in ACI moment coefficient. Deflection coefficients and moment coefficients of edge supported slabs have been calculated from elastic FE analysis. It is logical to use elastic moments for the calculation of immediate deflection (considering cracking) of edge supported slab. The deflection coefficients are presented in Table 3.6 for easy calculation of elastic deflection. A designer can calculate the elastic deflection at the center of any categories of slab using the following equation:

$$\text{Elastic deflection, } \delta = D_a \frac{wl^4}{Et^3} \quad (3.4)$$

where,

$D_a$  = elastic deflection coefficient in short direction

$w$  = total load applied on the slab

$l$  = span length of slab in short direction

$E$  = modulus of elasticity of concrete

$t$  = total thickness of slab

From finite element analysis, it has been observed that under service load, most of the edge supported slabs are cracked i.e., developed flexural stresses are greater than modulus of rupture of concrete. It is obvious that the immediate deflection of slab will be greater than the elastic deflection due to cracking of slab. For calculation of immediate deflection considering cracking, it is important to find the maximum stress developed in the slab. For this purpose the elastic moment coefficients are also proposed in Table 3.7 for calculation of elastic stress developed in the slab without FE analysis. From FE analysis the stresses developed at the most cracked zone of slabs (nine categories) have been computed and moment coefficients of those respective zone have been proposed. Using Eqn. (3.1) the maximum stress developed in the slab can be calculated without FE analysis.

**Table 3.6** Deflection coefficients for elastic deflection of two-way edge supported slab center, considering short direction

Aspect Ratio ( $m = l_x/l_y$ )	Case-1 ( $10^{-2}$ )	Case-2 ( $10^{-2}$ )	Case-3 ( $10^{-2}$ )	Case-4 ( $10^{-2}$ )	Case-5 ( $10^{-2}$ )	Case-6 ( $10^{-2}$ )	Case-7 ( $10^{-2}$ )	Case-8 ( $10^{-2}$ )	Case-9 ( $10^{-2}$ )
1.00	4.8332	1.4817	2.2542	2.5977	2.2542	3.3789	3.3789	1.8824	1.8824
0.95	5.3403	1.6346	2.6233	2.8652	2.3654	3.6324	3.8357	2.1365	2.0212
0.90	5.8970	1.7956	3.0585	3.1581	2.4741	3.8963	4.3553	2.4208	2.1615
0.85	6.5050	1.9635	3.5701	3.4673	2.5797	4.1679	4.9434	2.7368	2.3019
0.80	7.1650	2.1347	4.1703	3.7889	2.6800	4.4433	5.6053	3.0811	2.4367
0.75	7.8762	2.3052	4.8693	4.1256	2.7738	4.7184	6.3445	3.4545	2.5705
0.70 ++	8.6363	2.4706	5.6761	4.4743	2.8584	4.9872	7.1617	3.8563	2.6947
0.65	9.4385	2.6265	6.5951	4.8013	2.9333	5.2471	8.0521	4.2573	2.8051
0.60	10.271	2.7673	7.6256	5.1483	2.9949	5.4992	9.0088	4.6809	2.9035
0.55	11.124	2.8870	8.7539	5.4484	3.0420	5.7371	10.013	5.0783	2.9800
0.50	11.971	2.9801	9.9548	5.7246	3.0752	5.9472	11.048	5.4410	3.0390

**Table 3.7** Moment coefficients for calculation of maximum stress in the slab

Aspect ratio ( $m = l_a/l_b$ )	Case-1	Case-2	Case-3	Case-4	Case-5	Case-6	Case-7	Case-8	Case-9
	$C_a(+)$	$C_a(-)$	$C_b(-)$	$C_a(-)$	$C_a(-)$	$C_a(-)$	$C_b(-)$	$C_a(-)$	$C_a(-)$
1.00	0.0403	0.0439	0.064	0.0577	0.064	0.0762	0.0767	0.0468	0.0529
0.90	0.0483	0.0505	0.0588	0.0668	0.0681	0.0844	0.0683	0.0557	0.0589
0.80	0.0578	0.0572	0.0523	0.0761	0.0717	0.0919	0.0587	0.066	0.0643
0.70	0.0688	0.0646	0.0446	0.0856	0.0755	0.1002	0.0482	0.0783	0.07
0.60	0.081	0.0704	0.0357	0.0947	0.0778	0.107	0.0373	0.0904	0.0741
0.50	0.0941	0.0746	0.0261	0.1024	0.0787	0.112	0.0267	0.1012	0.0766

### 3.9 Conclusion

In this chapter the performances of the softwares FE-77 and ANSYS have been studied. A mesh sensitivity analysis revealed the required mesh size for a correct FE analysis. The moment coefficients of edge supported slabs have been calculated using program FE-77 and ANSYS and compared with ACI coefficients. Most of the slab cases the ACI coefficients are significantly different from FE results. The deflection coefficients have been calculated from both programs for easy calculation of elastic deflection of slab. The midpoint deflections of one-way slab for different end conditions have been verified with FE-77 and ANSYS. The elastic deflections of slabs by 3-D full building modeling and single slab modeling have been compared and conservative results have been found in single slab modeling. For calculation of elastic deflection of slab, deflection coefficients and for calculation of maximum stress, moment coefficients have been proposed in tabular forms. However, it must be noted that slabs are usually cracked under service loads and deflection calculations need to include effect of cracking which is done in the next chapter.



## CHAPTER 4

### NONLINEAR FINITE ELEMENT ANALYSIS

#### 4.1 Introduction

In Chapter 2, the methods for calculation of slab deflection using elastic and nonlinear analysis have been discussed. In Chapter 3, the performances of the software FE-77 and ANSYS have been studied and moment coefficients and deflection coefficients of edge supported slabs have been proposed for calculation of slab deflection. In the current chapter, Hossain's (1999) nonlinear finite element model is presented for calculation of immediate deflection of slab. The performance of Hossain's nonlinear FE module incorporated in FE-77 is verified with the experimental results of McNeice (1971) corner supported slab, McNeice (1967) one-way slab and Shukla and Mittal (1976) slabs. A thorough parametric study to identify the effects of different parameters on deflection of two-way edge supported slabs is carried out. The difference of immediate deflection considering cracking and elastic deflection is compared with variation of applied load on the slab. Mesh sensitivity analysis is performed for the calculation of immediate deflection of slab. The effects of concrete strengths ( $f'_c$ ), excess reinforcement and slab thickness on slab deflection are studied. The immediate deflections of slab are checked against ACI allowable limits for varying slab thickness and loads.

To prepare a new approach for calculation of immediate deflection of slab considering cracking deflection ratio vs. stress ratio curves are proposed. From this approach, a designer will be able to calculate the immediate deflection of slab without FE analysis. To identify the effects of different parameters on deflection ratio vs. stress ratio curves a thorough parametric study is carried out.

#### 4.2 Description of Hossain's Nonlinear Finite Element Program Module

A program module based on global plate stiffness approach has been developed by Hossain (1999) to incorporate the different short- and long-term models for predicting deflection of reinforced concrete slabs. The module acts as an integral part of the FE package FE-77 (1999) and calculates modified elastic properties to represent cracking, creep and shrinkage for each element, on the basis of stresses of FE solution, which are then fed back into the assembly module of the FE package. Hossain and Vollum (2002) found good correlation in the analysis of the real full scale 7 storied building at Cardington using this FE module employing EC2 (1992) and CEB-FIP Model Code 1990 (MC-90, 1990) where creep and shrinkage deflections have been dealt with more rigorously along with the effect of construction load. Deflection estimation procedure in ACI Code is simpler than these codes where long-term deflections are calculated from instantaneous deflection using multiplier. Branson's crack model (1977) which is adopted in the ACI Code (2002) has been used in the current work to calculate instantaneous deflection.

Within the FE program, elastic moments in two principal directions for each element are calculated in the first run which are then used to calculate the effective moment of inertia in two principal directions using Branson's (1977) equation:

$$\begin{aligned}
 I_{e1} &= \left( \frac{M_{cr}}{M_1} \right)^3 I_g + \left[ 1 - \left( \frac{M_{cr}}{M_1} \right)^3 \right] I_{cr1} \\
 I_{e2} &= \left( \frac{M_{cr}}{M_2} \right)^3 I_g + \left[ 1 - \left( \frac{M_{cr}}{M_2} \right)^3 \right] I_{cr2}
 \end{aligned}
 \tag{4.1}$$

where,  $I_g$  and  $I_{cr}$  are gross and cracked moment of inertia of slab element.  $M_{cr}$  is the moment at which cracks occur and  $M_1$  and  $M_2$  are the principal moments.

### 4.3 Sequence of Analysis

A flow chart describing the incorporation of the ACI / Branson's model is shown in Fig. 4.1. First, the analysis is carried out on the slab with gross concrete section (without reinforcement) using QD09 (general shell and plate bending element with nine nodes) elements. The FE solution gives deflections and stresses at all nodes. Stresses are calculated in principal directions from x-y directional stresses. Gross moment of inertia  $I_g$  and cracked moment of inertia  $I_{cr}$  are calculated for two principal directions. Effective moment of inertias are calculated using  $\sigma/\sigma_r$  ratios in both principal directions. Factors to modify the  $[E']$  matrices in the principal directions are calculated comparing effective moment of inertia and corresponding gross moment of inertia. The modified  $[E']$  matrices are then transformed into global x-y directions from principal directions. With the modified set of  $[E']$  matrices, the FE package gives the desired solution of stresses and deflections.

The incorporation of the ACI model to calculate the effective moment of inertia are presented in section 4.4. Once modification factors are calculated using Eqn. (4.5), modified  $[E']$  matrices are formed in the principal directions and then transformed into global x-y directions as described in section 4.5.

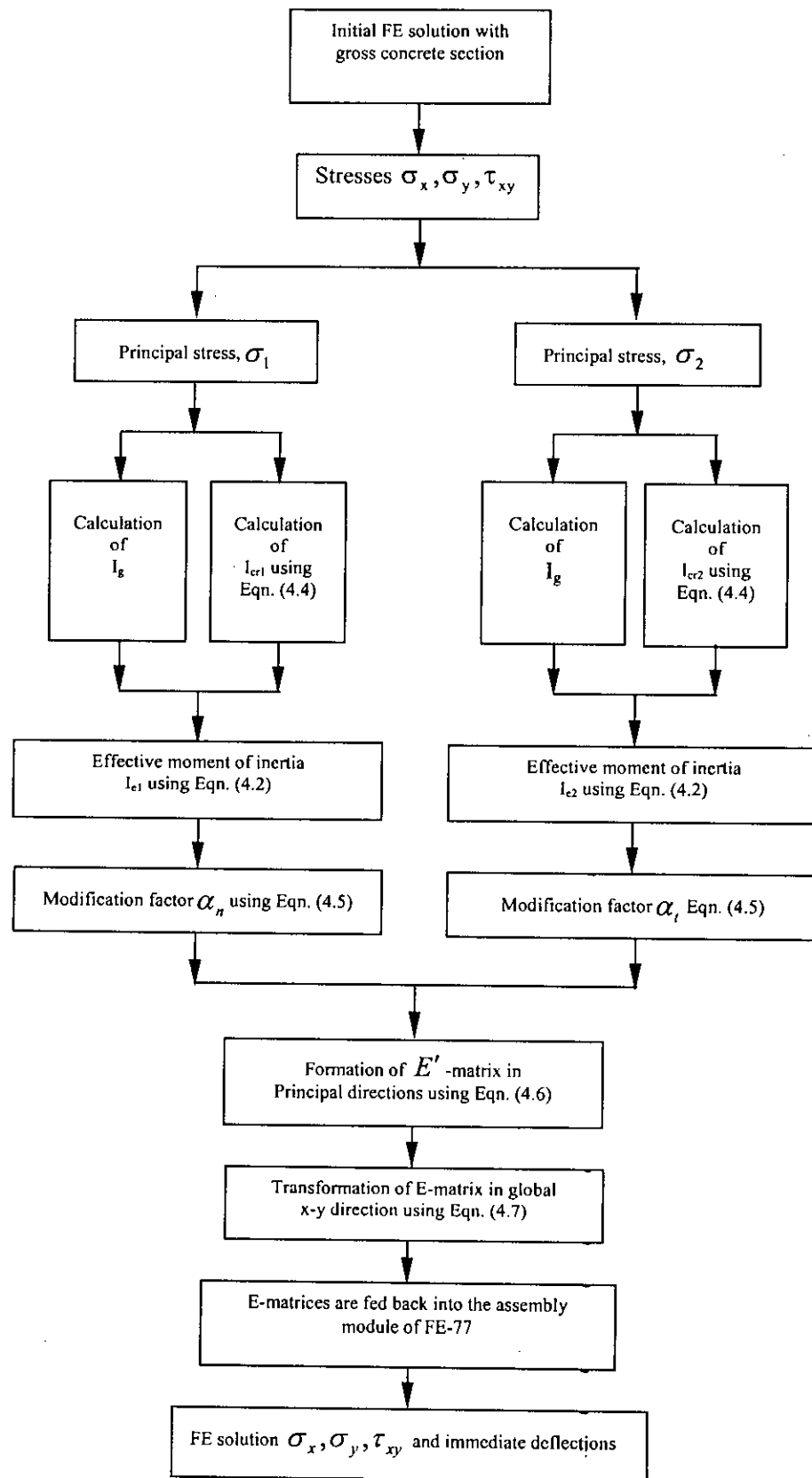


Figure 4.1 Flow chart showing the sequence of calculation

#### 4.4 Incorporation of ACI Method

The effective moment of inertia adopted by the ACI Building Code (2002) was discussed in section 2.5.1. The method uses the ratio of the section cracking moment to the applied moment to interpolate between uncracked and fully cracked states. In the present work, the ratio of modulus of rupture to principal tensile stress at the face of the section i.e.  $(f_r/\sigma_1)$  or  $(f_r/\sigma_2)$  is used instead of  $(M_{cr}/M)$  in Eqn. (2.6). The following equations are used to calculate the effective moment of inertia in the major and minor principal directions, respectively:

$$I_{e1} = \left(\frac{f_r}{\sigma_1}\right)^3 I_g + \left[1 - \left(\frac{f_r}{\sigma_1}\right)^3\right] I_{cr1} \quad (4.2)$$

$$I_{e2} = \left(\frac{f_r}{\sigma_2}\right)^3 I_g + \left[1 - \left(\frac{f_r}{\sigma_2}\right)^3\right] I_{cr2}$$

where  $\sigma_1$  and  $\sigma_2$  are the two principal stresses at the surface of slab and  $I_{cr}$  is the moment of inertia of the fully cracked transformed section. Jofriet & McNiece (1971) used Eqns (2.27) and (2.26), respectively, to calculate the depth of neutral axis and the second moment of area of a fully cracked section. These equations do not take into account the presence of compression steel. In the current work, the depth of neutral axis and the second moment of area of a fully cracked section are calculated considering both tension and compression steel. The depth of neutral axis of a fully cracked section, considering both tension and compression steel, is given by:

$$c_n = \frac{-a_2 + \sqrt{a_2^2 - 4a_1 a_3}}{2a_1} \quad (4.3)$$

where,

$$a_1 = b/2$$

$$a_2 = nA_s + (n-1)A_{sp}$$

$$a_3 = -nA_s d - (n-1)A_{sp} d'$$

The second moment of area around the neutral axis is:

$$I_{cr} = \frac{bc_n^3}{3} + nA_s (d - c_n)^2 + (n-1)A_{sp} (d' - c_n)^2 \quad (4.4)$$

### The modification factor

For the ACI method, the modification factors, to account for cracking, are obtained similarly to Scanlon & Murraray approach (Eqn. 2.23) where calculations were performed in x and y directions. However, in the present work they are calculated in the major and minor principal directions:

$$\alpha_n = \frac{I_{e1}}{I_g}$$

$$\alpha_t = \frac{I_{e2}}{I_g}$$
(4.5)

where,  $\alpha_n$  and  $\alpha_t$  are the modification factors for major and minor principal directions respectively.

### 4.5 Formation of [E] Matrices

In the FE analysis, initially the 6×6 elasticity matrices for all the elements are defined as anisotropic, so that they can have different values in orthogonal directions. These matrices are then modified for each element using the modification factors  $\alpha_n$  and  $\alpha_t$  to incorporate cracking, by using Eqn. (4.5). The modified matrix in the principal directions is thus follows:

$$[E'] = \begin{bmatrix} \frac{\alpha_n E_c}{(1 - \alpha_n \alpha_t \nu^2)} & \frac{\alpha_n \nu \alpha_t E_c}{(1 - \alpha_n \alpha_t \nu^2)} & 0 \\ \frac{\alpha_t \nu \alpha_n E_c}{(1 - \alpha_n \alpha_t \nu^2)} & \frac{\alpha_t E_c}{(1 - \alpha_n \alpha_t \nu^2)} & 0 \\ 0 & 0 & \frac{E_c \sqrt{\alpha_n \alpha_t}}{2(1 + \nu \sqrt{\alpha_n \alpha_t})} \end{bmatrix}$$
(4.6)

These  $[E']$  matrices are then transformed into global directions using Eqn. (4.7).

$$[E] = [C_2]^T [E'] [C_2]$$
(4.7)

where  $[C_2]$  are transformation matrices.

A set of  $3 \times 3$  matrices for all the elements are obtained:

$$\begin{Bmatrix} \sigma_x \\ \sigma_y \\ \tau_{xy} \end{Bmatrix} = [E] \begin{Bmatrix} \varepsilon_x \\ \varepsilon_y \\ \gamma_{xy} \end{Bmatrix} \quad (4.8)$$

The global  $[E]$  matrix is then adjusted so that it can be used in the FE package (Hitchings, 1994). These  $[E]$  matrices for all the elements are written in a file which is subsequently read by the FE package in the next run and it modifies the global stiffness matrix accordingly. As the material elasticity, and hence the structural stiffness is modified, there will be redistribution of stresses. Hossain's module has the capability of continuing until a state of equilibrium between stress redistribution and material properties is reached. However, in the current work, effect of stress redistribution has been ignored and FE analyses are carried out only once with modified elastic properties. Polak's (1996) approach, discussed in section 2.5.4, also used a similar procedure ignoring effect of stress redistribution, as the effect of redistribution of stress on deflection is small.

#### 4.6 Comparison of Experimental Results

In this section, FE analysis results are verified with available experimental results. McNeice corner supported slab, McNeice one-way slab and Shukla & Mittal slabs have been analyzed for this purpose.

##### 4.6.1 McNeice Corner Supported Slab

McNeice slab (McNeice, 1967) has been widely used as a benchmark of modeling of slabs. It was 914 mm (36 in.) square by 44.45 mm (1.75 in.) thick and reinforced with an isotropic mesh giving a reinforcement ratio  $100A_s/bh = 0.85$ . It was supported at four corners and loaded by a central point load. All the material properties and details are taken from Jofriet & McNeice (1971); as modulus of rupture is not specified, it is assumed to be  $0.62\sqrt{f'_c}$  N/mm<sup>2</sup> ( $7.5\sqrt{f'_c}$  psi), according to ACI Code (2002). Details of the material properties, slab dimension, reinforcement and the finite element mesh used in the present analysis are shown

Fig. 4.2. Load verses immediate deflection curves for four nodes of experimental results and modeled results are presented in Figs 4.3 to 4.6. The FE results are similar to the experimental results.

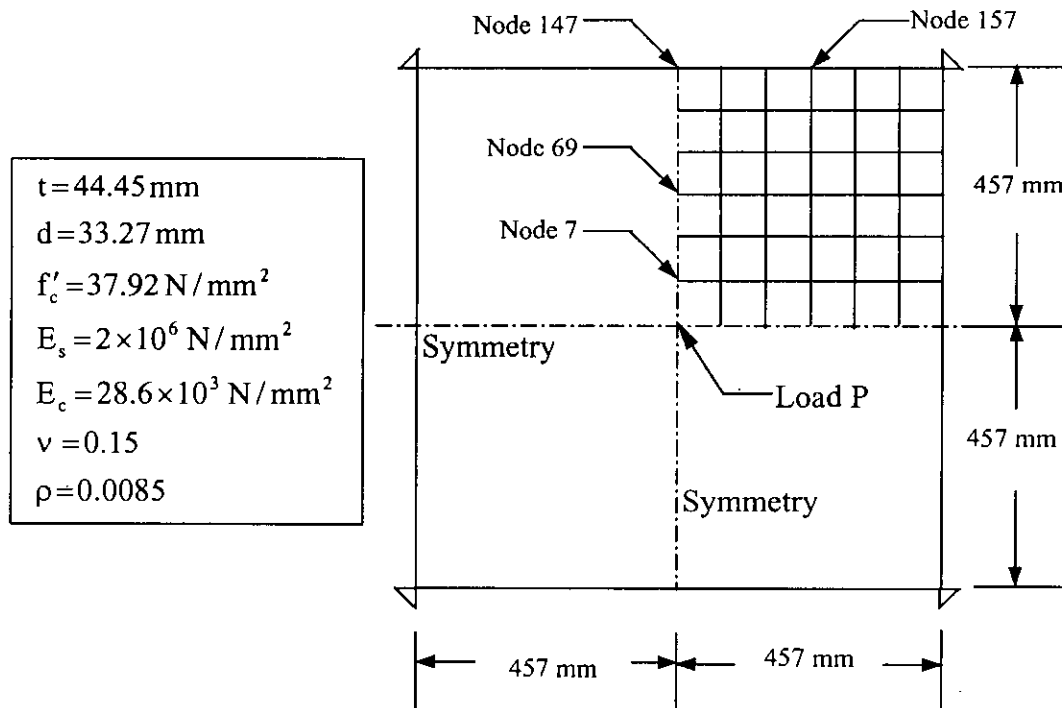


Figure 4.2 Details of corner-supported two-way slab tested McNeice.



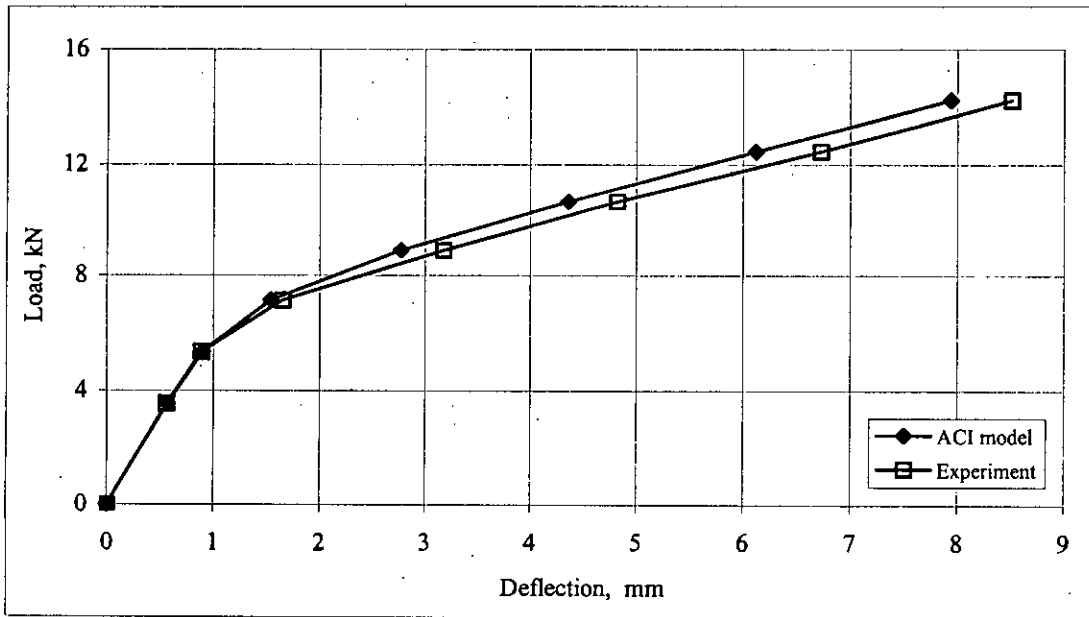


Figure 4.3 Load-deflection curve for the corner supported slab at node-7

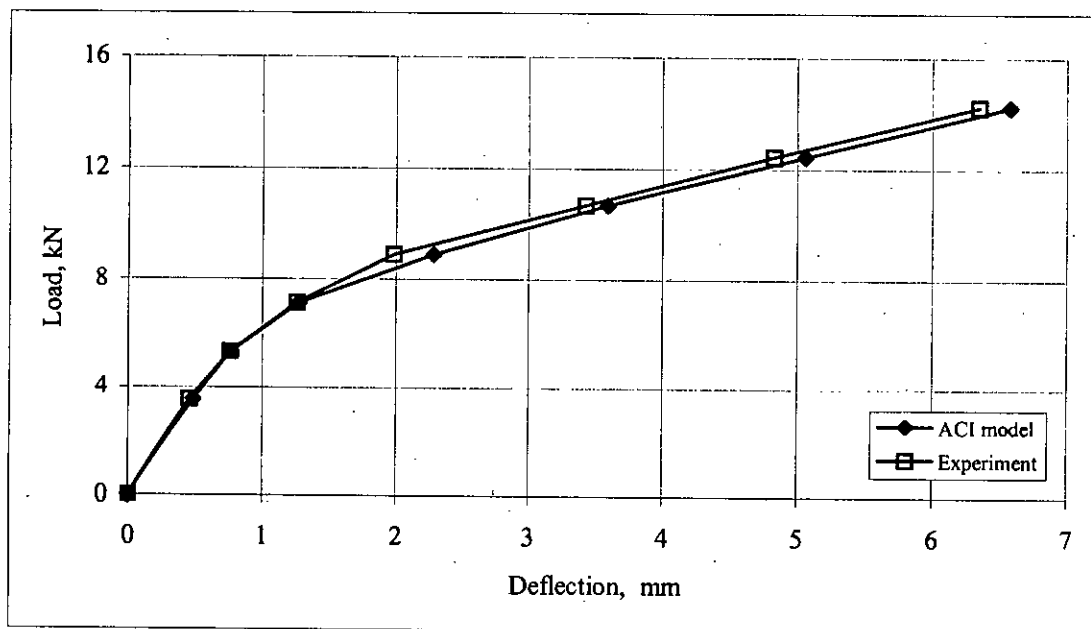


Figure 4.4 Load-deflection curve for the corner supported slab at node-69

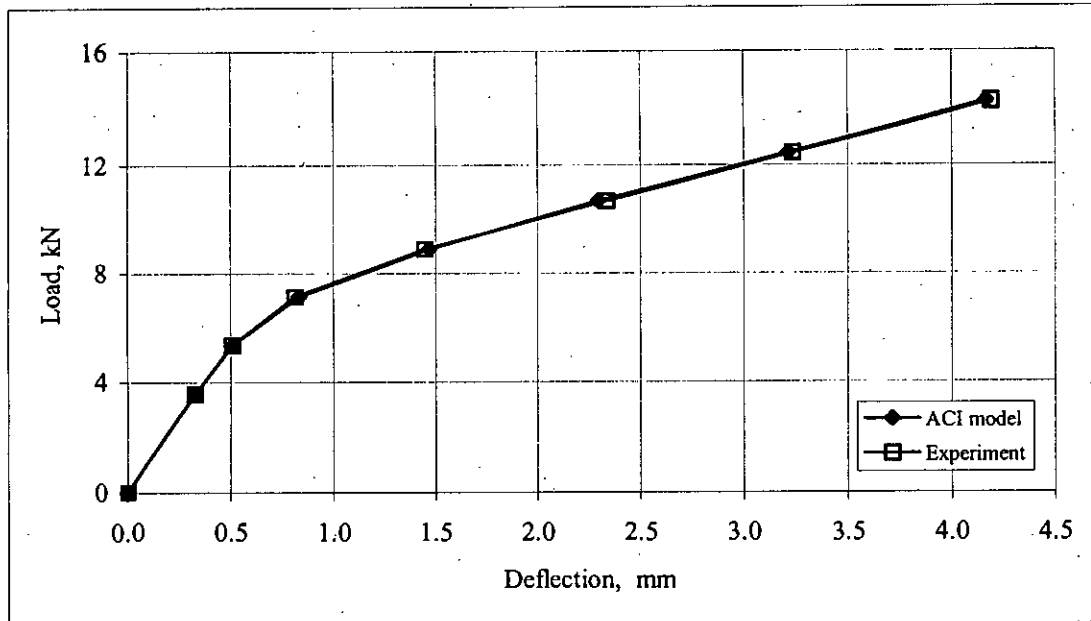


Figure 4.5 Load-deflection curve for the corner supported slab at node-147

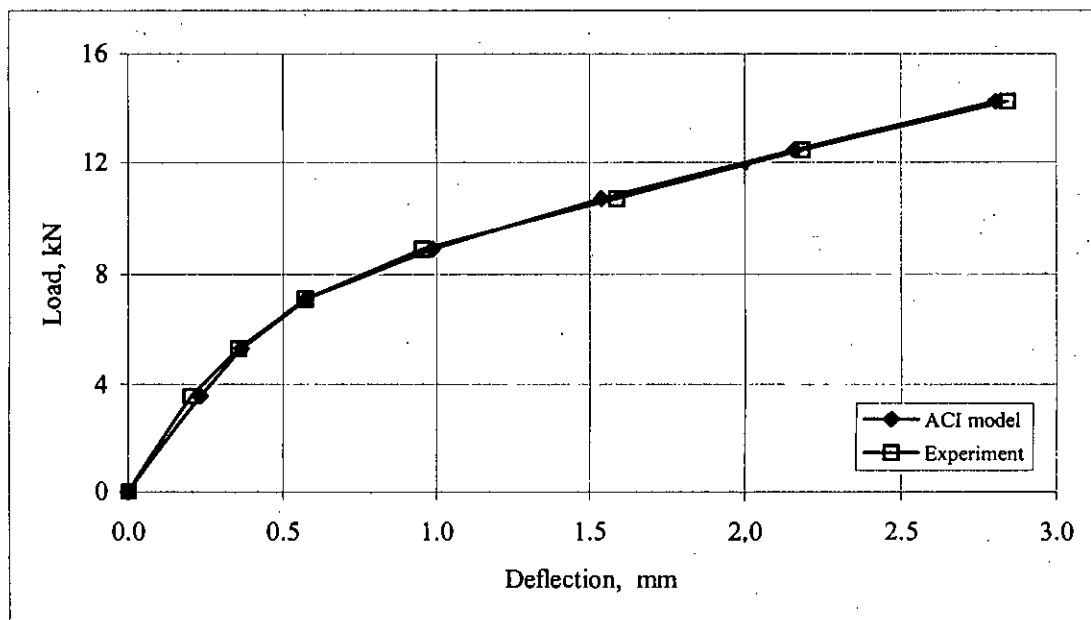


Figure 4.6 Load-deflection curve for the corner supported slab at node-157

#### 4.6.2 McNeice One-way Slab

A one-way slab, 304.8 mm wide by 44.5 mm thick, simply supported with a span of 863 mm and reinforced with 0.8 percent steel, was tested by McNeice (1967). Details of the materials properties and slab dimensions are shown in Fig. 4.7. Central deflections have been calculated with FE-77 analysis employing ACI model and compared with the experimental results shown in Fig. 4.8. The FE analysis results are similar to the experimental results.

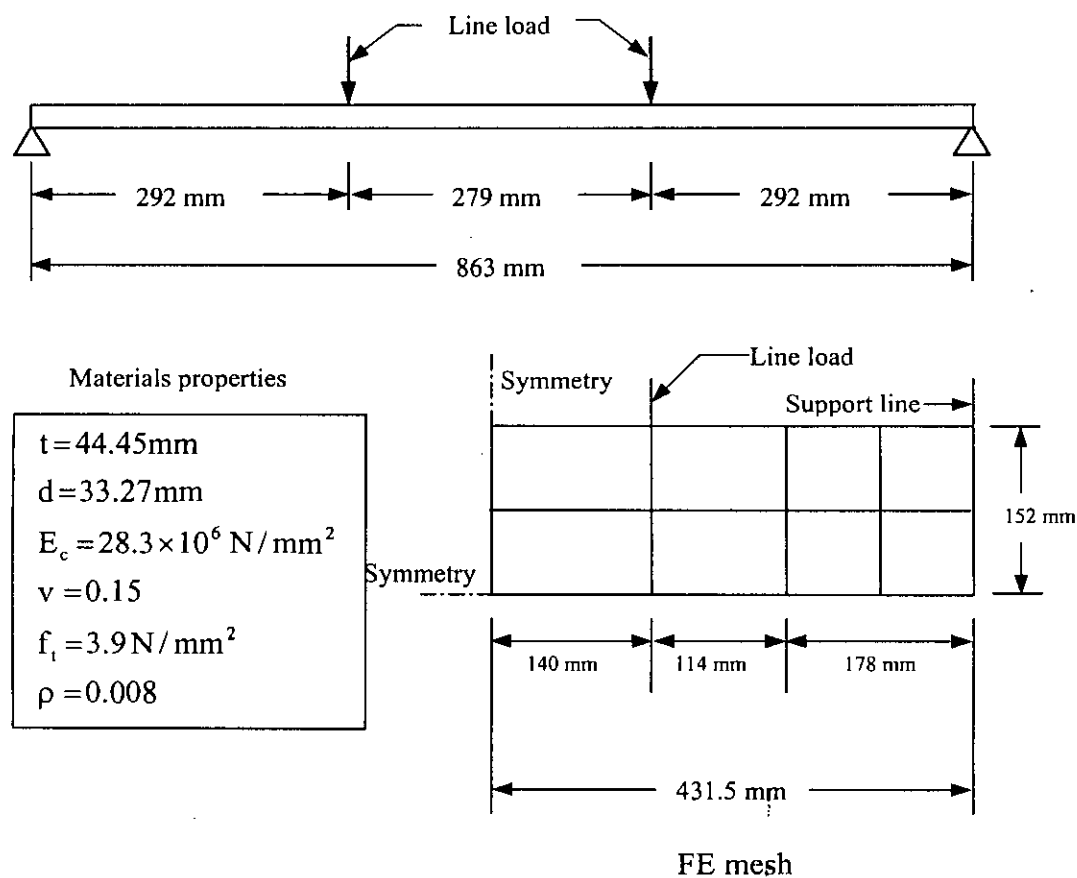
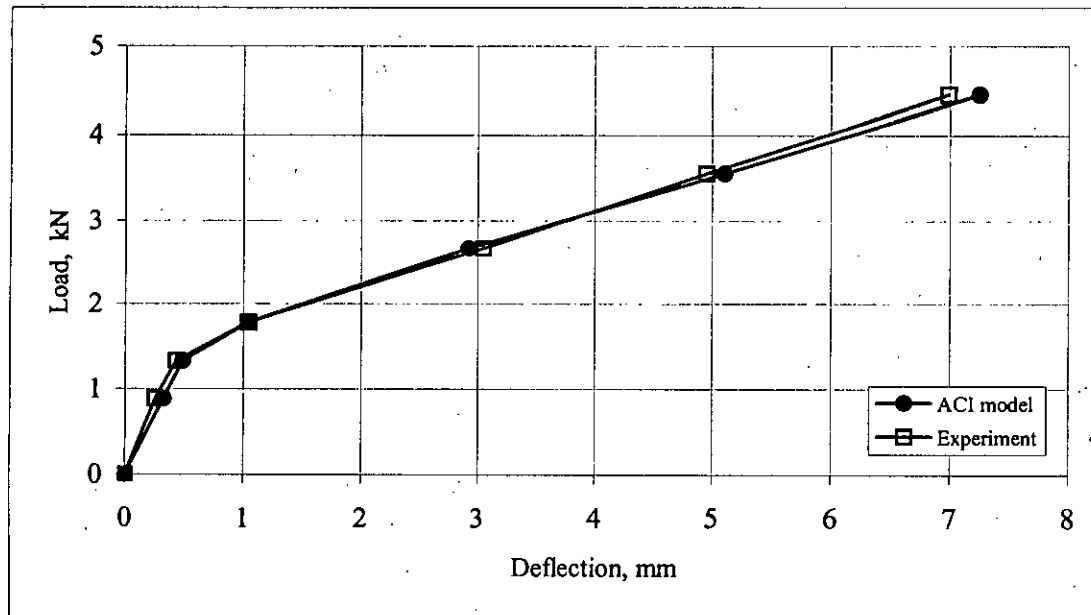


Figure 4.7 Details of simply supported one-way slab tested by McNeice: adapted from Jofriet & McNeice (1971)



**Figure 4.8** Load versus deflection curve for the simply supported one-way slab tested by McNeice

#### 4.6.3 Shukla and Mittal Slabs

Shukla & Mittal (1976) carried out a series of test on two-way edge supported slabs. All the slabs were 214 cm square and 8 cm thick. The slabs were supported on reinforced concrete walls with center to center span of 183 cm each way. Their corners were held down by means of 40 mm diameter steel rods anchored to the floor. Loads were applied to the test slab in increments of 2 Tons each through an inverted waffle-tree system, which transferred load at 16 equidistant point of the slab. Three slabs (S-8, S-11 and S-12) from this series have been analyzed here. S-8 and S-11 were isotropically reinforced with 10 mm bars to provide 5.24 and 4.36  $\text{cm}^2/\text{m}$  steel in each direction respectively. S-12 is reinforced with 10 mm and 6 mm bars to make an orthotropic slab with 5.24 and 1.35  $\text{cm}^2/\text{m}$  steel in two directions. The amount of top steel is not specified by the authors and it is assumed to have the same amount of steel as the bottom layer. The three slabs differ in concrete strength, which were 15.9 (S-8), 22.0 (S-11), 19.1(S-12)  $\text{N}/\text{mm}^2$ . Moduli of rupture and elasticity were not reported and hence have been estimated using the ACI equations (in  $\text{N}/\text{mm}^2$ ):

$$E_c = 4733 \sqrt{f'_c} \quad (4.9)$$

$$f_r = 0.62 \sqrt{f'_c} \quad (4.10)$$

Details of the slab dimensions and FE mesh are shown in Fig. 4.9. Experimental and FE based short-term load-deflection curves are compared for the central nodes of all the three slabs, and are presented in Figs 4.10 to 4.12. The results are similar to the experimental deflections.

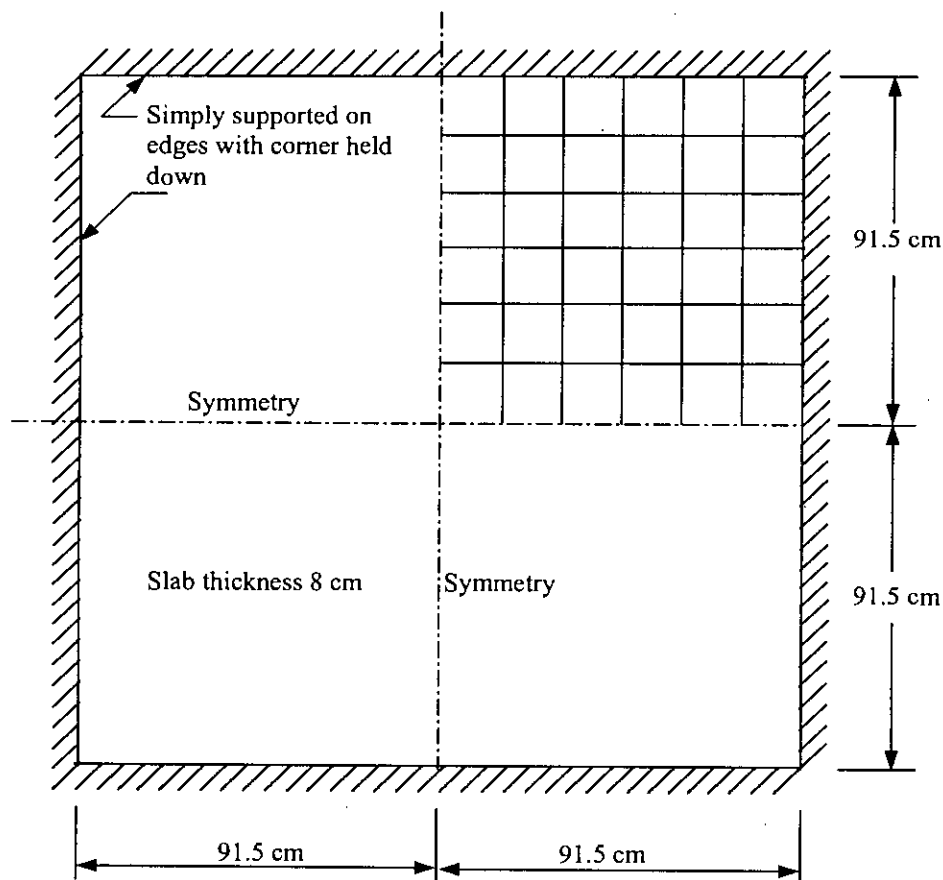


**Figure 4.9** Details of edge supported two-way slabs tested by Shukla & Mittal (1976).

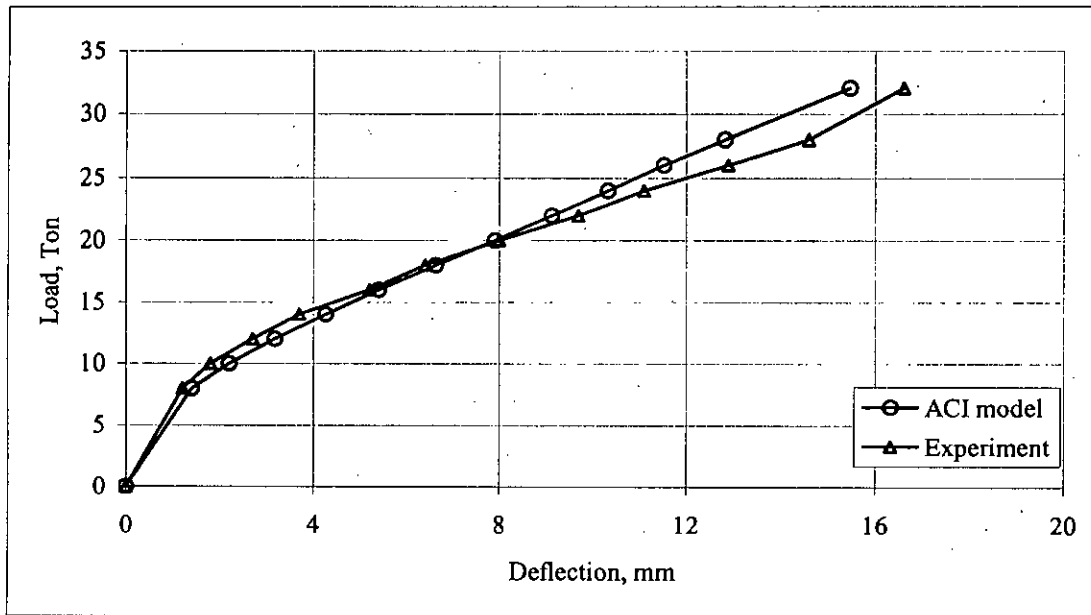


**Figure 4.10** Load versus deflection curves for the edge supported Shukla & Mittal slab S-8 using FE-77 analysis, employing ACI model.

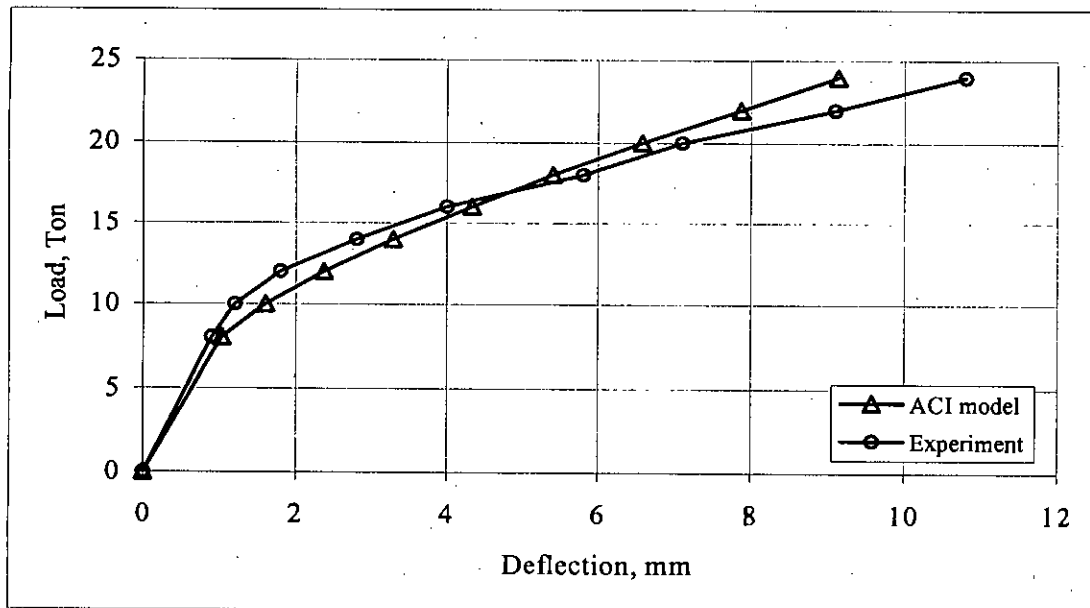


**Figure 4.11** Load versus deflection curves for the edge supported Shukla & Mittal slab S-11 using FE-77 analysis, employing ACI model.

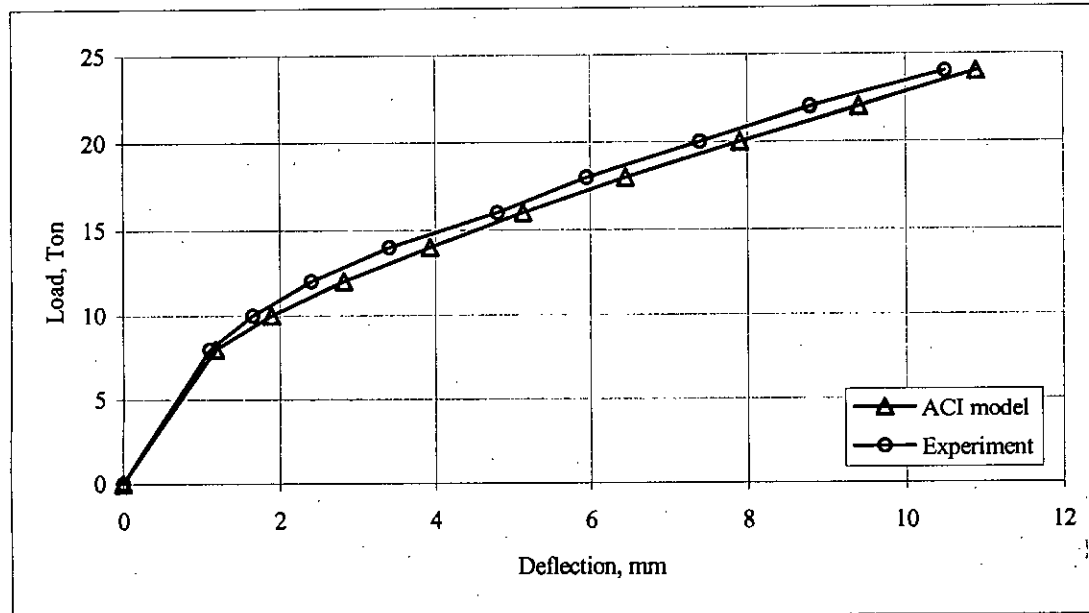


**Figure 4.12** Load versus deflection curves for the edge supported Shukla & Mittal slab S-12 using FE-77 analysis, employing ACI model.

#### 4.7 Sensitivity Analysis

To estimate the optimum number of elements for the purpose of the prediction of correct results, a sensitivity analysis has been performed with changing the number of elements and other parameters are taken as unchanged. For this purpose, two 4572 mm × 4572 mm (15' × 15') simply supported (case-1) and fixed supported (case-2) slabs have been modeled. For both slabs, the following parameters are used in the FE analysis:

- The slab thickness = Panel perimeter / 180 = 101.6 mm (4 inch)
- Total load applied on the slab for slab case-1 = 6.22 kN/m<sup>2</sup> (130 psf)
- Total load applied on the slab for slab case-2 = 19.63 kN/m<sup>2</sup> (410 psf)
- Concrete cylinder strength,  $f'_c = 20.7 \text{ N/mm}^2$  (3000 psi)
- Yield strength of steel,  $f_y = 413.7 \text{ N/mm}^2$  (60000 psi)
- Modulus of elasticity of concrete,  $E_c = 20685 \text{ N/mm}^2$  ( $3 \times 10^6$  psi)
- Modulus of elasticity of steel,  $E_s = 206850 \text{ N/mm}^2$  ( $30 \times 10^6$  psi)
- Poisson's ratio,  $\nu = 0.18$

- Modular ratio,  $n = 10$
- Modulus of rupture of concrete,  $f_r = 0.62\sqrt{f'_c}$  N/mm<sup>2</sup> ( $7.5\sqrt{f'_c}$  psi)
- The number of plate elements used in the analysis are  $4 \times 4 = 16$ ,  $6 \times 6 = 36$ ,  $8 \times 8 = 64$ ,  $10 \times 10 = 100$ ,  $12 \times 12 = 144$ ,  $16 \times 16 = 256$  and  $20 \times 20 = 400$  for  $1/4^{\text{th}}$  portion of the slab.

The effect of the variation of element number used in the finite element analysis has been verified by calculating the elastic and immediate deflection of slabs. In Figs 4.13 and 4.14, variation of elastic and immediate deflections with respect to number of elements are shown for slab case-1 and 2, respectively. From FE analysis, it has been observed that for both elastic and immediate deflections the number of plate elements equal or finer than  $10 \times 10 = 100$  have given more or less same results of deflections. So it can be concluded that the optimum number of element for  $1/4^{\text{th}}$  portion of a slab square panel is  $10 \times 10 = 100$ .

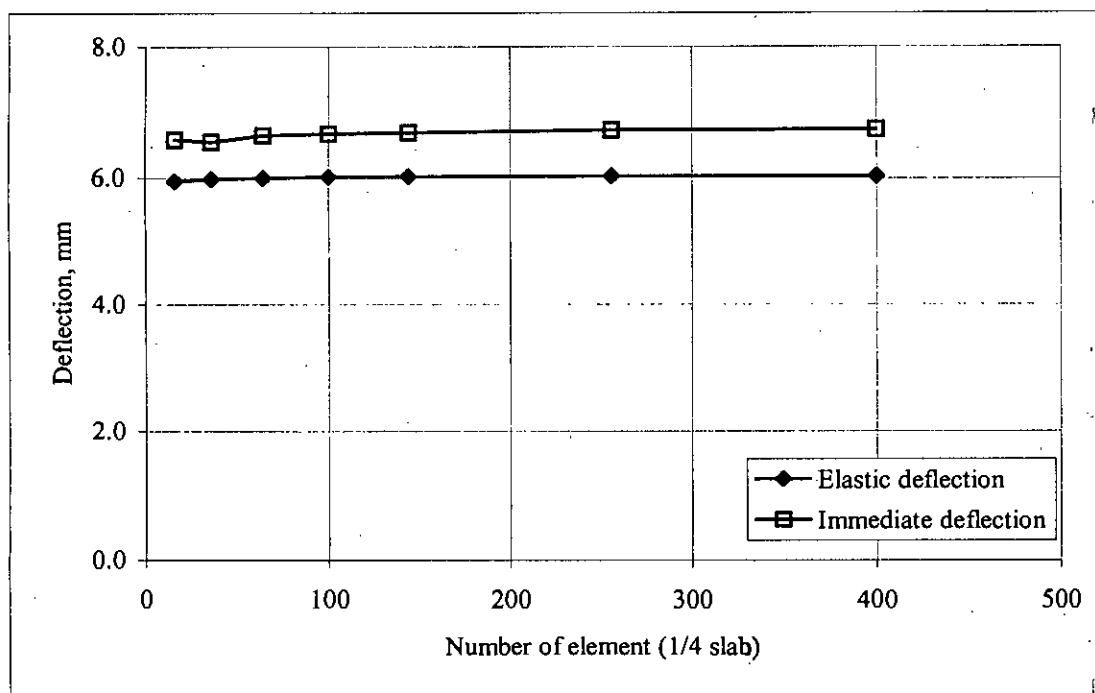


**Figure 4.13** Comparison of elastic and immediate deflection with respect to number of element of 4572 mm  $\times$  4572 mm slab for case-1.



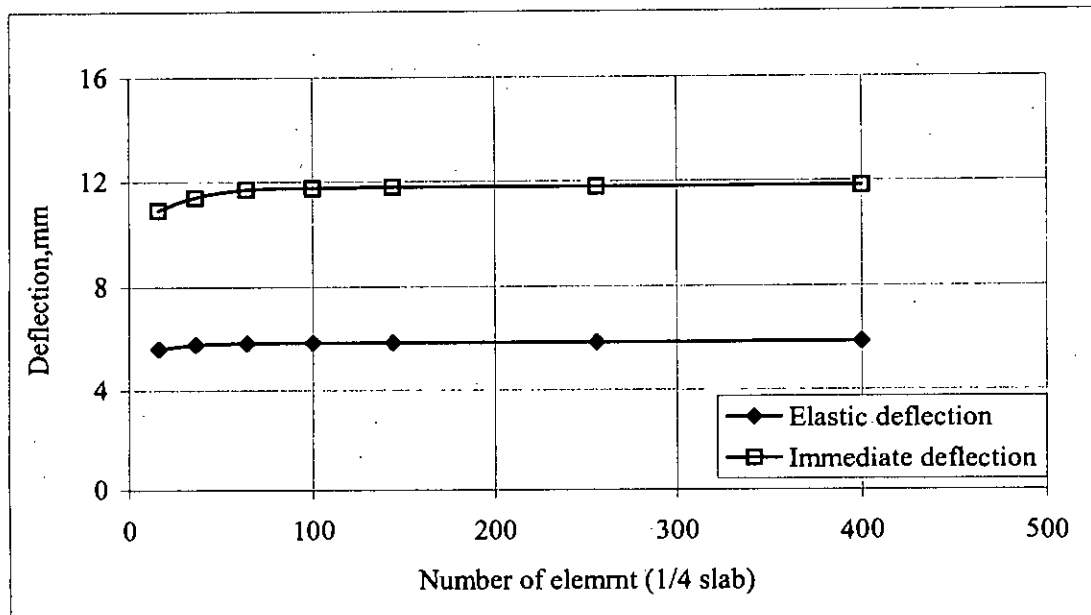


**Figure 4.14** Comparison of elastic and immediate deflection with respect to number of element of 4572 mm×4572 mm slab for case-2.

#### 4.8 Effect of Different Parameters on Deflection

The deflection of edge supported slab depends on different material and geometric parameters. It is important to study the effect of these parameters on deflection of slab. The parameters related to the deflection of edge supported slab are slab thickness, panel dimensions, loadings, material properties i.e. concrete compressive strength, modulus of rupture of concrete, modulus of elasticity of concrete etc. In this section the effects of the variation of these parameters on slab deflection are studied.

##### 4.8.1 Effect of Load on Elastic and Immediate Deflection of Slab

When a reinforced concrete member is subjected to bending at low range of loading it behave nearly elastically i.e. stress and strains are quite closely proportional. In this proportional range of stress-strain curve the corresponding deflection of a loaded slab is called elastic deflection. For a heavily loaded slab or flexural member

when the stress-strain curve is not proportional or the tensile stress of a concrete member exceeds its modulus of rupture then crack propagates from tension zone to neutral axis and reduces the effective area of concrete as well as moment of inertia. Due to effect of cracking the deflection of slab might be more excess than elastic deflection and it is called immediate or short-term deflection. To study the change in elastic and immediate deflection for varying loads a 7620 mm×5334 mm (25'×17.5') slab is modeled with FE analysis considering following parameters presented in the Table 4.1.

**Table 4.1** Parameters for elastic and immediate deflection of slab for varying load.

Concrete cylinder strength, $f'_c$	Modulus of elasticity of concrete, $E_c$	Poisson's ratio, $\nu$	Modulus of elasticity of steel, $E_s$	Slab thickness
27.6 N/mm <sup>2</sup> (4000 psi)	24856 N/mm <sup>2</sup> ( $3.6 \times 10^6$ psi)	0.18	206850 N/mm <sup>2</sup> ( $30 \times 10^6$ psi)	$t = \text{perimeter}/180$ (143.93 mm)

The two levels of modulus of rupture of concrete used in this analysis are  $f_r = 0.62\sqrt{f'_c}$  N/mm<sup>2</sup> ( $7.5\sqrt{f'_c}$  psi) and  $0.33\sqrt{f'_c}$  N/mm<sup>2</sup> ( $4\sqrt{f'_c}$  psi). The total load applied on the slab in the range of 7.22 to 12 kN/m<sup>2</sup> (150 to 250 psf). The modeling details of the slab are shown in the Fig. 4.15. The half portion of the slab is modeled with  $16 \times 24 = 384$  number of plate elements. From FE analysis the results of elastic and immediate deflections for both rupture strengths of concrete have been presented in Fig. 4.16. It has been observed that the immediate deflection is greater than the elastic deflection for different loadings and both deflections increased almost linearly against increasing of load applied on the slab.

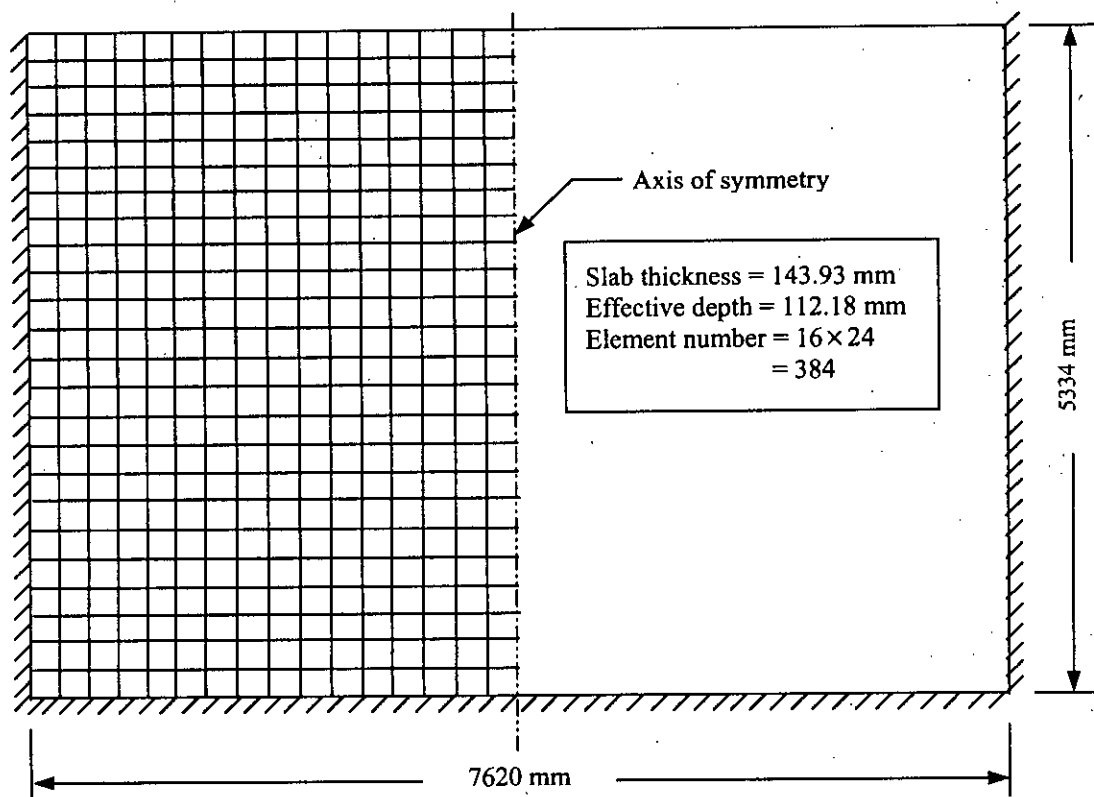


Figure 4.15 Details of slab modeling with FE meshing for case 8.

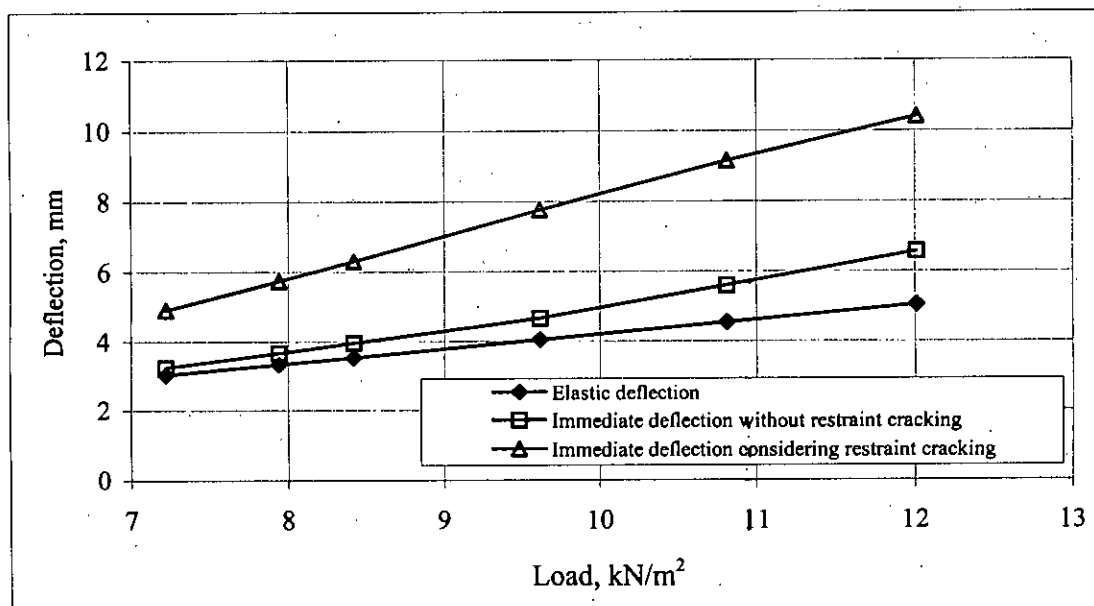
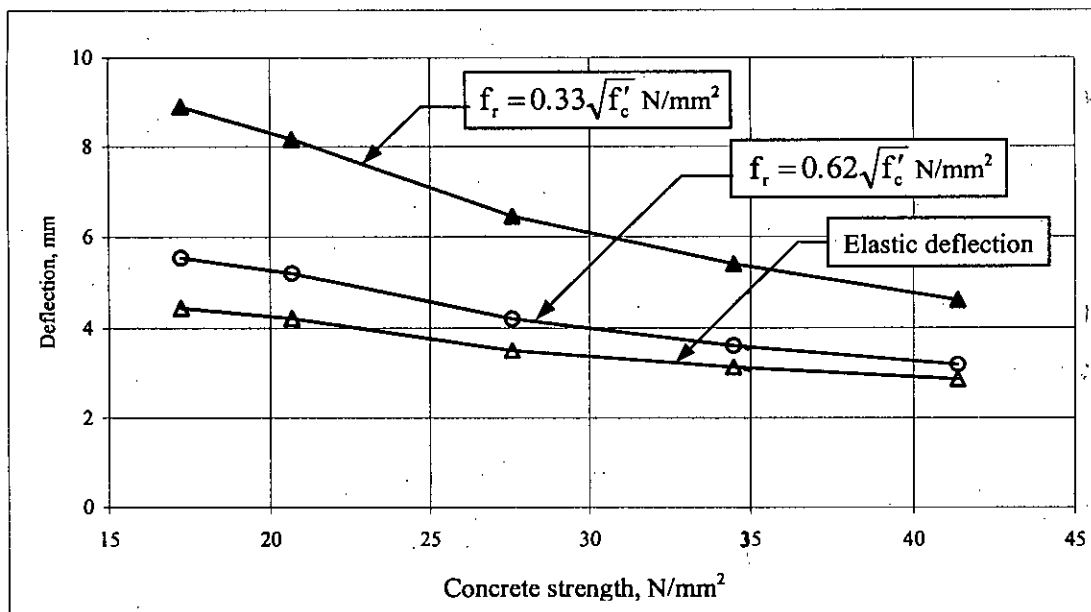


Figure 4.16 Comparison of elastic and immediate deflection of 7620 mm  $\times$  5334 mm slab for case-8.

#### 4.8.2 Effect of concrete strength on deflection

To identify the effect of concrete strength ( $f'_c$ ) on deflection, a 6096 mm  $\times$  6096 mm (20'  $\times$  20') slab for case-2 has been modeled considering ACI Code (1963) suggested slab thickness i.e. panel perimeter divided by 180 ( $t = 135.47$  mm) and total uniformly distributed load applied on the slab is 10.6 kN/m<sup>2</sup>. The 1/4<sup>th</sup> portion of the slab has been modeled with  $16 \times 16 = 256$  number of shell elements. The concrete strength was varied from 17.2 N/mm<sup>2</sup> to 41.4 N/mm<sup>2</sup> (2500 psi to 6000 psi). The modulus of rupture of concrete has been considered in the FE analysis are  $f_r = 0.62\sqrt{f'_c}$  N/mm<sup>2</sup> and  $0.33\sqrt{f'_c}$  N/mm<sup>2</sup>. The immediate deflection at central point of the slab has been considered for different concrete strength and modulus of rupture. The variation of immediate deflections for different concrete strength and rupture strength of concrete are presented in the Fig. 4.17. From the FE analysis it has been observed that the concrete strength and rupture strength of concrete has significantly affected the deflection of slab.



**Figure 4.17** Variation of mid point deflection of slab with respect to concrete strength and rupture strength of concrete, for case-2.

### 4.8.3 Effect of Reinforcement on Deflection

To study the effect of reinforcement on deflection, a 4572 mm  $\times$  4572 mm (15'  $\times$  15') two-way edge supported slab has been modeled with varying the percentage of required reinforcement from 100% to 200%. The slab end has been considered as monolithic to the support (case-2). The slab thickness is 101.6 mm and total load applied on the slab is 7.8 kN/m<sup>2</sup> (163 psf) in the FE analysis. The parameters used in the FE are as follows:

- Concrete cylinder strength,  $f'_c = 20.7 \text{ N/mm}^2$  (3000 psi)
- Modulus of elasticity of concrete,  $E_c = 20685 \text{ N/mm}^2$  ( $3 \times 10^6$  psi)
- Modulus of elasticity of steel,  $E_s = 206850 \text{ N/mm}^2$  ( $30 \times 10^6$  psi)
- Poisson's ratio,  $\nu = 0.18$
- Modular ratio,  $n = 10$
- The number of plate elements used in the analysis  $16 \times 16 = 256$  for 1/4<sup>th</sup> portion of the slab.

The analysis has been performed with rupture strength of concrete  $f_r = 0.62\sqrt{f'_c}$  N/mm<sup>2</sup> and  $0.33\sqrt{f'_c}$  N/mm<sup>2</sup>. The calculated deflections of slab for different percentage of reinforcement have been presented in the Fig. 4.18. It has been observed that the effect of reinforcement on deflection of slab is negligible for  $f_r = 0.62\sqrt{f'_c}$  N/mm<sup>2</sup> and is more noticeable for  $f_r = 0.33\sqrt{f'_c}$  N/mm<sup>2</sup>. Thus it may be concluded that the effect of reinforcement becomes more significant when slab is severely cracked.

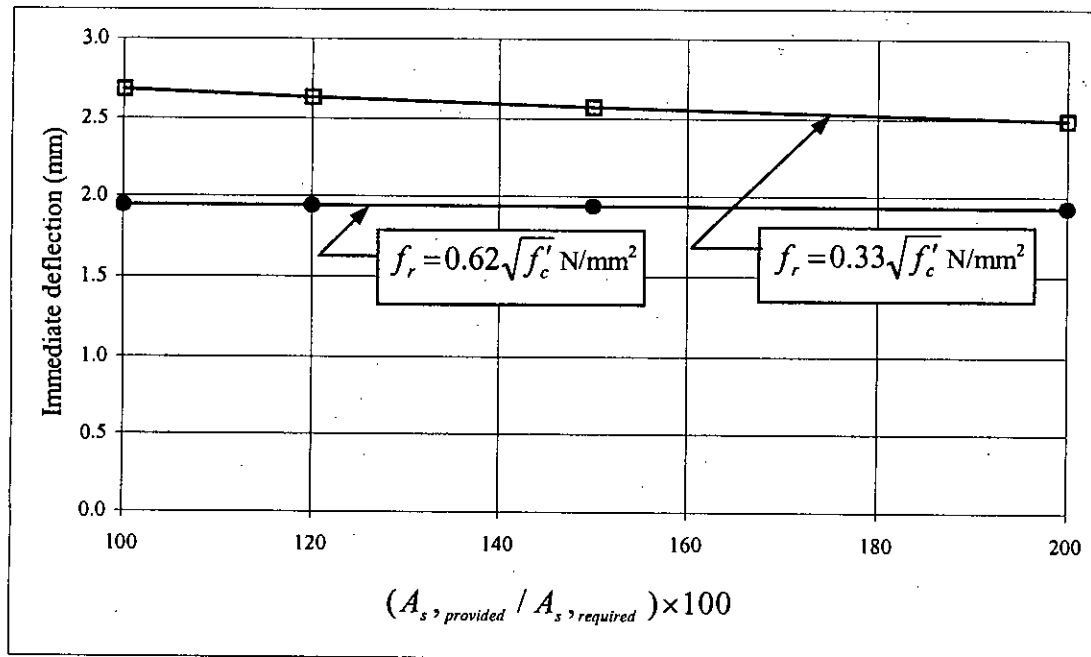


**Figure 4.18** Variation of immediate deflection of 4572 mm  $\times$  4572 mm (15 ft  $\times$  15 ft) slab with % reinforcement for case-2.

#### 4.8.4 Effect of Slab Thickness on Deflection

The effect of slab thickness on deflection has been observed in this section. For this purpose a 4572 mm  $\times$  4572 mm (15'  $\times$  15') slab for case-1 and a 7620 mm  $\times$  7620 mm (25'  $\times$  25') slab for case-2 have been modeled with changing their slab thickness at constant live load with the following parameters presented in the Table 4.2. The slab thickness have been changed as 1.2t, t, 0.9t and 0.75t; where t = panel perimeter/180 according to ACI Code (1963). For both modulus of rupture of concrete,  $f_r = 0.62\sqrt{f'_c}$  N/mm<sup>2</sup> and  $0.33\sqrt{f'_c}$  N/mm<sup>2</sup> have been used in the finite element analysis. The number of plate element used in the modeling of 1/4<sup>th</sup> portion of slab is  $16 \times 16 = 256$ .

From FE analysis the elastic deflection and immediate deflection (considering cracking) are presented in Figs 4.19 and 4.20 for slab case-1 and case-2 respectively. It has been observed that the variations of elastic and immediate deflections are affected significantly with change in slab thickness.

**Table 4.2** Parameters for calculation of elastic and immediate deflection of slab for varying slab thickness.

Concrete cylinder strength, $f'_c$	Modulus of elasticity of concrete, $E_c$	Poisson's ratio, $\nu$	Modulus of elasticity of steel, $E_s$	Total live load
20.7 N/mm <sup>2</sup> (3000 psi)	20685 N/mm <sup>2</sup> ( $3 \times 10^6$ psi)	0.18	206850 N/mm <sup>2</sup> ( $30 \times 10^6$ psi)	2.6 kN/m <sup>2</sup> (55 psf)

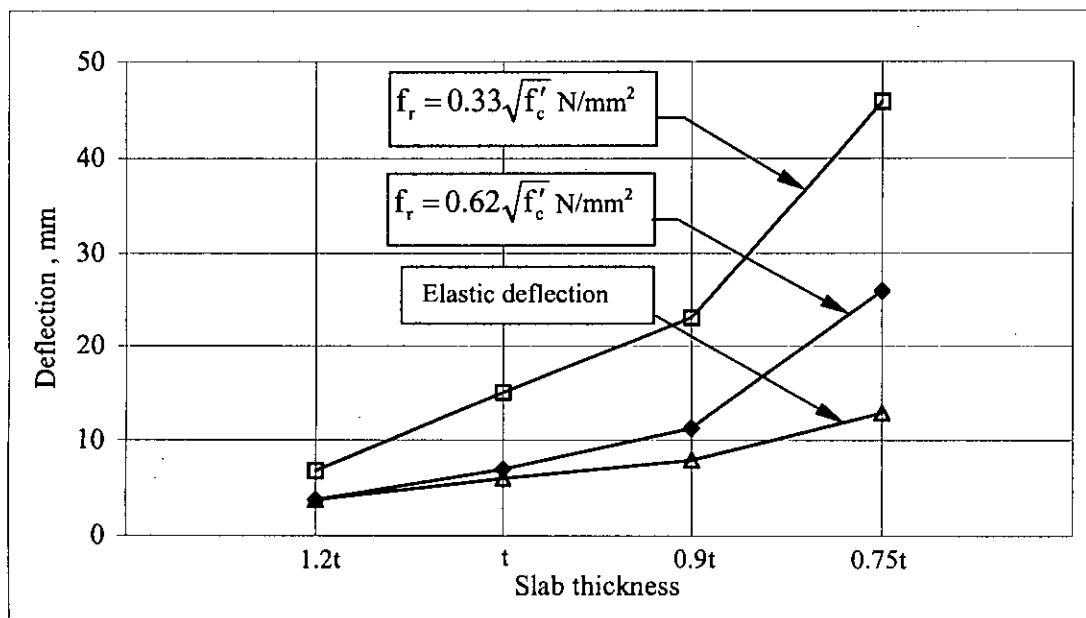


**Figure 4.19** Variation of elastic and immediate deflection of 4572 mm × 4572 mm slab for varying thickness with constant live load, for case-1.

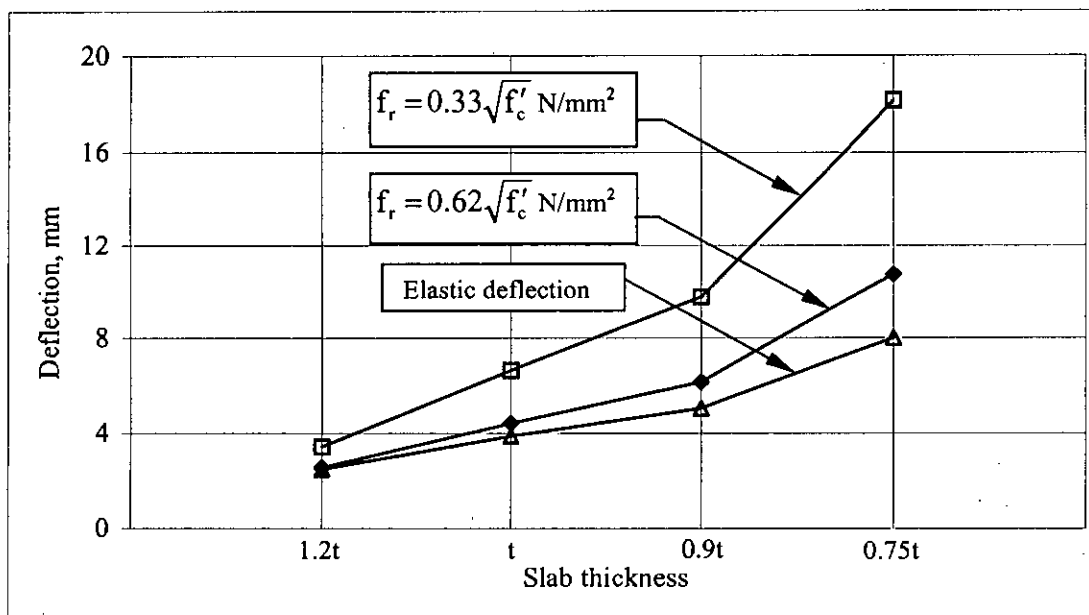


**Figure 4.20** Variation of elastic and immediate deflection of 7620 mm × 7620 mm slab for varying thickness with constant live load, for case-2.

#### 4.9 Deflection Limitations

To study the effect of slab thickness and span length on immediate deflection of edge supported slab, FE analysis has been done here. The immediate deflection of two-way edge supported slab has been computed with varying the slab thickness i.e. 75% to 120% of ACI Code (1963) suggested slab thickness and varying span length of slab for aspect ratio,  $m = 1.00$ . Three slabs have been modeled for case-2 whose span lengths are 4572 mm (15 ft), 6096 mm (20 ft), and 9144 mm (30 ft). The number of plate elements used in the modeling for  $1/4^{\text{th}}$  portion of the slab is  $16 \times 16 = 256$ . The common parameters used in the FE analysis are as follows:

##### (a) Loads

Live load = 2.4 kN/m<sup>2</sup> (50 psf)

Floor finish = 1.2 kN/m<sup>2</sup> (25 psf)

Partition wall = 1.44 kN/m<sup>2</sup> (30 psf)

##### (b) Material properties

Modulus elasticity of steel,  $E_s = 206850$  N/mm<sup>2</sup> ( $30 \times 10^6$  psi)

Modulus elasticity of concrete,  $E_c = 20685$  N/mm<sup>2</sup> ( $3 \times 10^6$  psi)



Compressive strength of concrete,  $f'_c = 20.7 \text{ N/mm}^2$  (3000 psi)

Poisson's ratio,  $\nu = 0.18$

(c) The total load applied on the slab has been calculated as follows:

Total load = Self-weight of slab + partition wall + floor finish + live load.

In some cases the slab thickness has been considered below the ACI (1963) range of 89 mm (3.5 inch). The immediate deflection has been calculated using above parameters and the ratio of immediate deflection to span length of slab has been determined and presented in the Table 4.3 in the form of  $\frac{\Delta}{L}$  (where,  $\Delta$  = immediate deflection computed from nonlinear FE analysis for full live load and  $L$  = span length of slab). The Fig. 4.21 shows the variation of immediate deflection for different slab thicknesses and span lengths of slab. It has been clearly found that the immediate deflection of slab does not exceed the ACI allowable limit  $\left(\frac{\Delta}{L} = \frac{1}{360}\right)$  for slab thickness up to 80% of ACI Code (1963) suggested guidelines and the variation of immediate deflection with span length has been observed almost linear for normal range of loading. It can be concluded from the above analysis that ACI minimum slab thickness or even less thickness may be found to be sufficient to satisfy immediate deflection limit, i.e. 1/360 under normal loading.

**Table 4.3** Immediate deflections versus span length of slab for different span length and slab thickness for full live load, for case-2.

	120% of ACI thickness	ACI thickness	80% of ACI thickness	75% of ACI thickness
Slab dimension	$\Delta / L$			
4572 mm × 4572 mm (15 ft × 15 ft)	$\frac{1}{2445}$	$\frac{1}{1194}$	$\frac{1}{461}$	$\frac{1}{370}$
6096 mm × 6096 mm (20 ft × 20 ft)	$\frac{1}{2088}$	$\frac{1}{1004}$	$\frac{1}{425}$	$\frac{1}{338}$
9144 mm × 9144 mm (30 ft × 30 ft)	$\frac{1}{1480}$	$\frac{1}{760}$	$\frac{1}{370}$	$\frac{1}{307}$

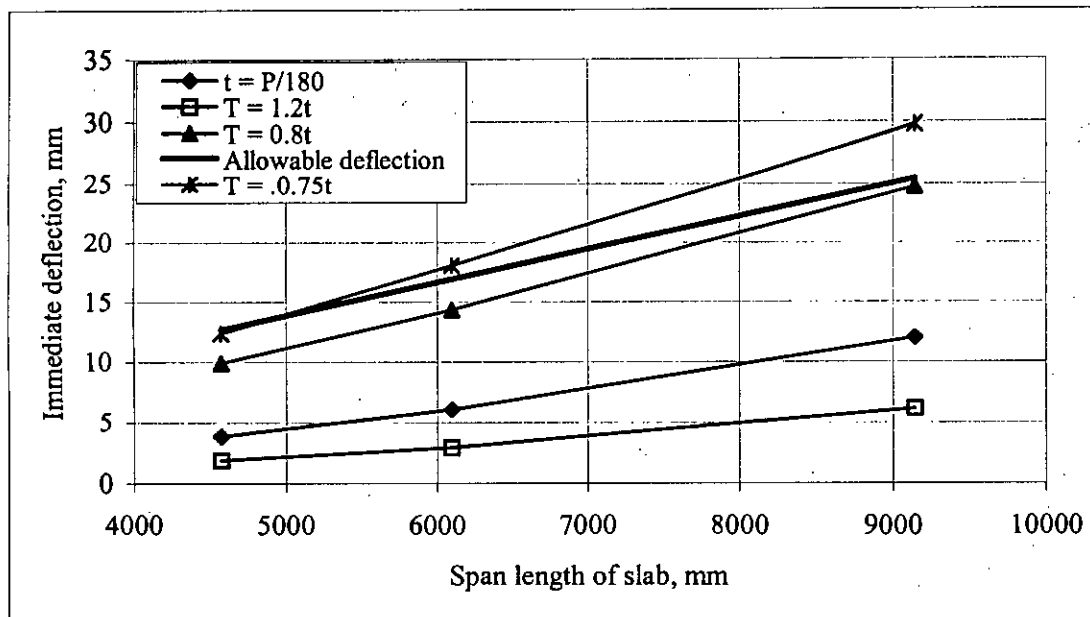


**Figure 4.21** Variation of immediate deflection of slab for application of full load with varying span length and slab thickness, for case-2.

#### 4.10 Deflection against Live Load

The effect of live load on immediate deflection of two-way edge supported slab has been studied in this section. For this purpose a 7620 mm × 6096 mm (25' × 20') slab for case-4 has been modeled with different live load range of 1.92 kN/m<sup>2</sup> to 9.58 kN/m<sup>2</sup> (40 psf to 200 psf). In addition to this live load another 1.43 kN/m<sup>2</sup> (30 psf) of partition wall load has been considered as live load. The total dead load including self-weight of slab and 1.2 kN/m<sup>2</sup> (25 psf) of floor finish load has been considered. The slab thickness has been considered as according to the recent ACI Code (2002) guidelines. In the modeling the modulus of rupture of concrete has been considered as  $f_r = 0.33\sqrt{f'_c}$  N/mm<sup>2</sup> and other parameters are taken from section 4.7.

The maximum values of immediate deflection have been taken from nonlinear FE analyses of slabs for different live load applied on it and the calculated values have been presented in the Table 4.4. Figure 4.22 shows the variation of immediate deflection to span length of slab. It has been found from FE analysis that the immediate deflection of slab is within the range of ACI allowable ( $L / 360$ ) limits for

total load up to 13 kN/m<sup>2</sup> (270 psf) and variation of immediate deflection is significant with increase in load.

**Table 4.4** Immediate deflection of slab with varying live load for 7620 mm × 6096 mm slab, for case-4.

Total load (kN/m <sup>2</sup> )	7.14	8.09	9.05	10.0	11.92	14.80
Live load (kN/m <sup>2</sup> )	1.92	2.87	3.83	4.79	6.71	8.58
$\Delta/L$	$\frac{1}{1116}$	$\frac{1}{873}$	$\frac{1}{703}$	$\frac{1}{581}$	$\frac{1}{420}$	$\frac{1}{290}$

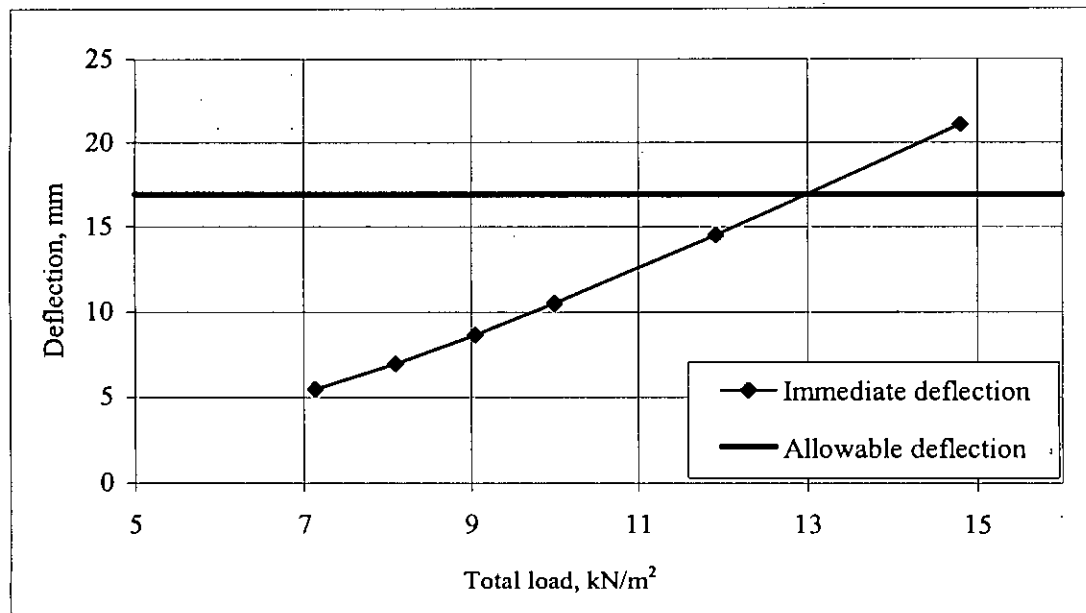


**Figure 4.22** Variation of immediate deflection with varying live load of 7620 mm × 6096 mm (25' × 20') slab, for case-4.

#### 4.11 Deflection Ratio vs. Stress Ratio Curve

From section 4.8, it is clearly observed that most of the slabs are cracked due to normal range of loadings and the immediate deflection is higher than the elastic deflection. It has also been observed that there is a unique relationship between immediate and elastic deflections which only depends on aspect ratio, boundary conditions and level of cracking. Under this circumstance, curves may be developed for the calculation of immediate deflection from elastic deflection without the help of FE analysis. The curve is termed as deflection ratio vs. stress ratio curve in which the abscissa of the curve is expressed as **stress ratio** and ordinate is **deflection ratio**. The stress ratio is the ratio between the maximum elastic stress developed in the slab and the modulus of rupture of concrete; and deflection ratio is the ratio of immediate deflection and elastic deflection of slab. From simple calculation a designer can predict the actual immediate deflection of slab from the proposed deflection ratio vs. stress ratio curve. To generate these curves, parametric studies have been performed with change in parameters like span length of slab, slab thickness, aspect ratio, concrete compressive strength, loading, modulus of rupture of concrete etc.

##### 4.11.1 Effect of Span Length

For the purpose of preparation of unique design charts, the effect of span length on deflection of slabs have been studied. For this purpose four types of slabs (case-1 to case-4) are analyzed with varying span length and varying live load applied on it. The panel dimensions are presented in the Table 4.5 for different slab case.

**Table 4.5** Panel dimension of slab for different slab case

Slab case	Case-1	Case-2	Case-3	Case-4
Slab dimension (mm × mm)	7620 × 7620 6096 × 6096 4572 × 4572 3048 × 3048	9144 × 9144 7620 × 7620 6096 × 6096 4572 × 4572 3048 × 3048	7620 × 7620 4572 × 4572 3048 × 3048	7620 × 6096 4572 × 3658

The common parameters used in the FE analysis are as follows:

(a) Loads

Live load = 2.4 kN/m<sup>2</sup> to 12 kN/m<sup>2</sup> ( 50 psf to 250 psf ) for slab case-1, case-3 and case-4.

Floor finish = 1.2 kN/m<sup>2</sup> ( 25 psf ).

Partition wall = 1.44 kN/m<sup>2</sup> ( 30 psf ).

(b) Material properties used in the modeling are the same as in section 4.7 and two levels of modulus of rupture of concrete,  $f_r = 0.62\sqrt{f'_c}$  N/mm<sup>2</sup> and  $0.33\sqrt{f'_c}$  N/mm<sup>2</sup> has been used.

(c) The sustained load applied on the slab has been calculated as follows:

Sustained load = Self weight of slab + floor finish + partition wall + 50% of live load.

(d) The slab thickness = Panel perimeter /180 for slab case-1, case-3 and case-4.

For case-2 the slabs have been modeled with varying thickness from 0.75t to 1.2t (where, t = Panel perimeter /180) of slab and varying span length with a constant live load of 2.63 kN/m<sup>2</sup> (55 psf). The respective thicknesses are presented in the Table 4.6.

**Table 4.6** Slab thickness for slab case-2.

Slab thickness	Panel dimension (mm × mm)				
	9144×9144	7620×7620	6096×6096	4572×4572	3048×3048
1.2t	243.84 mm	203.20 mm	162.56 mm	121.92 mm	81.28 mm
t	203.20 mm	169.33 mm	135.47 mm	101.60 mm	67.74 mm
0.9t	182.88 mm	152.40 mm	121.92 mm	91.44 mm	62.00 mm
0.8t	162.56 mm	135.67 mm	108.37 mm	81.28 mm	
0.75t	152.40 mm	127.00 mm			

The maximum stress has been taken at support for case-2, case-3 and case-4 and for case-1 at mid point of the slab. For all cases of slab the maximum immediate deflections at the center of slab have been monitored. Figures 4.23 to 4.26 show the variation of deflection ratio vs. stress ratio curve for case-1 to case-4 for modulus of

rupture of concrete,  $f_r = 0.62\sqrt{f'_c}$  N/mm<sup>2</sup>. In Figs 4.27 to 4.30 the variation of curves for case-1 to case-4 for modulus of rupture of concrete,  $f_r = 0.33\sqrt{f'_c}$  N/mm<sup>2</sup> are presented. The deflection ratio vs. stress ratio curves have been found to be almost identical for each slab case and same aspect ratio for both levels of modulus of rupture of concrete.

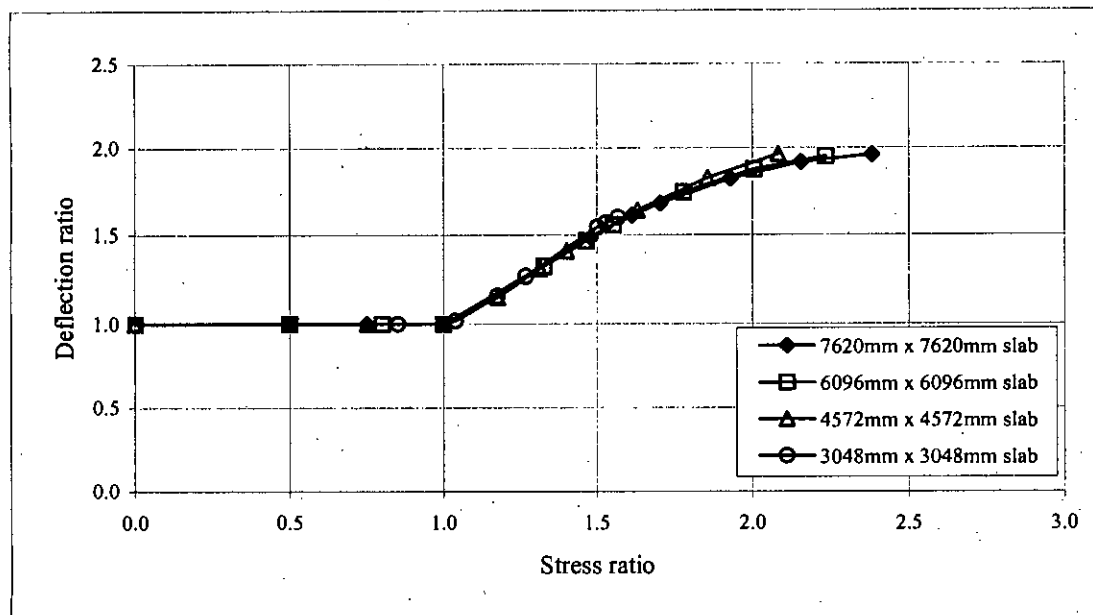


**Figure 4.23** Variation of deflection ratio vs. stress ratio curve of edge supported slab, for case-1,  $m=1.00$ ,  $f_r = 0.62\sqrt{f'_c}$  N/mm<sup>2</sup>

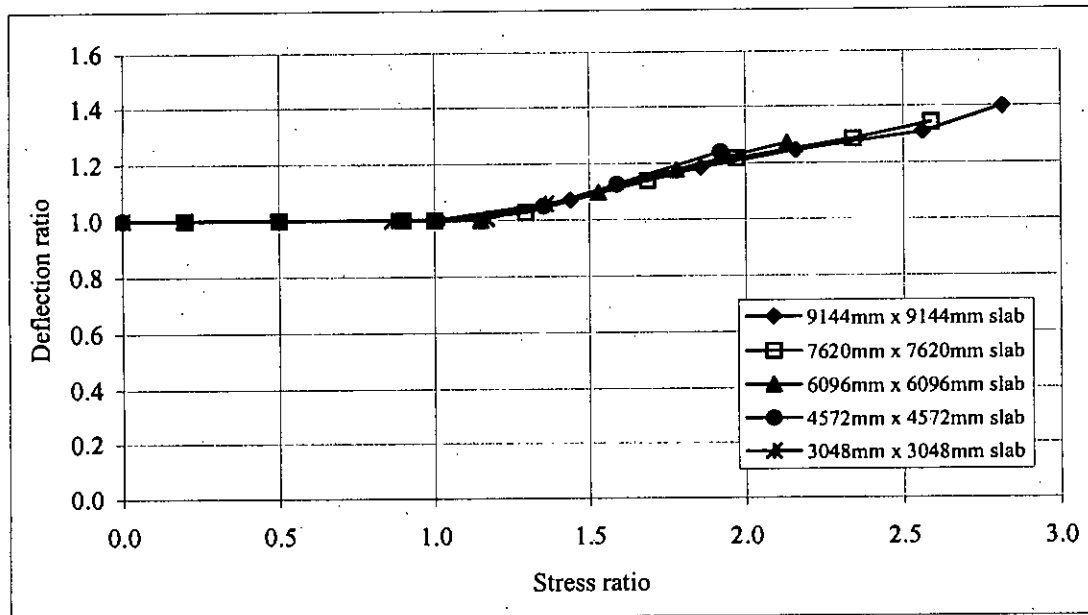


**Figure 4.24** Variation of deflection ratio vs. stress ratio curve of edge supported slab for case-2 with varying slab thickness,  $f_r = 0.62\sqrt{f'_c}$  N/mm<sup>2</sup>

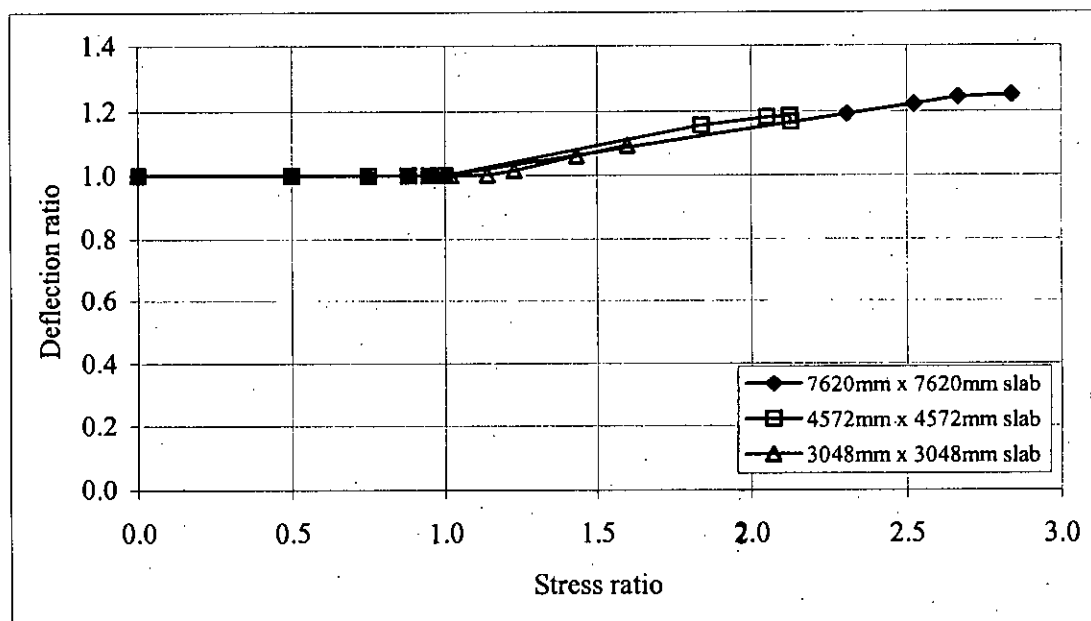


**Figure 4.25** Variation of deflection ratio vs. stress ratio curve of edge supported slab, for case-3,  $m=1.00$ ,  $f_r = 0.62\sqrt{f'_c}$  N/mm<sup>2</sup>

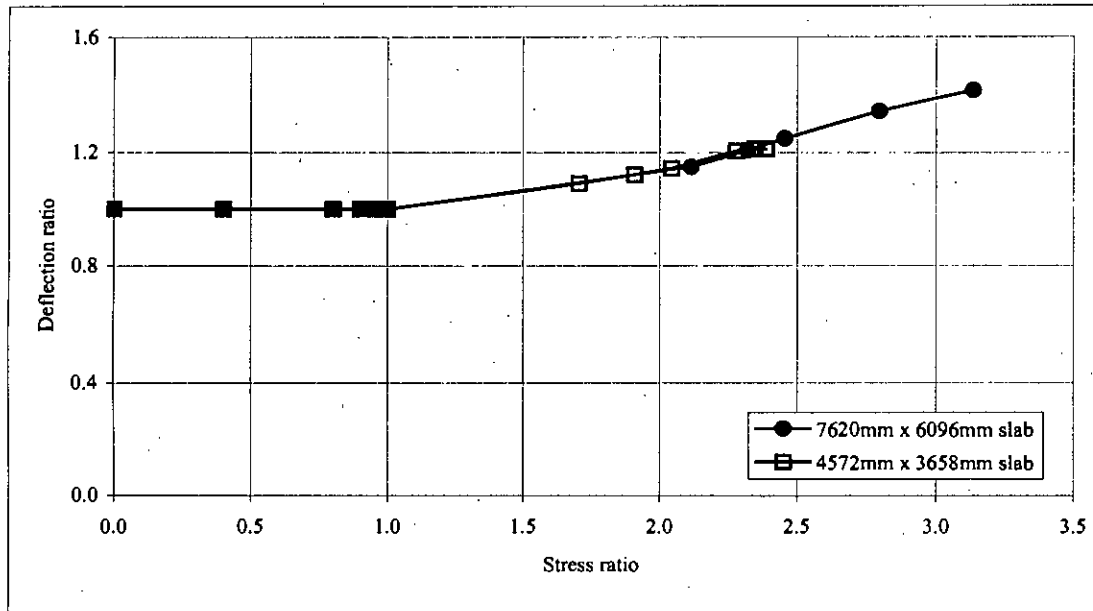


**Figure 4.26** Variation of deflection ratio vs. stress ratio curve of edge supported slab, for case-4,  $m = 0.80$ ,  $f_r = 0.62\sqrt{f'_c}$  N/mm<sup>2</sup>

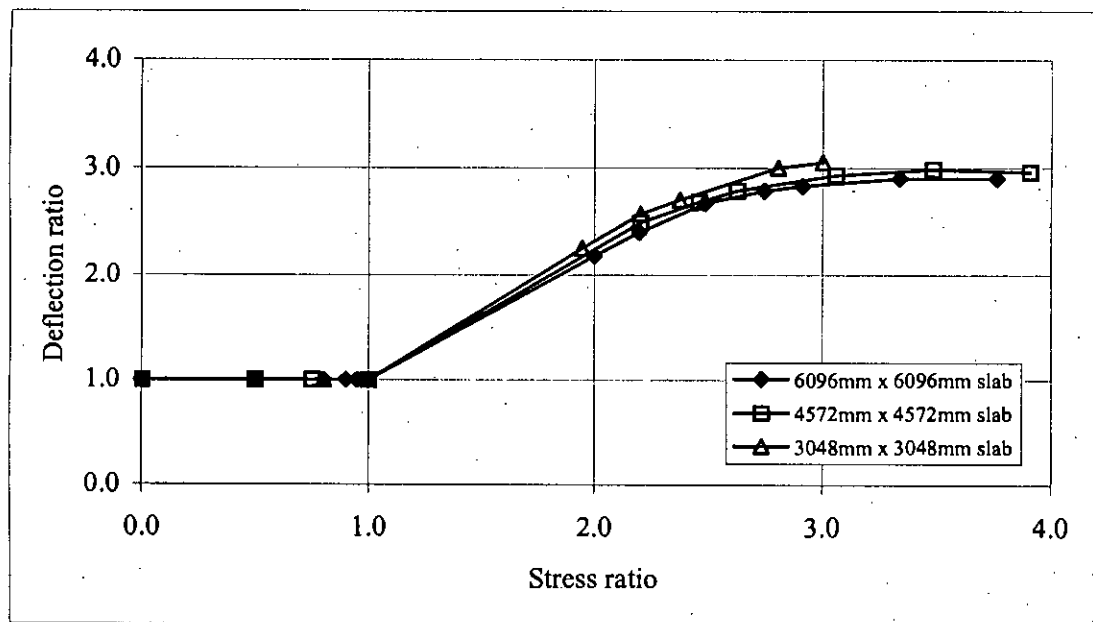


**Figure 4.27** Variation of deflection ratio vs. stress ratio curve of edge supported slab, for case-1,  $m = 1.00$ ,  $f_r = 0.33\sqrt{f'_c}$  N/mm<sup>2</sup>.



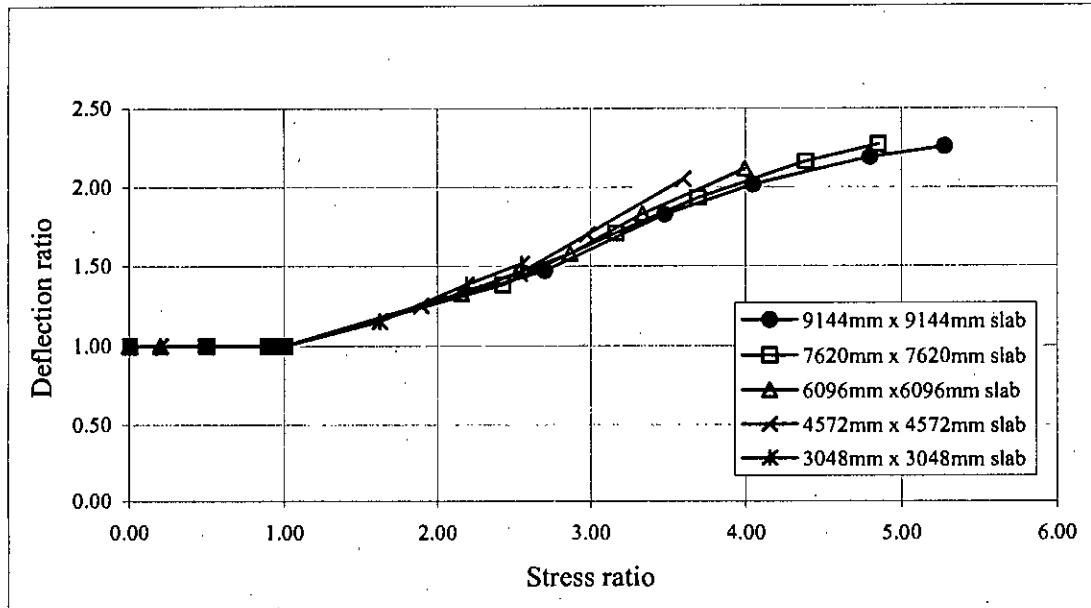


**Figure 4.28** Variation of deflection ratio vs. stress ratio curve of edge supported slab, for case-2 with varying slab thickness,  $f_r = 0.33\sqrt{f'_c}$  N/mm<sup>2</sup>

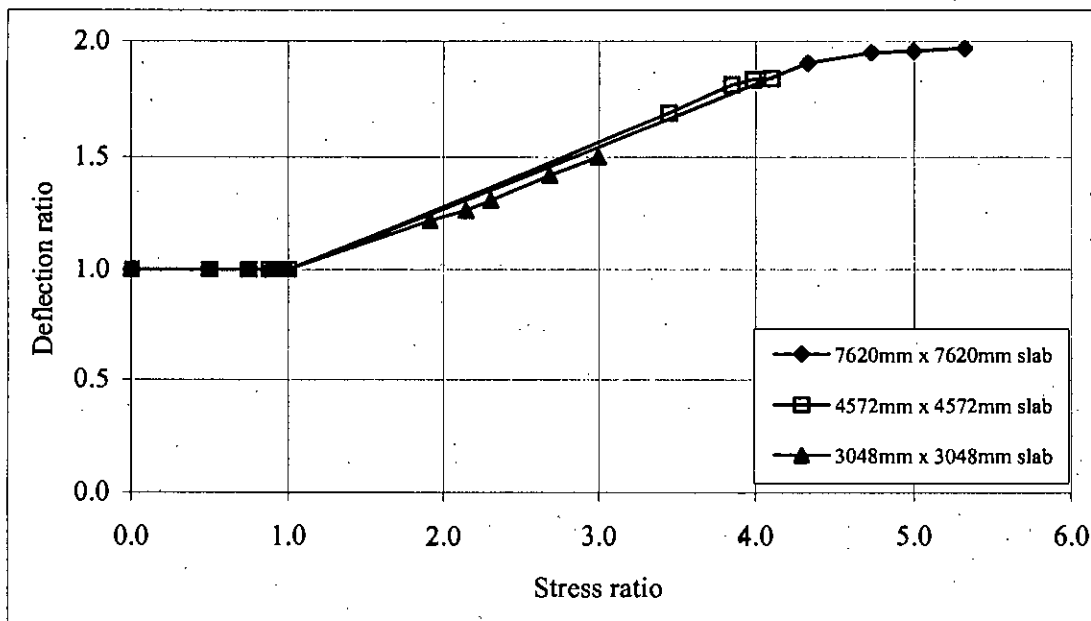


**Figure 4.29** Variation of deflection ratio vs. stress ratio curve of edge supported slab, for case-3,  $m = 1.00$ ,  $f_r = 0.33\sqrt{f'_c}$  N/mm<sup>2</sup>.

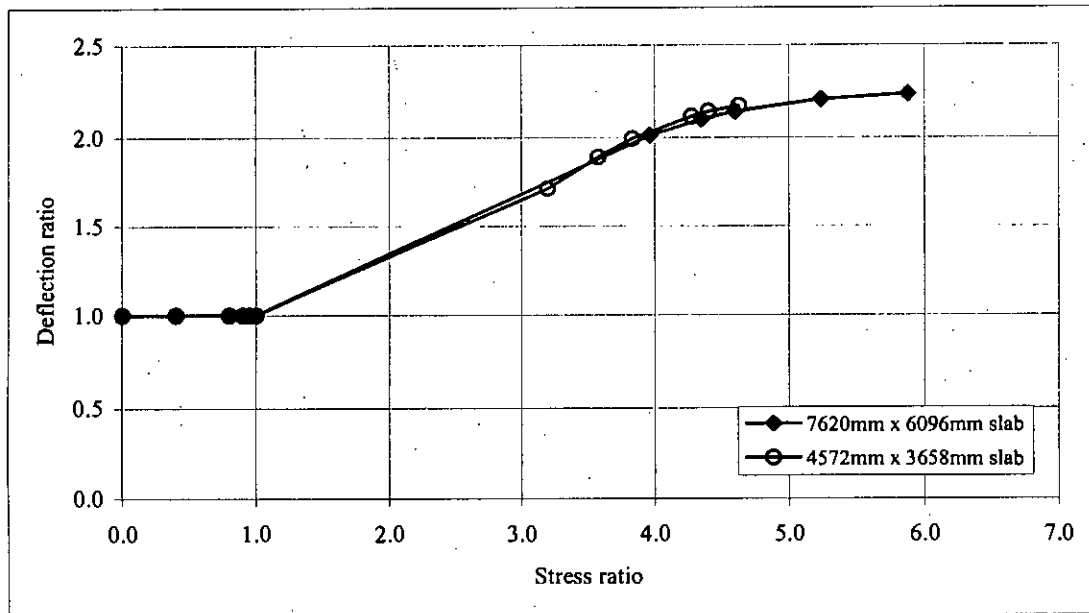


**Figure 4.30** Variation of deflection ratio vs. stress ratio curve of edge supported slab, for case-4,  $m = 1.00$ ,  $f_r = 0.33\sqrt{f'_c}$  N/mm<sup>2</sup>

#### 4.11.2 Effect of Applied Load and Slab Thickness

For the purpose of the preparation of unique deflection ratio vs. stress ratio curves, the effect of change of slab thickness and variation of live load have been compared. A 4572 mm × 4572 mm (15' × 15') slab (for case-1) and a 6096 mm × 6096 mm (20' × 20') slab (for case-2) have been modeled with varying live load of 2.4 kN/m<sup>2</sup> to 12 kN/m<sup>2</sup> (50 psf to 250 psf) keeping constant ACI Code (1963) suggested slab thickness. The above slabs have also been modeled with constant live load of 2.63 kN/m<sup>2</sup> (55 psf) and varying slab thickness from 0.75t to 1.20t, where, t = panel perimeter divided by 180. The moduli of rupture of concrete used in the FE analysis are,  $f_r = 0.62\sqrt{f'_c}$  N/mm<sup>2</sup> and  $0.33\sqrt{f'_c}$  N/mm<sup>2</sup> for both cases of slabs. The parameters used in this FE analysis from section 4.9.

From the FE analysis, the results of stress ratio and deflection ratio have been presented in Table 4.7 to 4.10 for varying live load and varying slab thickness. The variation of deflection ratio vs. stress ratio curves have been shown in Figs 4.31 and 4.32 for slab case-1 and case-2, respectively, using rupture strength of concrete,

$f_r = 0.62\sqrt{f'_c}$  N/mm<sup>2</sup> and Figs 4.33 and 4.34 that for  $0.33\sqrt{f'_c}$  N/mm<sup>2</sup>. It has been observed that for thin slabs, the deflection ratio vs. stress ratio curves has some difference when they are severely cracked. Slab thickness up to 0.90t and live load up to 4.79 kN/m<sup>2</sup> (100 psf), an insignificant difference has been found. So, with the help of these charts it would be possible to calculate immediate deflections for slabs with thickness even 90% of ACI minimum thickness.

**Table 4.7** Stress ratio and deflection ratio with changing live load and slab thickness

for case-1,  $f_r = 0.62\sqrt{f'_c}$  N/mm<sup>2</sup>

4572 mm × 4572 mm slab for varying live load, t = Panel perimeter/180.			4572 mm × 4572 mm slab for varying slab thickness Sustained live load = 2.63 kN/m <sup>2</sup> (55 psf)		
Live load (kN/m <sup>2</sup> )	Stress ratio	Deflection ratio	Slab thickness	Stress ratio	Deflection ratio
2.4	1.176	1.152	1.20t	0.883	1.000
3.83	1.313	1.311	t = Perimeter/180	1.176	1.152
4.79	1.402	1.412	0.90t	1.40	1.418
7.19	1.631	1.642	0.75t	1.882	2.019
9.58	1.857	1.828			

**Table 4.8** Stress ratio and deflection ratio with changing live load and slab thickness

for case-2,  $f_r = 0.62\sqrt{f'_c}$  N/mm<sup>2</sup>

6096 mm × 6096 mm slab for varying live load, t = Panel perimeter/180			6096 mm × 6096 mm slab for varying slab thickness Sustained live load = 2.63 kN/m <sup>2</sup> (55 psf)		
Live load (kN/m <sup>2</sup> )	Stress ratio	Deflection ratio	Slab thickness	Stress ratio	Deflection ratio
1.92	1.462	1.081			
2.87	1.562	1.105	1.20t	1.15	1.000
3.83	1.670	1.135	t = Perimeter/180	1.529	1.097
4.79	1.770	1.160	0.90t	1.779	1.177
9.58	2.288	1.233	0.80t	2.132	1.270
12	2.546	1.239			

**Table 4.9** Stress ratio and deflection ratio with changing live load and slab thicknessfor case-1,  $f_r = 0.33\sqrt{f'_c}$  N/mm<sup>2</sup>

4572 mm × 4572 mm slab for varying live load, t = Panel perimeter/180.			4572 mm × 4572 mm slab for varying slab thickness Sustained live load = 2.63 kN/m <sup>2</sup> (55 psf)		
Live load (kN/m <sup>2</sup> )	Stress ratio	Deflection ratio	Slab thickness	Stress ratio	Deflection ratio
2.4	2.204	2.488	1.20t	1.655	1.800
3.83	2.463	2.683	t = Perimeter/180	2.204	2.488
4.79	2.628	2.785	0.90t	2.615	2.909
7.19	3.058	2.932	0.75t	3.528	3.567
9.58	3.482	2.985			
12	3.906	2.990			

**Table 4.10** Stress ratio and deflection ratio with changing live load and slabthickness for case-2,  $f_r = 0.33\sqrt{f'_c}$  N/mm<sup>2</sup>

6096 mm × 6096 mm slab for varying live load, t = Panel perimeter/180			6096 mm × 6096 mm slab for varying slab thickness Sustained live load = 2.63 kN/m <sup>2</sup> (55 psf)		
Live load (kN/m <sup>2</sup> )	Stress ratio	Deflection ratio	Slab thickness	Stress ratio	Deflection ratio
1.92	2.740	1.534			
2.87	2.933	1.612	1.20t	2.158	1.327
3.83	3.130	1.689	t = Perimeter/180	2.866	1.577
4.79	3.323	1.755	0.90t	3.336	1.829
9.58	4.290	1.939	0.80t	3.998	2.117
12	4.773	1.954			

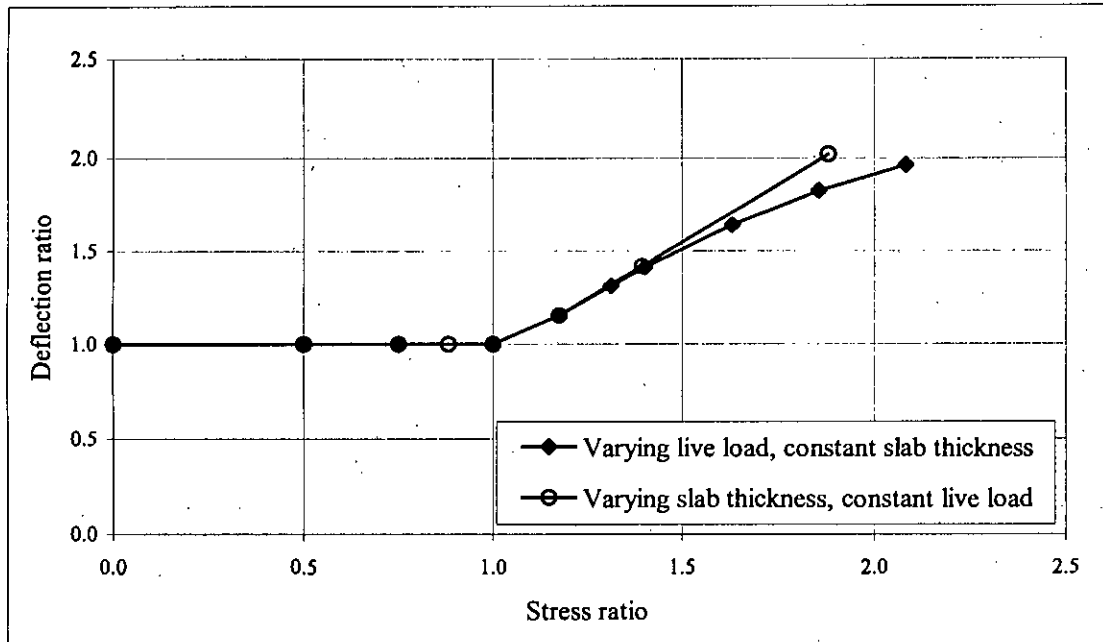


**Figure 4.31** Variation of deflection ratio vs. stress ratio curve of slab for varying live load and slab thickness, for case-1,  $f_r = 0.62\sqrt{f'_c}$  N/mm<sup>2</sup>.

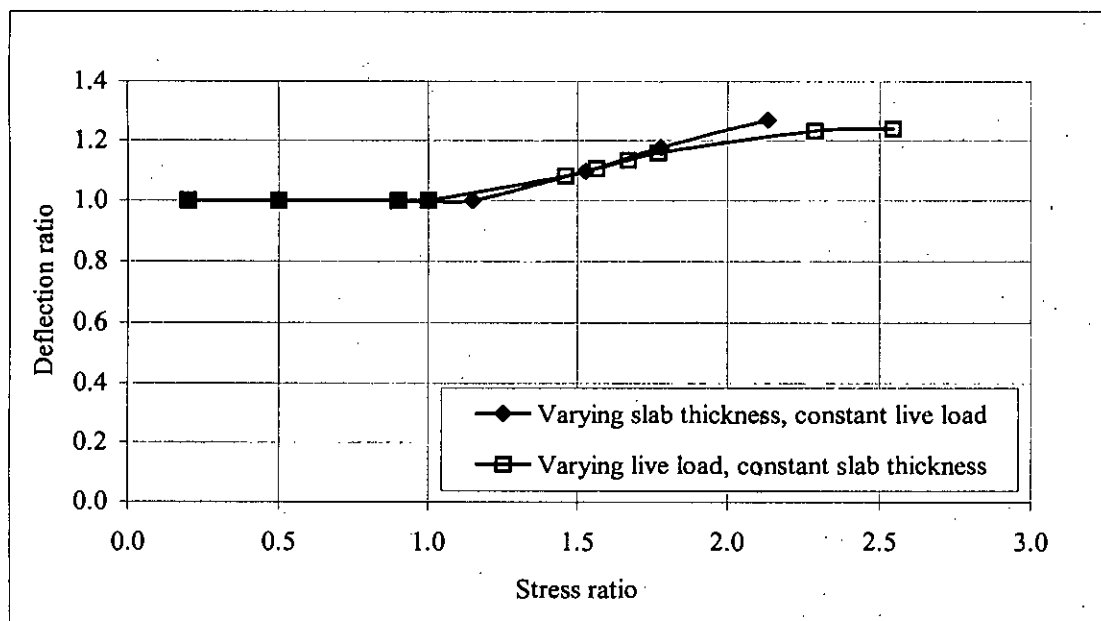


**Figure 4.32** Variation of deflection ratio vs. stress ratio curve of slab for varying live load and slab thickness, for case-2,  $f_r = 0.62\sqrt{f'_c}$  N/mm<sup>2</sup>.

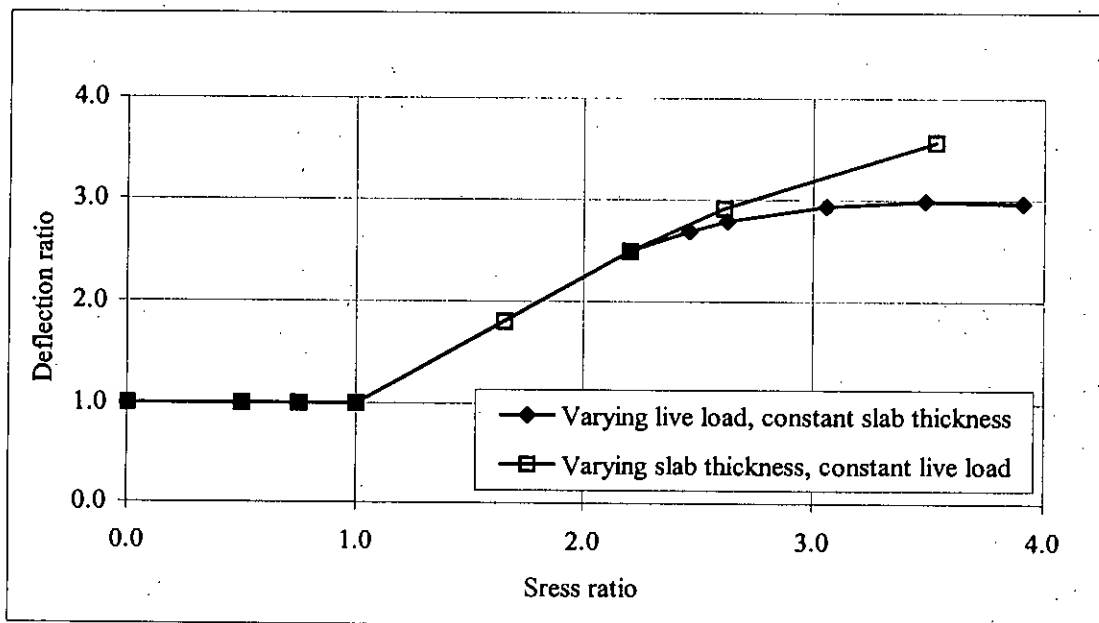


Figure 4.33 Variation of deflection ratio vs. stress ratio curve of slab for varying live load and slab thickness, for case-1,  $f_r = 0.33\sqrt{f'_c}$  N/mm<sup>2</sup>.

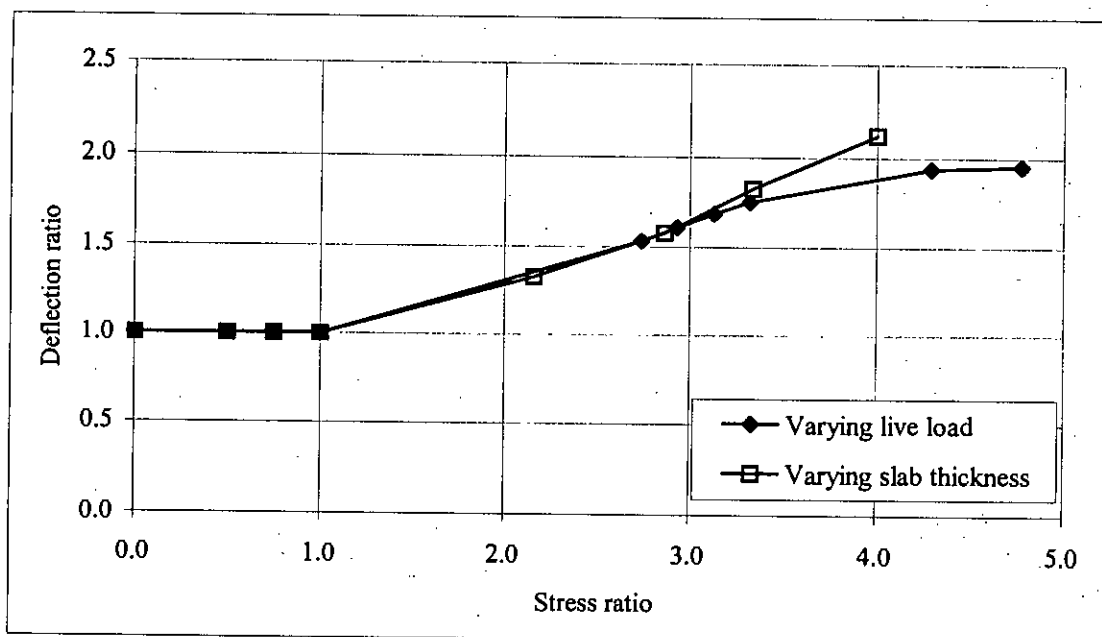


Figure 4.34 Variation of deflection ratio vs. stress ratio curve of slab for varying live load and slab thickness, for case-2,  $f_r = 0.33\sqrt{f'_c}$  N/mm<sup>2</sup>.

### 4.11.3 Effect of Live Load and Concrete Strength

To identify the effect of varying concrete compressive strength and varying live on deflection a study has been carried out. Two sets of deflection ratio-stress ratio curve have been developed with changing parameters of concrete strengths and live loads. The parameters are tabulated in Table 4.11 and 4.12. The moduli of rupture of concrete separately used in the FE analysis are  $0.62\sqrt{f'_c}$  N/mm<sup>2</sup> and  $0.33\sqrt{f'_c}$  N/mm<sup>2</sup>.

The deflection ratio vs. stress ratio curves are presented in Figs 4.35 and 4.36. It is clearly observed that the variation of concrete strength and live load does not affect the deflection ratio vs. stress ratio curve. So it would be possible to develop unique curves irrespective of concrete strength and live load for a specified aspect ratio and boundary condition of slab.

**Table 4.11** Data for varying concrete strength of 6096 mm × 6096 mm slab.

Concrete strength		Modulus of elasticity of concrete	Live load	Slab thickness
N/mm <sup>2</sup>	psi	N/mm <sup>2</sup>	kN/m <sup>2</sup>	mm
17.2	2500	19650	9.58	135.47
20.7	3000	20685		
27.6	4000	24856		
34.5	5000	27790		
41.4	6000	30442		

**Table 4.12** Data for varying live load of 6096 mm × 6096 mm slab.

Live load		Modulus of elasticity of concrete	Concrete strength	Slab thickness
kN/m <sup>2</sup>	psf	N/mm <sup>2</sup>	N/mm <sup>2</sup>	mm
1.92	40	20685	20.7	135.47
2.87	60			
3.83	80			
4.79	100			
9.58	200			
12	250			
14.37	300			

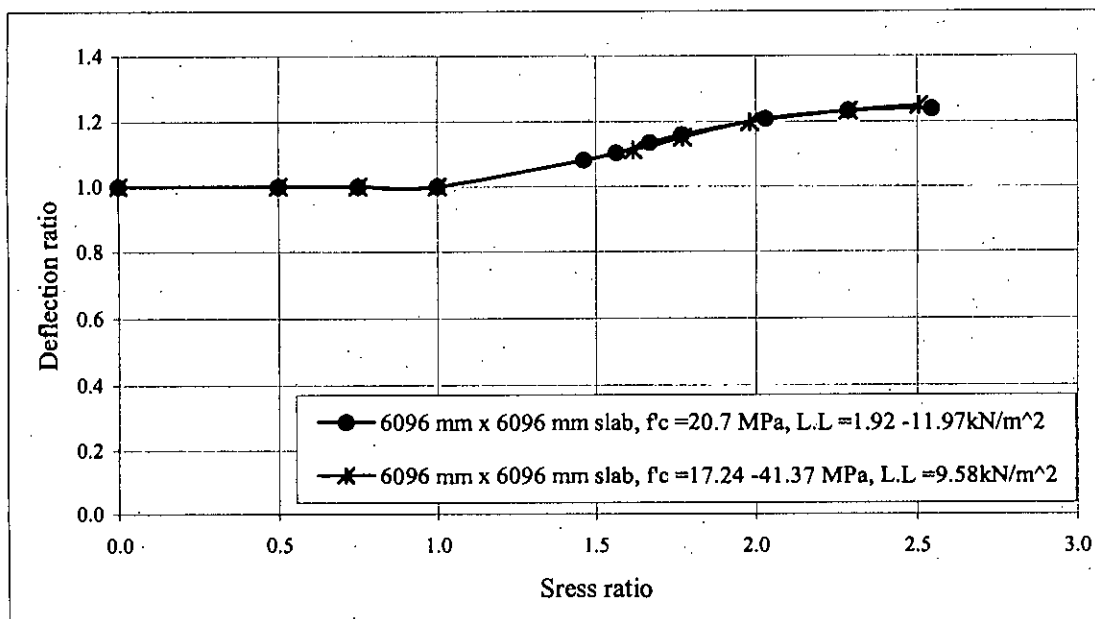


**Figure 4.35** Variation of deflection ratio vs. stress ratio curve of slab for varying live load and concrete strength, for case-2,  $f_r = 0.62 \sqrt{f'_c}$  N/mm<sup>2</sup>



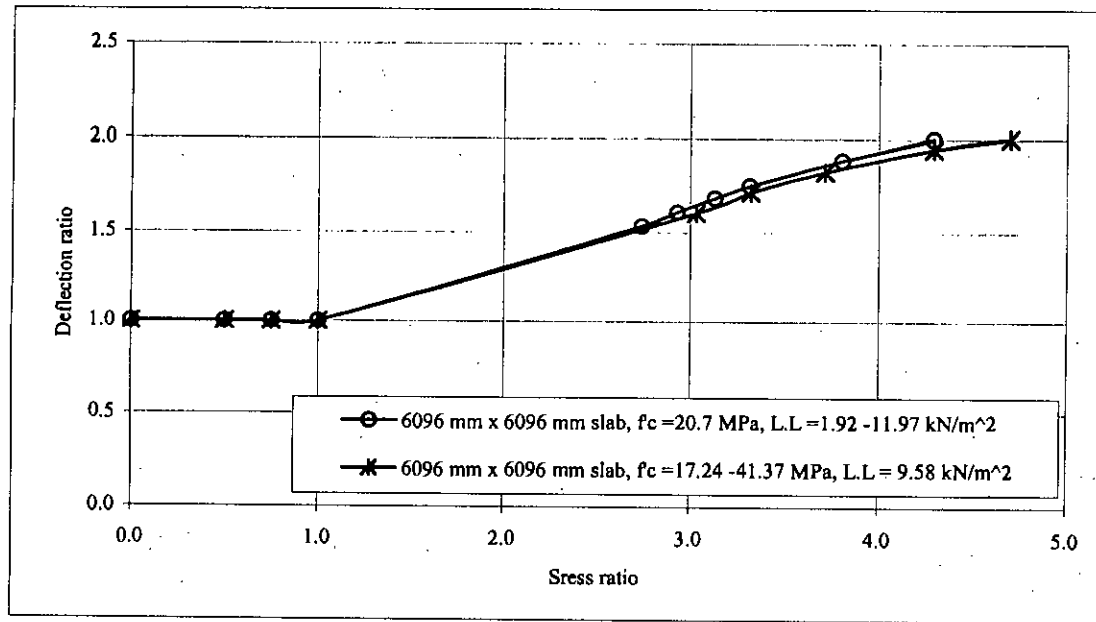


**Figure 4.36** Variation of deflection ratio vs. stress ratio curve of slab for varying live load and concrete strength, for case-2,  $f_r = 0.33 \sqrt{f'_c}$  N/mm<sup>2</sup>

#### 4.11.4 Effect of Live Load, Concrete Strength and Span Length

To produce a unique deflection ratio vs. stress ratio curve the effect of live load, span length of slab, concrete strength for individual type of slabs have been studied. For this purpose three types (case-4, case-5 and case-8) of slab have been modeled. The common parameters used in the FE analysis for above three slabs are presented in the Table 4.13, and other parameters are presented below as slab case-wise. Two levels of modulus of rupture of concrete  $0.62\sqrt{f'_c}$  N/mm<sup>2</sup> and  $0.33\sqrt{f'_c}$  N/mm<sup>2</sup> have been used in the FE analysis for all slabs mentioned above.

**Table 4.13** Common parameters used FE analysis.

Modulus of elasticity of steel	Poisson's ratio	Partition wall load treated as live load	Floor finish treated as dead load
206850 N/mm <sup>2</sup>	0.18	1.44 kN/m <sup>2</sup>	1.2 kN/m <sup>2</sup>

**Varying parameters for slab case-4:**

For slab case-4 three slabs have been modeled with following dimensions. The slab dimensions are 4572 mm × 3658 mm (15 ft×12 ft) and 7620 mm×6096 mm (25 ft×20 ft) having aspect ratio,  $m = 0.80$ . The first slab has been modeled with varying concrete strength with constant live load and second slab for varying live load with constant concrete strength. The second slab has also been modeled for varying concrete strength with constant live load.

**Varying parameters for slab case-5:**

For slab case-5 three slabs having aspect ratio,  $m = 0.6$  have been modeled with following dimensions. The slabs 7620 mm × 4572 mm (25 ft× 15 ft) and 4877 mm×2926 mm (16 ft×9.6 ft) have been modeled for varying concrete strength with constant live load, and 7620 mm×4572 mm (25 ft×15 ft) slab also for varying live load with constant concrete strength.

**Varying parameters for slab case-8:**

For slab case-8 four slabs have been modeled with varying live load, concrete strength having aspect ratio,  $m = 0.70$ . The slab dimensions are 7620 mm×5334 mm (25 ft×17.5 ft) and 6096 mm×4267 mm (20 ft×14 ft). The first slab has been modeled with varying concrete strength and varying live load and second slab with only varying the concrete strength.

The FE results are presented in Figs 4.37 to 4.39 for modulus of rupture of concrete,  $f_r = 0.62\sqrt{f'_c}$  N/mm<sup>2</sup> and Figs 4.40 to 4.42 for  $f_r = 0.33\sqrt{f'_c}$  N/mm<sup>2</sup> and almost identical curves have been found for all cases of slabs. From above analyses, it has been clearly observed that the deflection ratio vs. stress ratio curves are not affected by the variations of concrete strength, span length of panel and load applied on the slab. So it is possible to produce a unique curve for individual aspect ratio and rupture strength of concrete irrespective of span length, concrete strength and loadings.

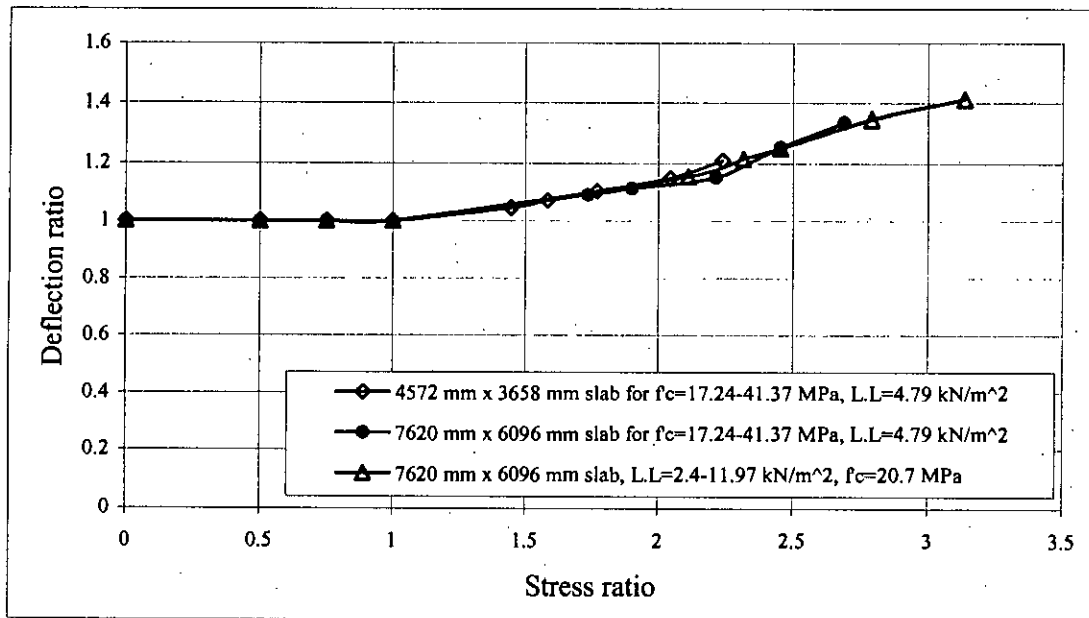


Figure 4.37 Variation of deflection ratio vs. stress ratio curve of slab for varying live load, concrete strength and span length, for case-4,  $f_r = 0.62 \sqrt{f'_c}$  N/mm<sup>2</sup>

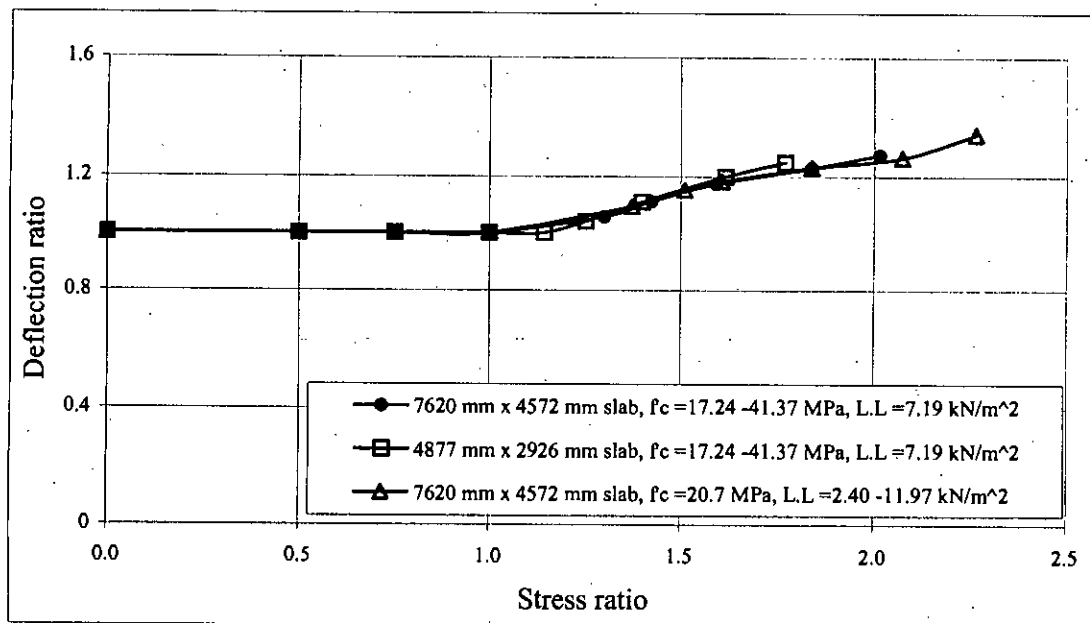
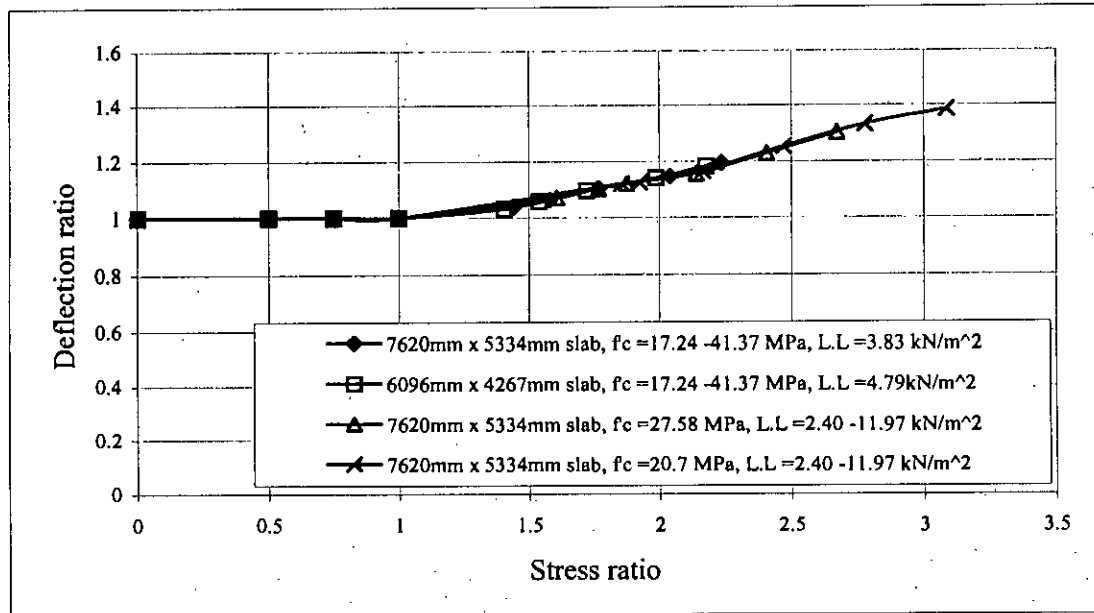
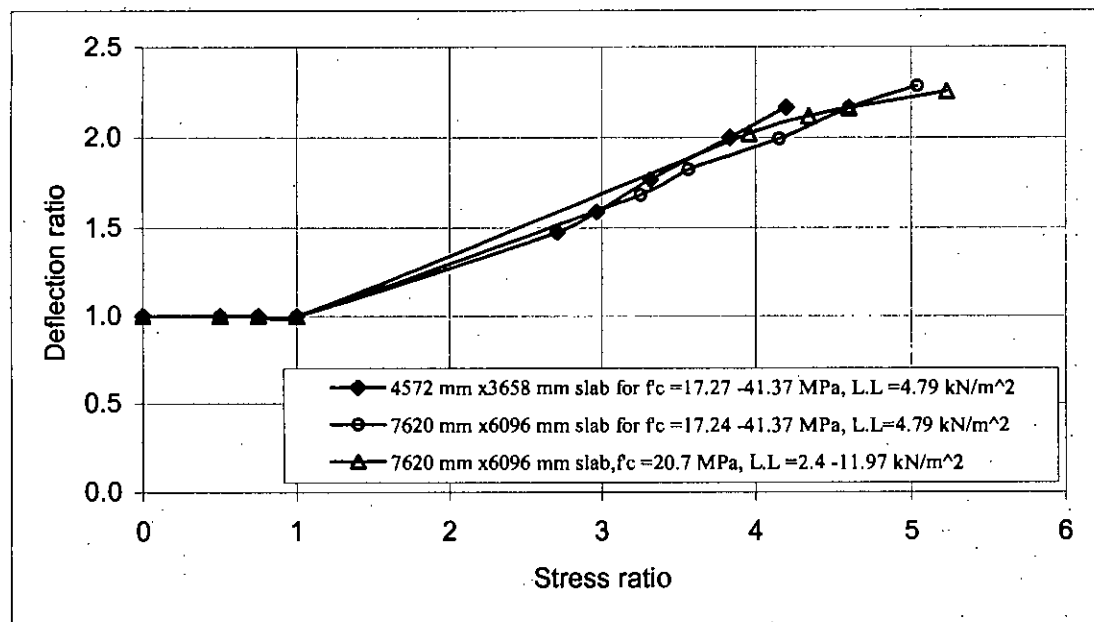


Figure 4.38 Variation of deflection ratio vs. stress ratio curve of slab for varying live load, concrete strength and span length, for case-5,  $f_r = 0.62 \sqrt{f'_c}$  N/mm<sup>2</sup>



**Figure 4.39** Variation of deflection ratio vs. stress ratio curve of slab for varying live load, concrete strength and span length, for case-8,  $f_r = 0.62 \sqrt{f'_c}$  N/mm<sup>2</sup>



**Figure 4.40** Variation of deflection ratio vs. stress ratio curve of slab for varying live load, concrete strength and span length, for case-4,  $f_r = 0.33 \sqrt{f'_c}$  N/mm<sup>2</sup>

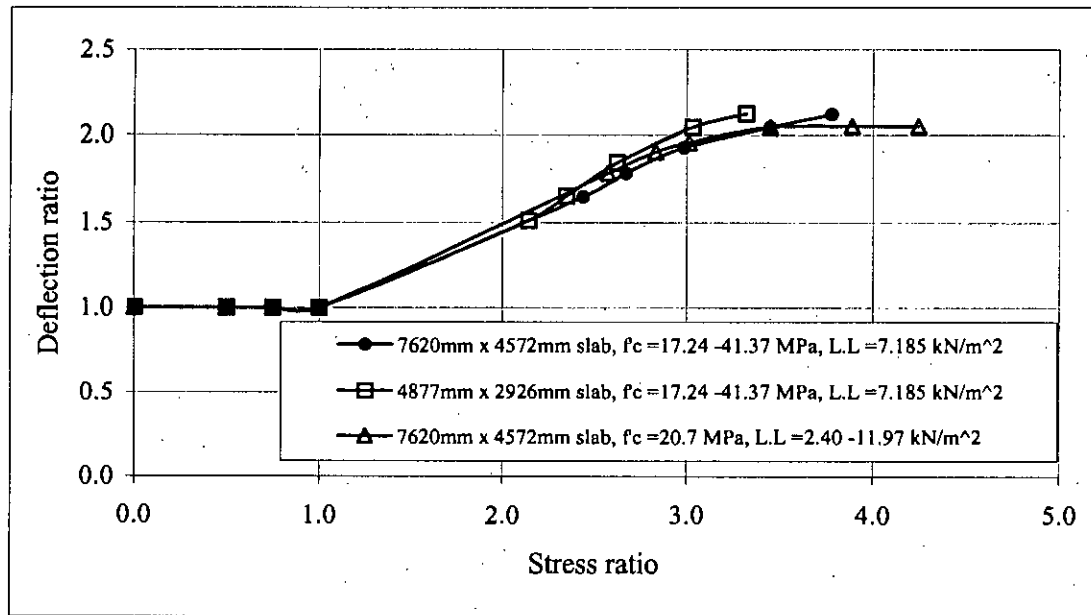


Figure 4.41 Variation of deflection ratio vs. stress ratio curve of slab for varying live load, concrete strength and span length, for case-5,  $f_r = 0.33 \sqrt{f'_c}$  N/mm<sup>2</sup>

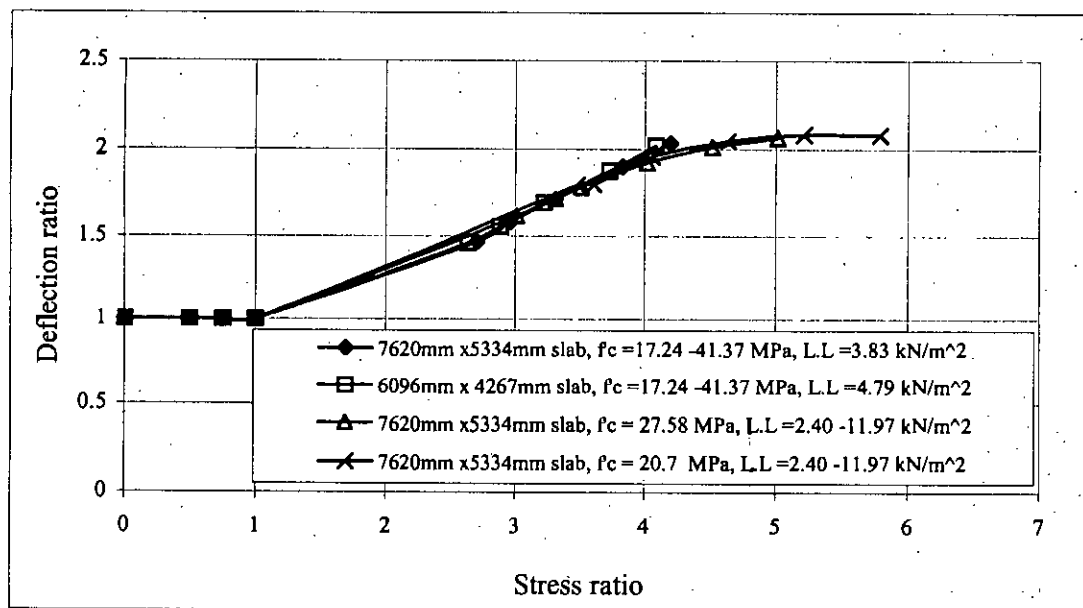
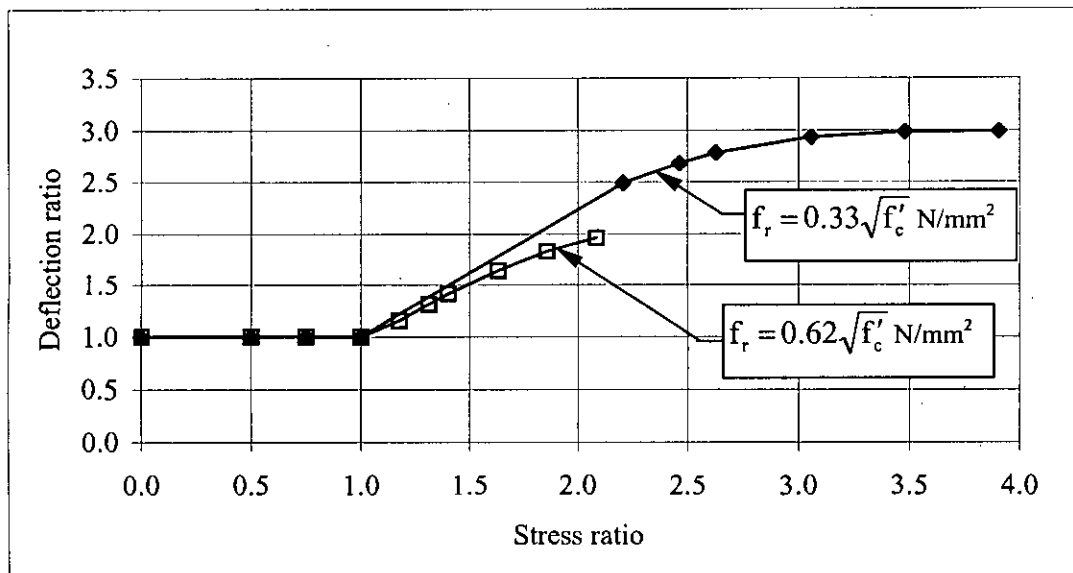


Figure 4.42 Variation of deflection ratio vs. stress ratio curve of slab for varying live load, concrete strength and span length, for case-8,  $f_r = 0.33 \sqrt{f'_c}$  N/mm<sup>2</sup>

#### 4.11.5 Effect of Modulus of Rupture of Concrete

The effect of modulus of rupture of concrete on deflection ratio vs. stress ratio curve has been studied for  $f_r = 0.62\sqrt{f'_c}$  N/mm<sup>2</sup> and  $0.33\sqrt{f'_c}$  N/mm<sup>2</sup>. For this purpose a 4572 mm×4572 mm (15 ft×15 ft) has been modeled. The parameters used in FE analysis are those used in section 4.7. The live load is varied from 2.4 to 12 kN/m<sup>2</sup>.

From this analysis it has been observed that deflection ratio vs. stress ratio curve are separate for different levels of modulus of rupture of concrete. In Fig. 4.43, the variation of deflection ratio vs. stress ratio curve for simply supported slab for varying load applied on the slab has been shown. So it is not possible to produce unique curves for two levels of modulus of rupture of concrete.



**Figure 4.43** Variation of deflection ratio vs. stress ratio curve of slab for varying rupture strength of concrete, for case-1

#### 4.11.6 Effect of Aspect Ratio

To check the effect of aspect ratio ( $m = l_a / l_b$ ) on deflection two slabs have been modeled with considering  $2.4 \text{ kN/m}^2$  (50 psf) of live load,  $1.2 \text{ kN/m}^2$  (25 psf) floor finish,  $1.44 \text{ kN/m}^2$  (30 psf) partition wall and ACI Code (1963) suggested slab thickness. In this analysis the long dimension of slab has been taken as  $l_b = 7620 \text{ mm}$ . The slab dimensions are changed with following aspect ratios of 1.00, 0.90, 0.80, 0.70, 0.60 and 0.50 and separate deflection ratio vs. stress ratio curves for each aspect ratio have been found. In Figs 4.44 and 4.45 the variation of deflection ratio vs. stress ratio curves for slab case-1 and slab case-2 have been shown. Different curves are obtained for different aspect ratio. From this type of chart a designer can find the immediate deflection for any aspect ratio, loading and dimension of two-way edge supported slab. Finally designer can predict the long-term deflection using ACI multiplier (ACI Code, 2002) approach.

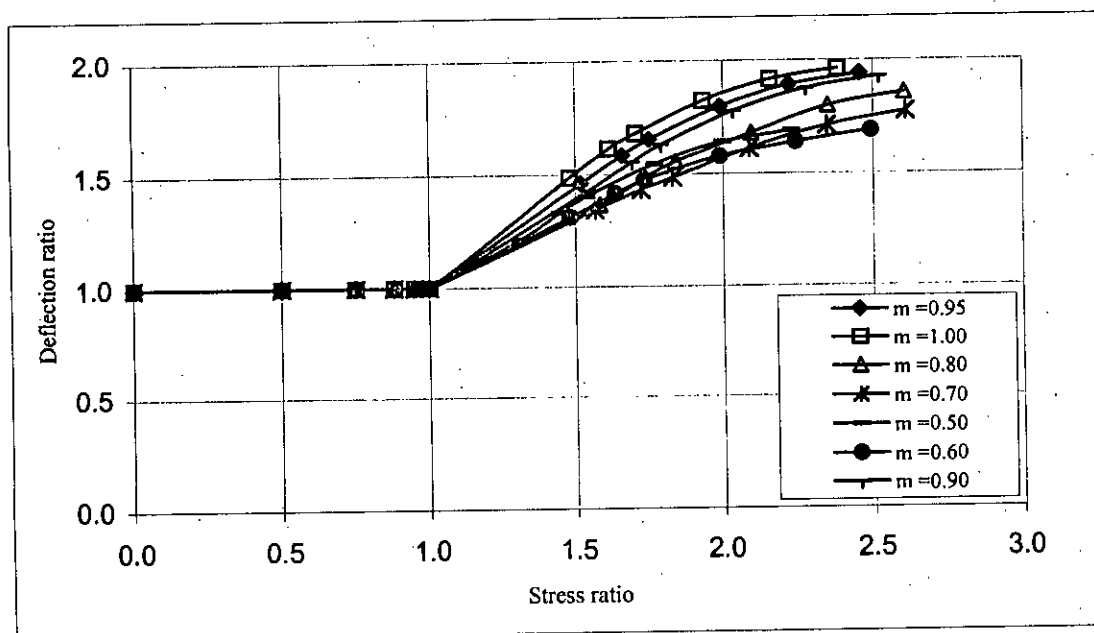


Figure 4.44 Deflection ratio vs. stress ratio curve of two-way edge supported slab,

for case-1,  $f_r = 0.62\sqrt{f'_c}$  N/mm<sup>2</sup>.

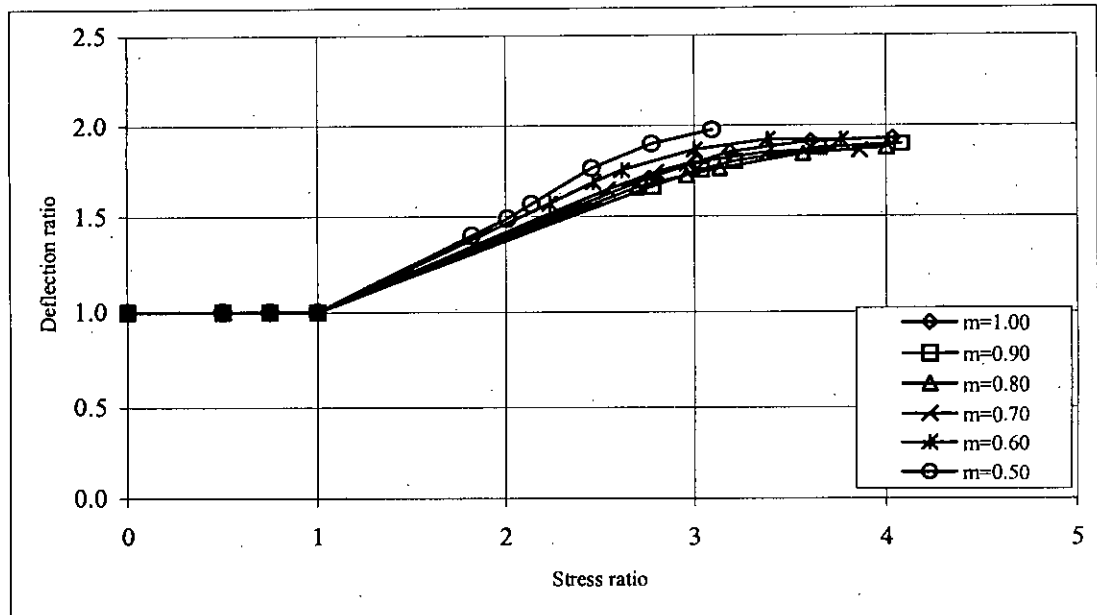


Figure 4.45 Deflection ratio vs. stress ratio curve of two-way edge supported slab,  
for case-2,  $f_r = 0.33\sqrt{f'_c}$  N/mm<sup>2</sup>



#### 4.12 Conclusion

In this chapter it has been observed that most of the edge supported slabs are cracked and immediate deflection is higher than elastic deflection. Performance of Hossain's nonlinear finite element module using ACI / Branson's crack model has been verified against experimental results of McNeice (1971) corner supported slab, McNeice (1967) one-way slab and Shukla and Mittal (1976) slabs. The parametric analyses have been performed with changing panel dimension, live load, slab thickness, concrete strength, and modulus of rupture of concrete, aspect ratio and percentage reinforcement required in the slab. It has been observed that the deflection ratio vs. stress ratio curves are not affected by the change of panel dimension, concrete strength and live load for particular aspect ratio and modulus of rupture of concrete. Deflection magnification is only affected by level of cracking  $f/f_r$ , aspect ratio and boundary conditions. This curve is valid for slab thickness up to 90% of ACI Code (1963) suggested thickness. From FE analysis, it has been observed that for a particular slab case, the deflection ratio vs. stress ratio curves for different aspect ratio form a band zone. It is possible to develop deflection ratio vs. stress ratio curves for different boundary conditions of slab to help easy calculation of immediate deflection.

## CHAPTER 5

### DEFLECTION ESTIMATION USING DESIGN CHARTS

#### 5.1 Introduction

A method of calculating deflection considering cracking using Branson's equation has been presented in Chapter 4 with appropriate validation against test data and a thorough parametric study has been carried out to identify effects of different parameters on deflection. It has been observed that even under service loads, the slabs do experience cracking and calculating deflection based on elastic analysis ignoring cracking may result in very unconservative design. But deflection calculation as shown in Chapter 4, considering cracking may prove to be complicated for the designer. In the current chapter a simplified method is proposed to help the designer to calculate short-term deflection considering cracking. Several design charts are proposed considering different boundary conditions and aspect ratio. The immediate deflection estimated from design charts are compared with the results of FE analysis. The estimated immediate deflections are also compared with experimental deflection of slabs tested by Shukla & Mittal (1976). An example for simple calculation of elastic and immediate deflection has been presented at the end of the chapter.

#### 5.2. Selection of Parameters

In order to produce design charts for deflection calculation for all possible cases, geometric and material parameters are varied in usual ranges. The main parameters are slab thickness, loading, material strength, support conditions, aspect ratio etc.

### 5.2.1 Slab Thickness

The FE analyses have been performed with ACI Code (1963) permitted slab thickness, which is equal to total panel perimeter divided by 180 and not less than 89 mm (3.5 inch). For all slab cases, the thickness has been taken equal to ACI thickness and rounding is avoided for exact modeling. For relatively smaller sizes of panel the thickness has been considered less than 89 mm (3.5 inch) for the purpose mentioned above. For heavily loaded slab the thickness has exceeded from ACI thickness for some slab cases and for that cases the slab thickness has been taken from strength point of view. The recent ACI Code (2002) specified slab thickness has been verified with ACI Code (1963) and comparatively higher thickness has been observed for all cases of slab. From FE analysis it has been observed that in the section 4.11.1 and 4.11.2 the variation of slab thickness (20% more and 10% less of ACI Code (1963) suggested thickness) not affected the deflection ratio vs. stress ratio curve.

### 5.2.2 Loading

The design charts are intended to be used for the whole range of load usual for common buildings. The slabs are designed for the purpose of modeling in USD system and dead loads and live loads have been considered in the analysis. The self-weight of slab and  $1.2 \text{ kN/m}^2$  (25 psf) of floor finish load are treated as total dead load. The total live load is calculated with the sum of  $1.35 \text{ kN/m}^2$  (30 psf) of partition wall load and live load applied on the slab. FE analysis has been performed using total load. The live load is varied from  $2.4 \text{ kN/m}^2$  (50 psf) to  $12 \text{ kN/m}^2$  (250 psf) for design and modeling of each slab with constant floor finish and partition wall load.

### 5.2.3 Support Conditions

The nine types of slab have been modeled with respect to end condition of slabs. The slab fixed to the support or continuous to the adjacent panel is expressed with hatching line and discontinuity is expressed without hatching line. All nine cases of slabs are presented in Fig. 3.34 with support conditions.

### 5.2.4 Span Ratio and Span Length

The span ratio or aspect ratio,  $m = l_a / l_b$  is varied from 0.50 to 1.00. The analyses have been performed for  $l_b = 7620$  mm (25 ft) and variation of aspect ratio  $m = 1.00, 0.90, 0.80, 0.70, 0.60$  and 0.50 with 0.10 interval of  $m$  for all slab cases. For slab cases 1, 2, 3 and 4 some additional slabs have been modeled with  $l_a = 3048$  mm (10 ft).

### 5.2.5 Reinforcement Ratio

Calculation of required reinforcement has been followed by the ACI Code (1963) coefficient method. The minimum reinforcement has been taken equal to  $0.0018bt$  in which  $b =$  width of slab (considered as unity) and  $t =$  slab thickness.

### 5.2.6 Material Properties

The material properties used in the modeling are concrete strength  $f'_c$ , modulus of elasticity of concrete  $E_c$ , modulus of rupture of concrete  $f_r$ , yield strength of steel  $f_y$ , Poisson's ratio  $\nu$  and Modular ratio  $n$ . The material properties used in the modeling are as follows:

$$f'_c = 20.7 \text{ N/mm}^2 \text{ (3000 psi), } 27.58 \text{ N/mm}^2 \text{ (4000 psi), } 34.48 \text{ N/mm}^2 \text{ (5000 psi) and } 41.3 \text{ N/mm}^2 \text{ (6000 psi).}$$

$$f_y = 413.7 \text{ N/mm}^2 \text{ (60000 psi)}$$

The modulus of elasticity of concrete,  $E_c$  has been considered according to ACI Code, i.e.  $E_c = 57000 \sqrt{f'_c}$  psi.

The values of Poisson's ratio,  $\nu$  of concrete fall in the range between 0.15 and 0.25. In the study the value of  $\nu$  is taken equal to 0.18.

The values of rupture strength of concrete  $f_r$  used in the modeling has been equal to  $0.33 \sqrt{f'_c}$  N/mm<sup>2</sup> ( $4 \sqrt{f'_c}$  psi) instead of  $0.62 \sqrt{f'_c}$  N/mm<sup>2</sup> ( $7.5 \sqrt{f'_c}$  psi). Tam and

Scanlon (1986) produced good correlation between calculated deflection with  $0.33\sqrt{f'_c}$  N/mm<sup>2</sup> value and mean field-measured deflection. This approach of using reduced modulus of rupture to take into the effect of cracking due to restraint shrinkage is reported in a series of papers [ACI Committee 435 (1991), Thompson & Scanlon (1988), Scanlon & Murraray (1982), Ghali (1990)].

### 5.3 Mesh Sensitivity of the Modeling

The modeling of edge supported slab has been performed for the preparation of deflection ratio vs. stress ratio curves to facilitate the easy calculation of immediate deflection. In previous sections 3.2 and 4.7 the mesh sensitivity of the modeling of slab deflection have been discussed. It has been found that the number of element less than  $10 \times 10 = 100$  for  $1/4^{\text{th}}$  portion of a square panel insignificantly affected the FE results. To get correct result, based on previous mesh sensitivity analysis, following mesh sizes are used for different slab cases and aspect ratios. For calculation of immediate deflection, nine types of slabs have been modeled with the following mesh density. The slab cases 1, 2, 3 and 5 the  $1/4^{\text{th}}$  portion of the slab have been modeled considering axis of symmetry. The number of plate element used in analysis for aspect ratio  $m = 1.00$  equal to  $16 \times 16 = 256$  for  $1/4^{\text{th}}$  portion of above slab cases and reduction of element number in the short direction has been considered with proportional to the aspect ratio. For slab cases 6 and 8 the half portion of the slab have been modeled with mesh density  $16 \times 32 = 512$  for aspect ratio 1.00 and reduction of meshing has followed by the other aspect ratios. For slab cases 7 and 9 the half portion of the slabs are also modeled with mesh density  $32 \times 16 = 512$  for aspect ratio 1.00 and other slabs with aspect ratios less than 1.00 are followed with same. The slab case 4 the full slab is modeled with  $20 \times 20 = 400$  number of plate element for aspect ratio 1.00 and 0.90 and  $24 \times 18 = 432$  for  $m = 0.80$ ,  $24 \times 16 = 384$  for  $m = 0.70$ ,  $24 \times 14 = 336$  for  $m = 0.60$  and  $24 \times 12 = 228$  for  $m = 0.50$ .

### 5.4 Moment and Deflection Coefficients for Calculation of Deflection

The bending moment coefficients of two-way edge supported slabs have been calculated from the finite element program FE-77 and ANSYS. The results were compared with ACI moment coefficient discussed in the section 3.4 and observed that both FE programs have shown identical results. The coefficients predicted from FE analysis are presented in the Table 3.7 for calculation of maximum flexural stress developed in the slab. The results have been found from elastic FE analysis and are different from ACI moment coefficient, which considers inelastic redistribution. For calculation of elastic deflection of slab elastic deflection coefficients are presented in Table 3.6. With help of elastic deflection coefficients designer can calculate the elastic deflection of edge supported slab without FE analysis.

### 5.5 Deflection Ratio vs. Stress Ratio Curve

Nine sets of design charts have been prepared to facilitate the easy calculation of deflection. For each boundary type and particular aspect ratio, a large number of analysis has been carried out with varying thickness, load etc. such that slabs with different levels of cracking are considered. For a particular type of boundary condition, deflection ratio vs. stress ratio curves are plotted with stress ratio in x-axis and deflection ratio in y-axis. The term stress ratio means the ratio between the maximum stress developed in the slab and modulus of rupture of concrete:

$$\text{Mathematically, stress ratio} = \frac{\text{Developed maximum stress}}{\text{Modulus of rupture of concrete}}$$

and the term deflection ratio means the ratio between immediate deflection and elastic deflection of slab:

$$\text{Mathematically, deflection ratio} = \frac{\text{Immediate deflection}}{\text{Elastic deflection}}$$

When the slab is not cracked then immediate deflection must be equal to the elastic deflection and deflection ratio is equal unity.

The stresses are calculated from the most cracked zone of edge supported slabs. From analysis, it has been observed that the slabs are more cracked at support than the other portions. For slab case-1, to check the level of cracking, the stress at midspan of the slab has been considered along the shorter direction. For slab cases 3 and 7 the stresses are considered at support along the longer direction and rest of the slab cases the stresses are checked at the support along shorter direction of slabs. The stress has been considered in the middle strip of the slab.

A designer can calculate the actual immediate deflection of slab from design charts. In each slab case, separate curves for different aspect ratios have been found and formed a band of curves. For slab case-1, the upper range of the curve corresponds to aspect ratio 1.00 and lower range to 0.50 and rest of the slab cases, i.e. 2 to 9, have shown reverse trends. The deflection ratio vs. stress ratio curves are shown in the Figs 5.1 to 5.9. The stress ratio up to unity means no cracking of slab and immediate deflection will be equal to elastic deflection. The stress ratio greater than unity represents cracking of slab and immediate deflection will be greater than the elastic deflection and it can be calculated by multiplying factor called deflection ratio. All curves are proposed for modulus of rupture of concrete,  $f_r = 0.33\sqrt{f'_c}$  N/mm<sup>2</sup> ( $4\sqrt{f'_c}$  psi). Similar design charts are prepared with modulus of rupture of  $0.62\sqrt{f'_c}$  N/mm<sup>2</sup> ( $7.5\sqrt{f'_c}$  psi) which are presented in Appendix A. They correspond to a condition where restraint shrinkage is negligible.

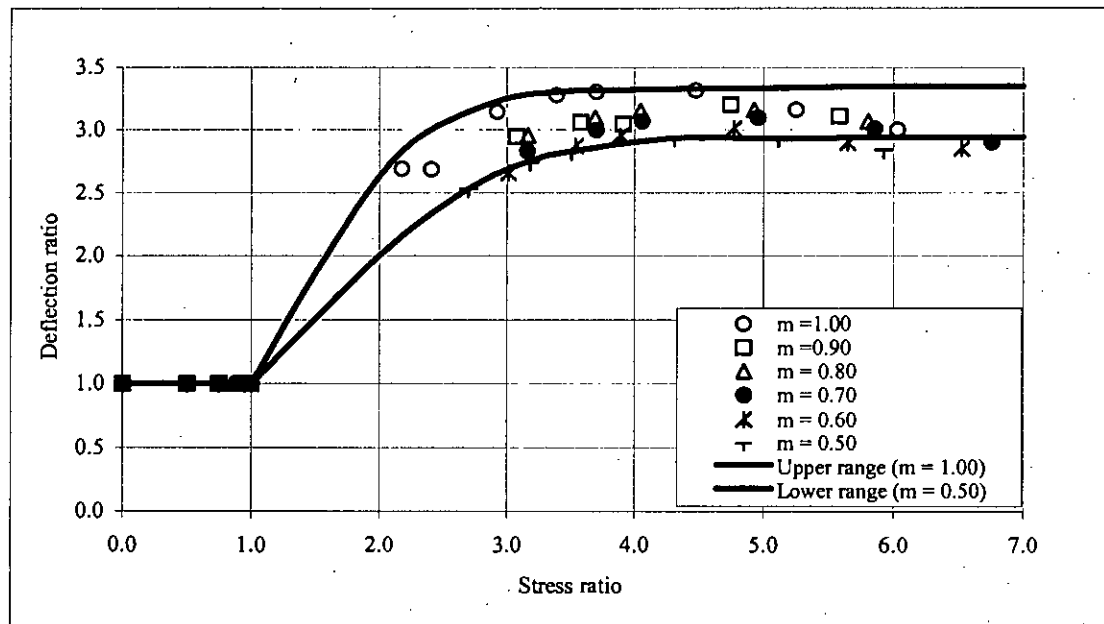


Figure 5.1 Deflection ratio vs. stress ratio chart of edge supported slab for case-1,

$$f_r = 0.33 \sqrt{f'_c} \text{ N/mm}^2$$

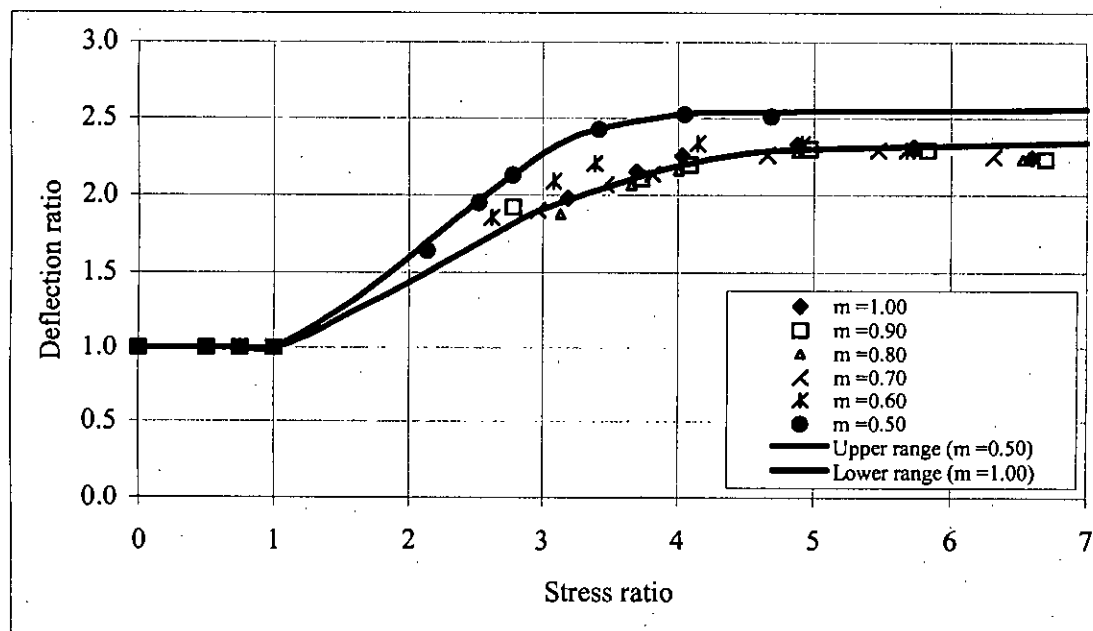


Figure 5.2 Deflection ratio vs. stress ratio chart of edge supported slab for case-2,

$$f_r = 0.33 \sqrt{f'_c} \text{ N/mm}^2$$



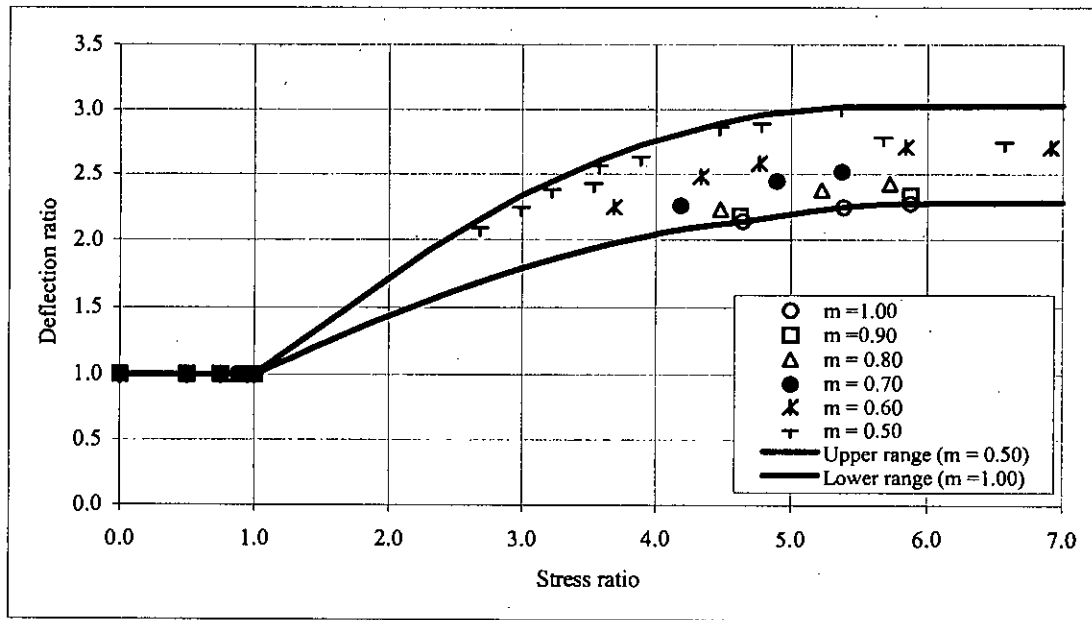


Figure 5.3 Deflection ratio vs. stress ratio chart of edge supported slab for case-3,

$$f_r = 0.33 \sqrt{f'_c} \text{ N/mm}^2$$

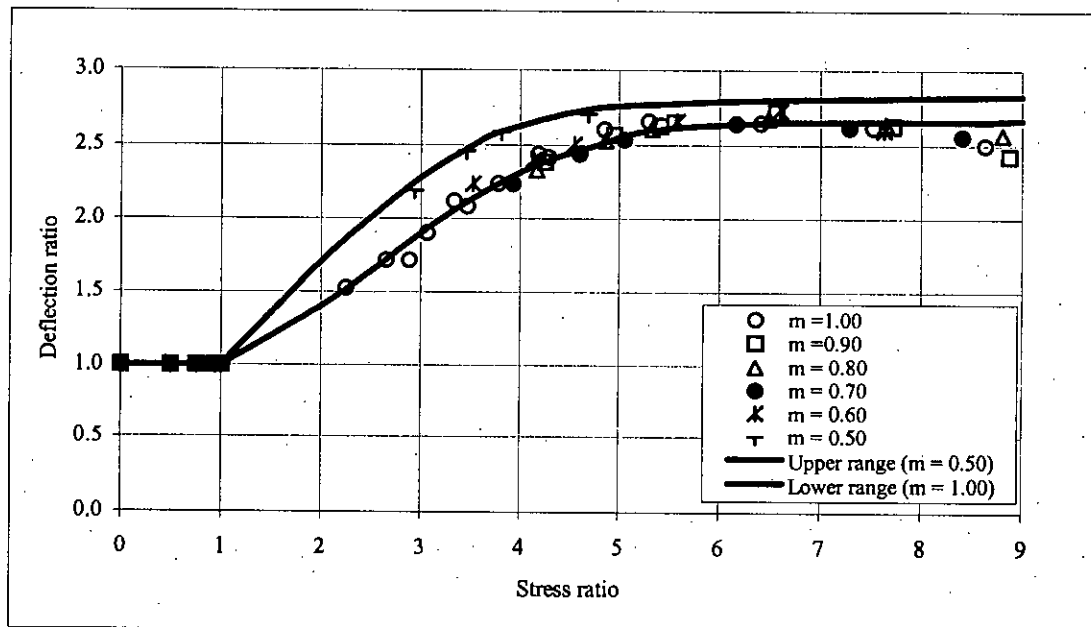


Figure 5.4 Deflection ratio vs. stress ratio chart of edge supported slab for case-4,

$$f_r = 0.33 \sqrt{f'_c} \text{ N/mm}^2$$

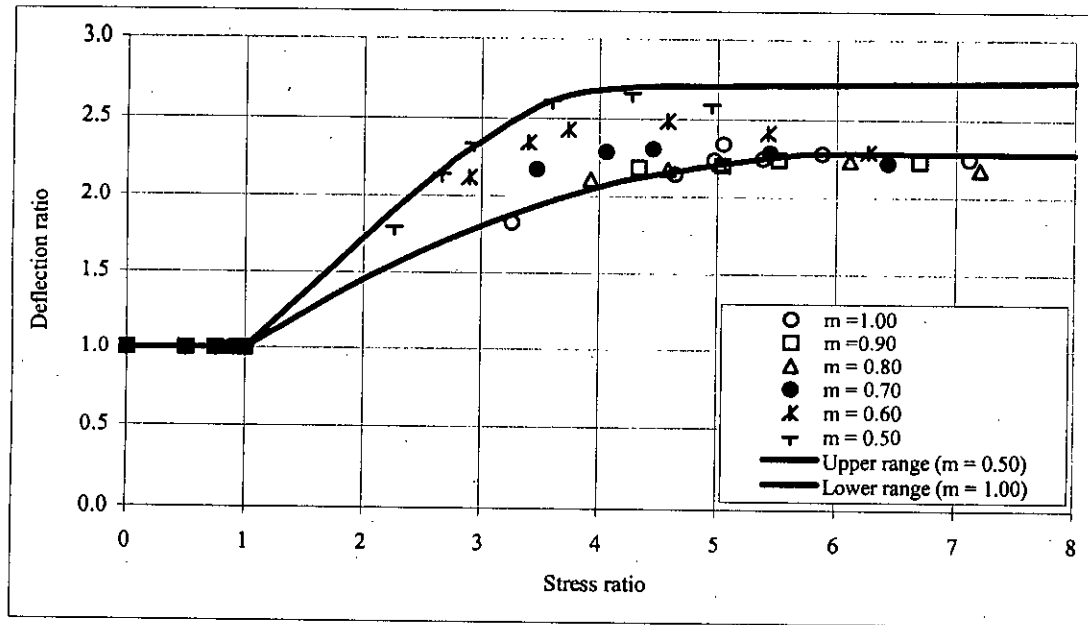


Figure 5.5 Deflection ratio vs. stress ratio chart of edge supported slab for case-5,

$$f_r = 0.33\sqrt{f'_c} \text{ N/mm}^2$$

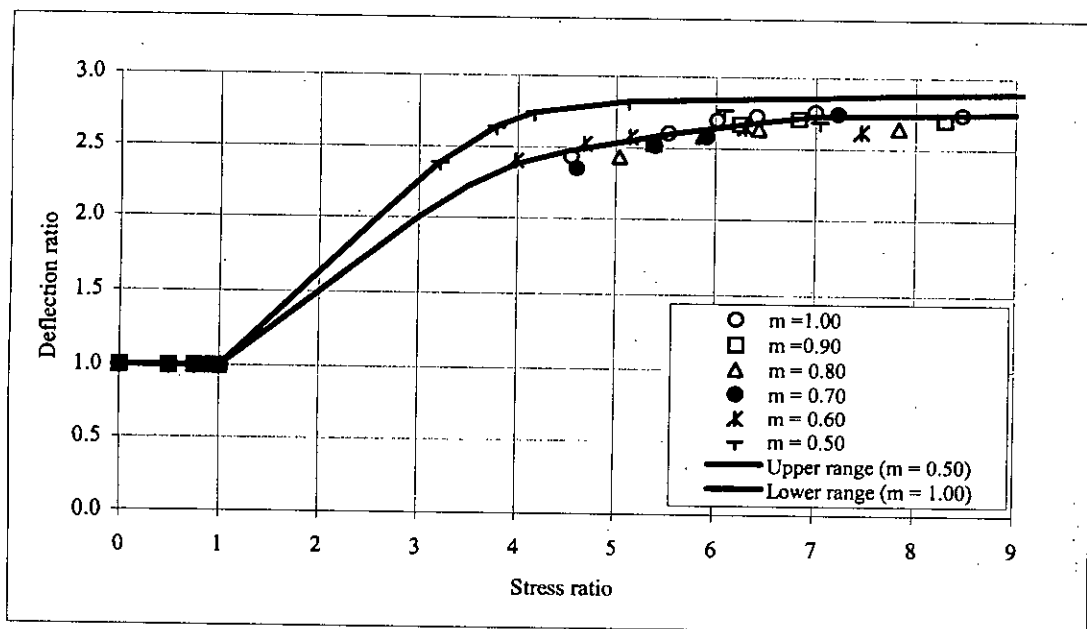


Figure 5.6 Deflection ratio vs. stress ratio chart of edge supported slab for case-6,

$$f_r = 0.33\sqrt{f'_c} \text{ N/mm}^2.$$

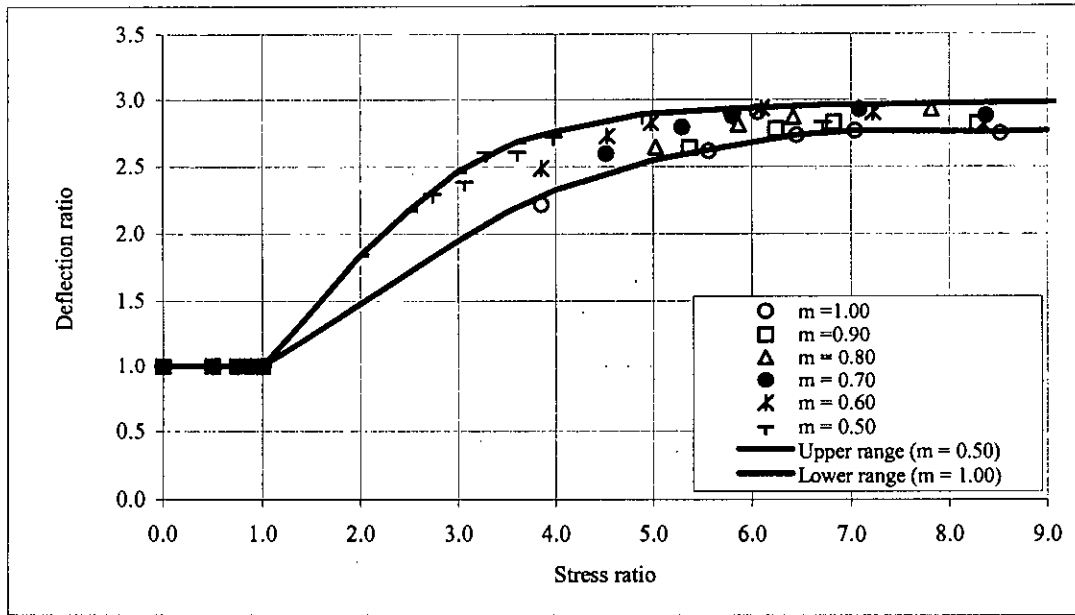


Figure 5.7 Deflection ratio vs. stress ratio chart of edge supported slab for case-7,

$$f_r = 0.33 \sqrt{f'_c} \text{ N/mm}^2$$

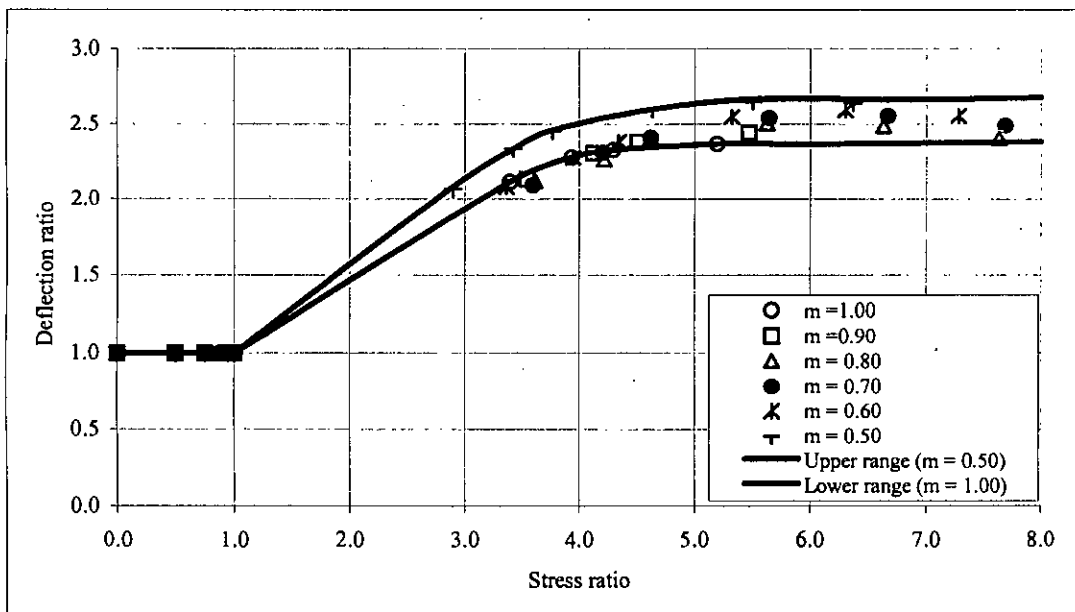
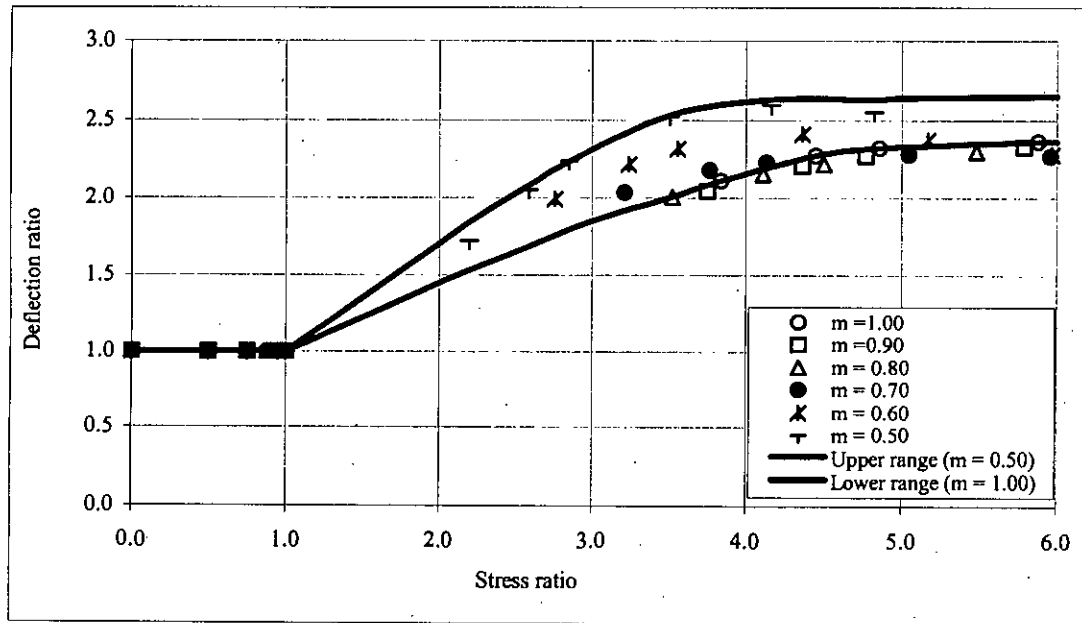


Figure 5.8 Deflection ratio vs. stress ratio chart of edge supported slab for case-8,

$$f_r = 0.33 \sqrt{f'_c} \text{ N/mm}^2$$



**Figure 5.9** Deflection ratio vs. stress ratio chart of edge supported slab for case-9,

$$f_r = 0.33 \sqrt{f'_c} \text{ N/mm}^2$$

## 5.6 Calculation of Elastic and Immediate Deflection of Slab

In Chapter 3, elastic deflections of different types of slabs have been calculated by finite element softwares ANSYS and FE-77. Also, in Chapter 4, immediate deflections considering cracking have been determined employing Branson's equation in FE-77 software. Both calculation of elastic and immediate deflection using finite element software are not simple and not particularly suitable for use in design office. To simplify the calculation, design charts are proposed in section 5.5. In the current section, use of these design charts are discussed.

### 5.6.1 Calculation of Elastic Deflection of Slab

The elastic deflections of two-way edge supported slabs have been calculated by the softwares ANSYS and FE-77 and same results are found for any support condition and aspect ratio. From finite element analysis, deflection coefficients have been

proposed (Table 3.6) for the calculation of elastic deflection of edge supported slabs. Chowdhury (2000) has also proposed deflection coefficients for the calculation of deflection and observed that the deflection coefficients are more or less same which has been discussed in the section 3.5. The elastic deflection coefficients of edge supported slabs are presented in the Table 3.6. The designer can easily calculate the elastic deflection at the center of the edge supported slab by using Eqn. (3.4).

### 5.6.2 Calculation of Immediate Deflection of Slab Using Design Charts

The calculation procedure of immediate deflection of two-way edge supported reinforced concrete slabs using design charts for different edge conditions and aspect ratios are presented here. The designer select a slab panel and assume the slab thickness and calculate the total load acting on it. Using material properties the elastic deflection can be calculated from Eqn. (3.4). The maximum flexural stress developed at support or midspan is then calculated for selected slab thickness and total load as follows:

$$f = \frac{6M}{bt^2} = \frac{6cwl^2}{bt^2} \quad (5.1)$$

where,

$f$  = flexural stress developed in the slab

$b$  = width of slab usually taken as unity

$t$  = total thickness of slab, and

$$M = cwl^2 \quad (5.2)$$

where,

$M$  = bending moment of slab

$c$  = moment coefficient from Table 3.7

$w$  = total load applied on the slab

$l$  = span length of slab

After calculation of the developed stress, the stress ratio ( $f/f_r$ ) is to be determined. The corresponding deflection ratio is then read from deflection ratio vs. stress ratio curve for the particular boundary type. Appropriate interpolation may be necessary

to obtain a deflection ratio for an intermediate aspect ratio. Finally the immediate deflection is calculated from multiplication of elastic deflection and deflection ratio.

$$\text{Immediate deflection} = \text{Deflection ratio} \times \text{Elastic deflection.} \quad (5.3)$$

A designer can easily calculate the immediate deflection of two-way edge supported reinforced concrete slabs for different edge conditions and aspect ratios without help of any finite element program.

### 5.7 Comparison of Immediate Deflection with FE Analysis

The immediate deflections predicted using proposed design charts is verified here. For this purpose, a large number of slabs with different end conditions has been considered with changing aspect ratio, loading and slab dimensions. In any aspect ratio between upper and lower range (0.5 and 1) the respective deflection ratio has been taken as weighted average value from the deflection ratio vs. stress ratio chart. Both deflections computed from FE analysis and estimated using design charts are presented in the Table 5.1 and variation in results have been observed to be insignificant. In most cases conservative results of immediate deflection have been found when using charts.

#### Estimation of immediate deflection

To estimate the immediate deflection of two-way slab, a 7620 mm  $\times$  7620 mm (25 ft  $\times$  25 ft) corner panel has been considered with following parameters. Total dead load = 5.19 kN/m<sup>2</sup> (108 psf), live load = 5.27 kN/m<sup>2</sup> (110 psf), slab thickness = 169.33 mm (6.67 inch),  $E_c = 20685 \text{ N/mm}^2$  ( $3 \times 10^6$  psi),  $f'_c = 20.7 \text{ N/mm}^2$  (3000 psi) and modulus of rupture of concrete,  $f_r = 0.33\sqrt{f'_c} \text{ N/mm}^2$  ( $4\sqrt{f'_c}$  psi).

The aspect ratio of the panel,  $m = 1.00$  and corresponding deflection coefficient and moment coefficient have been calculated from Table 3.6 and 3.7 respectively. The required values for calculation of elastic and immediate deflection are:

Deflection coefficient,  $D_a = 2.5977 \times 10^{-2}$

Moment coefficient,  $c = 0.0577$

Span length,  $l_a = 7620$  mm

Total load on slab,  $w = 10.46 \times 10^{-3}$  N/mm<sup>2</sup> (218.33 psf)

Modulus of rupture of concrete,  $f_r = 1.51$  N/mm<sup>2</sup>

$$\begin{aligned} \text{Elastic deflection, } \delta &= \frac{D_a w l_a^4}{E t^3} \\ &= \frac{2.5977 \times 10^{-2} \times 10.46 \times 10^{-3} \times (7620)^4}{20685 \times (169.33)^3} \\ &= 9.116 \text{ mm.} \end{aligned}$$

The flexural stress developed at support in the short direction,

$$\begin{aligned} f &= \frac{6c w l_a^2}{b t^2} \\ &= \frac{6 \times 0.0577 \times 10.46 \times 10^{-3} \times (7620)^2}{1 \times (169.33)^2} \\ &= 7.33 \text{ N/mm}^2 \end{aligned}$$

The stress ratio,  $f/f_r = 7.33 / 1.51 = 4.85$

The deflection ratio determined from design chart (Figure 5.4) = 2.6

The immediate deflection = Elastic deflection  $\times$  Deflection ratio

$$= 9.116 \times 2.6$$

$$= 23.7 \text{ mm.}$$

From FE analysis of the slab the immediate deflection has been found = 23.612 mm

% variation with respect to FE analysis = 0.40

**Table 5.1** Comparison of calculated and FE analyzed deflections for different slab cases.

Slab case	Slab dimension (mm×mm)	Slab thickness (mm)	Total load (kN/m <sup>2</sup> )	Immediate deflection from deign chart (mm)	Immediate deflection from FE analysis (mm)	% variation wrt FE analysis
Case-1	3048×3048	67.73	6.624	12.47	12.49	-0.1
	4572×4572	101.60	7.425	22.04	21.42	2.9
	7620×6096	152.40	11.013	46.74	46.18	0.9
	7620×3810	127.00	12.808	22.49	22.29	0.9
Case-2	7620×3810	127.00	10.418	3.36	3.27	2.8
	7620×6096	152.40	13.41	12.89	12.27	5.0
	7620×4572	135.47	17.803	10.40	9.55	8.8
	6096×6096	135.47	8.22	6.08	6.07	0.2
Case-3	7620×6858	160.87	10.258	10.50	9.96	4.0
	7620×5334	143.93	8.422	15.49	14.12	9.7
	5486×2743	91.44	14.37	15.36	15.39	-0.2
	7620×4572	135.47	10.617	19.11	17.70	8.0
Case-4	7620×6096	152.40	11.017	21.99	20.94	5.0
	4877×4877	108.37	10.50	14.70	15.06	-2.5
	7620×6858	160.87	8.339	14.44	14.60	1.1
	7620×6858	160.87	10.258	21.93	21.24	3.2
Case-5	7620×6096	152.40	10.06	17.48	18.08	-3.3
	7620×4572	135.47	10.617	12.49	11.57	8.0
	6096×6096	135.47	9.66	13.04	13.15	-0.9
	7620×5334	143.93	9.86	9.02	8.43	7.0
Case-6	7620×4572	135.47	10.617	6.70	6.54	2.5
	7620×4572	127.00	12.813	5.09	5.09	0.0
	7620×7620	169.33	9.02	27.11	26.58	2.0
	7620×6096	152.4	11.017	25.53	24.26	5.2
Case-7	7620×5334	143.93	9.86	17.55	16.22	8.2
	7620×4572	135.47	15.4	20.07	18.85	6.4
	7620×6858	160.87	10.25	31.83	31.79	0.1
	7620×6096	152.40	8.622	24.35	24.01	1.4
Case-8	7620×4572	135.47	15.407	34.78	34.10	2.0
	5486×2743	91.44	8.62	8.86	8.85	0.1
	7620×3810	127.00	9.46	14.02	13.51	3.8
	7620×7620	169.33	10.46	15.19	14.99	1.4
Case-9	7620×6858	160.87	13.61	20.81	20.61	1.0
	7620×6096	152.40	8.62	11.32	10.60	6.0
	7620×5334	143.93	13.21	17.25	16.96	1.7
	7620×3810	127.00	15.21	6.02	5.94	1.3
Case-9	7620×4572	135.47	10.617	6.31	6.04	4.4
	7620×6096	152.40	10.06	10.77	9.934	8.4
	7620×7620	169.33	11.416	16.95	16.71	1.4



### 5.8 Validation of the Design Charts with Experimental Results and FE Analysis

Considering modulus of rupture of concrete,  $f_r = 0.62\sqrt{f'_c}$  N/mm<sup>2</sup> (7.5 $\sqrt{f'_c}$  psi) a design chart has been developed for calculation of immediate deflection for slab case-1, as shown in Fig. 5.10. The developed design chart for prediction of immediate deflection of two-way edge supported slab has been verified with the experimental results tested by Shukla & Mittal (1976). For this purpose three slabs S-8, S-11 and S-12 have been considered. These slabs are single panel and resting on masonry walls and as a result extra tensile stress was not generated due to restraint shrinkage and a value of  $0.62\sqrt{f'_c}$  N/mm<sup>2</sup> (7.5 $\sqrt{f'_c}$  psi) for modulus of rupture is logical. The details Shukla & Mittal (1976) slab are discussed in section 4.6.3. The deflections predicted using design chart and experimental results are presented in Figs 5.11 to 5.13. It has been observed that the calculated immediate deflections from design chart compare well with those obtained from experiments.

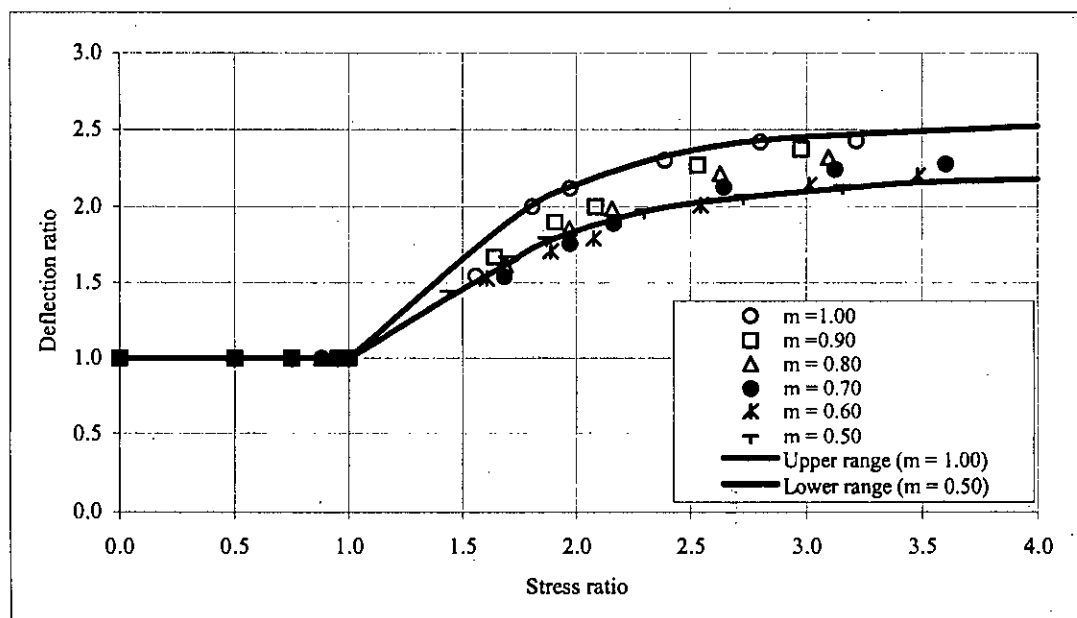


**Figure 5.10** Deflection ratio vs. stress ratio chart of two-way edge supported slab for case-1,  $f_r = 0.62\sqrt{f'_c}$  N/mm<sup>2</sup> (7.5 $\sqrt{f'_c}$  psi).

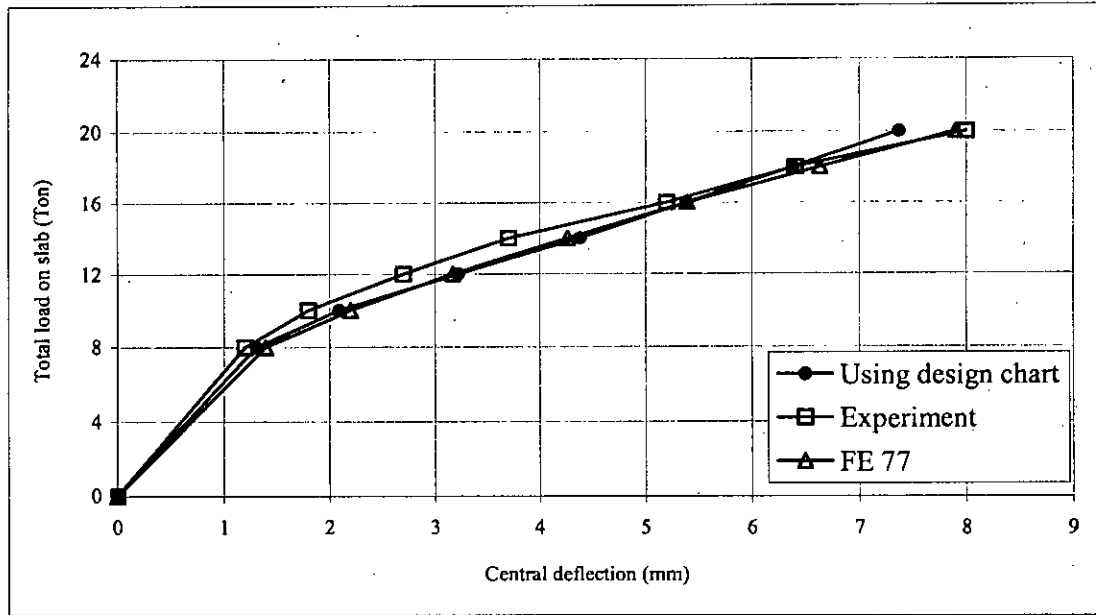


Figure 5.11 Load-deflection curve for Shukla & Mittal slab, S-8.

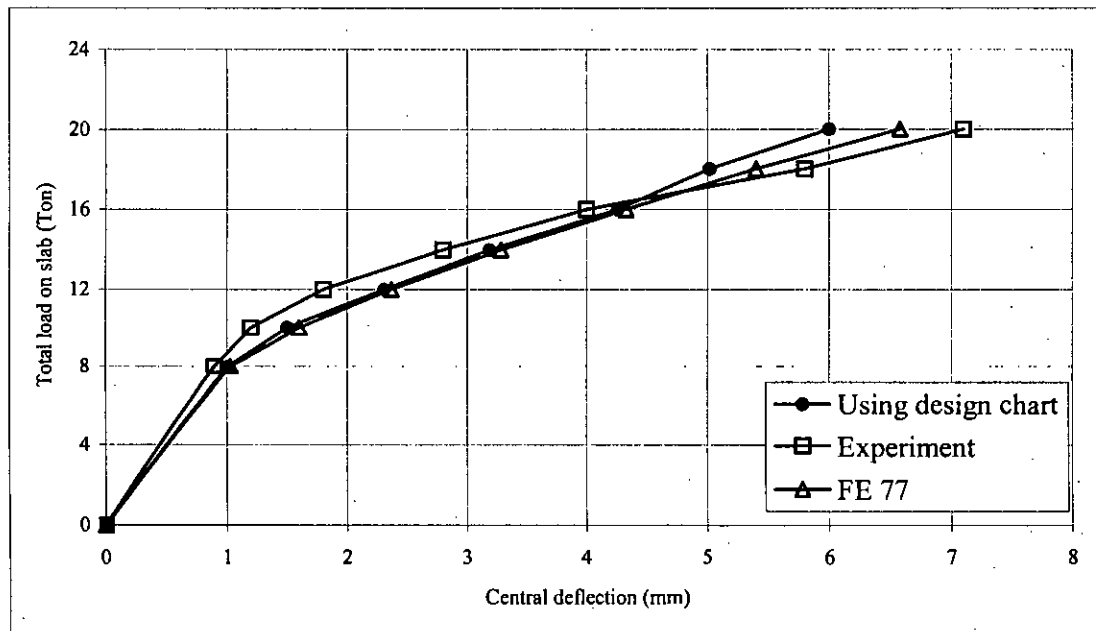
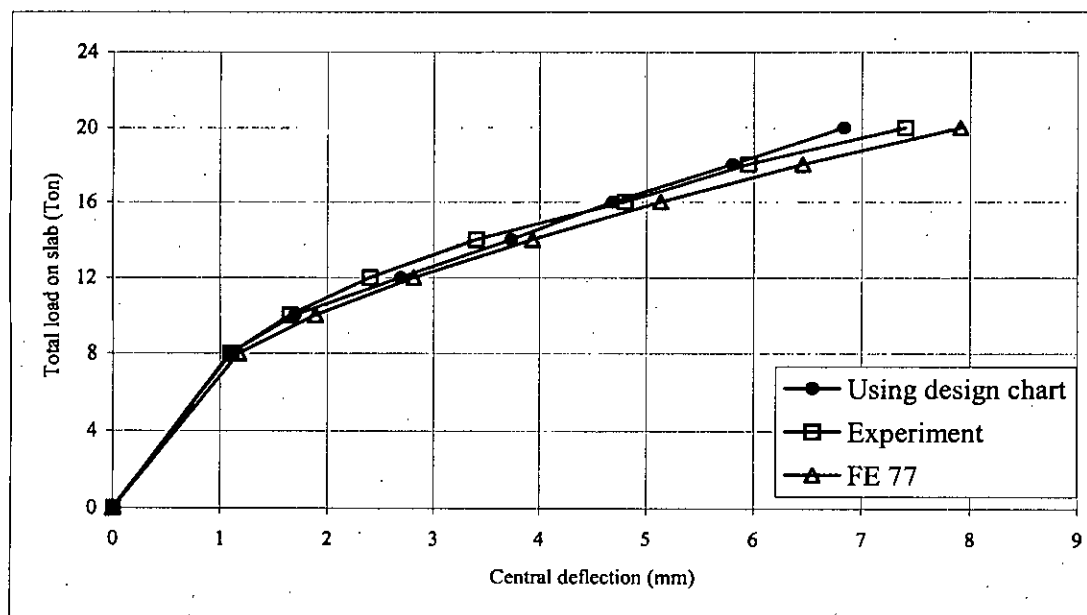


Figure 5.12 Load-deflection curve for Shukla & Mittal slab, S-11.



**Figure 5.13** Load-deflection curve for Shukla & Mittal slab, S-12.

### 5.9 Conclusion

In this chapter the calculation procedure of elastic and immediate deflection of two-way edge supported slabs have been presented. Nine sets of design charts have been proposed for the calculation of immediate deflection of two-way edge supported slabs for different boundary conditions and aspect ratio to facilitate the designer. The calculation procedure of elastic and immediate deflection of edge supported slab with an example has been worked out. The immediate deflections calculated from finite element analysis and those obtained using design charts compare reasonably well. Finally the immediate deflections calculated from design charts have been compared with experimental results and deflections predicted from FE analysis. Design charts have been proved to yield very good estimation of immediate deflection.

## CHAPTER 6

### ESTIMATION OF LONG-TERM DEFLECTION

#### 6.1 Introduction

In Chapter 5, the calculation of immediate deflection of slab using design charts for different end conditions has been discussed. In this chapter the calculation of long-term deflection of two-way edge supported slab are discussed using FE analysis and design charts. ACI Code (2002) simplified multiplier approach has been used to consider the effects of creep and shrinkage. The adequacy of ACI minimum thickness of slab for different live load, span length and concrete strength are verified in a parametric study by checking incremental and total deflection. The calculation procedures of incremental and total deflection are demonstrated with examples.

#### 6.2 Example Showing Short- and Long-term Deflections Estimation

To demonstrate the method of deflection calculation following ACI Code, an example is worked out here. Unlike the approach shown in Nilson (1997), cracking in slab is considered in the FE analysis. In the current example, short- and long-term deflections of a 4267 mm×3658 mm (14 ft×12 ft) corner panel slab has been estimated with following parameters.

Slab thickness has been calculated using recent formula shown in Eqn. (2.47) and found to be 95 mm (3.73 inch), the following parameters are assumed:

$f'_c = 20.7 \text{ N/mm}^2$  (3000 psi),  $f_y = 413.7 \text{ N/mm}^2$  (60000 psi),  $E_c = 20685 \text{ N/mm}^2$  ( $3 \times 10^6$  psi), Poisson's ratio = 0.18 and Modular ratio,  $n = 10$ .

A reduced value of  $0.33 \sqrt{f'_c}$  N/mm<sup>2</sup> ( $4 \sqrt{f'_c}$  psi) has been used for rupture strength of concrete instead of  $0.62 \sqrt{f'_c}$  N/mm<sup>2</sup> ( $7.5 \sqrt{f'_c}$  psi). The total dead load with 1.2 kN/m<sup>2</sup> (25 psf) of floor finish was 3.45 kN/m<sup>2</sup> (72 psf) and live load was 3.83 kN/m<sup>2</sup> (80 psf). Full panel has been modeled with  $24 \times 20 = 480$  plate elements and from FE analysis using ACI crack model, the immediate deflection has been found for total dead and live load. The calculation of long-term deflection has been performed using ACI multiplier method as discussed in section 2.6.1 with a sustained load of 30% live load and  $\xi = 3.0$  as proposed by Branson for slabs.

### 6.2.1 Long-term Deflection Calculation from FE Analysis

Long-term deflection calculation method demonstrated in this section is adapted from Nilson (1997). Immediate deflection for dead load and live load from FE analysis,  $\Delta_{d+1} = 4.44$  mm

The time-dependent portion of dead load deflection is,

$$\Delta_d = 4.44 \times \frac{3.45}{7.28} \times 3 = 6.31 \text{ mm}$$

The long-term deflection due to sustained portion of the live load is

$$\Delta_{0.3L} = 4.44 \times \frac{3.83}{7.28} \times 0.3 \times 4 = 2.80 \text{ mm}$$

The instantaneous deflection due to application of short-term portion of the live load is

$$\Delta_{0.7L} = 4.44 \times \frac{3.83}{7.28} \times 0.7 = 1.63 \text{ mm}$$

The total incremental deflection is  $\Delta = 6.31 + 2.80 + 1.63 = 10.75$  mm

The ACI Code limitation of incremental deflection is  $\frac{1}{480} = 7.62$  mm, it is observed that the slab thickness needs to be increased to control the incremental deflection of slab.

The total deflection is  $\Delta_{\text{total}} = 6.31 \times \frac{4}{3} + 2.80 + 1.63 = 12.84$  mm

The ACI Code limitation of total deflection is  $\frac{1}{240} = 15.24$  mm. From calculation, slab thickness is found to be adequate regarding total deflection.

### 6.2.2 Long-term Deflection Calculation from Design Charts

In Chapter 5, the calculation of immediate deflection of a slab for different end conditions from design charts are discussed. With the help of those design chart the immediate deflection of the above slab has been estimated to be 4.8 mm. The calculation of incremental and total deflections from above procedure are presented as follows.

Immediate deflection for dead load and live load from design chart,  $\Delta_{d+l} = 4.8$  mm

The time-dependent portion of dead load deflection is,

$$\Delta_d = 4.8 \times \frac{3.45}{7.28} \times 3 = 6.82 \text{ mm}$$

The long-term deflection due to sustained portion of the live load is

$$\Delta_{0.3L} = 4.8 \times \frac{3.83}{7.28} \times 0.3 \times 4 = 3.03 \text{ mm}$$

The instantaneous deflection due to application of short-term portion of the live load is

$$\Delta_{0.7L} = 4.8 \times \frac{3.83}{7.28} \times 0.7 = 1.77 \text{ mm}$$

The total incremental deflection is  $\Delta = 6.82 + 3.03 + 1.77 = 11.62$  mm

The ACI Code limitation of incremental deflection is  $\frac{1}{480} = 7.62$  mm, it is observed that the slab thickness needs to be increased to control the incremental deflection of slab.

The total deflection is  $\Delta_{\text{total}} = 6.82 \times \frac{4}{3} + 3.03 + 1.77 = 13.89$  mm

The ACI Code limitation of total deflection is  $\frac{1}{240} = 15.24$  mm. From calculation, slab thickness is found to be adequate regarding total deflection.

### 6.3 Parametric Study Showing Adequacy of Thickness

To study the adequacy of minimum thickness of ACI Code (2002), a parametric study has been carried out varying live load, concrete strength, slab thickness and panel size. Incremental and total deflections have been calculated using the approach shown preceding section. The effects of these parameters on incremental and total long-term deflections have been monitored.

#### 6.3.1 Live Load

To investigate the role of live load, it has been varied from  $1.92 \text{ kN/m}^2$  to  $6.71 \text{ kN/m}^2$  (40 psf to 140 psf) for a  $4267 \text{ mm} \times 3658 \text{ mm}$  (12 ft  $\times$  14 ft) slab. The panel under consideration is a corner panel, the thickness has been chosen using Eqn. (2.47) and Direct Design Method was employed. The FE analysis was carried using  $20 \times 24 = 480$  number of plate elements. Plate stiffness was reduced considering cracking using Branson's equation (Eqn. 4.1). Incremental and total deflections were calculated following the procedure described in the previous section assuming that only 30% of the live load remains sustained. In the analysis, deflection calculations under dead and live load were carried out with both elastic and cracked sections. Two levels of modulus of rupture, i.e.  $f_r = 0.33 \sqrt{f'_c} \text{ N/mm}^2$  and  $0.62 \sqrt{f'_c} \text{ N/mm}^2$  ( $4 \sqrt{f'_c} \text{ psi}$  and  $7.5 \sqrt{f'_c} \text{ psi}$ ) were used to show the effect of restraint shrinkage induced cracks. Incremental and total deflection variations with live load along with the allowable value have been plotted in Figs 6.1 and 6.2, respectively. The results show that if a reduced modulus of rupture is used in the analysis to cater for restraint shrinkage, the incremental deflections seem excessive even at  $2.87 \text{ kN/m}^2$  (60 psf) live load. The total deflection limit, which is generally easier to satisfy, is also exceeded at higher loads. The curves also show the effect of considering cracking which is often ignored in calculations of slab deflections.

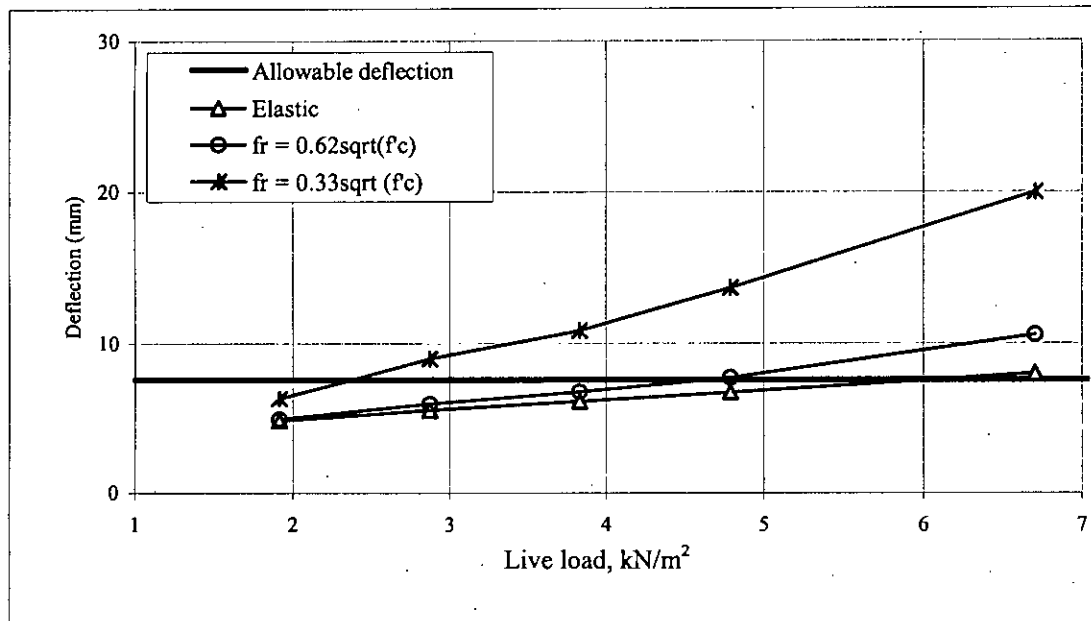


Figure 6.1 Variation of incremental deflection with varying live load for a 3658 mm  $\times$  4267 mm (12'  $\times$  14') corner panel.

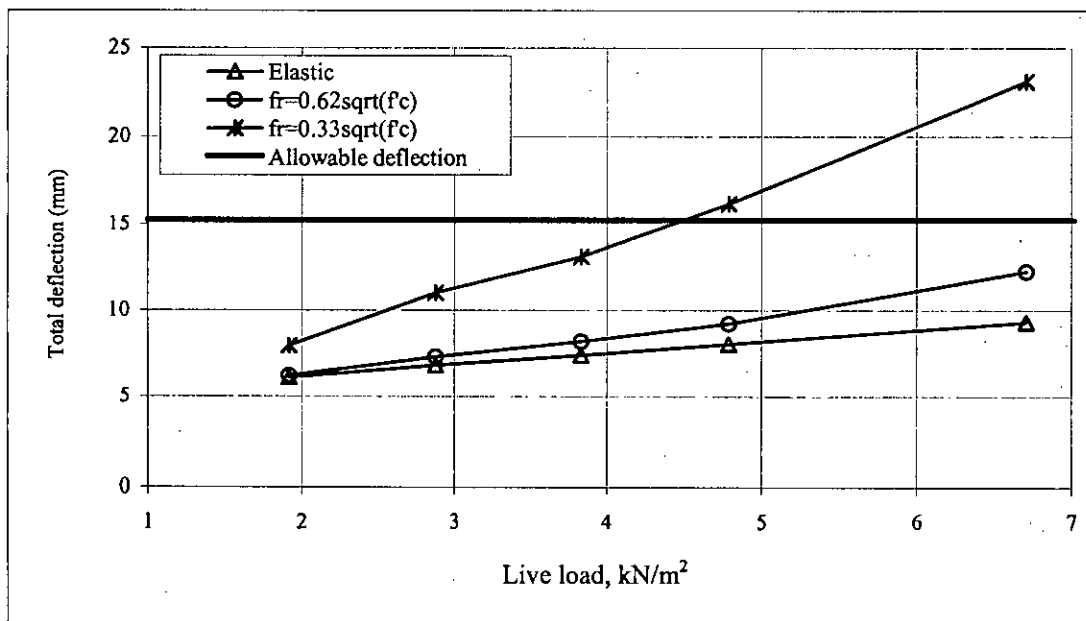
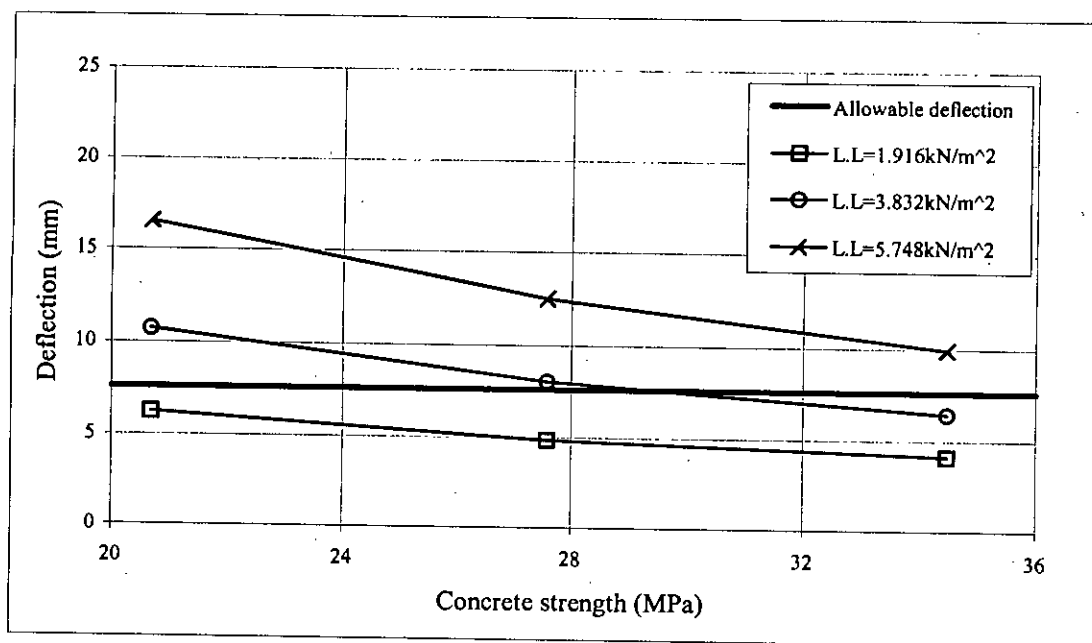


Figure 6.2 Variation of total deflection with varying live load for a 3658 mm  $\times$  4267 mm (12'  $\times$  14') corner panel.



### 6.3.2 Concrete Strength

Thickness selection based on ACI Code does not consider the effect of concrete strength. To identify the effect three concrete strengths, 20.7, 27.58 and 34.48 N/mm<sup>2</sup> (3000, 4000 and 5000 psi) were used in the analysis. Change in concrete strength changes modulus of rupture  $f_r$  and modulus of elasticity of concrete  $E_c$ . The variations of incremental and total deflections with concrete strength are plotted in Figs 6.3 and 6.4. The analysis is based on  $f_r = 0.33\sqrt{f'_c}$  N/mm<sup>2</sup> ( $4\sqrt{f'_c}$  psi). The results show that for higher live loads where slab is more cracked, the effect of providing higher concrete strength may prove beneficial. However, for lightly loaded slabs, which are mostly uncracked, the effect is not significant.



**Figure 6.3** Variation of incremental deflection with varying live load and concrete strength for a 3658 mm × 4267 mm corner panel,  $f_r = 0.33\sqrt{f'_c}$  N/mm<sup>2</sup>

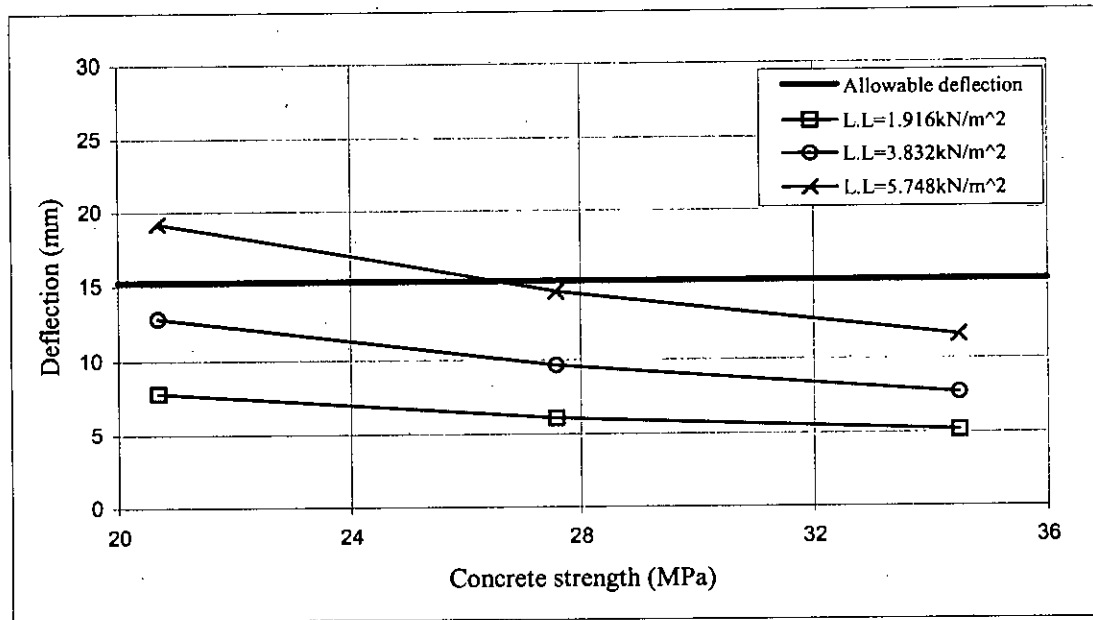


**Figure 6.4** Variation of total deflection with varying live load and concrete strength for a 3658 mm × 4267 mm corner panel,  $f_r = 0.33\sqrt{f'_c}$  N/mm<sup>2</sup>

### 6.3.3 Slab Thickness

To demonstrate the effect of slab thickness on deflection, a study has been carried out where slab thickness were chosen using both 1963 ACI Code (perimeter /180) and 2002 ACI Code (using Eqn. 2.47); at the same time, thickness 20% more and less than obtained from Eqn. (2.47) were used in the analysis. The comparative thickness of slab calculated from both Codes for corner panels are presented in the Table 6.1 and higher thickness are yield in ACI Code (2002). Two levels of live load, 1.92 and 3.82 kN/m<sup>2</sup> (40. and 80 psf), were used in the analysis. Incremental and total deflections with different thickness are plotted in Figs 6.5 and 6.6. The results show that deflections are reduced drastically if an increase in thickness results in reduction in cracking. For slabs, which are mostly uncracked, a thickness increase will not reduce deflections appreciably.

**Table 6.1** Slab thickness predicted from ACI Code 1963 and ACI Code 2002.

Slab dimension (mm × mm)	Beam dimension (mm × mm)		Slab thickness (mm)		% variation with respect to ACI Code 1963
	Breadth	Depth including slab thickness	ACI Code 1963	ACI Code 2002	
7620 × 7620	254	508	169	180	6.34
7620 × 6858	254	508	161	176	9.41
7620 × 6096	254	508	152	171	12.29
7620 × 5334	254	508	144	165	14.77
7620 × 4572	254	508	135	158	16.47
7620 × 3810	254	508	127	148	16.76

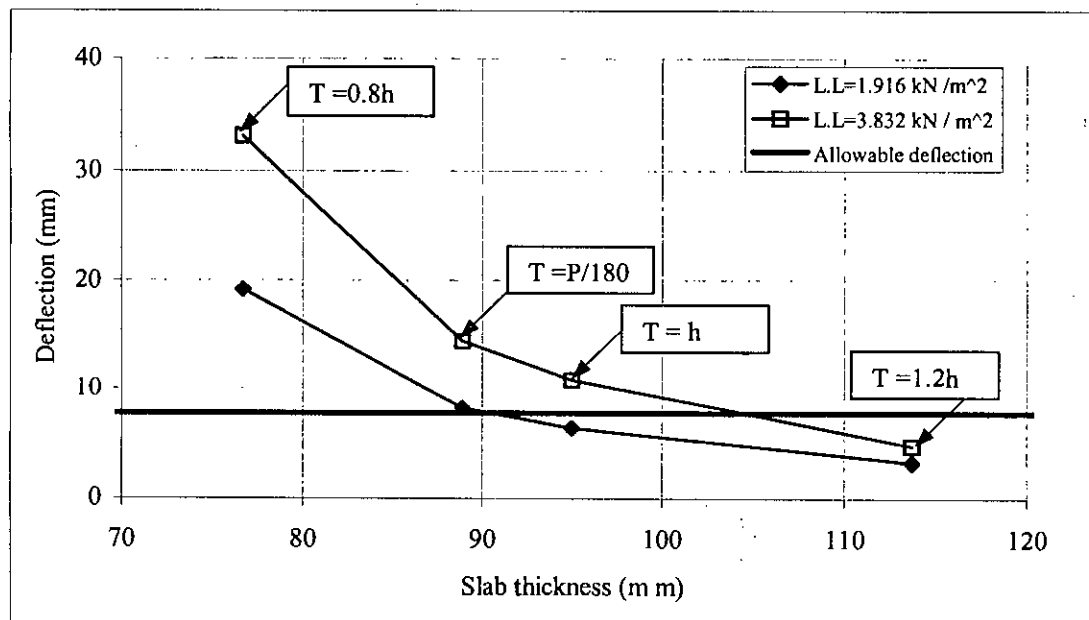


**Figure 6.5** Variation of incremental deflection with varying slab thickness for a 3658 mm × 4267 mm (12' × 14') corner panel,  $f_r = 0.33\sqrt{f'_c}$  N/mm<sup>2</sup>

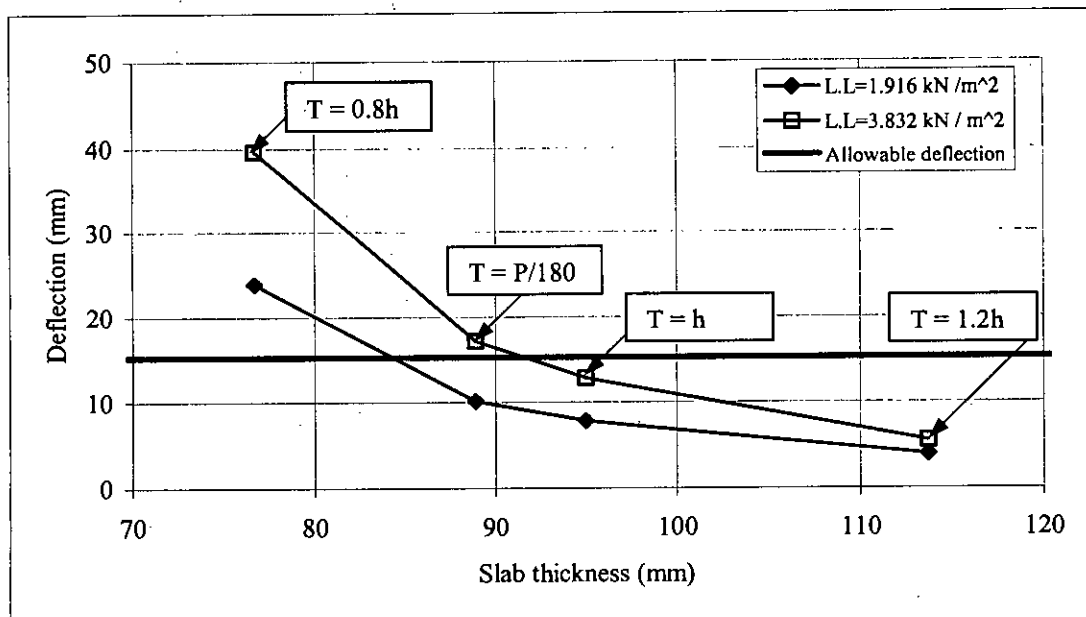


**Figure 6.6** Variation of total deflection with varying slab thickness for a 3658 mm × 4267 mm (12' × 14') corner panel,  $f_r = 0.33\sqrt{f'_c}$  N/mm<sup>2</sup>

### 6.3.4 Panel Size

To identify the effect of span length of two-way edge supported slabs on deflection, different panel sizes with varying live loads have been analyzed. The panel sizes are 3658 mm × 4267 mm, 4877 mm × 4877 mm and 6096 mm × 7620 mm. The analyses were carried out for concrete strength of 20.7 N/mm<sup>2</sup> (3000 psi) and reduced value of rupture strength. The live load was varied from 1.92 to 4.79 kN/m<sup>2</sup> (40 to 100 psf). The variation of incremental and total deflections with varying live loads are plotted in Figs 6.7 and 6.8. The results show that for smaller spans with relatively light loads the estimated deflections are within tolerable limits.

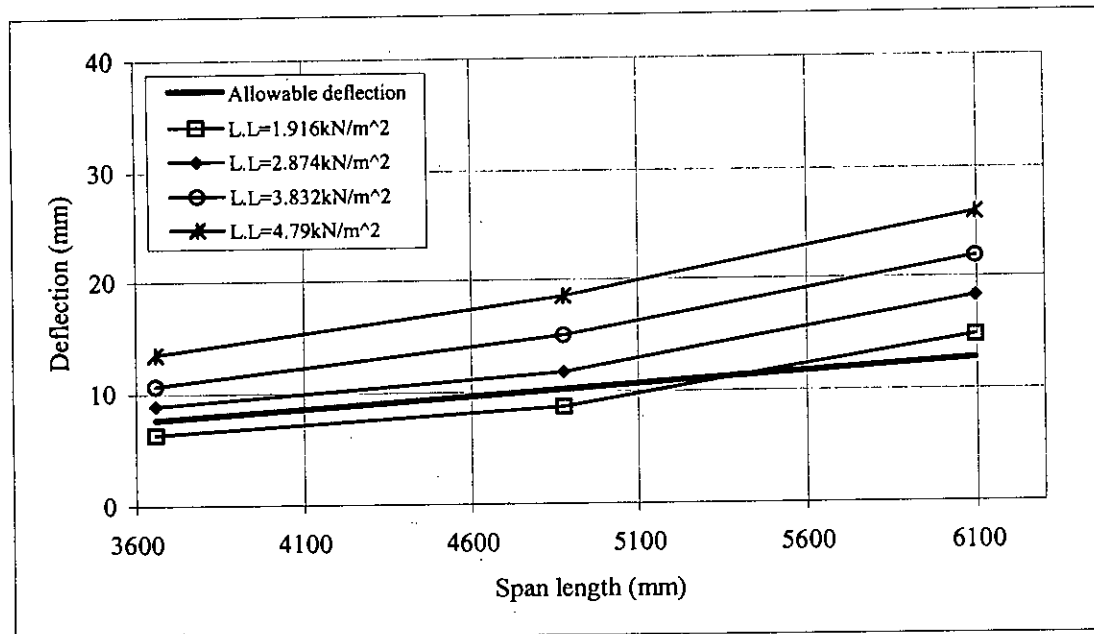


Figure 6.7 Variation of incremental deflection with varying span length and live load.

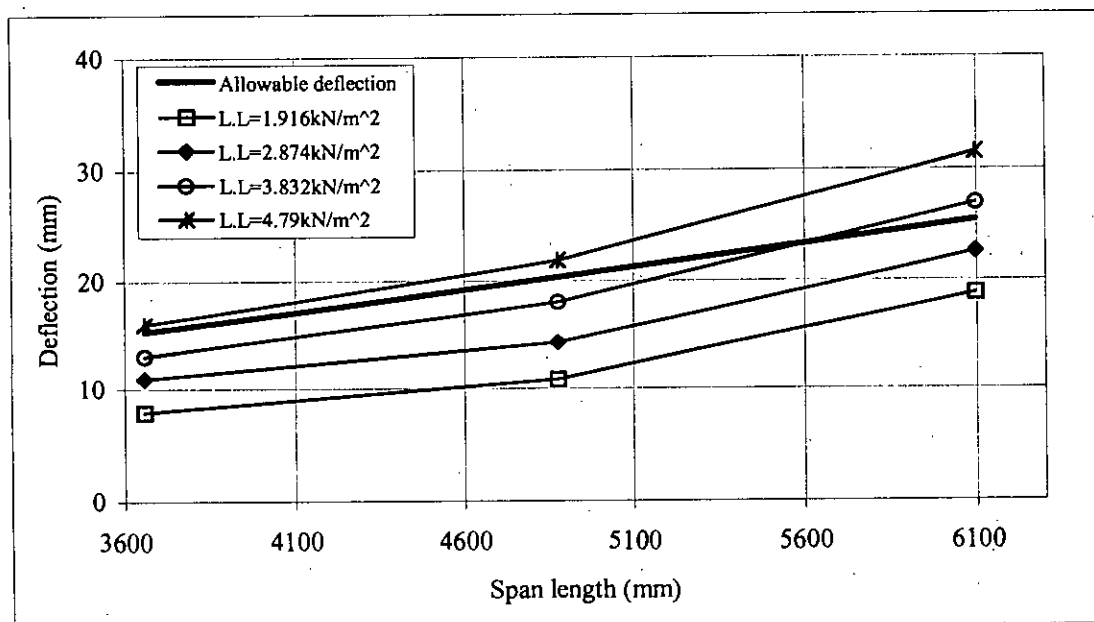


Figure 6.8 Variation of total deflection with varying span length and live load.

## 6.4 Conclusion

The results of the study show that in most cases the thickness provided by the ACI Code (2002) proved to be adequate where spans, live loads, concrete strength etc. are in normal range. However, for shorter spans with lighter loads, a smaller thickness may suffice from serviceability point of view. The ACI Code allows slab thickness less than the specified value if calculated values are within code-specified limits. So it would be economical to use thinner slabs in such situations where deflection analysis permits so. On the contrary, for excessive live load and larger panels, providing ACI Code minimum thickness may not be adequate. In such conditions, deflection calculations should be mandatory to decide a higher thickness. Nevertheless, it must be noted that deflection estimation procedure embodied in ACI Code, as discussed in section 2.6.1 and used in the current chapter to calculate long-term deflection, is crude in nature and does not intend to calculate deflection precisely.

## CHAPTER 7

### CONCLUSIONS AND RECOMMENDATIONS

#### 7.1 Introduction

The main objective of this research work is to develop a simplified method for prediction of immediate as well as long-term deflections of two-way edge supported slabs. In recent years, realistic estimation of slab deflections under service loads has become more important than ever due to increasing use of high-strength materials and due to the use of ultimate limit state design which generally result in thinner members. Deflection calculation is difficult since slabs designed according to ACI Code are mostly cracked even under service loads which demands use of nonlinear finite element analysis. Long-term deflections, which are the main concerns of serviceability, are also affected by creep and shrinkage which make analysis further complicated. In this work, nonlinear finite element method using Branson's equation is employed to simulate cracking. Based on the results of a large number nonlinear analyses simplified design charts have been prepared. With some accompanying charts to calculate elastic deflections and stresses, these simplified charts can be used to calculate immediate deflections with ease and reasonable accuracy. Calculation of long-term deflection using ACI Code multiplier approach is shown with examples to demonstrate the proposed deflection calculation procedure.

## 7.2 Conclusions

Within the scope and limitation of this research work the conclusions can be summarized as follows:

1. The deflection coefficients based on elastic FE analysis have been computed for the calculation of elastic deflection of slabs for the most common boundary conditions and for different aspect ratios. These will be useful in deflection calculation without time consuming FE analysis. However, from FE analysis it has been observed that most of the edge supported slabs are cracked even under service load when restrained shrinkage is significant. It is important to check the maximum stress developed in the slab and include the effect of cracking if stresses exceed modulus of rupture.
2. The moment coefficients based on elastic FE analysis for nine cases of boundary conditions of slabs have been proposed for calculation of maximum elastic stress in slabs which will be useful in deciding whether there is cracking in slab. The elastic stresses are also used to determine level of cracking which is needed in simplified deflection calculation. The moment coefficient calculated from FE analyses are compared with the ACI Code (1963) moment coefficient and some variations have been observed. This is due to the fact that the ACI Code (1963) has accounted for inelastic redistribution of stresses. It would be logical to use elastic stresses which represent state before cracking.
3. Branson's model to reduce stiffness due to cracking has been employed. The results obtained from nonlinear FE analysis have been compared with a number of experimental results and good correlations have been observed.
4. The effect of tensile reinforcement on deflection of slab has been studied and it has been found that providing more steel has little effect on deflection when slabs are lightly cracked. For slabs which are severely cracked, effect of reinforcement on deflections is more pronounced.
5. A large number of slabs with a combination of most common boundary conditions and aspect ratio has been analyzed. For certain end condition with a particular aspect ratio, all slabs show an identical pattern in deflection magnification due to cracking. Deflection magnification is only determined by the level of cracking  $f/f_r$ , aspect ratio and end conditions.



6. Deflection calculation using FE analysis considering cracking is time consuming and may prove to be complicated for the designer. A simplified method of deflection estimation has been proposed. First the designer needs to calculate the elastic deflection using the proposed charts of deflection coefficients. Based on the maximum flexural stress developed in the slab, which can be found from proposed elastic moment coefficients, the designer can determine the level of cracking of the slab. Using this level of cracking, one can estimate the deflection magnification factor. Nine sets of design charts for different boundary conditions and aspect ratios are prepared based on a large number of FE analyses using Branson's equation to incorporate effect of cracking. The immediate deflection can be found by multiplying the elastic deflection with this magnification factor. Immediate deflections of a large number of slabs have been calculated following this approach and they are found to be in good agreement with those obtained from rigorous FE analysis and some limited experimental results.
7. A parametric study has also been carried out and adequacy of ACI minimum thickness has been studied. ACI simplified multiplier method has been used in the analysis. Both incremental and total deflections of smaller sized panel designed with ACI thickness remain within tolerable limits when loads are light. For larger panels, ACI thickness provisions are found to be inadequate particularly when loads are high. When slabs are severely cracked due to excessive live loads, use of high strength concrete may prove beneficial.
8. It is easier to satisfy total deflection tolerable limits whereas incremental deflection limits are found to be frequently exceeded in case of high loads and/or larger panels.

### 7.3 Recommendations for Future Work

The following research topics are possible future extensions of the current work:

- This study was performed for single slab modeling and some differences have been observed when compared with 3-D elastic analysis. More realistic results of immediate slab deflection would be found if a full 3-D building is modeled.
- In this study the design charts containing deflection magnification factors are presented in the form of two bounding lines which correspond to aspect ratio 0.5 and 1.0. If more lines corresponding to intermediate aspect ratios can be generated, deflection calculation will be more accurate.
- Further study is possible to develop design charts for flat plate and flat slabs for calculation of immediate deflection.
- Crack width is another important aspect of serviceability and affects the corrosion of reinforcing bar or may be visually objectionable. Study is possible for prediction of crack width.
- Experiments involving measuring immediate and long-term deflections of edge supported slabs for different boundary conditions are needed for further verification of the proposed numerical analysis.
- A neural network based deflection prediction tool can be developed which will be useful in selection of slab thickness.

## REFERENCES

- ACI Committee 435. State-of-the-Art Report on Control of Two-way Slab Deflection. American Concrete Institute, Detroit, 1991.
- ACI Committee 318-02. Building Code Requirements for Structural Concrete (ACI 318-02) and Commentary (ACI 318R-02). American Concrete Institute, Michigan, 2002.
- ACI Publication 318-63. Building Code Requirements for Reinforced Concrete. American Concrete Institute, Detroit, 1963.
- Ahmed, B. and Chowdhury, S. R. (1999). Simplified Calculation Method for Serviceability Deflection of Edge Supported Slabs; Part-1 & Part-2: Modeling Slab Response. Journal of Civil Engineering, The Institution of Engineers, Bangladesh. Vol. CE 27, No. 1, June 1999, pp. 29-57.
- ANSYS 5.4, Operation Guide, SASIP Inc, 201 Johnson Road, Houston, PA 15342-1300.
- Asamoah, K. O. and Gardner, N. J. (1997). Flat Slab Thickness Required to Satisfy Serviceability Including Early Age Construction Loads. ACI Structural Journal. Vol. 94, No. 6, pp. 700-707.
- Beeby, A. W. (2001). Criteria for the Loading of Slab During Construction. Structures & Buildings 146 Issue 2, pp. 195-202.
- Branson, D. E . Deformation of Concrete Structures, McGraw-Hill Book Co., New York. 1977.
- Chang, K. Y. and Hwang, S. J. (1996). Practical Estimation of Two-way Slab Deflections. Journal of Structural Engineering, ASCE, Vol. 122, No.2, pp. 150-159.
- Chowdhury, S. R. (2000). Numerical Modeling of Edge Supported Slab Response, M. Sc. Engineering thesis, BUET, Dhaka.
- Cope, J. R. and Clark, A. L. (1984). Concrete Slabs: Analysis and Design, Elsevier Applied Science Publishers, London & New York.
- Ganeswarn, R. and Rangan, B. V. (1996). Long-term Deflections of High Strength Concrete Beams and One-way Slabs. Recent Developments in Deflection Evaluation of Concrete. Nawy, E. G. (ed) ACI, Michigan. SP-161, pp. 243-266.

- Ghali, A. and Azarnejad, A. (1999). Deflection Prediction of Members of Any Concrete Strength. *ACI Structural Journal*, Vol. 96, No. 5, pp. 807-816.
- Ghali, A. (1993). Deflection of Reinforced Concrete Members: A Critical Review. *ACI Structural Journal*, Vol. 90, No. 4, pp. 364-373.
- Ghali, A. (1990). Deflection of Prestressed Two-way Floor Systems. *ACI Structural Journal*, Vol. 87, No. 1, Jan-Feb, pp 60-65.
- Ghali, A. (1989). Prediction of Deflection of Two-way Floor Systems. *ACI Structural Journal*, Vol. 86, No. 5, pp. 551-562.
- Gilbert, R. I. (1999). Deflection Calculation for Reinforced Concrete Structures- Why We Sometimes Get It Wrong. *ACI Structural Journal*, Vol. 96, No. 6, pp. 1027-1032.
- Gilbert, R. I. (1985). Deflection Control of Slabs Using Allowable Span to Depth Ratios. *ACI Journal*. Vol. 82 No. 6, pp. 67-72.
- Hitchings, D. (1999). FE-77 User Manual Version 2.54. Aeronautics Dept., Imperial College. University of London
- Hwang, S. J. and Chang, K. Y. (1996). Deflection Control of Two-Way Reinforced Concrete Slabs. *Journal of Structural Engineering, ASCE*, Vol.122, No. 2, pp. 160-168.
- Hossain, T. R. (1999). Numerical Modeling of Deflections of Reinforced Concrete Flat Slabs Under Service Loads. PhD thesis, University of London
- Hossain, T. R. and Vollum, R. L. Prediction of Slab Deflections and Validation Against Cardington Data. *Structures and Building*, 2002, Vol. 152, No. 3, pp. 235-248.
- Joforiet, J. C. and McNeice, G. M. (1971). Finite Element Analysis of Reinforced Concrete Slabs. *Journal of the Structural Division, ASCE*, 97(3), pp. 785-806.
- Kong, F. K., Evans. R. H., Cohen. E., and Roll. F. (1983). *Hand Book of Structural Concrete*, McGraw- Hill Book Co. New York, St. Louis, San Francisco, pp. 11.1 – 12.88.
- Kripanayanan, M. K. and Branson E. D. (1976). Short-term Deflections of Flat Plates, Flat Slabs, and Two-Way Slabs. *ACI Journal*, Vol.73 (December), pp. 868-690.
- May, I. M., Montague, P., Samad, A. A. A., Lodi, S. H. and Fraser, A. S. (2001). The Behavior of Reinforced Concrete Elements Subject to Bending and Twisting Moments. *Structures & Buildings* 146, Proceedings of the Institute of Civil Engineering, May 2001, Issue 2, pp. 161-171.

Montague, P., May, I. M., Samad, A. A. A., and Tye, C. (2001). An Experimental Rig to Test the Behavior of Reinforced Concrete Slabs Subjected to Bending and Torsion. Structures & Buildings 146, Proceedings of the Institute of Civil Engineering, May 2001, Issue 2, pp. 173-182.

Nizamud-Doulah, S. M. and Kabir, A. (2001). Non-linear Finite Element Analysis of Reinforced Rectangular and Skew Slabs. Journal of Civil Engineering, The Institution of Engineers, Bangladesh. Vol. CE 29, No. 1, June 2001, pp. 1-16.

Nilson, A. H. Design of Concrete Structures, 12<sup>th</sup> Edition, McGraw- Hill Book Co. New York, 1997.

Nilson, A. H. and Walters, Jr. D. B. (1975). Deflection of Two-way Floor Systems by the Equivalent Frame Method. ACI Journal, May 1975, pp. 210-218.

Oforu-Asamoah, K. and Gardner, N. J. (1997). Flat Slab Thickness Required to Satisfy Serviceability Including Early Age Construction Loads. ACI Structural Journal, Vol. 94, No. 6, pp. 700-707.

Polak, M. A., Scanlon A., and Phillips. D. V. (1996). Deflection Analysis of Reinforced Concrete Members Using Finite Element Method. Pages 75-96 of : Nawy, E. G. (ed), Recent Developments in Deflection Evaluation of Concrete. ACI, Michigan. SP-161.

Rangan, B. V. (1976). Prediction of Long-term Deflections of Flat Plates Slabs. ACI Journal, Vol. 73 (April), pp. 223-226.

Rosowsky, D. V., Stewart M. G. and Khor, E. H. (2000). Early-age Loading and Long-term Deflections of Reinforced Concrete Beams. ACI Structural Journal, Vol. 97, No. 3, pp. 517-524.

Scanlon, A. and Choi, B. S (1999). Evaluation of ACI 318 Minimum Thickness Requirements for One-way Slabs. ACI Structural Journal, Vol. 96, No. 4, pp. 616-621.

Scanlon, A. and Thompson, D. P. (1990). Evaluation of ACI 318 Requirements for Control of Two-way Slab Deflections. ACI Structural Journal, Vol. 87, No. 6, pp. 657-661.

Shukla, S. N. and Mittal, M. K. Short-term Deflection in Two-way Reinforced Concrete Slabs After Cracking. ACI Journal, 1976, Vol. 73 (July), pp 416-419.

Thompson, D. P. and Scanlon, A. (1988). Minimum Thickness Requirements for Control of Two-way Slab Deflections. ACI Structural Journal, Vol. 85, pp. 12-22.

Tam, K.S.S. and Scanlon, A. (1986). Deflection of Two-way Slabs Subjected to Restraint Volume Change and Transverse Loads. *ACI Structural Journal*, Vol. 83, No. 5, pp. 737-744.

Ugural, A. C. (1999). *Stress in Plates and Shells*, Second edition, McGraw- Hill Book Co, pp. 141-191, 305-320.

Vollum, R. L. and Hossain, T. R. (2002). Are Existing Span-to-Depth Rules Conservative for Flat Slabs? *Magazine of Concrete Research*, 2002,54, No. 6, December, pp. 411-421.

Zhang, J. W., Teng, J. G., Wong, Y. L. and Lu, Z. T. (2001). Behavior of Two-way Slabs Externally Bonded with Steel Plates. *Journal of Structural Engineering*, ASCE, Vol. 127, No. 4, pp. 390-397

## APPENDIX

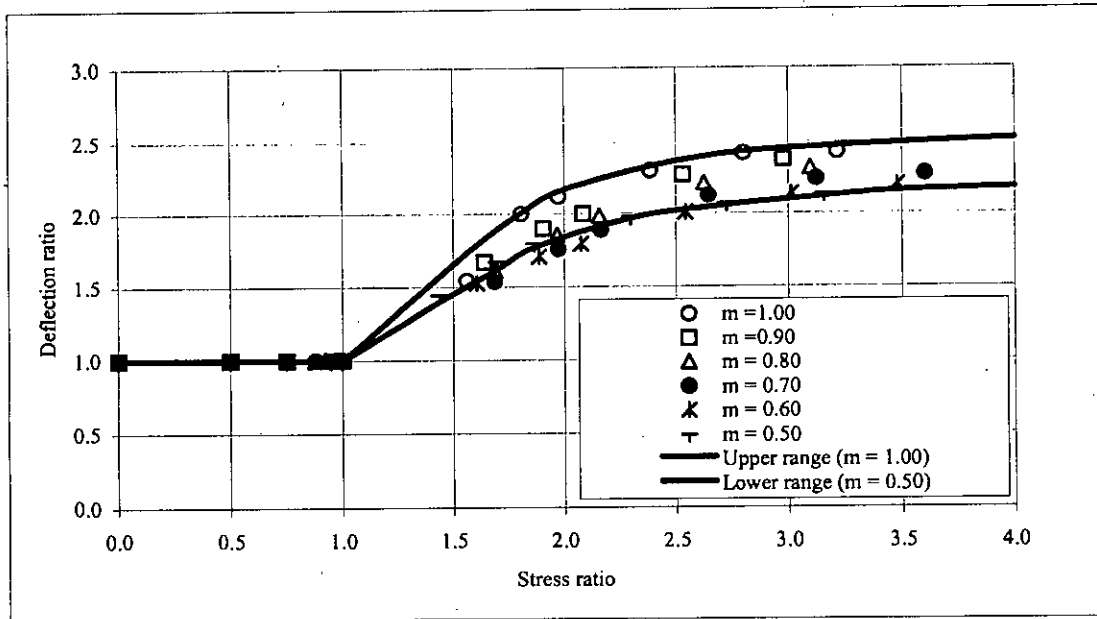


Figure A1 Deflection ratio vs. stress ratio chart for slab case-1,  $f_r = 0.62\sqrt{f'_c}$  N/mm<sup>2</sup>

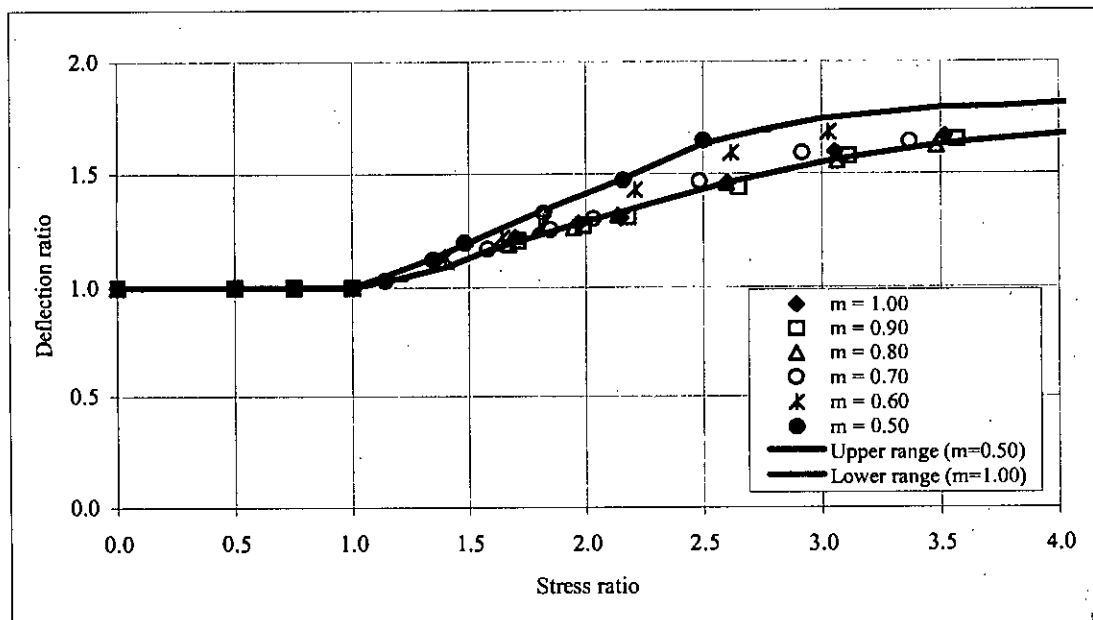


Figure A2 Deflection ratio vs. stress ratio chart for slab case-2,  $f_r = 0.62\sqrt{f'_c}$  N/mm<sup>2</sup>



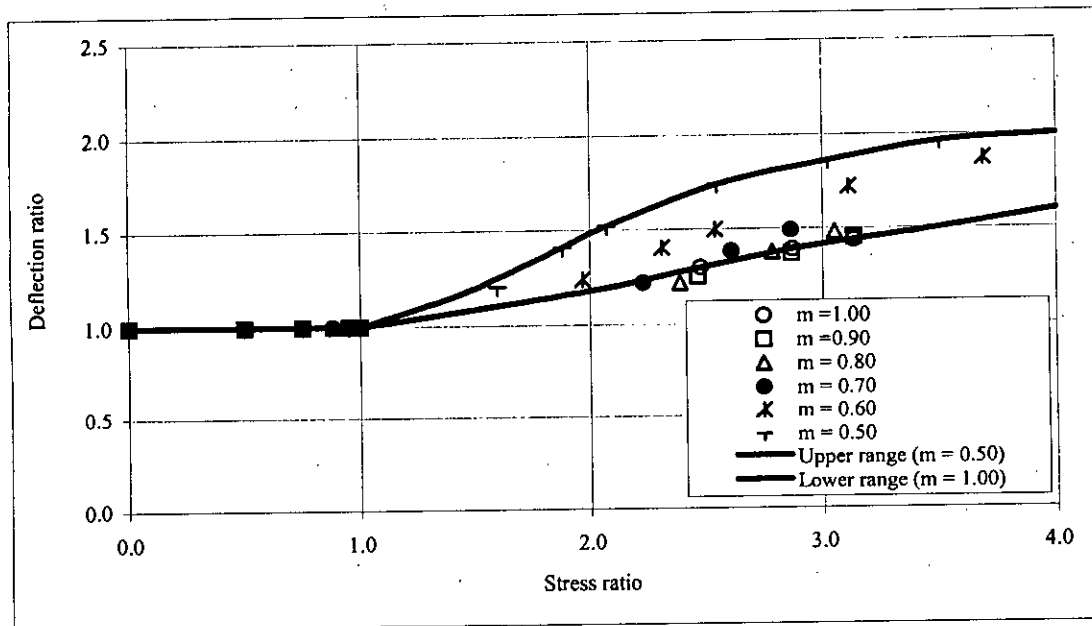


Figure A3 Deflection ratio vs. stress ratio chart for slab case-3,  $f_r = 0.62\sqrt{f'_c}$  N/mm<sup>2</sup>

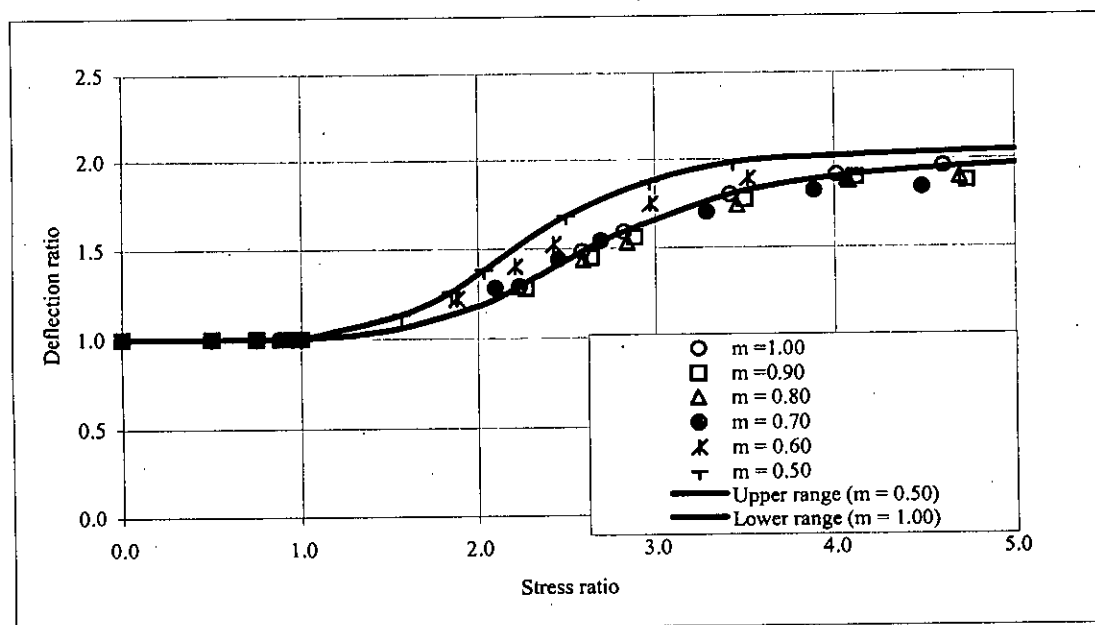


Figure A4 Deflection ratio vs. stress ratio chart for slab case-4,  $f_r = 0.62\sqrt{f'_c}$  N/mm<sup>2</sup>

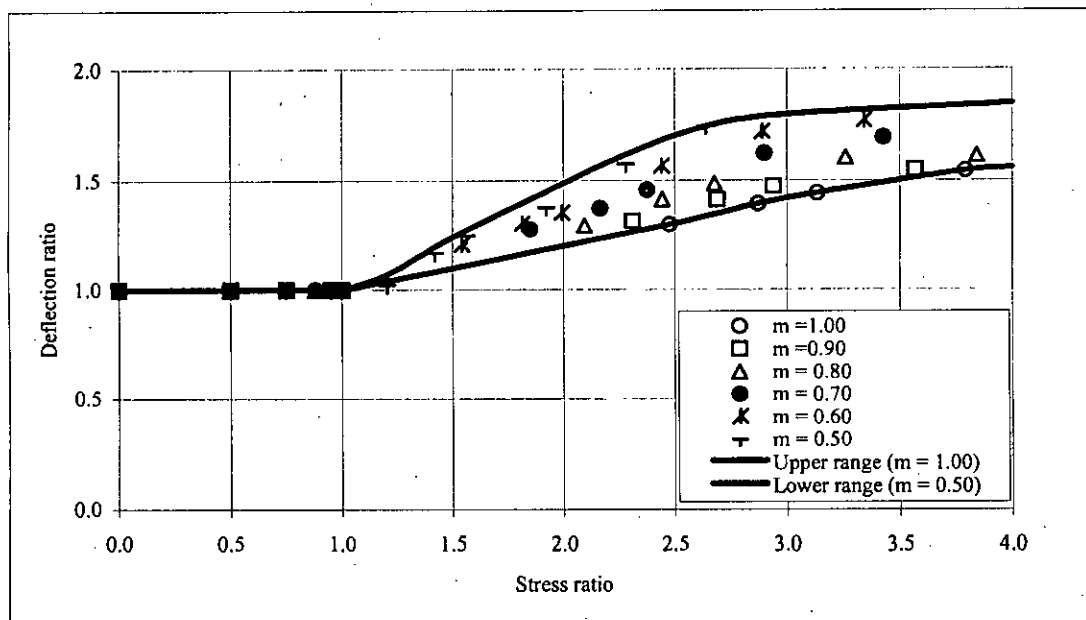


Figure A5 Deflection ratio vs. stress ratio chart for slab case-5,  $f_r = 0.62\sqrt{f'_c}$  N/mm<sup>2</sup>

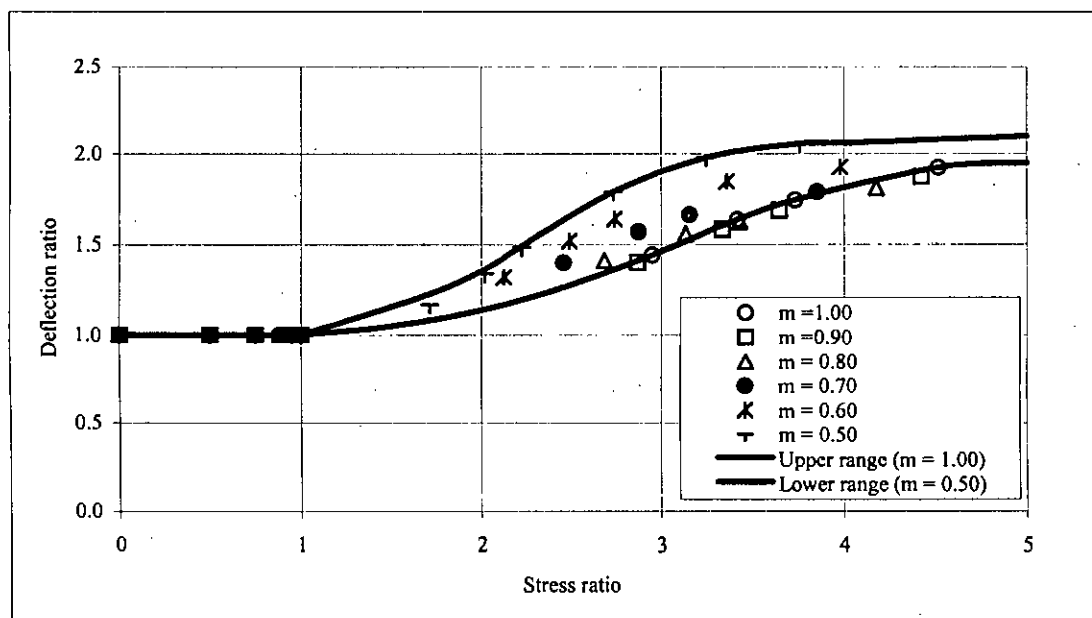


Figure A6 Deflection ratio vs. stress ratio chart for slab case-6,  $f_r = 0.62\sqrt{f'_c}$  N/mm<sup>2</sup>

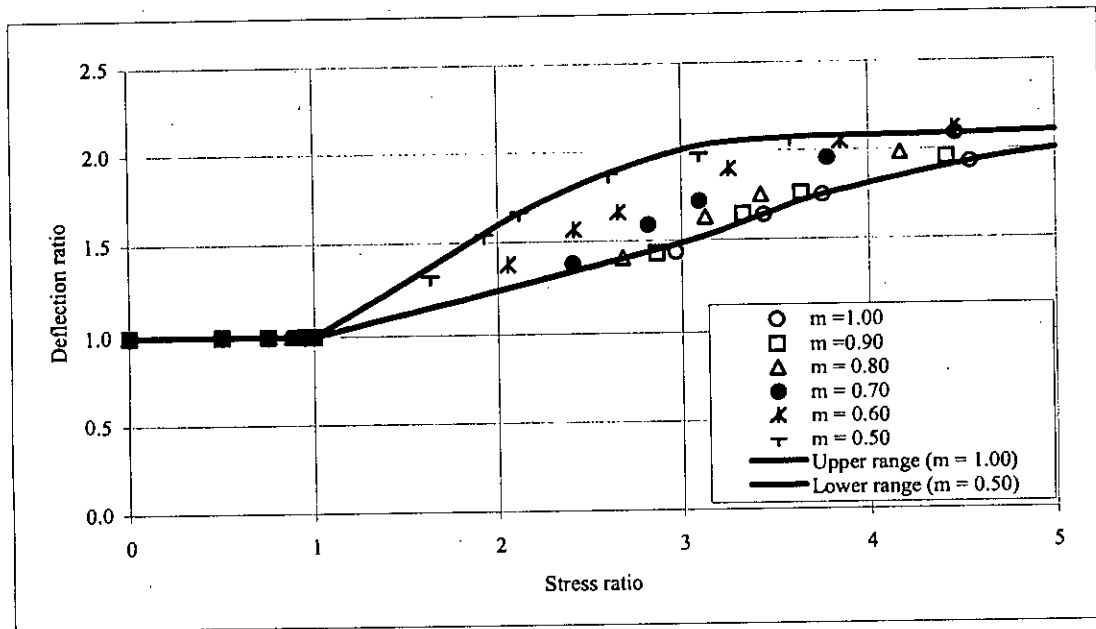


Figure A7 Deflection ratio vs. stress ratio chart for slab case-7,  $f_r = 0.62\sqrt{f'_c}$  N/mm<sup>2</sup>

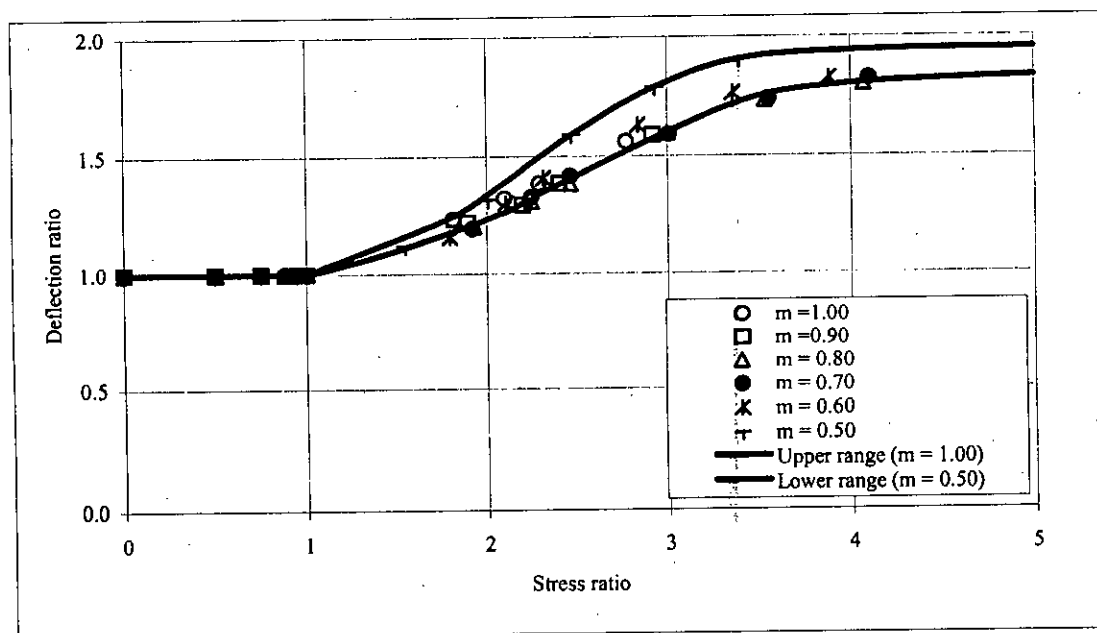


Figure A8 Deflection ratio vs. stress ratio chart for slab case-8,  $f_r = 0.62\sqrt{f'_c}$  N/mm<sup>2</sup>

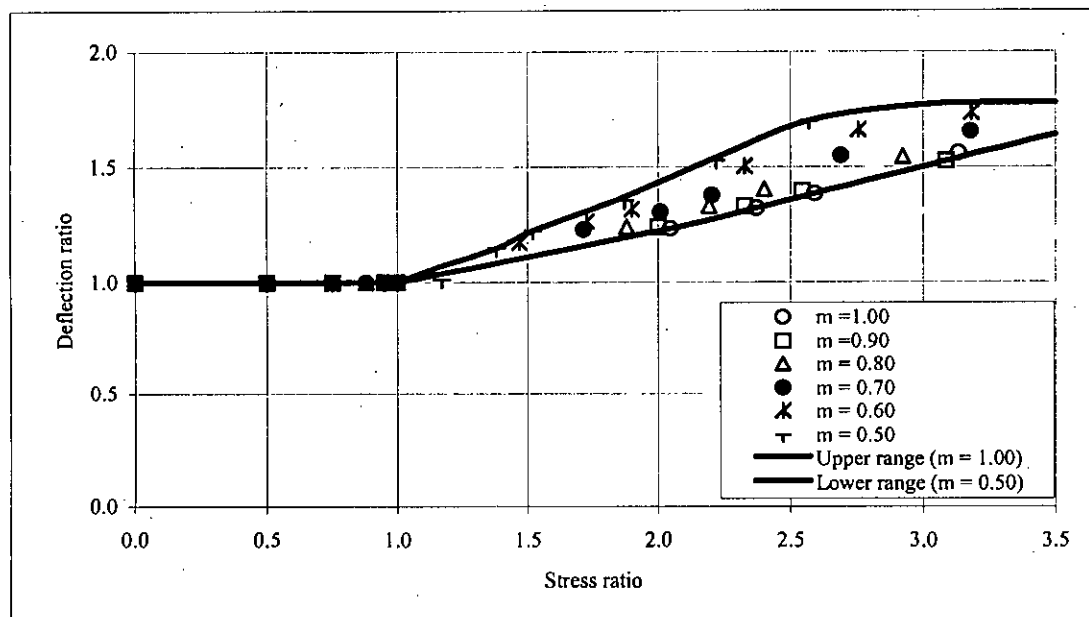


Figure A9 Deflection ratio vs. stress ratio chart for slab case-9,  $f_r = 0.62\sqrt{f'_c}$  N/mm<sup>2</sup>

